The Facial Musculature
Characterisation at a Motor Unit Level

Bernd G. Lapatki

The Facial Musculature
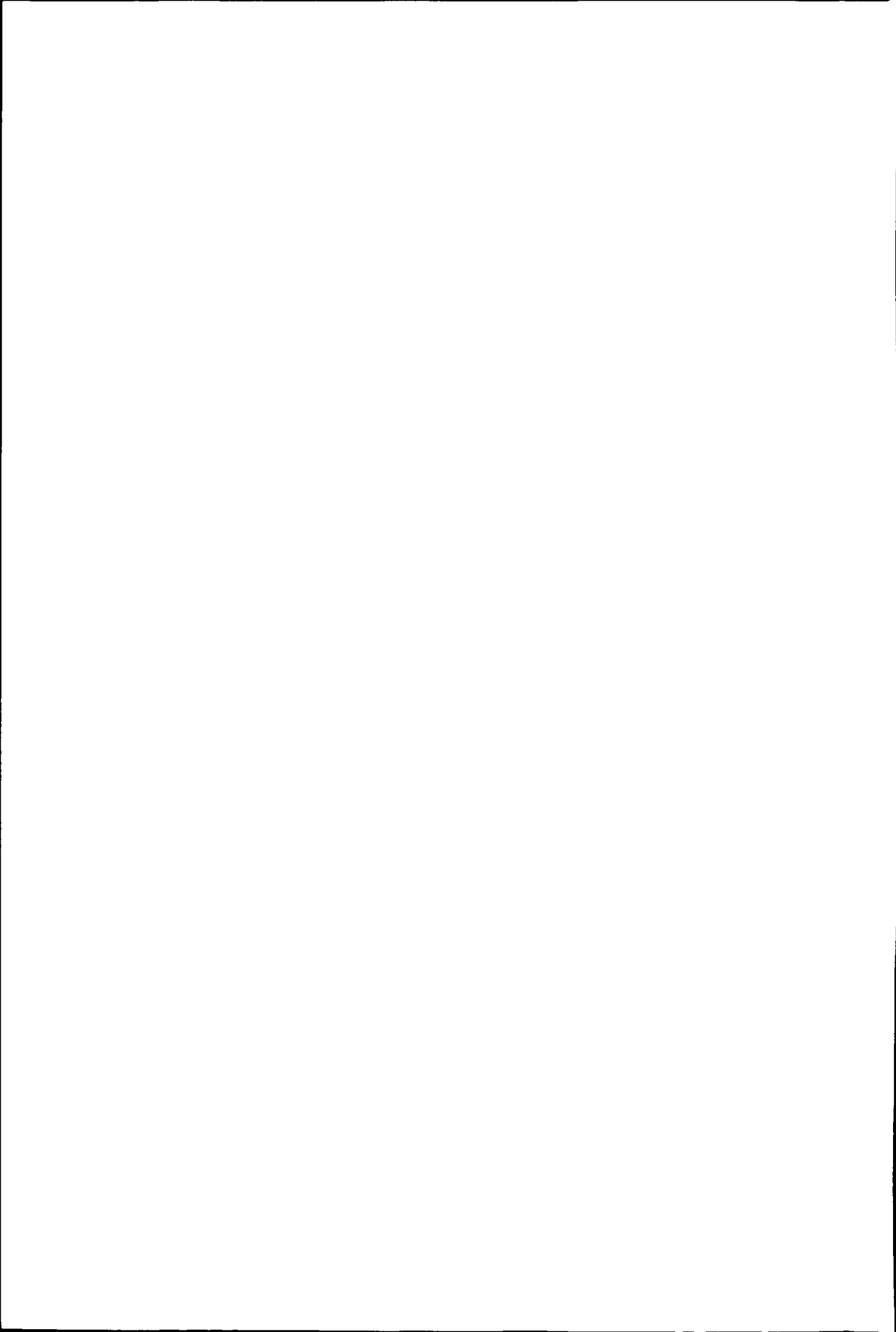## Characterisation at a Motor Unit Level

Bernd G. Lapatki

The Facial Musculature

Characterisation at a Motor Unit Level

Bernd G. Lapatki

The Facial Musculature

Characterisation at a Motor Unit Level

Een wetenschappelijke proeve op het gebied
van de Medische Wetenschappen

Proefschrift

ter verkrijging van de graad van doctor
aan de Radboud Universiteit Nijmegen
op gezag van de rector magnificus prof mr S C J J Kortmann,
volgens besluit van het college van decanen
in het openbaar te verdedigen op vrijdag 4 juni 2010
om 13 00 uur precies

door

Bernd G. Lapatki
geboren op 16 mei 1966
te Rottweil, Duitsland

Promotores:
Prof. dr. ir. D.F. Stegeman
Prof. dr. M.J. Zwarts

Copromotor:
Dr. ir. R. Oostenveld

Manuscriptcommissie:
Prof. dr. ir. N.J.J. Verdonschot
Prof. dr. B.R. Bloem
Prof. dr. P.M.N. Werker (Rijksuniversiteit Groningen)
Prof. dr. S.J. Bergé
Dr. J. Delbeke (Katholieke Universiteit Leuven)

The Facial Musculature

Characterisation at a Motor Unit Level

An academic essay in
Medical Sciences

Doctoral Thesis

To obtain the degree of doctor
from Radboud University Nijmegen
on the authority of the rector magnificus prof dr S C J J Kortmann,
according to the decision of the Council of Deans
to be defended in public on Friday June 4, 2010
at 13.00 hours

by

Bernd G. Lapatki
born on 16 May1966
in Rottweil, Germany

To Cris and my Dutch friends

Contents

Part I

Introduction

The anatomic and neurophysiologic literature on the complex facial musculature shows major deficiencies in knowledge about the basic morphological motor unit properties. In the last two decades measurement and data analysis methods have been developed that allow electrophysiological characterisation of topographical aspects of superficially located musculature at the level of single motor units. Measurements are performed with high-density surface EMG electrode arrays and their analysis uses a decomposition of the raw EMG with interference of many motor units into the action potentials of single motor units. The decomposition of the signal is possible by exploiting both the temporal information of the EMG, but also the spatial information provided by multiple electrodes distributed over the muscle. High-density surface EMG has been applied in numerous studies for single motor unit analysis in various muscle systems. Their results contributed significantly to the understanding of the structure and function of the neuromuscular system. Moreover, the non-invasive high-density surface EMG technique has demonstrated in recent years to be a useful clinical tool for studying functional alterations due to neuromuscular diseases. The facial musculature has been largely segregated from this development, mainly because available sensors and signal processing tools could not meet the high technical demands related to the special anatomical characteristics of the facial muscle system. The special aspects of the facial musculature as well as the methodological basics for its visual and electrophysiological examination are dealt with in the first part of this thesis. A summary of the methodological progression from conventional surface EMG to high-density surface EMG builds a bridge from this introductory part to the novel research that is described in the subsequent parts.

1

CHARACTERISTICS OF FACIAL MUSCLES

Functional importance

The muscles of the face are involved in various physical functions. Some muscles participate in the intake of solid and liquid food and in mastication. Others facilitate or impede the access of sensory stimuli to the organs of vision and taste and to the olfactory and acoustic organs. The mobility and suitable position of the facial muscles were probably important factors for their development as the main mediators of emotional and affective states. The relevance of facial muscles for non-verbal communication is also reflected in their second name: "mimic muscles". The perioral musculature furthermore plays an important role in articulation and – as expressed by the term "embouchure musculature" – in sound generation on wind instruments.

Facial muscles insert in the facial skin, or in fasciae and cartilage that are inter-connected with the skin. Thus, functions of facial muscles are always related to movement of the facial soft tissues. As only little force is necessary for moving the soft tissue, facial muscles are much thinner and smaller compared to most other skeletal muscles.

A detailed understanding of the functions of the facial musculature and related facial movements requires profound knowledge of the development, macro- and micro-anatomical characteristics, and neural control mechanisms of this unique muscle system.

Developmental aspects

Many structural characteristics of facial muscles and different variants of their architecture can be explained by phylogenetic and developmental aspects (Braus and Elze 1954). Facial muscles evolve from two muscle layers, both originating from the tissue of the second branchial arch. Both layers undergo a complex, cranially directed migration process which can

be regarded as overflow of the head by muscle tissue. The different steps of this migration process are documented in the anatomy of lower and higher primates (phylogenesis) and in human embryogenesis.

The superficial layer (the original "platysma") has a cervical stream building the platysma and the depressor labii inferioris. Both muscles can be regarded as a single muscle sheet that is attached to the lower mandibular margin. Two streams of the superficial layer migrate further in the cranial direction - one behind, and one in front of the ear – and over-flow the face. During this migration in ventral-medial direction the apertures of the face (i.e., the eye, nose and mouth) separate the muscle sheets into smaller components which attach to the facial skeleton or other muscle subcomponents. Both zygomaticus muscles, the levator labii superioris alaeque nasi and the orbicu-laris oculi, are supposed to originate from the mid- and upper facial streams of the superficial layer, although there is a controversy in the literature on which individual muscle actually belongs to this layer (Braus and Elze 1954). The deep layer (the sphincter colli profundus) attaches early (i.e., already in the region of the cavum oris) to the skull and its migration ends at the lower margin of the orbita. Several lower and midfacial muscles, such as the orbicularis oris and both the depressor and levator of the mouth corner are considered to originate from this layer.

The complex topography of the facial musculature is closely related to special aspects of the migration process. Some of the descend-ents of the deep layer are – corresponding to the original relation – covered by the descend-ants of the platysma. Others emerge through gaps in the superficial layer on the surface or even migrate through this layer and even cover platysma descendents. The latter is exemplified by the depressor anguli oris which originates from the deep layer, but reaches the surface

1
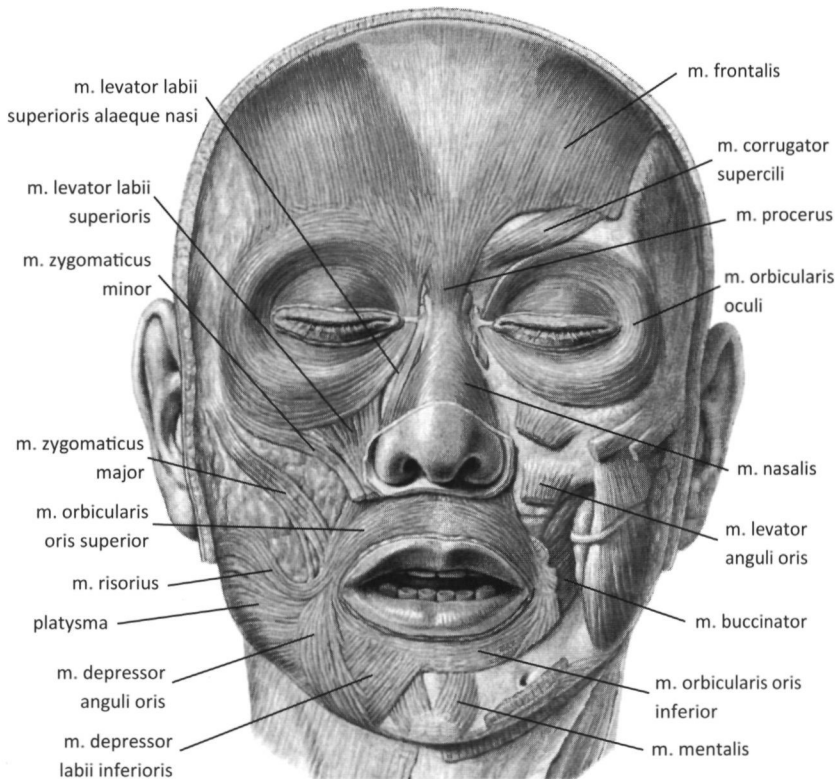
Figure 1-1. Frontal view on the facial musculature (adapted from (Sobotta 2000)).

of the face lateral to the mouth and overflows the depressor labii inferioris (i.e., a platysma descendent) in caudal direction. In general, the inversion of the two layers seems to be facilitated by the enlargement of the head and face leading to greater distances between the individual muscle subcomponents.

Macro-anatomical characteristics

The facial muscle architecture, i.e. the positions of individual muscle components and their fibre orientations, is described and illustrated in the form of drawings (Fig. 1-1) and photographs in a variety of anatomical textbooks, see

e.g. (Braus and Elze 1954; Nairn 1975; Rohen et al. 2006; Salmons 1995; Sobotta 2000). The available information usually refers to a limited number of dissected human cadavers. Systematic quantitative macro-anatomical data on the facial musculature is sparse. A few investigations included determination of muscle cross-sectional areas, e.g. (Ito et al. 2006), or localisation and quantitative evaluation of the different subcomponents of the orbicularis oris muscle in dissected human cadavers (Blair and Smith 1986; Hwang et al. 2007a). One dissection study conducted on 11 cadaveric specimen (Kennedy and Abbs 1979) quantitatively characterised the topology of

several facial muscles in relation to facial landmarks.

In the literature, facial muscle architecture is described as having special anatomical features when compared to other skeletal musculature: non-tendonous attachments to soft tissue, i.e. to facial skin or other muscle tissue (in some muscles even both the origin and attachment is non-tendenous), interdigitation and overlap in relatively small areas (especially in the lower facial area), absence of muscle fasciae and muscle spindles, and remarkably high inter- and intra-individual variability in both location and morphology of the muscles (Blair 1986; Braus and Elze 1954; Kennedy and Abbs 1979; Nairn 1975; Salmons 1995). The variability manifests itself in the inconsistency of facial muscles such as the risorius and zygomaticus minor, i.e. these often consist of only a few fibres or are even completely absent (Braus and Elze 1954; Freilinger et al. 1990; Sato 1968). The large structural variability further complicates the subdivision of the facial muscle system into the single muscle components (Blair and Smith 1986), which results in some controversies in the anatomical literature. The research in this thesis aims to contribute to the understanding of this complex muscle system by studying its individual subcomponents at the level of their basic functional building blocks: the motor units.

Motor units

Motor unit number and innervation ratio

A motor unit, i.e. the basic functional unit of the neuromuscular system, comprises an α-motoneuron and all the muscle fibres that innervated by this α-motoneuron (Buchthal 1959; Kugelberg 1976). Both from a structural and functional point of view, two variables are of particular importance regarding the fine motor skill necessary for performing most facial muscle functions and for monitoring the course of neuromuscular diseases: the number of motor units per muscle and the number of muscle fibres per α-motoneuron (innervation ratio).

Three fundamentally different approaches exist to estimate the number of motor units in a muscle. The first is based on histochemical determination of the number of α-axons in nerve cross-sections obtained from cadaveric material. The second approach includes electrophysiological measurements (McComas et al. 1971; Shefner 2001) and is referred to as MUNE (motor unit number estimation). The third uses intramuscular stimulation of motor nerve fibres combined with twitch force measurements of single motor units and measurement of the muscle's maximal force output. Each of these approaches has considerable limitations, explaining the large discrepancies that are observed when applying different methods to the same muscles (Daube 2006; Lawson et al. 2004; Mateika et al. 1998).

The innervation ratio can be determined in cadavers by counting the number of α-axons and muscle fibres in nerve and muscle cross-sections respectively, or more directly after depletion of a single motor unit of glycogen (using electrical stimulation) and subsequent identification of the depleted muscle fibres (Kugelberg 1976). Results from different musculature varied widely, ranging from thousands of fibres in large limb muscles to only a few fibres in extraoccular muscles (see (Enoka 1995) for a review). It is assumed that a low innervation ratio increases the ability for fine graded muscle activity.

At present, few studies exist on motor unit numbers and innervation ratios of facial muscles. Available data from a few individual subcomponents indicates a relatively greater number (when related to muscle size) of smaller motor units when compared to

limb muscles. For instance, in a histochemical study in the human platysma, ca. 1100 motor units and an innervation ratio of 25 were found (Feinstein et al. 1955). Based on twitch force measurements, 227 motor units were estimated for the tiny pars alaris of the human nasalis muscle (Mateika et al. 1998; McComas 1998). In contrast, a more recent electrophysiological study determined a much lower number (i.e., 30 motor units in average) for the whole nasalis muscle (Yayla and Oge 2008). In one of the first MUNE studies in the face, rough estimates of motor unit numbers for groups of facial muscles were reported; these were 156, 316 and 187 for eyelid, midfacial and perioral muscles, respectively (Delbeke 1982). Severe problems were reported in this study with regard to application of MUNE in the face. For example, limitations in selective muscle or nerve branch stimulation make it nearly impossible to estimate the motor unit numbers for individual facial muscles (the nasalis muscle seems to be an exception in this respect). Also relatively small electrical sizes of facial motor units and overlap of motor unit territories of different muscles are factors that decrease the reliability of the estimate (Daube 2006).

Territories and muscle fibre organisation

In general, the muscle fibres of different motor units intermingle. The fibres of a single motor unit are restricted to a particular region of the muscle, though the relative cross-sectional areas vary considerably between muscles (Bodine-Fowler et al. 1990). Motor unit territories are typically elliptical and muscle fibres tend to be distributed in clusters with the highest fibre density in the periphery of the motor unit territory (Arsos and Dimitriu 1995).

Muscle fibres of a single motor unit also tend to be constrained in the muscle's longitudinal dimension, i.e. they do usually not extend from one muscle end to the other

(Ounjian et al. 1991; Trotter et al. 1995). This implies that at least one fibre end terminates intramuscularly either on connective tissues or as a tapered fibre (Ounjian et al. 1991; Trotter 1993). Such muscle fibre organisation influences functional variables such as neural activation patterns and external force transmission (Trotter et al. 1995).

In some muscles, discrete regions can be activated independently of other regions in the same muscle (Armstrong et al. 1988; Scholle et al. 2001; Staudenmann et al. 2009). The human masseter muscle is a typical example showing this behaviour (Blanksma and van Eijden 1995; Phanachet et al. 2001; Schindler et al. 2005; Widmer et al. 2007). According to the typical pattern of terminal motor nerve branching and clustered endplate zone distribution (Happak et al. 1997), facial muscles might also show such compartmentalisation, since studies in the human biceps brachii indicate this phenomenon to be consistent with the branching pattern of the nerve (English and Letbetter 1982).

Investigations of topographical characteristics of facial motor units (such as territorial motor unit boundaries and spatial orientations of motor unit fibre populations) are sparse. To our knowledge, there is only one published study in which conventional surface EMG techniques were used to show that motor unit territories are located within the quadrants of the human lip musculature (Goffman and Smith 1994). This thesis contributes to this almost uncharted aspect of the facial muscular system by using a new technique of surface EMG. The results described in this thesis support the understanding of the already discussed macro-anatomical organisation of facial muscles.

Physiological and biochemical properties

Aside from morphologic variability, motor units and muscle fibres vary in their physiolo-

gical (force, contractile speed and fatigability) and biochemical properties. This is related to contractile behaviour, mitochondrial oxidative function, anaerobic capacity and availability of substrates. In addition, isoforms for several key enzymes can be determined using molecular methods. On the basis of the various motor unit and muscle fibre properties, a number of classification schemes has appeared in the literature (see e.g. (Burke and Gandevia 2003; Enoka 1995; Monti et al. 2001) for reviews).

These classifications are largely derived from studies of lower limb muscles in animals.

It seems that muscle fibre properties are uniform among fibres from the same motor unit (e.g. (Nemeth et al. 1986)). Moreover, strong associations between the metabolic and physiological motor unit features (Table 1-1) as well as the order in which the motor units are recruited during graduated muscle contraction are present (e.g., (Henneman and Mendell 1981; Kernell 1992)). For instance,

Table 1-1. Physiological, structural and biochemical characteristics of the major histochemical fibre types. Adapted from Gray's Anatomy (Wigley 2008).

Characteristic	Fibre types		
	Type I	Type IIA	Type IIB
Phyiological			
Function	Sustained forces / posture	Powerful, fast movements	
Motor neurone firing threshold	Low	Intermediate	High
Motor unit size	Small	Large	Large
Firing pattern	Tonic, low-frequency	Phasic, high-frequency	
Maximum shortening velocity	Slow	Fast	Fast
Rate of relaxation	Slow	Fast	Fast
Resistance to fatigue	Fatigue-resistant	Fatigue-resistant	Fatigue-susceptible
Power output	Low	Intermediate	High
Structural			
Capillary density	High		Low
Mitochondrial volume	High	Intermediate	Low
Z-band	Broad	Narrow	Narrow
T and SR systems	Sparse		Extensive
Biochemical			
Myosin ATPase activity	Low		High
Oxidative metabolism	High	Intermediate	Low
Anaerobic glycolysis	Low	Intermediate	High
Calcium transport ATPase	Low		High

the earliest recruited motor units, i.e. the type S (slow) units consisting of type I muscle fibres, generate the smallest forces with a slow contraction speed and show the greatest resistance to fatigue. Conversely, the last recruited motor units, i.e. the type FF (fast, fatigable) units consisting of type IIB fibres, exert relatively high forces, but fatigue fast. The type FR (fast, fatigue-resistant) units consisting of type IIA muscle fibres have most properties in between type S and FF units.

Fibre type composition and properties of facial muscles were investigated in several histochemical studies (Freilinger et al. 1990; Goodmurphy and Ovalle 1999; Happak et al. 1988; Hwang et al. 2007b; Johnson et al. 1973; Stal et al. 1987, 1990). The results were largely concordant. In that investigation including the greatest number of facial muscles (Happak et al. 1988), three muscle groups were distinguished. The buccinator and the occipitofrontal muscles (the "tonic" group) showed a predominance of type I fibres (57 - 77%). The zygomaticus major, levator labii superioris, levator and depressor anguli oris muscles and the platysma (the intermediate group) had type I proportions between 27 – 38%. The orbicularis oculi was considered in this study to be the only "phasic" muscle, as indicated by the smallest proportion of type I fibres (15%). This finding agrees with the relatively short contraction times observed for the orbicularis oculi (McComas and Thomas 1968).

One investigation (Stal et al. 1987) reported exceptionally high type II fibre proportions (up to 89%) also for the zygomaticus major and minor muscles, which indicates that these muscles might have properties similar to the "phasic" orbicularis oculi. Moreover, it was observed in the latter study that a relatively large proportion of the type II fibres were of a special subtype (called type IIAB) with properties between type IIA and IIB fibres. Detailed examination of the orbicularis oris muscle indicated a relatively high concentration of type I fibres in the marginal part of the upper lip, although it has been shown that the whole muscle contains only ca. 30% of this slow fibre type (Freilinger et al. 1990; Hwang et al. 2007b; Stal et al. 1990). One of these studies (Freilinger et al. 1990) even found three to five muscle fibre bundles immediately adjacent to the lip edges purely consisting of type I fibres.

Facial muscles show relatively high resistance to fatigue (van Boxtel et al. 1983). The fact that they are even less fatigable than the masseter which predominantly consists of type I fibres suggests that fatique resistance in the facial muscles is not only related to muscle fibre type alone. It can be speculated that their insertion in the movable skin prevents static contractions and, consequently, development of high tension and obstruction of blood circulation within the muscle (Stal et al. 1987).

In total, it seems that the great variability of fibre composition and contraction time of facial motor units reflects the highly different functional requirements on this musculature, such as producing facial tonus and emotional expression, reflectory protection of the sense organs (i.e., phasic activity), performance of integrated synergism during speech and forceful activity during mastication (Freilinger et al. 1990; Stal et al. 1990; Stal et al. 1994).

Recruitment and activation

Muscle force can be increased by recruitment of previously silent units and by increasing the discharge frequencies of active units. Sequentially recruiting motor units occurs in a relatively fixed order. As described in the "size principle", the recruitment order is determined by motor neuron size (Henneman 1977) which means that smaller motor neurons are recruited first. Motor neurons with the lowest thresholds also exert the smallest maximum force (Fleshman et al. 1981). It is a realistic assumption that maximal recruitment of 50%

of the motor neurons results in only ca. 10% of the maximal force output of the muscle (Kernell 1992; Stuart and Enoka 1983). In most muscles, recruitment of additional motor units continues up to 80% of the muscle's force maximum and the remaining increase in force is achieved only by increase of discharge rates. Minimal tonic discharge rates of motor units of limb muscles usually range between 5 – 7 Hz (Macefield et al. 1993), but are higher for motor units of facial (Petajan 1981) and masticatory muscles (Phanachet et al. 2004). Maximum frequencies seem to vary between 20 and 41 Hz (Enoka 1995). Some motor units in human muscle appear even capable discharging at rates up to 100 Hz for a short burst of activity (Grimby and Hannerz 1977).

Data on firing behaviour and recruitment patterns of facial motor units is sparse. In an investigation of firing and contractile properties of human lower lip motor units during generation of constant forces of small to near maximal levels recruitment of motor units at all levels of force could be observed (Blair 1988). Moreover, the recruitment level and the interspike intervals appear in this study to be highly variable from trial to trial for each unit. Another investigation on firing rate interactions reported similar firing rate variability as other skeletal musculature and a tendency for orbicularis oris inferior motor units to synchronise (Kamen and De Luca 1992).

Graduated muscle contraction requires activation of only a selected subset of the motor neuron pool, i.e. the entity of motor neurons innervating a certain muscle. As mentioned before, the recruitment order of motor units depends on motor neuron size and, therefore, is relatively stable within a motor neuron pool. This strategy relieves higher centres of the responsibility to select the motor neurons that must be activated for a specific task (Enoka 1995). However, it seems that the selection of the motor unit subset is not fixed for each

motor neuron pool which means that it may vary for different tasks in which the muscle is involved (Glendinning and Enoka 1994; Theeuwen et al. 1994). The presence of such flexible control mechanisms is also assumed in the perioral musculature consisting of many interdigitating and overlapping muscles with a wide range of distinct, finely modulated movements to accomplish (Abbs et al. 1984; Wohlert 1996a).

Neuromuscular junctions

Within a muscle, motor nerves travel through the epimysial and perimysial septa before they enter the endomysial tissue around the muscle fibres. α-Motor axons branch repeatedly before they lose their myelinated sheaths and terminate in a narrow zone usually located towards the centre of the muscle belly and known as the endplate region or the motor point. Clinically, the latter term is defined as the location on a muscle from which it is easiest to elicit a contraction with stimulating electrodes. The terminal branch of an α-motor axon gives off several short branches each ending in an elliptical area, the motor endplate. At the endplate, the α-motor axon contacts a muscle fibre with a specialised synapse, the neuromuscular junction.

The dogma of classical motor unit anatomy and physiology describes normal adult mammalian skeletal muscles as consisting of fibres with a single motor endplate in the middle forming a narrow band (the "motor band") which crosses the muscle's central region (Aquilonius et al. 1984; Christensen 1959). Results obtained in recent years from histological and electrophysiological studies in different musculature challenge the general validity of this dogma. For instance, in the human laryngeal muscles, fibres with more than one endplate have been observed (Perie et al. 1997; Rossi 1990). Sophisticated electrophysiological techniques revealed a variety

of architectural organisations of motor units including the presence of single and multiple endplate zones in central and non-central locations even in long human limb muscles (Lateva and McGill 2001; Lateva et al. 2002, 2003).

Such differences from the "classical" motor unit structure are particularly present in human facial muscles. Histochemical studies showed that these muscles have myoneural junctions distributed in round or oval-shaped clusters over the muscle's region (Happak et al. 1997). Histological analysis revealed a small number of clusters which always corresponded with the number of innervating terminal motor nerve branches. However, exceptions in this respect were the orbicularis oris, orbicularis oculi, and buccinator muscles, in which motor endplates were found to be evenly spread over the whole muscle resulting in a great number of small motor zones. Another characteristic finding of these studies was a predominance of one motor endplate cluster (in some of the examined muscles), and eccentric positions of the motor endplates on the corresponding muscle fibre bundles. Due to the observed high inter-individual and inter-muscular variability of endplate cluster distribution, which has been considered to result from the great variability of facial nerve routing (Davis et al. 1956), the exact specifications of endplate cluster locations with regard to the position on the muscle have not been at present provided in the literature.

Neural control mechanisms

Facial muscles are supplied by the facial nerve. Corresponding lower α-motorneurons are located in the facial nucleus which resides in the ventrolateral region of the inferior pons (Crossman 2008). Histologically, the facial nucleus can be subdivided at least into four subnuclei named according to their medial, lateral, dorso-medial, and intermediate loca-

tions (Jenny and Saper 1987; Kuypers 1958). Their musculotopic organisation seems to be reflected in a column structure (Jenny and Saper 1987; Morecraft et al. 2001; Satoda et al. 1987; Welt and Abbs 1990). Neuroanatomic findings and correlates of patients with central lesions support the current view of the regulation of the motor neurons in the facial nucleus through a complex network of multiple interactive systems. These systems involve cortical and subcortical neural structures which reflect the voluntary, emotional and affective influencing of facial muscle activity (Morecraft et al. 2004).

Based on a long history of neuroanatomic studies in nonhuman primates, and observations following cortical stimulation, functional neuroimaging and localised surgical resection in humans, it is widely acknowledged that at least five, selectively interconnected cortical face representations are involved in facial motor control (Morecraft et al. 2004). They comprise areas of the primary motor cortex (M1), ventral lateral premotor cortex (LPMCv), supplementary motor cortex (M2), rostral cingulate motor cortex (M3), and caudal cingulate motor cortex (M4). Recent neuronal anterograde and retrograde tracing studies in the nonhuman primate provided more detailed information on the topographical associations between the cortical face representations and the musculotopically organised facial subnuclei. In general, all cortical face representations have been found to project to each facial subnucleus (Jenny and Saper 1987; Morecraft et al. 2001). However, the absolute density of these projections varies considerably. More specifically, the face representations of M1 and LPMCv were found to project primarily to the contralateral lateral facial subnucleus which innervates the (upper and lower) perioral musculature. Also M4 demonstrated projections that preferentially ended in the contralateral lateral subnucleus,

though these connections were relatively weak. Projections of M2 terminate bilaterally in the medial subnucleus which probably supplies the lateral portion of the frontal belly of the occipitofrontalis. The projections of M3 have been found to end bilaterally, mainly in the dorsal and intermediate subnuclei innervating the frontalis, corrugator supercili and orbicularis oculi muscles. Considering the lateral locations of M1 and LPMCv in the territory of the middle cerebral artery and the medial locations of M2, M3 and M4 in the territory of the anterior cerebral artery, these neuronal tracing studies provided also plausible explanations for clinical symptoms and recovery of facial muscle weakness following infarction.

With respect to the differentiation between voluntary and involuntary facial movements, the recent findings for the face representations of M3 and M4 were particularly significant. They are located in the cingulated cortex which receives strong input from the limbic system (Holstege 1991; Morecraft and Van Hoesen 1998). This suggests that they play an important role in involuntary facial muscle activity associated with social communication, emotions, attention, and decision making. Recently, a prominent amygdala projection to the face region of M3 has been identified (Morecraft et al. 2007) which supports this theory.

In addition to the described direct projections certain cells of the cortical facial motor areas project also indirectly to the facial nucleus ((Jenny and Saper 1987; Keizer and Kuypers 1989; Kuypers 1958). These pathways end on ipsi- or contralateral interneurons in the reticular formation, and many of these interneurons were found to project, according to their lateral or medial location, either ipsi- or contralaterally to the cranial motor nuclei including the facial nucleus (Holstege et al. 1977; Holstege 1991). It has to be noted that other subcortical and cortical structures such as the basal ganglia, thalamus, hypothalamus and trigeminal complex are likely to contribute as well to emotional and voluntary facial muscle activity (Holstege et al. 1977; Holstege 2002; Hopf et al. 1992; Morecraft et al. 2004; Root and Stephens 2003; Urban et al. 1998). However, the nature of many of these subcortical systems and their direct and indirect interconnections with the cortical facial representations are not yet completely understood.

Local circuitries in the brainstem are also relevant for the reflex responses of facial muscles, e.g. the blink reflex. Important reflex connections of the facial nucleus are established by ipsilateral afferents from the nucleus solitarius and from the trigeminal sensory nucleus (Crossman 2008). Excitatory reflex responses of facial muscles can be produced by electrical stimulation of trigeminal nerve branches or mechanical stimulation of the facial soft tissues (Ekbom et al. 1952; Gandiglio and Fra 1967a, b; Kugelberg 1952). The blink reflex can be elicited also by means of corneal, auditory and photic stimulation (Rushworth 1962). Single motor unit recordings from perioral muscles provided evidence for muscle-specific projections between the trigeminal sensory system and facial motoneurons (McClean and Smith 1982).

Clinical aspects

The essential functions of the facial musculature can be significantly affected by developmental disorders (such as cleft lip), localised cortical lesions (following infarction or trauma), neoplasia, peripheral facial palsy and a number of neurological diseases, e.g. facioscapulohumeral dystrophy, congenital facial diplegia (Möbius syndrome), myotonic dystrophy, and oculopharyngeal muscular dystrophy. Focal dystonia of the embouchure in woodwind or brass instrumentalists is a

task-specific dysfunction characterised by loss of control of lip vibration and air flow into the mouthpiece (Frucht et al. 2001; Frucht 2009). Dysfunctions of the facial muscles may also produce tooth malposition, because the orofacial musculature represents the functional matrix for the maxillary and mandibular bones and dentoalveolar complex (Moss 1997).

Electromyography is the preferred technique for studying muscle function. Clinical neurology uses mainly needle EMG for examining single motor unit properties. Surface EMG, which provides a more global view of a muscle's activity, has proven to be a valuable research and diagnostic tool. Facial applications of this tool concern e.g. the fields of psychophysiology, speech physiology, and dentistry. Beside EMG examinations, some diseases and clinical pictures require visual examination of facial muscle functions. For instance, facial weakness deserves thorough evaluation and periodic reassessment, which has to include both visual functional analysis and scrutinising the patient's face for tone and asymmetry (mainly by comparing the two sides of the face).

2

Visual examination of facial muscle contractions

Introduction

The wide range of defects associated with facial nerve injury (May and Barnes 2000), as well as the difficulties in identifying the contribution of individual subcomponents to certain functions or deficits (e.g. for purposes of diagnosis, recording and reporting) demand comprehensive basic knowledge on how activation of the minimal functional units moves the facial soft tissues and changes facial appearance. Otherwise, diagnosis might be misleading and, consequently, the therapeutic interventions incorrect. It has to be noted that illustrative and descriptive material about selective facial muscle contractions and their effects on the facial soft tissues is only sparsely available in the literature. An exception is the so-called facial acting coding system (FACS) specially developed for diagnosis and research in neuropsychology (Ekman and Friesen 1977; Ekman et al. 2002).

This chapter includes photographs from selective contractions of all periorbital and perioral facial muscle subcomponents and describes the corresponding facial poses and the relevant anatomical and functional background in detail. Epicranial and nasal muscles are not considered, because they are of minor functional and clinical significance. For those contractions which are difficult to perform we describe typical co-activation patterns and mention possibilities to identify and avoid co-activation.

Contractions of individual facial muscles and corresponding facial poses

Selective contractions of individual facial muscles can best be characterised by describing the corresponding changes in positions of facial landmarks, and/or the changes in location of shadows and lines in the face relative to the facial appearance at rest.

Periorbital and palpebral muscles

Poses of the actions of these subgroup of muscles are illustrated in Fig. 2-1. Functions of these muscles concern (1) reduction or increase of the amount of light entering the eye by piling up the facial skin in the circumorbital area (m. orbicularis oculi pars orbitalis, OOC orb; m. corrugator supercili, CSC) or elevating the upper eyelid (m. levator palpebrae superioris, LPS), (2) gentle eyelid closure as part of the blink reflex or voluntarily (m. orbicularis oculi pars palpebralis, OOC pal), (3) voluntary maximal eye closure (all three portions of the m. orbicularis oculi, OOC), and (4) control of lacrimal flow (m.orbicularis oculi pars lacrimalis, OOC lac).

M. levator palpebrae superioris (LPS)

This muscle is innervated by the n. oculomotorius. It is the antagonist for the depressor action of the superior palpebral part of the OOC, i.e. it raises the upper lid (Fig. 2-1B).

M. corrugator supercili (CSC)

The fibres of the corrugator supercili muscle have their origin on the bone at the medial end of the superciliary arch and pass laterally and slightly upwards to insert in the skin and muscle tissue above the middle of the supraorbital margin.

The muscle draws (in cooperation with the OOC) the eyebrow medially and downwards and produces vertical furrows on the bridge of the nose and forehead as well as a hollow superior to the eyebrow's medial portion (Fig. 2-1C). Co-contraction of the OOC orb can be often observed during attempted isolated contraction of the CSC.

M. orbicularis oculi (OOC)

The OOC is a flat elliptical muscle which surrounds the circumference of the orbit and

Figure 2-1. (A) Face at rest and (B-F) facial poses corresponding to isolated contractions of the periorbital and palpebral muscles. These include the mm. levator palpebrae superioris (LPS), corrugator supercili (CSC), orbicularis oculi pars palpebralis (OOC pal), orbicularis oculi pars orbitalis (OOC orb), and all portions of the orbicularis oculi together (OOC). (G) Assignment of muscles and corresponding poses.

spreads into the eyelids and surrounding skin areas. Orbital, palpebral and lacrimal parts can be distinguished. The orbital part (OOC orb) arises from the bone near the medial angle of the orbit. Its upper and lower fibres are broadly arranged in an elliptical pattern, interdigitate into the lateral palpebral raphe (where there is no bony attachment) and blend with fibres from adjacent muscles. The palpebral part (OOC pal) arises mainly from the medial palpebral ligament, sweeps across the eyelids and interlaces at the lateral commissure. The lacrimal part (OOC lac) controls the tear flow and can be regarded as the deep, small subcomponent of the OOC pal.

Orbital and palpebral (inclusive lacrimal) parts of the OOC can be differentially contracted. Contraction of the OOC pal gently closes the lid (Fig. 2-1D), as in sleep or blink reflex. Activation of the OOC orb partially closes the eyelid (mainly by raising the lower lid) and draws the skin of the temple, forehead and infraorbital area, together with the upper and lower lids medially. As a consequence, the skin is thrown into folds that radiate from the lateral angle of the eyelid (Fig. 2-1E). Contraction of all OOC portions together deepens these folds and results in firm eye closure (Fig. 2-1F).

Perioral muscles

In functional respect, the three-dimensional assembly of muscles that control the shape of the buccal orifice can be divided into three groups:

- Retractors of the upper lip: mm. levator labii superioris alaeque nasi (LLS an), levator labii superioris (LLS), zygomaticus minor (ZYG min). Due to their common function, these three muscles can be considered as one group (Nairn 1975). Other authors have classified them as the three heads belonging to the M. quadratus labii superioris.

- Muscles that converge towards to the corners of the mouth: mm. levator anguli oris (LAO), zygomaticus major (ZYG maj), buccinator (BUC), depressor anguli oris (DAO), incisivus labii superioris et inferioris (INC), and orbicularis oris superior et inferior (OOR). This group of muscles is concerned with the closure and sealing of the oral commissure, with the development of pressure by the lips and cheeks, and two-dimensional displacement of the "modiolus" (the modiolus is a muscular-tendinous node lying just lateral to the corners of the mouth).

- Retractor and elevator of the lower lip: m. depressor labii inferioris (DLI) and mentalis (MEN).

Many activities of the perioral muscles take place in three phases (Salmons 1995). First, a particular modiolar muscle group becomes dominant over its antagonists and the modiolus is rapidly relocated. Then the modiolus is fixed in this new site by simultaneous contraction of other muscles radiating from the modiolus. Acting from this fixed position, the main physiological effectors, the BUC and OOR (which can be principally regarded as a horizontal, continuous muscular sheet drawn right across the lower face) perform their specific function.

Poses corresponding to the contractions of the midfacial and lower facial muscles are illustrated in Fig. 2-2 and Fig. 2-5, respectively. Contractions of distinct fibre groups of the m. orbicularis oris are shown in a frontal (Fig. 2-3) and lateral view (Fig. 2-4).

M. levator labii superioris alaeque nasi (LLS an), m. levator labii superioris (LLS), m. zygomaticus minor (ZYG min)

This group of three muscles arises from the upper part of the frontal process of the maxilla (LLS an), the inferior orbital margin above the infraorbital foramen (LLS) and the lateral

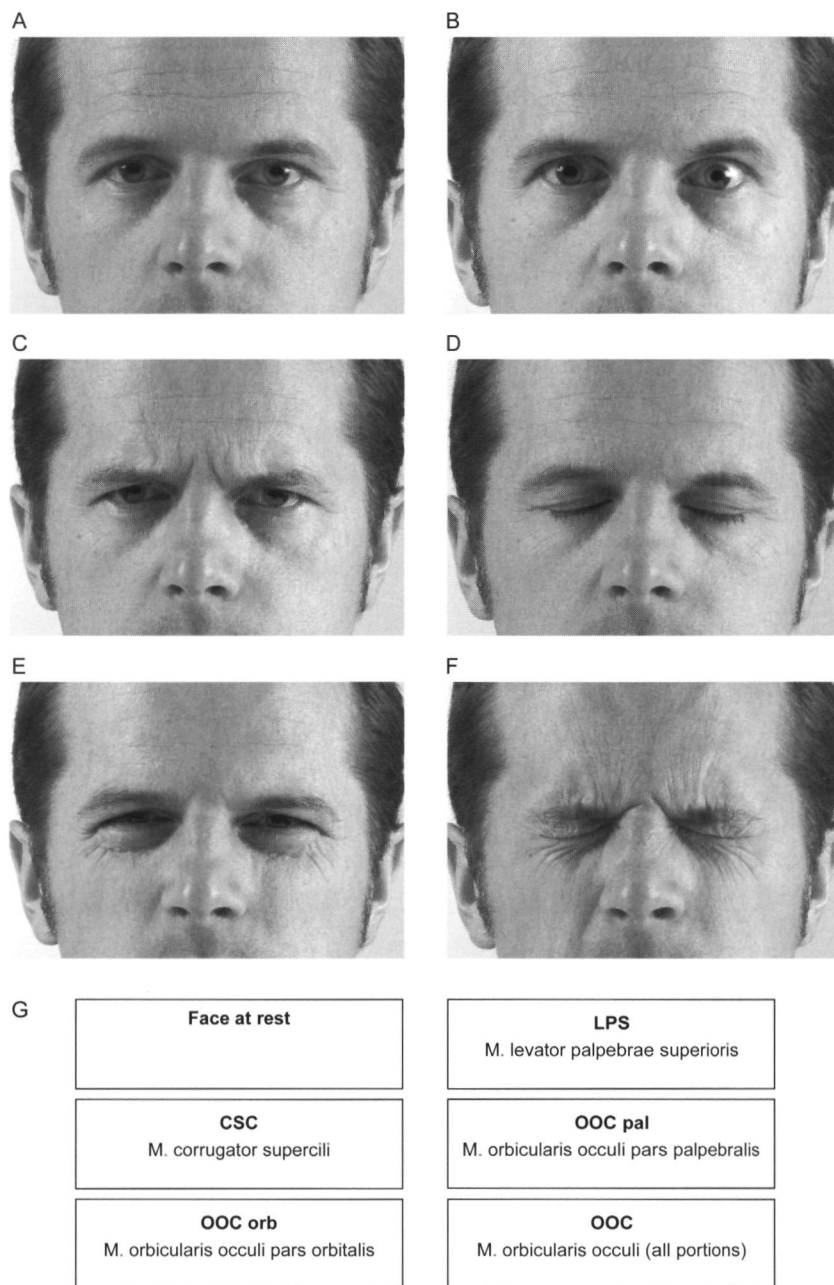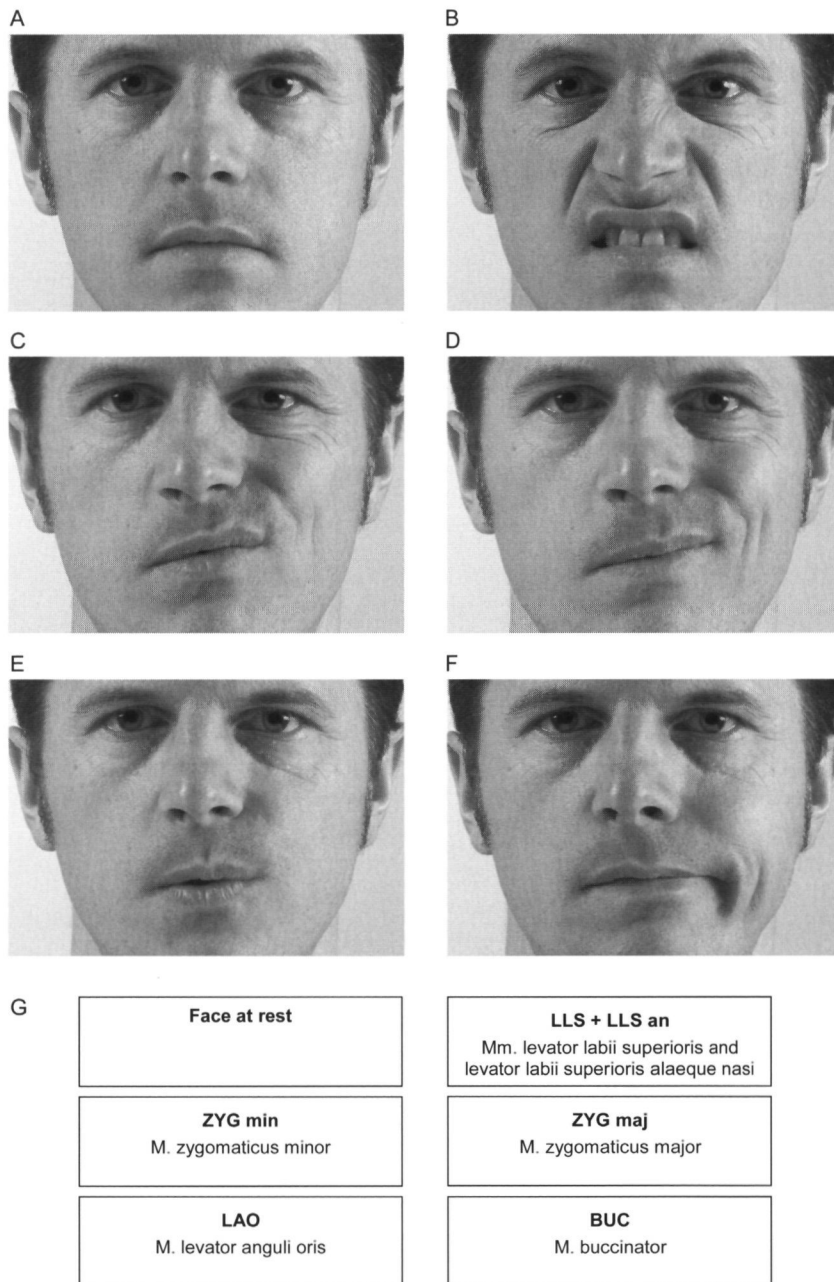**Figure 2-2.** (A) Face at rest and (B-F) facial poses corresponding to isolated contractions of the midfacial muscles. These include the mm. levator labii superioris and levator labii superioris alaeque nasi (LLS + LLS an), zygomaticus minor (ZYG min), zygomaticus major (ZYG maj), levator anguli oris (LAO) and buccinator (BUC). (G) Assignment of muscles and corresponding poses.

surface of the zygomatical bone (ZYG min). Their fibres pass downwards and blend, before they converge into the muscular substance of the upper lip.

Their common action raises and everts the upper lip and elevates the side of the nose. As a result, the upper lip adopts a rectangular shape and the upper frontal teeth become visible. In addition, the nasolabial fold as well as the inferior tarsal furrow (running inferior to the lower lid) deepen and delimit the infraorbital cheek. Horizontal wrinkles may also arise in the upper portion of the nose. Isolated activation of the LLS elevates and everts mainly the middle portion of the corresponding upper lip quadrant (i.e. uncovers only the incisor teeth) and straightens the nasolabial fold in superior direction (Fig. 2-2B), while contraction of the ZYG min elevates and everts only the lateral portion of the upper lip and keeps the convex curvature of the nasolabial furrow (Fig. 2-2C). However, such selective activations of single subcomponents of this muscle group are, even in trained individuals, relatively difficult.

Contraction of these muscles shows usually co-activation of the OOR, which can be observed by absent separation of the upper and lower lips. Moreover, activation of the LLS is often accompanied by co-activation of the m. procerus. Such co-activation can be palpated by placing a finger superior to the nasal bone.

M. zygomaticus major (ZYG maj)

This muscle originates from the zygomatic bone just anterior to the zygomaticotemporal suture and runs in medio-inferior direction to the modiolus where it blends with fibres from other muscles.

The ZYG maj elevates the corners of the mouth in lateral direction (Fig. 2-2D). In some individuals, the lower portion of the upper incisors and the canine, and in some cases also the buccal teeth of the corresponding side become visible. Contraction of the ZYG maj may modify the lateral portion of the nasolabial fold and also creates vertical, arched wrinkles on the cheek, which are – compared to those emerging during ZYG min contraction – more pronounced. The changes in facial appearance induced by activation of the ZYG maj are characteristic for smiling.

Contractions of adjacent facial muscles results in similar changes in facial appearance. Isolated ZYG maj contraction can be recognised by missing evertion of the upper lip's lateral portion (which is performed by the ZYG min) or absence of a dimple lateral to the corner of the mouth (caused by activation of the BUC).

M. levator anguli oris (LAO)

This relatively deeply located muscle arises from the fossa canina on the anterior surface of the maxilla just below the infra-orbital foramen. Running in latero-inferior direction, its fibres enter the modiolus.

Contraction of the LAO results in barely visible changes in facial appearance. The corner of the mouth is slightly elevated and displaced in medial direction (Fig. 2-2E). In addition, the lateral portion of the upper lip is compressed and bulges in a characteristic manner. Observation of these changes is facilitated by unilateral contraction and comparison to the non-contracted facial side.

With regard to isolated contraction, the LAO is one of the most difficult facial muscles. If not possible, one can first train to press the corners of the mouth against the teeth (thereby keeping the OOR and BUC relaxed), which corresponds to a combined contraction of the LAO and DAO. From this pose, one can attempt to relax the DAO while LAO activation is continued. Contraction of the LAO can easily be verified by palpation of the upper portion of the muscle in the region of the fossa canina (i.e. lateral and inferior to the nostril).

2

M. buccinator (BUC)

The origin of three bundles of fibres can be identified: small upper and lower groups are attached to the alveolar process of the maxilla and mandible, respectively (opposite the molar teeth); a large flat middle group arise from the pterygomandibular raphe which separates the muscle from the m. constrictor pharyngis. Thus this muscle is very deeply placed internal to the ascending portion of the mandible. The main part of BUC fibres converges towards the modiolus. The deep, that is, oral fibres from all three parts are attached to the mucous membrane of the cheeks which can be regarded as a site of insertion for these fibres.

Action of this muscle compresses the cheeks against the teeth and gums. When the cheeks have been distended with air, BUC contraction expels the air between the lips. The latter accounts for the name: "buccinator" (Latin) means "trumpeter". The change in facial contour characteristic for activation of the BUC is the dimple slightly lateral to the corner of the mouth resulting from traction on the deep portion of the modiolus and the submucosa in this area (Fig. 2-2F). This dimple is absent if the corner of the mouth is drawn laterally (only) by the ZYG maj. The facial appearance corresponding to contraction of the BUC expresses an "artificial smile".

M. orbicularis oris superior et inferior (OOR)

This muscle is actually a complex of muscles and, similar to the OOC, not a real sphincter. It consists of four substantially independent quadrants (upper, lower, left and right) each of which contains a peripheral part and a marginal part. Both parts are attached to the modiolus, continue towards the facial midline, and cross some millimetres into the contralateral segments. The peripheral parts of the upper and lower orbicularis oris muscles (OOR per) reach the nasal septum and

mentolabial fold, respectively, and lie close to and parallel with the inner mucosal surface of the lip. The marginal part (OOR mar) of each quadrant occupies the core of the red lip, and is therefore also curling outward. Moreover, the complex structure of the lip musculature includes also non-horizontal (i.e. tangential) fibres (OOR tan) that pass between the horizontal bundles to their submucosal attachments. They originate either outside the lips (these fibres are called extrinsic vertical orbicularis oris fibres, and probably belong to the retractors of the upper and lower lips (Blair 1986) or attach to the hairy skin of the lips (called intrinsic tangential orbicularis oris fibres (Blair 1986) or M. rectus (Braus and Elze 1954) and run (mainly in sagittal direction) diagonally through the vermilion part of the lips from the hairy epidermis adjacent to the outer vermilion border towards the inner part of the vermilion.

Lip movements (Fig. 2-3 and Fig. 2-4) are, in accordance with the complex muscular configuration, relatively complicated. In most movements, activity of the OOR is superimposed by activity of the direct labial tractors (i.e. the LLS and DLI) and muscles that insert into the modiolus. The resultant actions range from delicate adjustments of the tension and profile of the lip margins to large increases of the oral fissure with eversion of the lips and modiolar displacements (Salmons 1995) (Fig. 2-3B). Complicated lip movements with involvement of several perioral muscles are not considered in more detail here, but only isolated actions of the distinct intrinsic OOR fibre groups.

Isolated contraction of the OOR tan transforms the bulbous cross-sectional profiles of the lips into a narrower, wedge-shaped profile, called the "labial cord" (which is important e.g. in playing of brass instruments). Simultaneously, the flattened marginal parts of the upper and lower lips tilt slightly forward
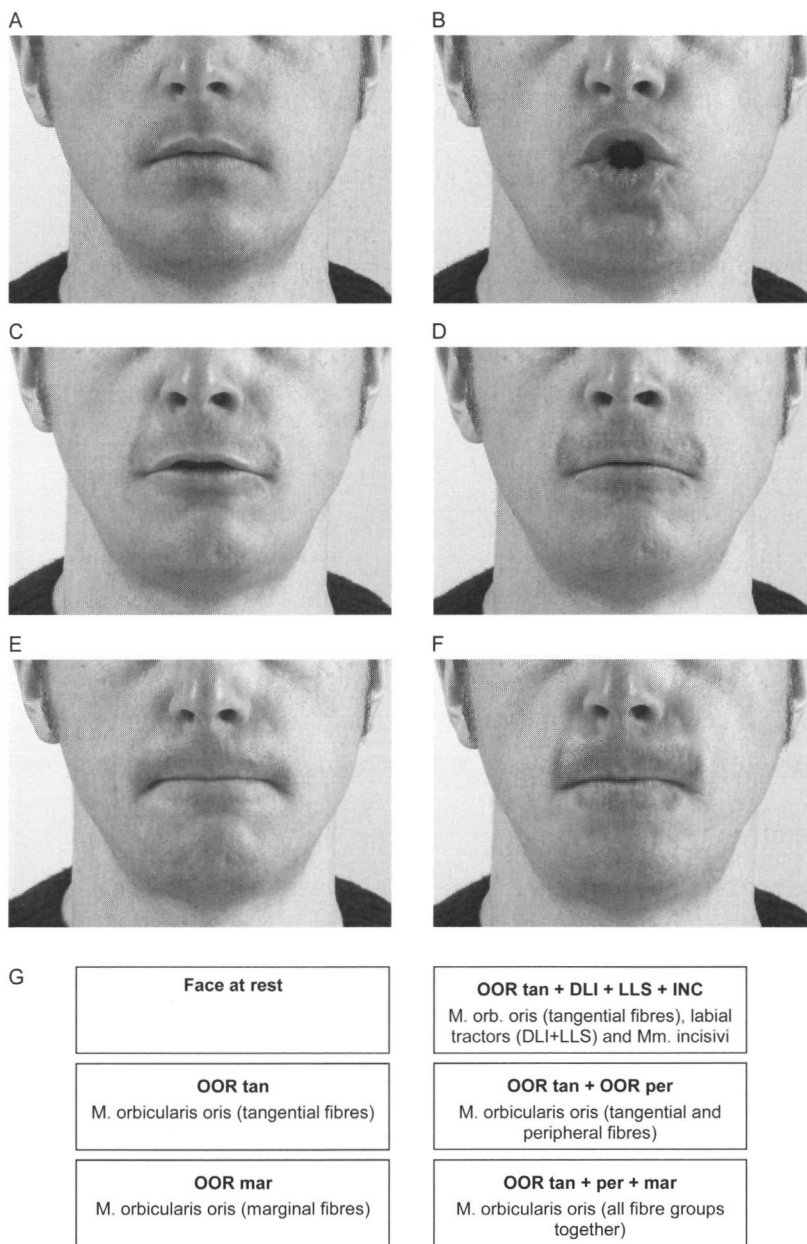
Figure 2-3. (A) Frontal view of the face at rest and (B-F) lip poses corresponding to isolated contractions of the distinct m. orbicularis oris (OOR) fibre groups. Differential contractions of the tangential fibres of the OOR including the mm. incisivi and the direct labial tractors Mm. levator labii superioris and depressor labii inferioris (OOR tan + DLI + LLS + INC), of the tangential orbicularis oris fibres alone (OOR tan), of the tangential and peripheral fibres (OOR tan + OOR per), of the marginal orbicularis oris fibres alone (OOR mar), and of all intrinsic orbicularis oris fibres together (OOR) are shown. (G) Assignment of muscles and corresponding poses.

and the part of the hairy skin (right next to the red-lip) in that the tangential fibres attach separates from the adjacent peripheral lip portion (Fig. 2-3C and Fig. 2-4B). Starting from this lip posture, the OOR per can tilt the marginal lip portions partly back (Fig. 2-3D and Fig. 2-4C). Contraction of only the OOR mar presses the upper and lower red lips toward each other (i.e. produces lip closure) and also narrows the red-lips, because the S-shape of the labial curl flattens out to a certain extent (Fig. 2-3E). The peripheral lip portion remains relaxed. If, in advance, the labial cord is formed by the OOR tan, contraction of the OOR mar results in tightening and retraction of the labial cord, i.e. hermetic lip closure. A contrary opinion in the literature – which does not agree with our experience – is that the labial cord is mainly formed and not only tightened and retracted by contraction of the OOR mar. Contractions of all OOR fibre groups together (OOR tan + per + mar) produces a high tonus in the whole labial area (as e.g. required in brass instrument playing), inverts the red-lips, and presses the lips towards each other and against the frontal teeth (Fig. 2-3F and Fig. 2-4D). To summarise: the main function of the intrinsic, tangential OOR fascicles (OOR tan) is to tilt the marginal lip portion forward and to produce the labial cord; peripheral (OOR per) and marginal fibres (OOR mar) tilt the peripheral and marginal lip portions, respectively, back and press them towards each other (i.e. act in the manner of a "sphincter"), simultaneously sealing the lips.

Attempted selective contraction of the OOR is often accompanied with co-activation of other muscles inserting into the modiolus. The latter can be verified by palpating the tension lateral to the corners of the mouth (which should be absent during contraction of only the OOR). Isolated contractions of the OOR tan is relatively difficult (if they have not been trained specially), but possible.

A common finding is co-contraction of the m. dilatator naris, i.e. widening of the nasal aperture. Especially in isolated contraction of this OOR portion, attention has to be paid to the fact that the corners of the mouth keep their resting position and tonus, i.e. they may not protrude or move against each other. A method to obtain the ability of selective activation of the OOR tan bases on the fact that this part of the OOR usually co-contract when the contracted DLI fatigues (Burba 1994).

Mm. incisivus labii superioris et inferioris (INC)

The four INC are considered to be accessory muscles of the oral orbicular complex. They have bony origins near the apices of the lateral incisors teeth. In their course towards the modiolus, the fibres of these muscles intermingle with and become part of the horizontal fibres of the OOR.

Simultaneous action of the four INC (Fig. 2-5B) moves the corners of the mouth against each other and rounds the marginal lip portion (as e.g. in whistling). Differential action of the four INC allows them to change the orientation of the lip line.

M. depressor labii inferioris (DLI)

This muscle arises from the lower border of the mandible and passes upwards and medially into the skin, muscular tissue and mucosa of the lower lip. Some authors classify the lateral fibres as belonging to the platysma (pars labialis). Near the insertion, the DLI crosses the facial midline and blends with the paired muscle from the opposite side and with fibres of the OOR.

Activity of the DLI uncovers the lower incisor teeth and flattens the mental soft tissue by stretching the chin downwards and laterally. Often, the medial boundary of the DAO (i.e. the mentolabial fold) emerges because of the superficial location of the latter muscle on

A   B   C   D

2

Face at rest	**OOR tan** M. orbicularis oris (tangential fibres)	**OOR tan+per** M. orbicularis oris (tangent. + periph.)	**OOR tan+per+mar** M. orbicularis oris (all fibre groups)
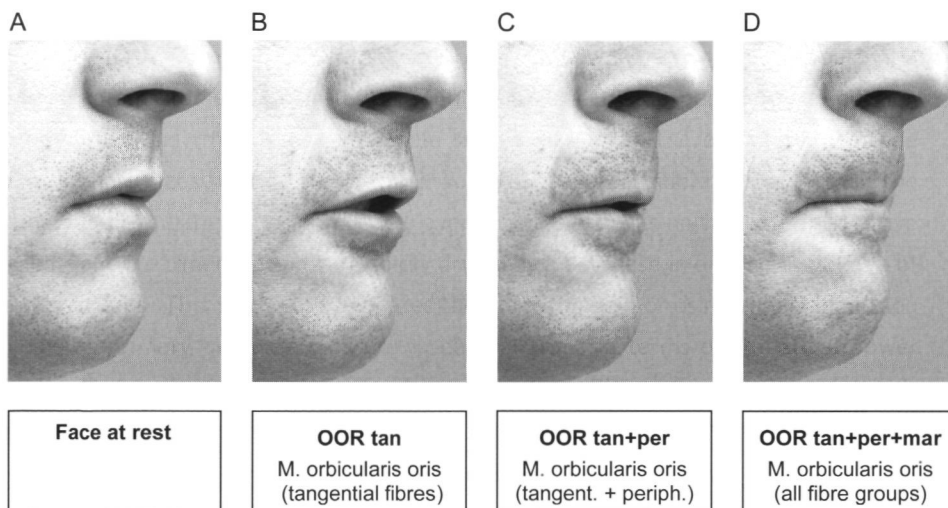
Figure 2-4. (A) Lateral view on a face at rest and (B-D) on lip poses corresponding to isolated contractions of the distinct fibre groups of the OOR. Contractions of the tangential orbicularis oris fibres (OOR tan), of the tangential and peripheral fibres (OOR tan + per), and of all intrinsic orbicularis oris fibres together (OOR) are shown. Note how the peripheral lip portions are tilted foreward (OOR tan) and backward (OOR tan + per), and how additional contraction of the marginal fibres (OOR tan + per + mar) tightens and retracts the labial cord.

the lateral and inferior portion of the DLI. Bilateral contraction of the medial portion of the DLI (DLI med) depresses mainly the middle portion of the lower lip (Fig. 2-5C). Contraction of the muscle's lateral portion (DLI lat) or the platysma pars labialis, respectively, draws the lateral portion of the lower lip downwards and laterally and simultaneously everts this part of the lower lip (Fig. 2-5D). In contrast to the isolated contraction of the DLI med, the lower lip thereby adopts the shape of a flattened "V" (and not those of a regular curve).

M. depressor anguli oris (DAO)

This muscle has a long, linear origin extending from the mental tubercle in an oblique line (along the base of the mandible) to the area of the lower first molar. Its fibres converge in superior direction before they insert into the modiolus, or (only some fibre bundles) into the skin of the upper lip's lateral portion. The characteristic triangular shape of the DAO reflects the synonym m. triangularis. In some anatomical textbooks, the latter name (m. triangularis) also includes the mm. transverses menti and risorius. The latter two highly variable muscles lie medially and laterally to the DAO, respectively, and are functionally of minor importance.

The DAO draws the corners of the mouth downwards and laterally. This action bulks the lower cheek (resulting in deep, arched skin furrows inferior and lateral to the modiolus) and straightens the upper lip in inferio-lateral direction (Fig. 2-5E). The corresponding facial appearance expresses sadness. The posture of the lower lip remains almost unchanged.

Attempted isolated contraction of the DAO is most often accompanied with co-contraction of the MEN.
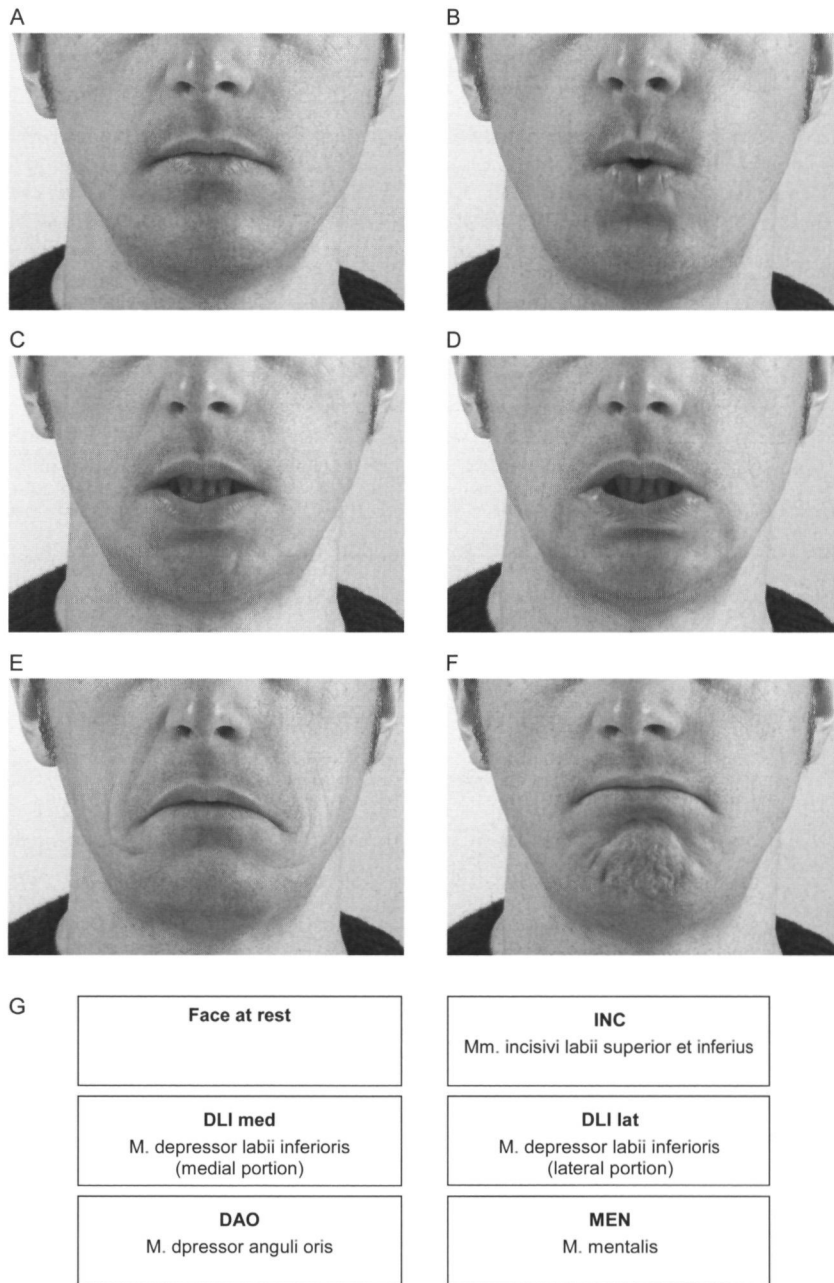
Figure 2-5. (A) Face at rest and (B-F) facial poses corresponding to isolated contractions of the lower facial muscles. These include the Mm. incisivius labii superioris et inferioris (INC), depressor labii inferioris pars medialis (DLI med) and lateralis (DLI lat), depressor anguli oris (DAO), and mentalis (MEN). (G) Assignment of muscles and corresponding poses.

M. mentalis (MEN)

The fibres of this conical muscle arise from the mandible inferior to the lower lateral incisor roots and descend in medial direction to attach to the dermis in the area of the chin. Medial fibres of the paired MEN intermingle, creating a muscular sling.

The MEN sling raises the whole mental soft tissues, separates the lateral and inferior boundary of the latter and produces the characteristic fine dimples and wrinkles on the chin (Fig. 2-5F), which may even be present in a relaxed face (as sign of an increased resting tonus of the MEN). As result of the shortening of the MEN sling, the lower lip is also pushed up. Moreover, in relaxed and closed lip position, both lips elevate and protrude in their middle part.

Attempted isolated MEN is often accompanied by co-activation of the DAO (which can be palpated).

Conclusions

Knowledge on how isolated facial muscle contractions change facial appearance is clinically relevant, e.g. for localising facial weaknesses or identifying the contributions of individual muscle subcomponents to certain orofacial dysfunctions. Difficulties in the examination of such deficits are mainly related to the complexity and special anatomical features of the facial muscle system. The only way for the clinician to face these difficulties, as well as to reduce the risk of misleading diagnoses and incorrect treatment, is to acquire corresponding anatomical background knowledge, and to learn and experience how isolated contractions of facial muscle subcomponents change facial contours and appearance. Especially in the latter respect, this chapter should complement the sparse descriptive and illustrative material available up to now.

2

3

EXAMINATION OF FACIAL MUSCLE FUNCTION USING BIPOLAR SURFACE EMG ELECTRODES

With previous surface electromyography (sEMG) electrodes it has been difficult to combine small outer dimensions and secure skin attachment. We resolved this problem by developing a new skin attachment technique that yields firm electrode fixation without requiring an acrylic housing. Consequently, we could reduce the outer electrode dimensions to 4-mm diameter and only 1.5-mm thickness. In a bipolar montage, this electrode allows an inter-electrode distance of 8 mm. This improves measurement selectivity and, because of the small dimensions, makes possible the non-invasive observation of multiple facial muscles with a minimum of obstruction. Our new technique was tested on a group of 11 professional trumpeters. They were instructed to perform a series of muscle-specific facial poses and to play exercises on their instruments while EMG signals were recorded simultaneously from seven different perioral muscles. Although the skin attachment was subjected to high stress during trumpet playing, more than 98% of electrode placements yielded a secure mechanical and electrical connection. Muscle selectivity of the signals recorded during the facial poses was similar to that obtained in a previous investigation using intra-muscular fine-wire electrodes. Cross-talk in the perioral area was estimated to be lower than 25%. The availability of an unobstructive sEMG electrode for simultaneously observing multiple facial muscles opens up a wide range of applications (e.g. in speech research, psychophysiology and orthodontics).

3

Introduction

Several methodological aspects of facial EMG are involved when considering the unique anatomy of facial musculature (Fridlund and Cacioppo 1986). Firstly, the high inter- and intra-individual variability in location and morphology of the individual muscles, as well as in the overlying soft-tissue (Braus and Elze 1954; Kennedy and Abbs 1979; Salmons 1995; Sato 1968), place serious limits on standardising the electrode positions (Fridlund and Cacioppo 1986; Kennedy and Abbs 1979; O'Dwyer et al. 1981; Tassinary et al. 1989). Secondly, electrodes suitable for facial sEMG must allow a very firm and secure skin attachment, because the facial muscles insert in the facial skin, resulting in skin distortions during their activities (Cole et al. 1983). Saliva also increases the risk of attachment loss. Further important aspects concern the electrode's outer dimensions. The simultaneous observation of multiple muscles in relatively small

areas is only possible when the electrodes do not occupy too much space. Moreover, the close proximity of the (mostly simultaneously active) muscles results in the need to suppress cross-talk. In a bipolar electrode montage (in most applications bipolar electrodes are preferred), cross-talk not only depends on the distance between the electrode pair and the adjacent muscle(s), but also on the inter-electrode distance (IED, defined as centre-to-centre distance between the two single electrodes). This is due to the close relation between IED value and uptake volume; the smaller the IED value, the smaller this volume and, consequently, the higher the measurement's selectivity (Andreassen and Rosenfalck 1981; Basmajian and De Luca 1985; De Luca and Knaflitz 1992). Cross-talk is adequately suppressed with IED values less than 10 mm (Loeb and Gans 1986). Another important rationale for using small electrodes has to do with methodological bias. Bulky (large and/or thick) electrodes can hinder facial movements

(e.g. the highly dynamic lip movements during speech) or they can alter subjects' behaviour in the study of emotional and cognitive processes (Fridlund and Cacioppo 1986).

In practice it has proven difficult to combine simple and firm skin attachment with small outer dimensions in one electrode. To ensure a simple and firm attachment, cup electrodes are commonly used in facial sEMG. This electrode type consists of a detection body recessed into an acrylic housing. However, although the housing simplifies the attachment procedure (by permitting the bonding of a double adhesive collar at its rim), it also significantly increases electrode's dimensions and mass, leading to the disadvantages previously mentioned.

The aims of this research project were (1) to combine small size and secure skin attachment in one electrode, (2) to test the new technique in practice, (3) to make sEMG recordings during a series of discrete facial actions (selected to activate only one of the examined muscles), and to evaluate these recordings with regard to signal selectivity and cross-talk, and (4) to quantitatively compare our results with those obtained in a previous

investigation using intra-muscular fine-wire electrodes (O'Dwyer et al. 1981).

Methods and Materials

Design and construction of electrode and double-sided tape for skin attachment

We used a sintermetallic Ag/AgCl disk (Zentner, Freiburg, Germany) of 4 mm diameter and 0.5 mm thickness (Fig. 3-1A and Fig. 3-1B). This material provides several desirable features concerning bioelectrical characteristics and maintenance (Cooper et al. 1980; Fridlund and Cacioppo 1986; Geddes 1972; Janz and Taniguchi 1953; Tassinary et al. 1990). This disk was connected to a 1 mm thick pure-silver lead by means of conducting silver bonding (H 20 E – PFC, Polytec GmbH, Waldbronn, Germany). For skin attachment of pairs of these electrodes, double-sided adhesive medical tape (thickness 0.1 mm, GS Stanztechnik, Villingen, Germany) was cut into pieces of 10 x 20 mm. In each of these pieces, two holes with a diameter of 4.5 mm were punched at a distance of 8 mm (centre-to-centre), predetermining the position of the two electrodes. The distance between the two
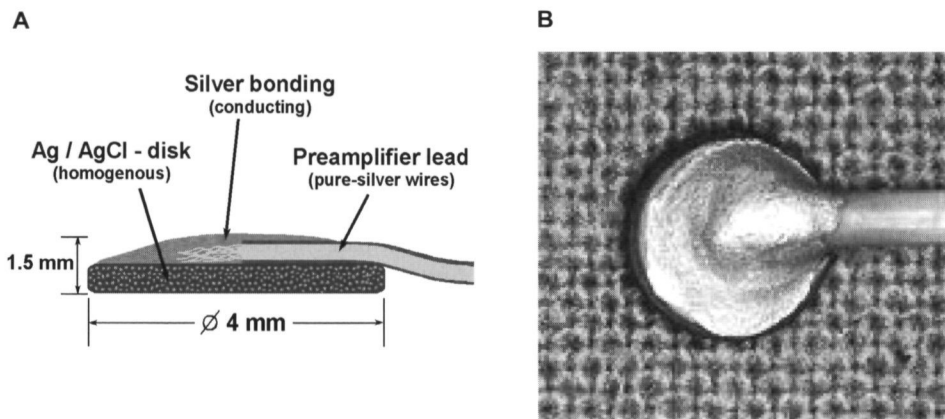
Figure 3-1. Miniature surface electrode specially designed for facial EMG. (A) Detection body consists of sintermetallic silver-silverchloride (Ag/AgCl) connected with a pure-silver lead by means of silver conduction bonding. (B) The electrode has an outer diameter of 4 mm and is only 1.5 mm thick. Photography of the electrode.

holes was obtained accurately with a specially manufactured double hole puncher.

Skin attachment of bipolar electrodes

The bipolar electrodes were attached to the skin as follows (Fig. 3-2). After shaving the skin in the corresponding area (if necessary) and cleansing it with an alcohol-wetted swab, we fixed the prefabricated double-sided adhesive tape in the correct position. Only in the areas of the two punched holes, we then treated the skin to reduce skin-electrode impedance. This procedure included a slight skin abrasion using a sandpaper pen (Fig. 3-2A) and the application of conducting cream (Electrodencreme®, Marquette-Hellige, Freiburg, Germany; Fig. 3-2B). In order to keep the double-sided tape's outer bonding surface free from cream, we did not remove the outer barrier foil until the cream had been applied. The two electrodes were then pre-fixed using thin plasters (Fixomull Stretch®, Beiersdorf, Hamburg, Germany; Fig. 3-2C). Finally, we bonded a piece of 15 x 25 mm of the same plaster material over the entire area of the electrode pair and firmly attached it around the electrode borders (Fig. 3-2D). Additional fixations were made at the cables to avoid attachment loss due to draughts (although these were not absolutely necessary, because the cables were held secure by the electrode-covering plaster).

Subjects tested and muscles observed

This new technique was tested on a group of 11 professional trumpeters (males n=9, females n=2) all of whom provided informed consent. Their mean age was 27.2 (24 - 32) years. The participants had no known neurological or general health disorders. Seven different perioral muscles (or muscle groups, respectively) were observed on the right side of the face (Fig. 3-3B); namely, the orbicularis oris superior (OOS) muscle, the orbicularis oris inferior (OOI) muscle, the depressor
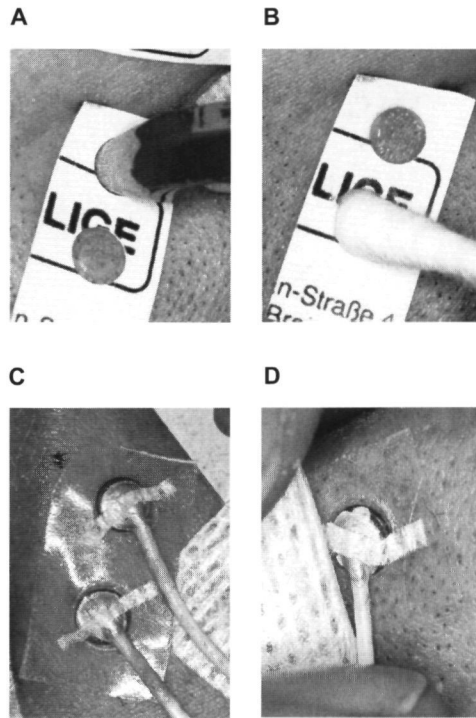
Figure 3-2. Skin attachment technique of our new sEMG electrode (in a bipolar montage). After a double adhesive collar was fixed, we preconditioned the skin in the area of the two punched holes; a slight abrasion with a sandpaper pen (A) was followed by application of electrode cream (B). After the double adhesive collar's outer barrier foil was removed, the two single electrodes were pre-fixed with help of tiny plasters (C). Finally, the electrode pair was securely fixed by means of a tightly drawn elastic plaster firmly attached at the electrode borders and the cables (D).

labii inferioris (DLI) muscle, the mentalis (MEN) muscle, the depressor anguli oris (DAO) muscle, the zygomaticus major (ZYG) muscle, and the levator labii superioris (LLS) muscle group (consisting of the levator labii superioris, the levator labii superioris alaeque nasi and the zygomaticus minor muscles). We examined the OOS and OOI muscles bilaterally, so that there was a total of nine bipolar electrodes attached to each subject (Fig. 3-3A).
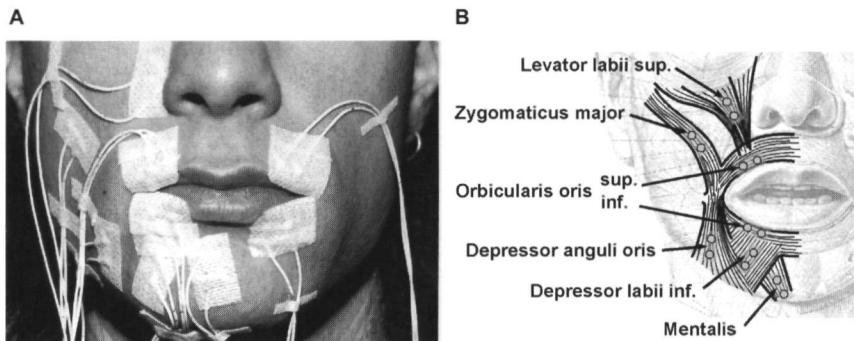
Figure 3-3. Attached bipolar electrodes and selected perioral muscles. Seven different perioral muscles on the right side of face were selected for the test. Observation of the OOS and OOI muscles occurred bilaterally. Additional fixations were made at the cables (A). Topographical relationship between the bipolar electrodes and underlying muscles (B).

Electrode positions

Recording sites were chosen on the basis of anatomical textbooks and experimental anatomical studies (Braus and Elze 1954; Kennedy and Abbs 1979; Salmons 1995). The bipolar montage was parallel to the supposed muscle fibre direction (Fig. 3-3B). The main criterion for determining the recording sites was to maximise the distance to the adjacent muscles (in order to reduce cross-talk). The locations of the innervation zones could not be considered in electrode positioning, because the facial motor units have neuromuscular junctions distributed over the whole muscle in several oval-shaped zones (Happak et al. 1997). The position of the ZYG electrode pair was verified by palpating the underlying muscle during contraction.

The OOS and OOI electrodes were positioned as close as possible to the vermillion border (due to the size of the double-adhesive tape used for attachment, there was a minimal distance of 4 mm between the electrode centres and the vermillion border). The medial electrodes were 18 mm from the facial midline (this distance was pre-determined by the trumpet mouthpiece's size). To establish the DLI recording site we determined the borders of the mental soft-tissue while subjects contracted the MEN muscle. In addition, a horizontal line was drawn level with the mentolabial sulcus. The DLI electrode pair was positioned so that the upper part of the corresponding double-adhesive tape touched the lateral border of the mental soft-tissue and the level of the mentolabial sulcus (here also, the centre of the upper DLI electrode had a distance of 4 mm to these reference lines). We angulated the DLI electrode pair approximately 30° relative to the face's midline. The MEN electrode pair was positioned on a line drawn from soft-tissue pogonion (most anterior point of the chin on the face's midline) towards the supposed apex of the lower lateral incisor. Pogonion was at the boundary of the lower electrode's inferior margin. To determine the DAO electrode position, we draw a line parallel to the face's midline through a point 8 mm lateral to cheilion (cheilion is the point where the vermillion borders of upper and lower lips meet). The point 8 mm lateral to cheilion approximately corresponds with the centre of the modiolus (a muscle-tendinous node in which several perioral muscles insert, see (Kennedy and Abbs 1979)). The electrode pair was positioned on the drawn line, located

midway between the modiolus and the inferior border of the mandible. To determine the ZYG muscle's position, we drawn a line from cheilion toward the origin of this muscle at the zygomatical bone (the muscle's origin can often be palpated as a bony dimple on the lateral surface of the zygomatical bone, inferior and lateral to the orbita's lateral margin, see (Braus and Elze 1954)). The bipolar montage was along this line, with the upper electrode placed midway between the origin and cheilion. The LLS electrode pair was positioned as close as possible (again with the electrode centres 4 mm

lateral) to the ala nasi baseline at the level of the alar curvature point (the most lateral point on the ala nasi baseline). Bipolar montage was made at an angle of approximately 30° to the face's midline.

Recording procedure

EMG recordings were made while the subjects performed a series of discrete facial actions and poses, respectively. Each pose was selected to activate a particular muscle (Fig. 3-4). Prior to these recordings, the poses were explained precisely and demonstrated

Orbicularis oris sup. et inf. m.
(OOS + OOI)

Depressor labii inferioris m.
(DLI)

Mentalis muscle
(MEN)

Depressor anguli oris m.
(DAO)

Zygomaticus major muscle
(ZYG)

Levator labii superioris m.
(LLS)

G

Perioral muscles	Instructions for recruiting selective contractions
OOS + OOI	Contract upper and lower lips (central and peripheral parts)
DLI	Depress lower lip in the centre (not laterally)
MEN	Raise chin soft-tissue and lower lip / wrinkle the chin
DAO	Depress corners of mouth
ZYG	Pull corners of mouth upwards and backwards
LLS	Raise upper lip

Figure 3-4. Facial poses (A-F) and corresponding instructions (G) chosen for recruiting a selective contraction of individual perioral muscles. It turned out to be almost impossible to contract the OOS and OOI muscles separately, so the subjects were asked to activate these muscles together (see A). In this subject, co-activation is visible in the DAO pose (co-activation of the MEN muscle), and in the LLS pose (co activation of the OOS, nasalis and orbicularis occuli muscles).

by the trained investigator. The subjects were helped in performing the experimental tasks by providing visual feedback. We made three recordings in each pose.

The ability of the skin-electrode-bonding to withstand moisture and mechanical stress was judged from observations made while the subjects played exercises on the trumpet (Fig. 3-5) for approximately 30 minutes. These exercises included tones from C3 up to C5, at piano and forte dynamics. Quantitative results concerning this study of trumpet playing will be reported separately.

Recording equipment and data analysis

The equipment for sEMG amplification and storage had a high input impedance (10 GΩ), a common mode rejection ratio of 120 dB and an input referred voltage noise of 0.7 μV_{RMS} (Biovision, Wehrheim, Germany). The ampli-
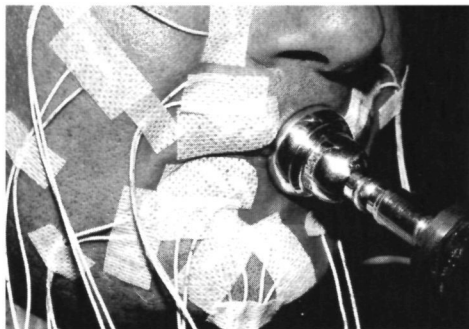
Figure 3-5. Test of the electrode's skin attachment during trumpet playing withstanding mechanical strain and moisture. Producing tones on the trumpet requires highly dynamic perioral muscle contractions and moistening of the vibrating lips.

fied signals were sampled with 12 bits (1 μV/bit) at 2000 Hz. The low- and high-cut-off frequencies of the amplifier were 10 Hz and 700 Hz, respectively. In order to exclude movement artefacts, we analysed a data segment of 2 seconds that started about 1 second after the subjects adopted the corresponding facial pose

(Fig. 3-6, upper diagram). Muscle activity was quantified by calculating Root Mean Square (RMS) values of the signals. In order to quantify muscle-selectivity of the signals recorded during the (attempted) isolated contractions, a so-called selectivity-index (SI) was individually calculated for each performance of a facial pose using

$$SI_{pose(i)} = \frac{nRMS_{sensor(i)}}{\left(\sum_{j=1}^{N} \left(nRMS_{sensor(j)} \right) - nRMS_{sensor(i)} \right) / (N-1)}$$

(Eq. 1)

This parameter was defined as the amplitude of the signal detected over the contracted muscle (i) divided by the mean amplitude of the signals detected over the other N-1 muscles (here N=7) during that pose. In order to give all muscles the same weight in this calculation, we used normalised RMS values (nRMS), i.e. RMS values were related to the maximal RMS value of the corresponding channel over all facial poses. From the three repetitions per pose, the one with the highest SI value was used for further calculations.

In order to estimate the amount of crosstalk that occurred from the (selectively) contracted muscle (i) to an adjacent recording site (j), a so-called cross-talk ratio (CTR) was defined as

$$CTR_{muscle(i)-sensor(j)} = \frac{RMS_{sensor(j)}}{RMS_{sensor(i)}}$$

(Eq. 2)

This parameter was separately calculated for each subject, facial pose and recording site and describes the relation between the amplitude detected by the adjacent bipolar electrode (j) and those detected by the bipolar electrode directly over the contracted muscle (i). Absolute RMS values were used in this calculation, because we assumed that the signals
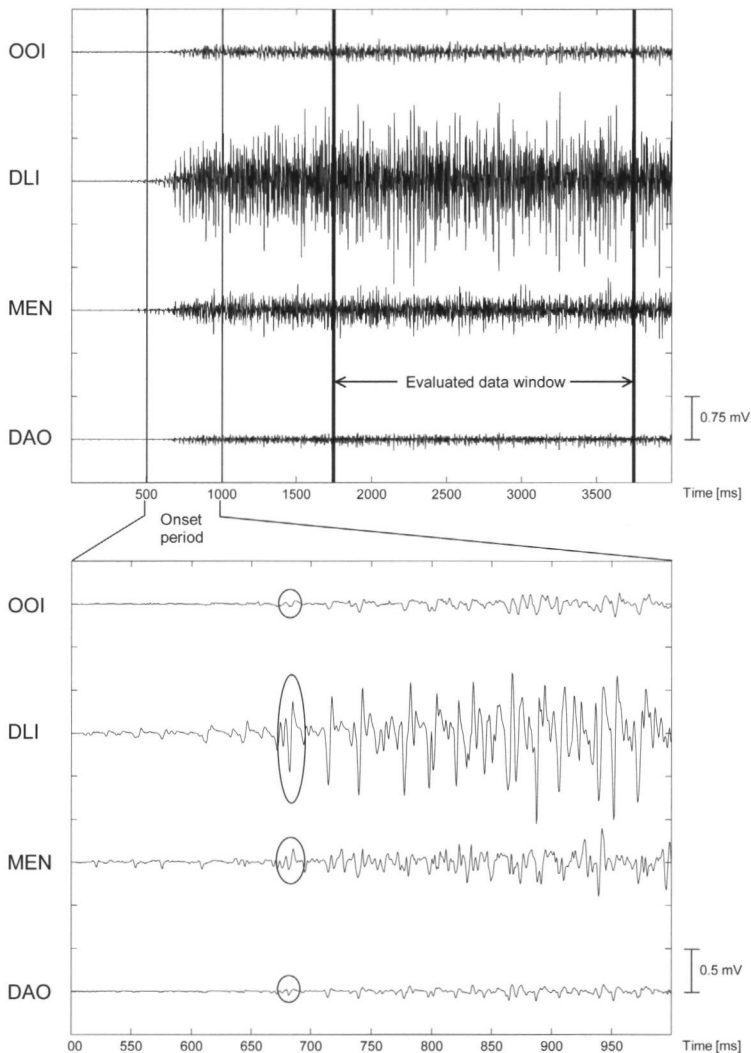
Figure 3-6. Subset of signals from the muscles of the lower face, i.e. from the OOI, DLI, MEN and DAO muscles, recorded during (attempted) selective contraction of the DLI. We analysed a data segment that started about 1 s after the subject adopted the corresponding facial pose (see upper diagram). The onset period of the contraction is shown in more detail in the lower diagram. Although forceful contraction of the DLI muscle results in a considerable downward movement of the lower lip (about 10-15 mm, see also Fig. 3-4B), signals hardly show any baseline instability typical for a movement artefact. The sufficiently high signal-to-noise ratio achieved with our new electrodes becomes obvious when the amplitudes at rest and at maximal activity are compared. The height of the large peaks in the DLI signal on the one hand, and simultaneously occurring smaller peaks in the OOI, MEN and DAO signals on the other, allows a rough, visual estimation of the amount of crosstalk from the DLI muscle to these adjacent recording sites (a subset of such peaks-probably representing a large DLI motor unit potential at different locations-is marked in the lower diagram). The fact that the OOI and DAO signals mainly consist of such small peaks simultaneously occurring with large DLI firings suggests that they indeed are mainly the result of crosstalk from the DLI muscle. In contrast, the MEN signal apparently contains 'independent' myoelectric activity, i.e. activity generated by co-activation of the MEN muscle.

detected at both locations result from the contraction of muscle (i). Using the normalised RMS values would result in a bias of the CTR by the 100%-reference contraction of the adjacent muscle (j).

The minima of the CTR across the study group were used for estimating the amount of cross-talk from the selectively contracted muscle (i) to the respective adjacent recording site (j). We thereby assumed (1) that in that subject with the smallest CTR, the respective adjacent signal was only caused by cross-talk (and not by co-activation of muscle (j), see discussion), and (2) that the inter-individual variability in facial anatomy had no significant influence on these calculations.

Results

Verification of the new technique and bioelectrical performance in practical application

Only two of the 94 bipolar electrode pairs lost their firm attachment to the skin during the experiments. This occurred during trumpet playing in both cases. After a short period of habituation, the subjects reported that their labial movements and ability to play the trumpet were barely hindered by the electrodes. In three subjects, the skin-electrode impedance was measured relative to a common reference (placed mid-forehead) at a frequency of 100 Hz (sEMG contains most of its power around this frequency). Impedance values varied between 5.2 and 9.6 kΩ. Differences within bipolar electrode pairs ranged from 1.7 to 3.6 kΩ. From the signals shown in Fig. 3-6 it is obvious that the signal-to-noise ratio was sufficiently high.

Evaluation of the recording selectivity and cross-talk during the facial poses

SI values revealed great inter-individual and inter-muscle variability (Table 3-1B). The

elevation of the upper lip (executed by the LLS muscle) produced the most selective signals. The corresponding median SI of 6.4 indicates that in this facial pose, the activity registered over the LLS muscle was over six times higher than the averaged activity registered over the other six muscles. In one subject this ratio was even 16.2. Highly selective signals were also found while raising the soft tissues of the chin (pose for the MEN muscle). The corresponding median and maximum values were 3.6 and 13.2, respectively. In contrast, signals recorded during contraction of the upper and lower lips were rather unselective. The corresponding median values of 1.4 indicate that, in the attempted isolated contraction of the OOS and OOI, the signal amplitude over these two muscles was not much higher than the averaged amplitude over the other five muscles.

The calculations for estimating cross-talk during the facial poses are illustrated in Fig. 3-7. In all poses, the minima of the calculated RMS ratios were not higher than 0.25. That means that in each facial pose there was at least one subject having a signal amplitude from the contracted muscle of at least four times that recorded from adjacent muscles. The highest CTR minima were found during DLI muscle contraction; the corresponding values were 0.25 and 0.23 for the OOI and MEN recording sites, respectively (an exemplary subset of signals illustrating cross-talk from the DLI muscle to bipolar electrodes positioned over adjacent muscles is shown in Fig. 3-6, lower diagram). Relatively high CTR minima were also calculated for the DLI recording site during the MEN muscle contraction (0.22), as well as for DLI recording site during the DAO muscle contraction (0.21).

Discussion

The usefulness of the new electrode design and application technique has been demonstrated.

Table 3-1. Median values, minima and maxima of muscle activity (A) and signal selectivity (B) during the facial poses

A

Pose for	Muscle Activity [% of Maximum / Channel]						
	OOS	**OOI**	**DLI**	**MEN**	**DAO**	**ZYG**	**LLS**
OOS + OOI	**100** (100 / 100)	**100** (196/ 100)	100 (19 / 100)	49 (25 / 100)	70 (20 / 100)	92 (43 / 100)	25 (12 / 64)
DLI	7 (2 /50)	43 (13 / 70)	**89** (21 / 100)	56 (21 / 100)	17 (7 / 46)	15 (11 / 25)	8 (2 / 21)
MEN	36 (2 / 84)	31 (8 /100)	16 (10 / 100)	**100** (36 / 100)	6 (3 / 100)	24 (12 / 100)	9 (5 / 84)
DAO	18 (6 / 38)	18 (5 / 55)	32 (17 / 86)	27 (9 / 100)	**100** (27 / 100)	48 (17 / 100)	11 (7 / 50)
ZYG	18 (4 /43)	28 (4 / 75)	47 (3 / 93)	31 (13 / 93)	37 (3 / 100)	**89** (47 / 100)	27 (14 / 100)
LLS	14 (3 / 80)	7 (2 / 84)	5 (1 /92)	16 (2 / 88)	4 (1 / 80)	41 (19 / 67)	**100** (100 / 100)

B

Pose for	Selectivity Indices (SI)		
	Minima	**Median**	**Maxima**
OOS	1.2	1.4	4.1
OOI	1.2	1.4	4.1
DLI	1.8	2.6	4.7
MEN	1.1	3.6	13.2
DAO	0.8	2.5	5.9
ZYG	0.8	2.2	6.1
LLS	1.3	6.4	16.2

In the upper table (A), minima and maxima are given in braces. In order to enable inter-individual as well as inter-muscular comparisons, amplitudes (i.e. RMS values) were individually normalised to the maximal amplitude of that channel over all facial poses. Selectivity indices (SI) were separately calculated for each subject and facial pose using the normalised RMS values and Eq. (1).

During experimentation, skin attachment was lost in less than 2% of electrodes. This did not occur until the attachment had been subjected to the high stress during trumpet playing, where the tension and dynamic of the skin as well as the presence of moisture are much greater than under most other conditions (i.e. during speech or other physiological orofacial functions). From the different measures of the attachment procedure, the pre-fixation of the electrodes and their exact positioning during the definitive fixation demanded the most attention and time (attaching one electrode pair took about five minutes). We plan to have a future electrode version with two detection bodies permanently connected by means of a 2 mm wide and 50 µm thick flexible plastic strip (i.e. from Polyimid material) embedded
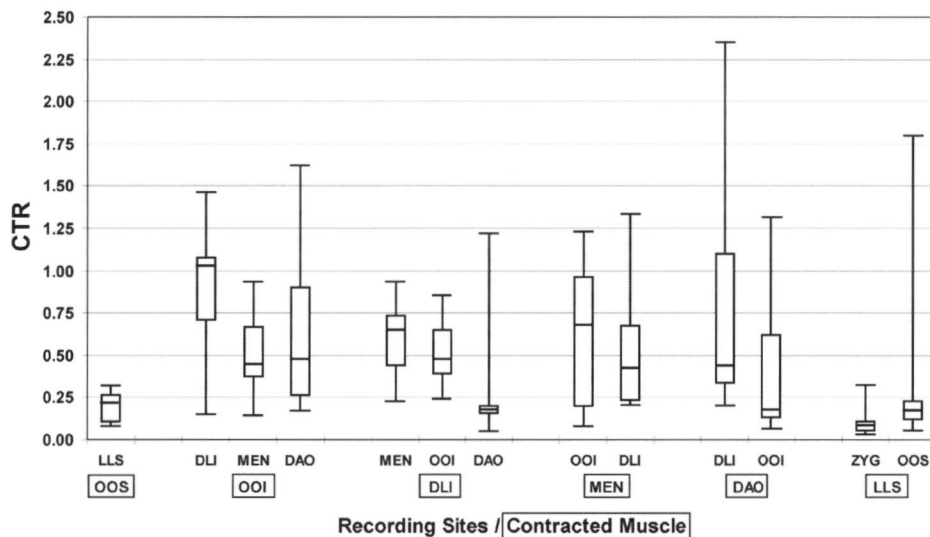
Figure 3-7. Crosstalk during the facial poses (from the contracted muscles to bipolar electrodes positioned over adjacent muscles). Crosstalk ratios (CTR) were calculated according to Eq. (2). Since crosstalk is a largely distance dependent phenomenon, only CTR of recording sites in close proximity of the contracted muscle were illustrated in this diagram. Estimations of the amount crosstalk were made on the basis of the CTR minima. We assumed that in the CTR minima, the superimposition of the factor 'crosstalk' by the factor 'co-activation' was largely eliminated.

into the silver bonding layer. In so doing, the separate pre-fixation step could be omitted; the connecting plastic strip would firmly fix the two electrodes at the double adhesive collar after their placement in the punched holes.

The skin-electrode impedance measurements revealed that absolute values and imbalances within electrode pairs were sufficiently low. In the bipolar recording technique, these are important parameters regarding the signal-to-noise ratio and the avoidance of differential common mode detection (De Luca and Knaflitz 1992; Freriks et al. 1999).

A miniature sEMG electrode especially for the use in facial area was previously designed by Cole et al. (Cole et al. 1983). The detection body used corresponds to that of our electrode with regard to the size and material. However, in Cole et al.'s design, the detection body is recessed into an acrylic housing, leading to a total electrode size of 6.5 mm diameter and

3 mm thickness. The miniature surface electrode types used in other previous facial EMG investigations were also cup electrodes, with total dimensions (at least thickness alone) larger than those of our electrode. As a consequence, their disadvantages are also greater. An often mentioned advantage of such cup electrodes (compared to electrodes with a detection surface directly contacting the skin, as those described in this article), is their reduced tendency to movement artefacts in dynamic contractions. This assumption is based on the theory that in cup electrodes, the depot of electrode gel or crème minimises the effect of the relative movement between the detection surface and the underlying skin (which actually causes some of the baseline instability). Movement artefacts generally were not a problem in our study because the analysed data segment started after the subjects adopted the corresponding facial pose (i.e. only after facial

soft-tissue movement occurred). Nevertheless, it seems that also under dynamic conditions, signals recorded with our electrodes show a relatively high baseline stability. This is demonstrated by the exemplary subset of signals (low cut-off-frequency: 10 Hz) which includes the onset period of a facial muscle contraction (Fig. 3-6) and was also confirmed in a pilot experiment in which we compared the baseline stability achievable with our electrodes and cup electrodes. Thus, we suggest that the described technique is also suitable for studying dynamic facial muscle contractions (e.g. in speech research). Possible reasons for the relative high baseline stability of our electrodes are (1) the sinter-metallic detection surface, (2) the reduced electrode size and mass, as well as (3) the very firm fixation of the electrodes and cables (which hardly allows any relative movement between the detection surface and the underlying skin).

From previous studies it is known that the size of the conductive area of sEMG electrodes as well as the inter-electrode distance in bipolar montages have an influence on both the amplitude and the frequency content of the detected signal. The potential of an electrode reflects the mean voltage under the detection surface. (1) An increase of the electrode size in muscle fibre direction therefore has a temporal, but also a spatial low pass effect. The latter means that an electrode with a larger area in muscle fibre direction spans - to a greater extent - positive and negative components of the EMG interference pattern and, therefore, detects signals of decreased amplitudes. (2) On condition that the electrodes are optimally placed over the muscle, the amplitude should also decrease in case of enlarging the electrode's dimensions perpendicular to the muscle fibre direction (Roeleveld et al. 1997c). However, this condition is difficult to ensure in practical circumstances. (3) Upon an increase of the IED value it is known that this decreases the bandwidth

of the signal and increases its amplitude (De Luca and Knaflitz 1992). In total, the small conductive area of our new electrode as well as the small IED value should theoretically lead to signals having relatively high frequency variables; due to opposing and more complex effects, the influence on the amplitude is unpredictable. In a pilot study, in which we compared the bioelectrical performance of our electrode to that of a commonly used cup electrode type (having a conductive area of 7 mm in diameter and an IED value of 11 mm), the theoretical effect on the frequency content of the signals could be corroborated; the median frequency calculated from the signals detected with our electrodes was approximately 10% higher than the corresponding value of the cup electrode's signals. A second finding was that the signals recorded with our small bipolar electrodes frequently had higher amplitudes. We intend to verify and investigate these preliminary results in a separate systematic study.

The selectivity of the signals recorded during the muscle-specific facial poses showed very high inter-individual variability. Moreover, clear inter-muscular differences were observed. In some of the muscles examined (especially the LLS and the MEN muscles), the activity during (attempted) isolated contraction was clearly above the average of the other muscles. In other tasks, however (especially in those to selectively contract the OOS and OOI muscles), signal selectivity was relatively low. O'Dwyer et al. (O'Dwyer et al. 1981) made recordings from a comparatively large number of facial muscles during a series of similar facial poses. In contrast to us, they obtained EMG signals using an invasive technique (bipolar intra-muscular fine-wire electrodes). Since these electrodes are believed to record more selectively than sEMG electrodes (Fridlund and Cacioppo 1986; O'Dwyer et al. 1981), the results of this former study may be regarded as

3

a 'gold standard' (from the results published in an earlier report (Isley and Basmajian 1973), it was not possible to quantify signal selectivity; for this reason, O'Dwyer et al.'s study was preferred for comparison). From their mean values, SI values were calculated using (Eq. 1). The results were quite similar to those calculated from our mean values (Table 3-2).

The greatest difference was found in the LLS muscle pose, where signal selectivity in O'Dwyer et al.'s recordings was more than twice as high as in the present study. However, this difference should not be overemphasised, since there were also subjects in our study with very high indices (up to 16.2) for this pose.

In general, one should note that the selectivity of EMG signals (expressed in our study by the SI values) is determined by (1) the selectivity of the neural drive to the muscle and (2) the selectivity of the recording technique (i.e. its ability to suppress cross-talk).

(1) Higher neural drive selectivity means less co-activation of other muscles. Since directed facial actions are generally difficult to perform, co-activation can present a particular problem in facial EMG. That means that, when confronted with facial action tasks,

subjects may adopt alternative strategies to achieve them (Tassinary et al. 1989). This very probably was the reason for the relatively high inter-individual variability of the CTR and SI values and also explains why one must be cautious in interpreting results from facial EMG recordings. A second problem is that in some facial muscles it is difficult to relate a certain facial pose to their selective contraction, because the latter is not accompanied by an easily visible and characteristic facial movement. This is especially the case in the OOS and OOI muscles and therefore explains the relatively low signal selectivity found while the subjects contracted their lips. Another aspect concerning the selectivity of neural input relates to the composition of the study sample; we examined professional trumpeters, which might be more skilled in performing facial actions than other subjects (although our trumpeters had not undergone any special training prior to the recording session). This could have exercised an influence in favour of the selectivity indices calculated from our results, when compared to those calculated from the results of O'Dwyer et al..

(2) Cross-talk is a largely distance-

Table 3-2. Selectivity indices (SI) calculated from the recordings of O'Dwyer et al. (O'Dwyer et al. 1981) obtained with intra-muscular fine-wire electrodes.

Pose for	Selectivity Indices (SI)	
	O'Dwyer (1981), N = 6	Present study, N = 11
OOS	1.5	1.6
OOI	2.4	1.5
DLI	3.1	2.8
MEN	2.2	2.6
DAO	2.7	2.5
ZYG	1.9	2.2
LLS	10.2	4.4

The results of this previous study were evaluated by calculating SI from the published mean values of muscle activity. In order to allow a quantitative comparison with those results, we made identical calculations from our recordings also using the mean values of the whole study group.

dependent phenomenon and therefore another key problem in facial EMG. In this regard, one must be cautious in attributing facial EMG signals to specific muscles or functions (Blair and Smith 1986; Fridlund and Cacioppo 1986). In some of the facial muscles (e.g. the OOI muscle), it is definitely not possible to record selectively from a homogenous fibre population. This is true for both surface and invasive EMG electrodes (Blair and Smith 1986). We attempted to separate cross-talk from co-activation by taking only the most selectively executed poses into account, i.e. by estimating the amount of cross-talk on the basis of the CTR minima. Since even in the most selectively executed poses, the signals registered over adjacent muscles probably still contained some myoelectrical activity generated by co-activation (of the respective underlying muscle), cross-talk should have indeed been even lower than was indicated by the CTR minima. One might verify this assumption by studying subjects especially trained in selective facial actions. The fact that most cross-talk was noted during the DLI muscle contraction (with minima of 25% and 23% for the OOI and MEN recording sites, respectively) might be explained by the anatomical situation in the corresponding facial area; the DLI fibres intermingle with horizontal OOI fibres within the lower lip (Blair 1986) and extend in the medial dimension to the MEN

electrode site (Leanderson et al. 1971).

In total, our results suggest that as long as bipolar sEMG electrodes with optimised selectivity (i.e. a small IED value) are used, it is possible to keep the amount of crosstalk within an acceptable limit for most muscles. Due to general limitations in interpreting data obtained during selective facial muscle contractions (Blair and Smith 1986), as well as the fact that professional trumpeters were examined in our study, we hesitate to make concrete statements regarding the recording selectivity achievable with surface EMG electrodes vs. invasive EMG electrodes. However, comparing signal selectivity gives us reason to believe that there is probably no large difference in this respect. Undoubtedly, invasive techniques still have their specific indications. These mainly concern applications on the motor unit level. However, surface EMG electrodes offer several advantages when compared to intra-muscular electrodes (Cole et al. 1983; Fridlund and Cacioppo 1986). This is especially true for clinical investigations due to the much greater acceptance among patients or participants. The availability of an unobstructive sEMG electrode for simultaneously observing multiple muscles in a relative small area opens up a wide range of applications in the facial musculature (e.g. in speech research, psychophysiology and orthodontics) as well as in other muscle groups.

3

4

HIGH-DENSITY SURFACE EMG

Zwarts M.J., Lapatki B.G., Kleine B.U., Stegeman D.F.

Introduction

Surface EMG is a non-invasive method to measure the electrical activity evoked by activation of muscle fibres through the intact skin. Although the clinical application of sEMG measurements in the context of nerve conduction studies is well accepted and its superiority in comparison with needle recording of the compound muscle action potential is undisputed, further usefulness of sEMG measurements as a diagnostic tool is judged to be negligible (Haig et al. 1996; Pullman et al. 2000). Intuitively, needle EMG is usually regarded as precise and informative. A more rational approach would be to use the electrode type best suited for the particular clinical question. The above mentioned use of sEMG in nerve conduction studies is a good example. This application requires the measurement of the summed activity of a large number of simultaneously activated motor units (MUs) and for that purpose, surface EMG electrodes possess superior properties.

Basic to all sEMG measurements is the determination of the voltage difference between two surface electrodes. In the case of a monopolar recording, one electrode is far away from the target muscle. Combining the activity of one electrode with that of one or several surrounding electrodes results in "higher order" derivations or montages. The effect is a "spatial (high pass) filtering" or a narrowing of the spatial view. Subtracting the signals from two nearby electrodes over the muscle, results in a bipolar recording. This is the classical configuration. One step further in complexity leads to the "double differential" recording (Merletti et al. 1999). The EMG signal of a central electrode is doubled, and the summation of the activity of the electrodes on both sides is subtracted (Fig. 4-1). A Laplacian configuration is again more complex: the central electrode is connected with four surrounding electrodes (Disselhorst-Klug et al. 1997). This is similar to the "source derivation" montage in EEG. The exact montage to be used depends on the clinical or research ques-

4

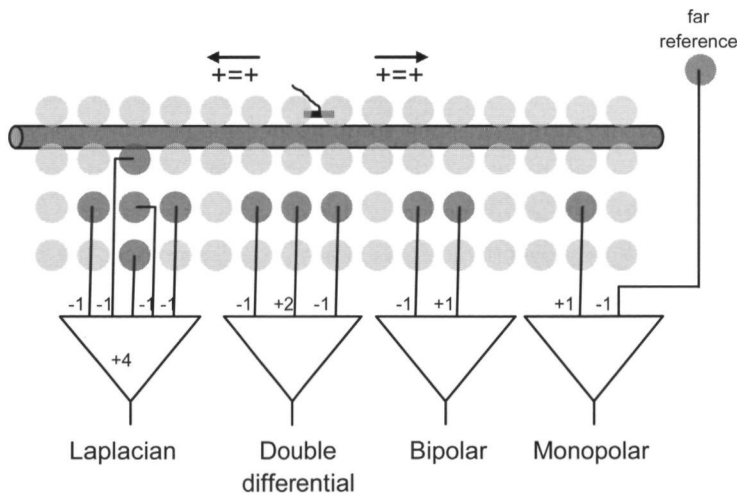**Figure 4-1.** Starting with an arbitrary grid of electrodes different montages can be constructed by combining the electrodes in different ways. From right to left: the monopolar montage, in this way the signals are actually recorded and stored. Bipolar: the classical recording between two nearby electrodes. Double differential and Laplacian: higher order derivations that combine one electrode with several surrounding electrodes.

tion. It should be realised that the recording area of the electrodes becomes progressively smaller with shorter inter-electrode distances and higher order derivations. The bipolar and higher order montages record mainly the traveling part of the motor unit action potential (MUAP) and suppress the far field activity originating during the start and extinction of the action potential. Also, a short inter-electrode distance diminishes cross-talk from nearby muscles. With a higher order montage the amplitude of the signals usually decreases. The EMG signals contain progressively less low – spatial and generally also temporal – frequency components.

Multi-channel sEMG

Besides the different possibilities for recording montages it is also possible to further increase the number of channels. In this way, topographical information concerning the distribution of the EMG activity over a muscle and/ or the timing relationships between different muscles becomes accessible. This is an important facility of sEMG. In principle, there is no hindrance in increasing the number of electrodes over the muscle, the number of channels or arranging complex montages from different electrodes for each channel (Stegeman et al. 2004).

Connecting several bipolar recording electrodes placed in line, results in a linear array recording (Farina et al. 2000; Masuda and Sadoyama 1986). This enables the measurement of sarcolemmal propagation by comparing the time delay of the consecutive signals, provided they are aligned with the muscle fibre direction (Fig. 4-2). Here, we encounter the first spatial aspect of the MUAP: its origination at the endplate zone, propagation along the sarcolemma and extinction at the tendon. In a bipolar recording, the endplate zone is characterised by a low ampli-

tude (the two electrodes above the place of origination of the action potential "see" almost the same potential). The propagation of the MUAP is seen from the later arrival of the potentials at the consecutive electrode pairs. The lines connecting the peaks (Fig. 4-2) indicate a constant propagation along the muscle fibres. Note that the polarity of the signals is opposite (phase reversal) when comparing the two directions of MUAP propagation. This simplifies the recognition of the endplate zone.

A logical extension of the recording configuration is a two-dimensional grid of electrodes with an arbitrary number of electrodes and inter-electrode distances (Fig. 4-3). Such a configuration enables the localisation and size estimation of motor units as well as the determination of the position of the motor endplate zone. Using a two-dimensional grid, it also becomes possible to display the sEMG activity in an amplitude or spectral map (Roeleveld et al. 1997d).

Please note that it is recommended for all sEMG measurements, especially for multi-channel sEMG as discussed here, to record and
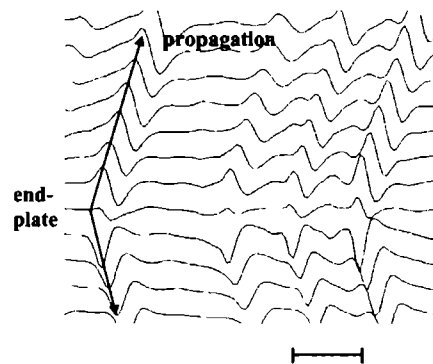

Figure 4-2. Example of sEMG measurements of a longitudinal array of electrodes in bipolar configuration is shown. Note the position of the endplates visible from the "phase reversal", the different MUs and the conduction visible from the time delay between the consecutive channels The amplitudes hardly change along the course of the muscle fibres The horizontal calibration is 10 ms.
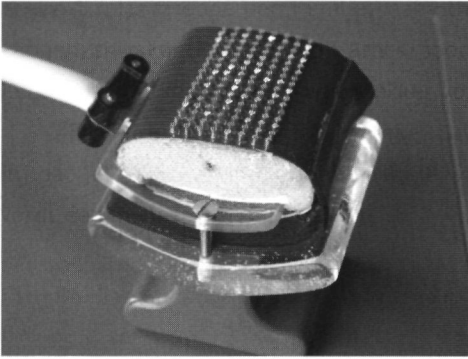
Figure 4-3. The 128-channel sEMG grid with gold-coated electrodes mounted on a flexprint base.

store the signals of the individual electrodes in the array or grid referenced to a remote electrode (thus in a monopolar fashion). We recommend this approach because it enables a versatile and purpose-dependent rearrangement afterwards, both with respect to the desired montages (bipolar, Laplacian etc) and to the way in which the EMG activity is displayed (column, row, map etc.).

Motor unit size estimation from high-density sEMG

An important piece of information from needle EMG is the 'size' of the motor unit. Changes in this 'size' reflect alterations due to reinnervation or loss of muscle fibres, e.g. due to a myopathic process. The motor unit size can be represented in different ways. Usually, the duration of the MUAP is measured or, alternatively, the area of the MUAP can be calculated. Since its size is an essential property of a motor unit, we investigated if it was possible to measure this feature of the motor unit noninvasively with sEMG. The size of the motor unit can – in the case of sEMG – be estimated from the measured amplitude (or area) of the surface MUAP. As in macro-EMG, estimation of MUAPs from a mono-

polar montage appears to be far superior to other montages. The major question to pose is how well do these monopolar surface MUAPs represent the motor unit size? Essentially, the depth of the motor unit influences the MUAP amplitude and wave shape. Roeleveld et al. (Roeleveld et al. 1997b) proposed to use the spatial characteristics of the MUAP template to solve this problem. Superficial motor units give a fast decline in amplitude with distance from the motor unit. Deep motor units show much less relative amplitude decline circumferentially (Fig. 4-4). Theoretically, a motor unit lying in the centre of a circular volume conductor has an even distribution over the skin. Using these differences, the depth of a motor unit can be estimated, allowing for "depth correction" of the MUAP amplitude. MUAPs were measured using macro needle EMG and a cross of sEMG electrodes. There were good correlation coefficients (in the order of 0.85) between the area and amplitudes of macro-EMG and sEMG measured MUAPs.
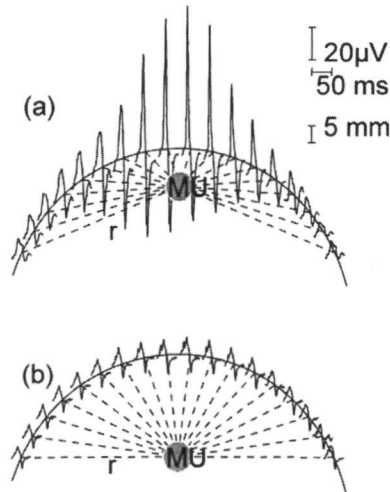

Figure 4-4. The distribution of bipolar sEMG over the skin from a motor unit at different depths. The location of the motor unit was determined with a macro-EMG needle. The measurements of 18 recordings along the circumference of the m. biceps brachii are depicted (Roeleveld et al. 1997d).

Extensions of this work for enlarged motor units due to a neurogenic condition confirmed this relationship (Roeleveld et al. 1998). Others also found enlarged sEMG MUAPs in motor neuron disease patients indicating reinnervation (Wood et al. 2001). The challenge with this approach is the identification of MUAPs, in the surface EMG pattern. The technique of using a bipolar montage for identification and subsequent averaging of the monopolar MUAPs can be fruitfully used here (see next section) (Kleine et al. 2000a).

Motor unit fingerprints

The recognition of motor units using sEMG is possible using their unique configuration of the spatial potential distribution over the skin (finger print). Kakuda et al. (Kakuda et al. 1991) described an early version of this idea using two sEMG channels in addition to a needle recording. Using the 126-channel sEMG grid, each motor unit has a specific topographic configuration: its end plate zone, direction of propagation, extent and rate of decline in lateral direction are all variables contributing to its specific topographical distribution of activity (Fig. 4-5). The study of Kleine et al. (Kleine et al. 2000a) showed the use of these characteristics in the unraveling of motor unit firing patterns. In a low level voluntary contraction with active several motor units, a first extraction was done by using a peak detection at a user-defined level. Such peak detection should be done repeatedly in several channels, since it is not known a priori where the maxima of different motor units lie. The resultant MUAP topograms were clustered on the basis of their similarity by using Ward's clustering algorithm followed by a visual verification. Next, templates could be formed by averaging the sEMG signals of all electrodes using the peaks as time-lock. Each resulting template thus consisted of 126 MUAPs (Fig.

4-5). Note that the main difference between the topograms is not in the temporal, but in the spatial domain. The fingerprints can be used to resolve all firings of the motor unit, including superimpositions. Up to five simultaneously active motor units could be detected in this way. The advantage of the sEMG approach is – compared with needle EMG measurements – that besides a list of all firing moments also basic information concerning motor unit properties becomes available. Using this technique in combination with magnetic cortex stimulation, impaired inhibition of the motor cortex in Parkinson's patients could be demonstrated (Kleine et al. 2000a).

Electrode grid developments

The development of multi-channel sEMG grids poses many, often conflicting technical demands (Blok et al. 2002). Our first grids consisted of metal pin electrodes, mounted in apertures of a substrate sheet and integrated in a single, rigid container (Fig. 4-3). To allow flexibility, the substrate sheet was mounted on 25 mm thick foam layer. Such arrays are suitable for clinical use, and can be easily applied on the large muscles of the extremities. A smaller electrode array (consisting of 16 rows of 8 electrodes with an inter-electrode distance of 3 mm) has been developed for intrinsic hand muscles. All of these grids were fixed with straps of Velcro or medical plaster, which may influence the contours of the muscle. The next step was to provide a universally adaptable and less obstructive sensor (see Chapter 5).

Basic limitations and advantages of sEMG

It is obvious that for phenomena at the level of the muscle fibre, the needle EMG electrode is indispensable. At the level of the motor unit, an overlap exists between the two techniques
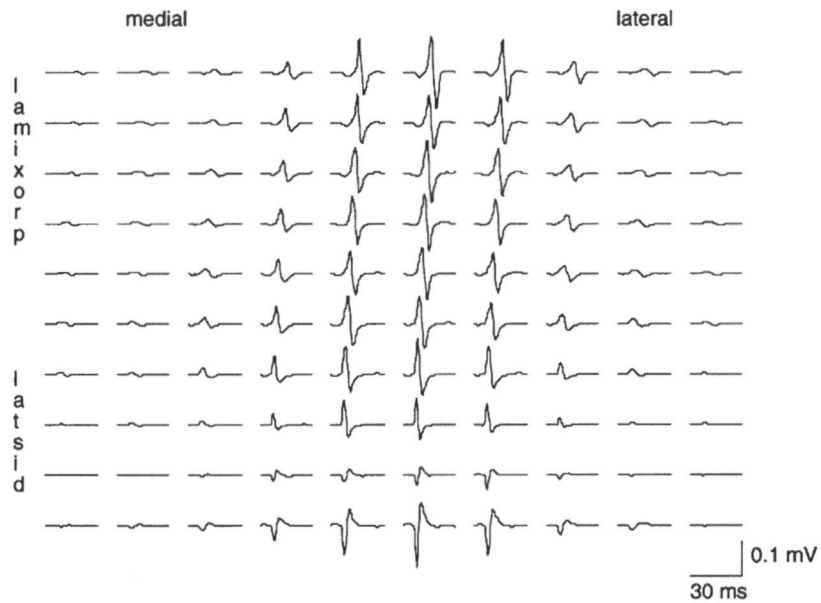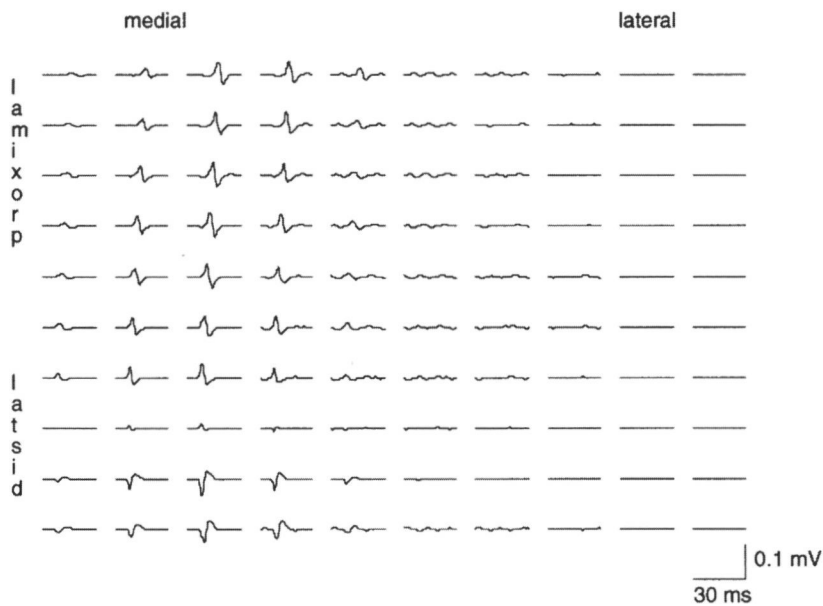
Figure 4-5. Two different templates of averaged MUPs over the skin of the biceps brachii muscle using the 126 channel sEMG grid (Kleine et al. 2000a). Note the differences in position of endplate zones, maximal over the muscle and lateral amplitude decline.

with respect to several important characteristics such as size and number of MUAPs (Zwarts et al. 2000). Presently, the use of needle EMG is well embedded in clinical neurophysiology, and it is a fast and versatile tool for many applications concerning motor unit changes in disease. This fast mode of application and measurement also has the drawback that, in clinical practice, the quantification of MUAPs is often subjective and less than optimal. Although it requires advanced software analysis, one of the most important variables in EMG, the motor unit size, can be reliably estimated using multichannel sEMG. For a number of indications, it is worthwhile to further explore the utility of sEMG, for example the use in children or for followup clinical or research studies. The noninvasive character is, of course, very appealing in all circumstances. Clinical applications concerning topographical information of the motor unit and activity distribution over the muscle clearly belong to the domain of sEMG. They await further exploration, as well. At the moment, it is clear that several pathophysiological mechanisms affecting MUAPs, such as the conduction block in myotonia congenital (Drost et al. 2001) and muscle fibre conduction velocity slowing in familial hypokalemic periodic paralysis (Zwarts et al. 1988) have completely escaped the keen eye of the needle EMG due to the topographic character of electrophysiological expression of its pathology.

How far can you go?

Surface EMG has finally become mature. It has a thorough and extensive theoretical background (Zwarts and Stegeman 2003). Multichannel sEMG grids and software tools enable measurements of MUAP size and number which – until now – were regarded standard needle EMG applications. New technical developments enable the use of flexible, high-density sEMG systems for measurements in the most challenging and difficult areas, such as the human face (see Chapter 5). Moreover, physiological and topographical information becomes available that is beyond the reach of needle EMG. This includes muscle fibre conduction, endplate localisation and MUAP classification using its unique amplitude distribution (finger print) over the skin. Thus, multi-channel sEMG provides both classic and new information regarding the neuromuscular system in health and disease. Its main advantage lies in the noninvasive addition of spatial information to our view on the motor unit. The exploration of the possibilities of this technique has only just begun.

4

Part II

Sensor development

Application of high-density surface EMG as a non-invasive tool for studying facial motor units has not been possible, mainly due to limitations of sensors and signal processing tools. This part describes the development of a special multi-electrode array and an optimised skin attachment technique that fulfil the specific requirements in the face. We aimed at developing a non-invasive recording technique which allows measurements in skin areas with very uneven contours and which does not impede facial movements. This required sensors which were more flexible and less bulky when compared to the up to then available high-density surface EMG electrode arrays. In addition, a skin attachment technique was demanded that did not use external fixations.

5

A THIN, FLEXIBLE MULTIELECTRODE GRID FOR HIGH-DENSITY SURFACE EMG

Lapatki B.G., van Dijk J.P., Jonas I.E., Zwarts M.J., Stegeman D.F.

A lthough the value of high-density surface electromyography (sEMG) has already been proven in fundamental research and for specific diagnostic questions, there is as yet no broad clinical application. This is partly due to limitations of construction principles and application techniques of conventional electrode array systems. We developed a thin, highly flexible, 2-D multi-electrode sEMG grid, which is manufactured using flexprint techniques. The material used as electrode carrier (Polyimid®, 50μm thick) allows grids to be cut out in any required shape or size. One universal grid version can therefore be used for many applications reducing costs. The reusable electrode grid is attached to the skin using specially prepared double-sided adhesive tape, which allows the selective application of conductive cream only directly below the detection surfaces. To explore the practical possibilities, this technique was applied in single motor unit analysis of the facial musculature. The high mechanical flexibility allowed the electrode grid to follow the skin surface even in areas with very uneven contours, resulting in good electrical connections in the whole recording area. The silver-chloride surfaces of the electrodes and their low electrode-to-skin impedances guaranteed high baseline stability and a low signal noise level. The electrode-to-skin attachment proved to withstand saliva and great tensile forces due to mimic contractions. The inexpensive, universally adaptable and minimally obstructive sensor allows to extend the principal advantages of high-density sEMG to all skeletal muscles accessible from the skin surface and may lay the foundations for more broad clinical application of this non-invasive, 2-D sEMG technique.

5

Introduction

Surface electromyography (sEMG) is applied in many areas of muscle research and patient care, for instance in human movement sciences, rehabilitation, ergonomics and clinical neurophysiology. The single bipolar montage, commonly used in these fields, is of value for diagnostic purposes, but offers little information at a single motor unit (MU) level. To deal with this limitation, sEMG techniques have been extended with the design of linear and two-dimensional electrode arrays and grids (Blok et al. 2002; Masuda et al. 1985; Prutchi 1995; Reucher et al. 1987; Stegeman et al. 1996; Yamada et al. 1987). These multi-electrode grids cover a larger part of the muscle and add spatial information that is largely independent of the "classical" temporal information. If electrode grids with small electrode sizes and inter-electrode spacing (so-called

"high-density sEMG arrays") are used, it is possible to decompose the sEMG interference pattern for single MU analysis and the determination of firing events of individual MUs (see Refs. (Farina et al. 2000; Kleine et al. 2000a; Masuda and Sadoyama 1987; Wood et al. 2001; Zwarts and van Dijk 1998)). Although single MU analysis is a key attraction of multichannel sEMG, spatial (or topographical) information from a muscle is also useful in other respects: (1) It allows the construction of higher order electrode montages for spatial filtering (Disselhorst-Klug et al. 1997; Huppertz et al. 1997); (2) the muscle's spatial functional properties can be studied and mapped, respectively (Kleine et al. 2000b; Ohyama et al. 1988; Schumann et al. 1994); (3) grid areas with high signal amplitude can be selected (on-line or off-line) for more detailed inspection or analysis (Kumagai and Yamada 1991).

High-density sEMG has proven its value for fundamental research and is acknowledged for specific diagnostic purposes (Drost et al. 2001; Zwarts et al. 2000), but there is as yet no broad clinical application. A crucial first step on this road is the availability of sEMG electrode grid systems that are (1) flexible in their use, i.e. their applicability should include as many skeletal muscles as possible, (2) inexpensive (at least the sensor component), and (3) easy to apply and to maintain (including sterilisation or at least sufficient disinfection). Although successful progress regarding these criteria has been made, sEMG grids available up to now still contain restrictions which mainly result from their construction principle; they usually consist of metal pins or bars (as single electrodes) mounted in apertures of a substrate sheet and integrated in a single container. A considerable disadvantage resulting from this construction is the fixed, i.e. unchangeable size of the array and the arrangement of the electrodes. Consequently, the examination of muscles which have largely different sizes and shapes requires a number of different grids. For large scale use, this might become ineffective and expensive. Other significant disadvantages of such container arrays are the unavoidably large outer dimensions (especially the large height of several cm) and the limitations regarding mechanical flexibility. In the examination of small muscles, bulky and relatively stiff electrode arrangements may hinder (or even alter) the functions to be studied (Fridlund and Cacioppo 1986). In uneven skin areas (e.g. in the face), grids with a limited mechanical flexibility do not completely follow the patient's anatomy; consequently, a good electrode-skin-contact cannot be achieved in the entire recording area.

For currently available sensor systems, it is not only the electrode arrangement itself, but also the technique by which the sensor is attached to the skin, that contains some principle problems. In most techniques, skin attachment is realised by means of external fixations. These consist either of bands of Velcro which are tied round a limb (Blok et al. 2002; Prutchi 1995) or medical plasters which are tightly drawn over the whole electrode containers and then adhered to the adjacent skin. In some areas (e.g. in the face), it is not practical or even possible to employ such an attachment technique. As a consequence, the application of these conventional sEMG grid systems is limited to certain muscles and/ or positions. Moreover, external fixations unavoidably compress the soft tissue in the area of the sensor. This pressure might cause problems if (1) the array consists of sharply contoured electrode surfaces used to reduce electrode-to-skin impedance in dry application (i.e. in application without conductive cream or gel), (2) the array is applied in areas where the skin is relatively thin and sensible, and (3) the underlying hard tissue has an uneven contour. These are factors causing uneven pressure distribution in the recording area, leading to electrode impressions on the skin and pain to the subjects and patients. In addition, there is a certain risk that sharp electrodes applied with pressure even slightly injure the skin. Together with the risk of insufficient cleaning and disinfection (which may occur in routine clinical applications), slight skin lesions may lead to transference of pathogens (although this infection risk can be considered small).

In this contribution, we describe the design and performance of a thin, highly flexible multi-electrode sEMG grid. The aim of this development was to provide a relatively inexpensive, easily adaptable and minimally obstructive sensor, thus laying the foundations for more broad clinical applications of high-density sEMG, and extending the use of this technique to all superficially located skeletal muscle groups. A crucial aspect connected with the application of such an electrode grid type

was the development of a special skin attachment technique that yields firm sensor fixation and sufficiently low electrode-to-skin impedances without requiring external fixations. In order to explore and demonstrate the practical possibilities, this newly developed sensor technique was applied in the facial musculature. The facial musculature was chosen because of the large methodological demands in this area relative to others (Cole et al. 1983; Lapatki et al. 2003).

Materials and Methods

Electrode grid design

The manufacturing process of the new multielectrode sEMG grid principally corresponds to that of a standard flexprint, i.e. the detection surfaces and connecting wires are chemically etched and electrochemically deposited on a highly flexible carrier material (Polyimid®, 50µm thick). The layout and design was made in cooperation with Digiraster Tetzner GmbH (Stuttgart, Germany). The printed rectangular grid consists of 7 columns of 13 electrodes each (Fig. 5-1A). The inter-electrode distance (IED) is 4mm centre-to-centre in both directions. This value was chosen on the basis of the spatial version of the Nyquist sampling criterion (see Ref. (Blok et al. 2002), as well as the relation between the number of available recording channels and the required size of the recording area. The thin electrode carrier substrate allows smaller grids, of any desired size, to be cut out of the basic grid version with a common scissors (in our application example, we used trimmed grids of 5x12 and 6x10 electrodes, respectively, see below). The flexprint includes a regular pattern of 1.2-mm diameter perforations (through holes) each centred between 4 electrodes.

The grid's electrodes have the shape of a solid circle with a diameter of 1.95mm, protruding 300µm from the Polyimid® mate-

rial. They consist of copper, which is surface coated with a pure-silver (99.99% Ag) layer (Fig. 5-1B). Before chloriding the electrodes, we roughen their outer silver surfaces using a fine glass fibre pen. Total thickness of the grid (electrode, carrier material, traces, protection lacquer) is 470µm in the area of the electrodes and 150µm between them. The high mechanical flexibility of the grid resulting from this minimal thickness and the material properties is demonstrated in Fig. 5-1C.

For electrical connection of the electrodes, traces of 80µm width are printed on the reverse side of the Polyimid® substrate (i.e. on the opposite side of the electrodes). Their position on the reverse side protects the traces against damage due to removal of the double-sided adhesive tape (used for skin attachment, see below) or cleaning of the grid's detection surface after the measurements. Printed trace lines are insulated with a flexible, non-conductive overlay lacquer. The traces of one electrode column (13 electrodes in our grid design) converge into groupings of parallel lines that lead to a 3mm wide and 50mm long tail (Fig. 5-1A). Every tail terminates at a connection end that has exposed electrically conductive surfaces and is dimensioned to mate with an external connector (13FLZ-SM1-TB, J.S.T. Deutschland GmbH, Winterbach, Germany).

Skin attachment of the electrode grid

An electrode grid is attached to the skin using 100µm thick double-sided adhesive tape (1522 Medical double coated tape, 3M, St. Paul, MN, USA). This tape has been specially prepared by creating regular patterns of holes of 2.2mm in diameter to leave the electrode areas blank, and smaller holes (1.2-mm diameter) that topographically match with perforations of identical size in the electrode grid (see Fig. 5-2A).

The attachment procedure is as follows: after shaving the skin in the corresponding

5

A

4 mm

B

C
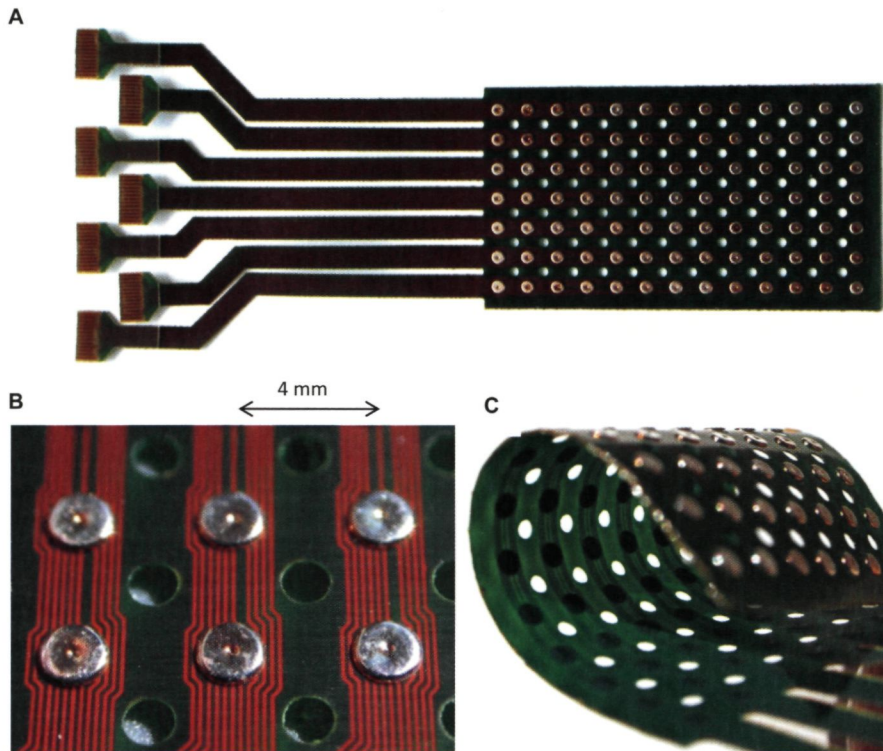
Figure 5-1. (A) Photograph of an sEMG multi-electrode grid (including the connection tails) manufactured using flexprint techniques. This grid has been specially designed for our application example and consists of 7 by 13 electrodes, with an inter-electrode distance (IED) of 4mm (centre-to-centre) in both directions. The thin (50μm) electrode carrying material (Polyimid®) allows smaller grids to be cut out from the basic grid. In principle, grids of any desired electrode sizes and arrangements can be manufactured. (B) Each electrode (1.95mm in diameter) consists of a copper body, which has been surface coated with pure-silver (99.99% Ag). The traces printed on the reverse side of the flexprint are visible in this photograph due to the translucency of the Polyimid® material. Perforations of 1.2mm in diameter (each centred between 4 electrodes) were made to facilitate skin attachment of the electrode grid. (C) Illustration of the high mechanical flexibility of the multi-electrode grid. Total thickness of the flexprint (electrode, carrier material, traces, protection lacquer) is 470μm in the area of the electrodes and 150μm between them.

area (if necessary) and cleansing it with an alcohol-wetted swab, we fix the prefabricated double-sided adhesive tape in the correct position. In order to reduce electrode-to-skin impedance we then evenly apply conductive cream (Elektrodencreme®, Marquette-Hellige, Freiburg i.Br., Germany) in the whole area of the attached tape. The surplus cream is removed on the outer barrier foil of the tape using a dental cotton roll, leaving only a thin cream layer on the skin of the blank electrode spaces (Fig. 5-2A). Since we peel off the outer

barrier foil after the cream has been applied, it is guaranteed that the tape's outer bonding surface is kept free from electrode cream. The next step is to accurately fixate the electrode grid on the outer bonding surface of the attached double-sided adhesive tape. Proper positioning is facilitated by identical patterns of 1.2-mm perforations in the electrode carrier material and the adhesive tape (see Fig. 5-2B); the detection surfaces are exactly centred in the blank 2.2-mm electrode spaces, if the 1.2-mm perforations of the electrode grid and the tape

A

B

Figure 5-2. (A) Double-sided adhesive medical tape (1522 Medical double coated tape, 3M, St. Paul, MN, USA) attached to the skin with surplus electr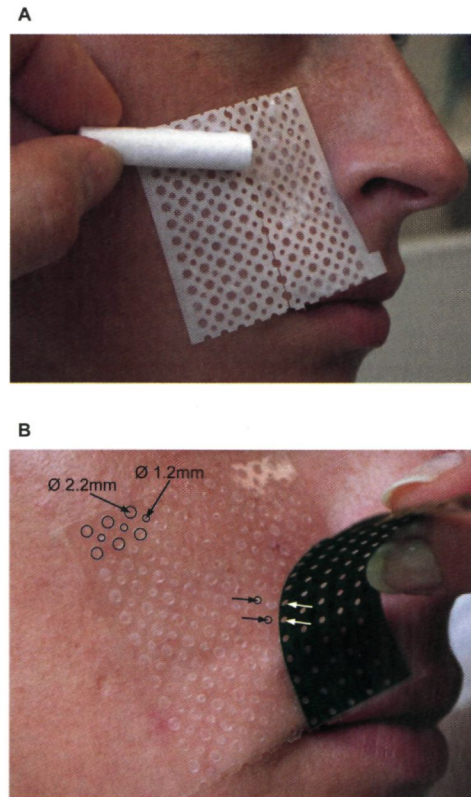ode cream and dental cotton roll used for surplus removal. Perforations of 2.2mm in diameter were punched out to leave the detection surface areas blank. Smaller (1.2-mm) perforations were made to facilitate the skin attachment procedure. (B) Attachment of the electrode grid on the double-sided tape after the outer protecting foil of the tape has been removed. The grid is accurately positioned on the adhesive tape if the 1.2-mm perforations in the electrode carrier material exactly meet the perforations of identical size in the adhesive tape.

exactly meet.

After the measurement, the grid and adhesive tape are detached from the skin by carefully pulling at the connection tails. The tape can then be pulled off from the flexprint. It is advisable to clean the electrode grid immediately after detachment with an alcohol-wetted gaze for subsequent usage.

Subjects

This new technique was tested in the facial musculature on a group of 13 healthy subjects (males n=6, females n=7, mean age 27.2 years). Nine of them were trumpet students or professional trumpeters, who were expected to have good facial motor control. The participants had no known neurological or general health disorders. The Ethics Commission of the University Medical Centre Nijmegen (NL) approved the protocol.

Setup for the measurements and data acquisition

In each subject, we observed the upper and lower facial muscles in two separate sessions (either on the right or left side of the face). In the upper face, sEMG measurements were made using two 5 by 12 electrode grids positioned side by side (see Fig. 5-3). In the lower face, we used two grids of 6 by 10 electrodes that were also positioned side by side, but vertically displaced by one electrode row (see below in Fig. 5-6A). Thus, in both recording areas 120 channels were simultaneously sampled. By using grids of different shapes in the upper and lower face, we could optimally adapt the dimension of the recording area to the anatomy of the underlying musculature.

A single, flexible and lightweight cable (132 conductors Junflon PFA coaxial round cable, J14B0596-A, W.L. Gore & Associates GmbH, Pleinfeld, Germany), 0.7m in length and 8mm in outer diameter, was used to electrically connect the electrode grids to the amplifiers. It contains 132 individually shielded leads and additionally has an outer shield. Especially for application in the face, the cable has been split in two parts behind the head. The two cords were separately guided to the face along movable arms, which are mounted on a headset (Fig. 5-3). The 3-dimensional flexibility of the arms allowed the connectors to be positioned in a manner that the tails of the electrode grid

5

Figure 5-3. Setup for high-density sEMG in the upper facial area. We used two trimmed electrode grids (each consisting of 5 by 12 electrodes) positioned side by side. The cable from the amplifiers was split in two parts behind the head, each containing the connections of one electrode grid. Both cords were guided along two 3-D movable arms that were fixed at the right and left sides of a headset. At the distal end of both arms, two hardprints were mounted serving as a strain relief. The hardprints were equipped with connectors having lockable slots that match with the connection ends of the electrode grids. We secured the borders of the electrode grids in areas that were exposed to moisture or high tensile forces using strips of elastic medical plaster (Fixomull Stretch® Beiersdorf, Hamburg, Germany).

adopt a curved course guaranteeing maximal freedom of movement between the attached electrode grid and the connectors.

Signals were recorded monopolarly, referred to an electrode positioned on the dorsum nasi. A second reference electrode provided a common mode signal (CMS). Both reference electrodes used (Mühl, Freiburg,

Germany) are 4mm in diameter and have been originally developed for conventional facial sEMG recordings (Lapatki et al. 2003). They consist of sintered Ag/AgCl and therefore have similar electrochemical properties as the grid electrodes. A driven right leg (DRL) electrode (see Ref. (Metting van Rijn et al. 1991)) was attached at the forehead. The 128-channel-

system used for data acquisition (Mark-6, BioSemi Inc., Amsterdam, NL) has an input impedance > 100MΩ and a CMRR > 120dB. Signals are band-pass filtered (3.2 - 400Hz; high-pass: first order Bessel, low-pass: fourth order Bessel) and synchronously sampled at 2000Hz with a resolution of 0.5μV over a range of +/- 16mV (16 bits). The acquisition software allows the experiments to be controlled by on-line inspection of the mono- or bipolar data of selected electrode rows or columns. Electrode-to-skin impedances can be measured using a 20mV (p-p), 62.5Hz square wave signal over a 1MΩ resistance in series with two electrodes (i.e. the corresponding grid electrode and the reference electrode). The maximal current is 20nA. Such low current will not disturb the skin-metal double layer, which would make the impedance current dependent. See also Ref. (Blok et al. 2002) for more technical details regarding the recording system.

Recording procedure
At the beginning of each recording session, subjects were instructed and trained in performing selective contractions of the muscles to be examined. After placing and electrically connecting the two grids, we performed an initial impedance measurement. Surface EMG signals were then recorded while each muscle in the recording area was selectively activated at different levels. Since especially in the facial muscles, contractions at a constant level are difficult to perform, we implemented an sEMG amplitude feedback tool into the acquisition program that visually displayed the activity level of a selected muscle to the subject via the PC monitor. Muscle activity level was determined by calculating the normalised mean value of the RMS values of selected bipolar signals (window duration for RMS calculation was 500ms, normalisation was made to a maximal reference contraction

of the muscle). Each recording session lasted for approximately 2 hours and was finished by a second impedance measurement.

Data analysis
Data analysis was performed off-line using algorithms programmed in Matlab, Version 6.5 (The Mathworks Inc., Natick, MA, USA). Impedance data (120 impedance values per measurement) were statistically evaluated by calculating boxplot percentiles separately for each subject, recording moment (initial and final impedance measurement), and measurement location (upper and lower face). For each of the five calculated boxplot percentiles (i.e. the 5th, 25th, 50th, 75th and 95th percentiles) we then determined the median values across the study group (separately for the initial and final recordings and the two measurement locations).

Noise performance of the grid was evaluated by calculating RMS values of signals recorded while the muscles were kept at rest. We only evaluated measurements taken in the upper face about one hour after electrode grid application. Similar to the impedance evaluation, we calculated percentiles for the 120 values (per measurement and subject, respectively) first; from these individual percentile values, median values across the study group were determined.

For analysing the topography of facial MUs, we decomposed the sEMG interference pattern by (1) detecting peaks in the bipolar signals of three selected channels, (2) classifying these peaks according to their differential spatio-temporal amplitude and firing characteristics, and (3) averaging the bipolar data windows around the detected peaks for all 120 channels. Peak classification was based on the Ward's clustering algorithm using "Euclidean distances" between the spatial and the temporal peak characteristics (for more details see Ref. (Kleine et al. 2000a).

5

Results

The evaluation of the impedance measurements (Fig. 5-4) indicate a statistically significant reduction of the electrode-to-skin impedance values during the recording sessions (Wilcoxon signed-rank test, p<0.01) from 163.7 and 137.6kΩ (median values of the 50th percentiles for the measurement in the upper and lower face, respectively) to 75.7 and 99.4kΩ. The difference between the initial and final impedance values appeared to be larger in the upper than in the lower face.

Fig. 5-5A shows a subset of bipolar sEMG signals derived from a single vertical column of electrodes during a short contraction of the depressor anguli oris (DAO) muscle (the orientation of the selected electrode column approximately corresponds to the muscle fibre direction). The bipolar montage was constructed by subtracting the monopolar signals of consecutive electrodes. As recognised by Masuda et al. (Masuda et al. 1983), the position of the motor endplate zone can be detected from the bidirectional propagation pattern of the action potentials, which also results in low amplitude at and opposite signal polarity on both sides of the endplate. Thus, in this recording the neuromuscular junctions are in the area of the 4th bipolar signal (from the bottom), i.e. they are located between the 4th and 5th monopolar electrodes.

In spite of considerable soft tissue movement during the onset period of the DAO contraction, the signals recorded with our new electrode grid showed very high base-line stability (see Fig. 5-5B, signal only band-pass filtered by hardware). The good signal quality
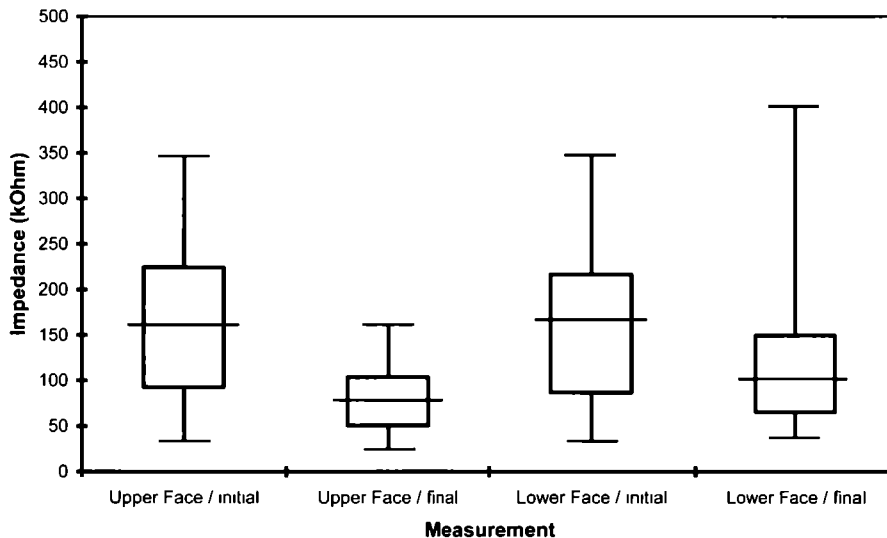
Figure 5-4. Results of the impedance measurements made at beginning and end of the recording sessions in the upper and lower face. Impedances were measured by applying a 62.5Hz square wave signal over a 1MΩ resistance in series with the reference electrode (which had a relatively low impedance value) and the corresponding grid electrode. The values given in these boxplot diagrams (from bottom to top 5th, 25th, 50th, 75th or 95th percentiles) are the median values across the study group calculated from the corresponding percentile values of the individual measurements (see also 'Data analysis' section)
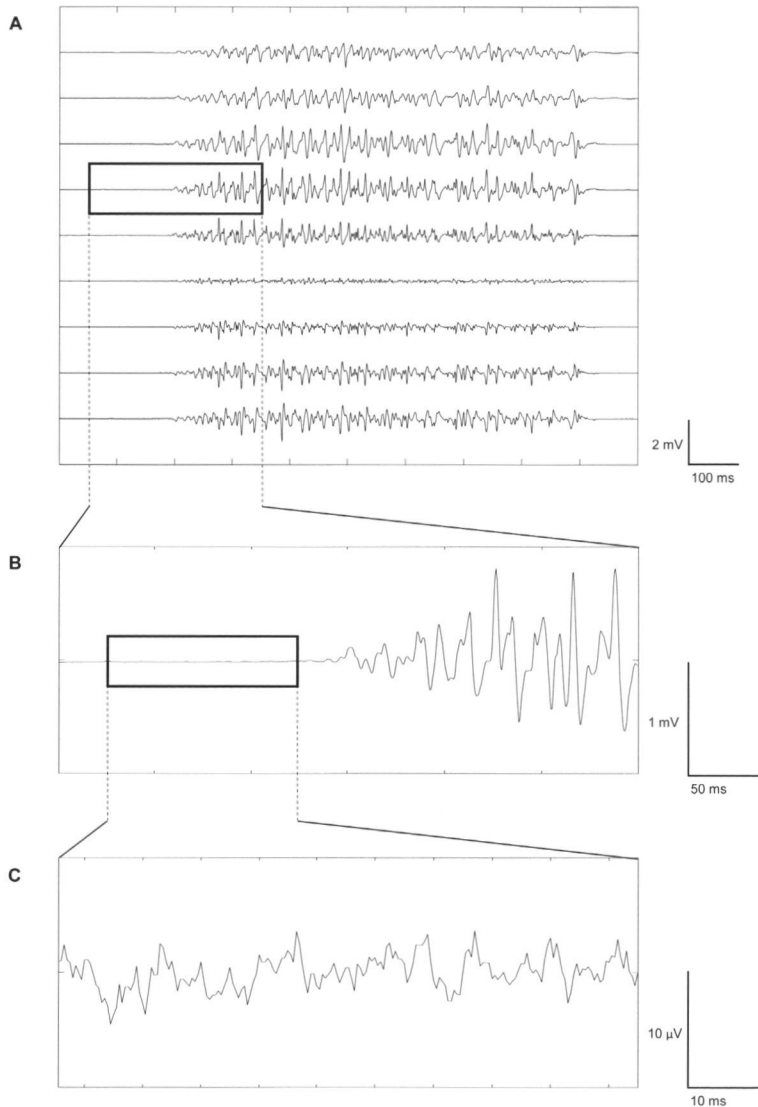
Figure 5-5. (A) Bipolar sEMG signals derived from a single vertical column of electrodes, placed approximately parallel to the fibres of the depressor anguli oris (DAO) muscle. The bipolar montage was constructed by subtracting consecutive monopolar signals. The relatively low amplitude of the 4th bipolar signal (from the bottom) and opposite signal polarity on both sides of this signal indicates an endplate location between the 4th and 5th monopolar electrodes (from the bottom) of the selected electrode column. (B) 300ms window of bipolar data (recorded around the onset of the short isotonic DAO contraction) revealing the good baseline stability of the signals derived from our new electrode grid. Note that the signal was only band-pass filtered by hardware (cut-off frequencies 3.5 / 400 Hz). (C) Bipolar data (100ms) recorded prior to the DAO contraction demonstrating the low noise level of the signals recorded with our electrode grid (note the voltage range in the diagram of +/- 10µV). The median value in the study group (calculated from the 50th percentile values of the individual measurements) was $2.32\mu V_{rms}$ (RTI) for sEMG recordings taken in the upper face at rest.

can be assessed from Fig. 5-5C, which shows a data window of 100ms EMG at large amplification recorded prior to the DAO contraction. For signals recorded in the upper face at rest, we calculated a median noise level of $2.32\mu V_{rms}$ (RTI) (RTI: referred to input). The corresponding median values of the 5th and 95th percentiles were 1.92 and $5.24\mu V_{rms}$ (RTI).

Using the algorithm described above, we decomposed sEMG data recorded during selective contractions of different facial muscles at a moderate level, i.e. contractions of 20 - 40% of the maximal voluntary contraction. As a result of these calculations, we obtained templates or "fingerprints" showing the spatio-temporal characteristics of individual MU action potentials (MUAPs). Fig. 5-6A shows two electrode grids attached for recordings in the lower face. The Figs. 5-6B-F show examples of MUAPs belonging to different facial muscles underlying the attached grids, i.e. the depressor anguli oris (DAO), depressor labii inferioris (DLI), mentalis (MEN) and orbicularis oris inferior (OOI) muscles.

The template decomposed from data recorded during the selective contraction of the DAO muscle (Fig. 5-6B) shows a relative symmetric amplitude distribution. The endplates are located in the cranio-caudal centre of the muscle. In contrast, the neuromuscular junctions of the MU belonging to the DLI muscle (Fig. 5-6C) are located inferior to the anatomical centre of the muscle (note that the DLI muscle was completely covered by the two 6 by 10 electrode grids). The finding of asymmetrically located endplate zones and oblique fibre direction in this muscle was consistent in all subjects. The template calculated from data recorded during the MEN muscle contraction shows quite an asymmetric amplitude distribution in the vertical direction (Fig. 5-6D); above the endplate zone, the signal amplitude rapidly decreases in the cranial direction. In the OOI muscle, we found MUs with small territories and neuromuscular junctions in distinct locations (Fig. 5-6E+F).

Discussion

Advantages of a new type of sEMG electrode grid have been demonstrated in a real applied situation. The flexibility of the new electrode grids, together with the possibility of mass/series production, are significant positive features for the development of clinical applications of high-density sEMG. Since the thin electrode carrier material allows grids of any desired size and shape to be cut out, one universal grid version can be used for many applications. If this basic grid is manufactured in large numbers, the unit price can be kept at relatively low level; for a grid size of 7 by 13 electrodes and an output of 1000 units, the manufacturer gives a rough estimate of €50 / unit.

The performance of the new sensor introduced in this contribution becomes clear from the results of the impedance and noise calculations as well as from the presented signal examples. The electrode-to-skin impedances obtainable with our technique were found to be relatively low. Nearly all impedance values were far below $300k\Omega$ (see Fig. 5-4). The latter value is – if obtained for the majority of electrodes – considered to be acceptable for such type of recording configuration (Blok et al. 2002). Impedance measurements with and without the use of electrode cream in three subjects revealed the great significance of electrode cream application regarding a good and stable electrical connection of the electrodes; impedance values with our non-serrated electrode design were found to be about 40 times higher in dry electrode application. Since the cream was applied only in the areas of the detection surfaces, we avoided short-circuits between adjacent electrodes. Short-circuiting indeed is a problem when the cream is evenly
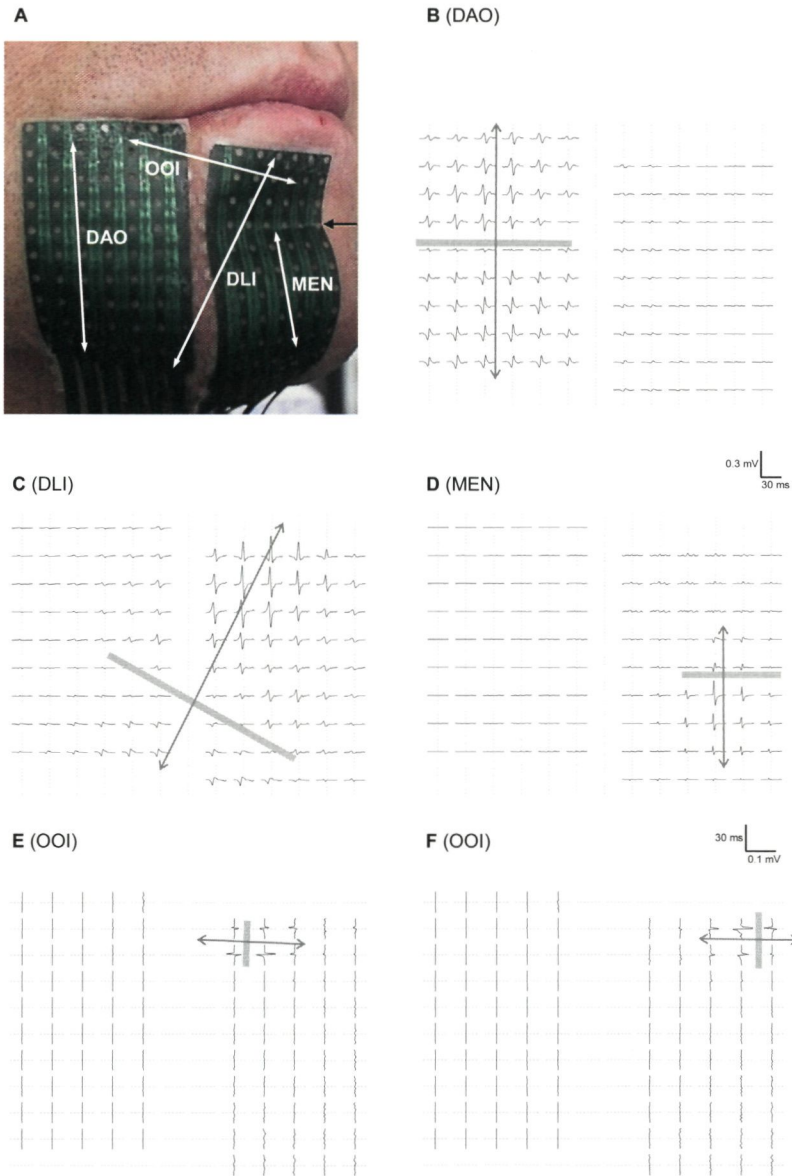
Figure 5-6. (A) Two multi-electrode grids attached to the lower face. The position and fibre direction of the underlying facial muscles are indicated by white arrows. (B-F) Five different bipolar MU templates decomposed from data recorded during selective, moderate contractions of (B) the depressor anguli oris (DAO), (C) the depressor labii inferioris (DLI), (D) the mentalis (MEN), or (E+F) the orbicularis oris inferior (OOI) muscle. According to the fibre orientation of the corresponding muscle, the bipolar montage was constructed by subtracting monopolar signals of consecutive vertical (in the DAO, DLI and MEN templates, see B-D) or horizontal electrodes (in the OOI templates, see E+F). The grey bar in each template indicates the location of the innervation zone. Note that in the two OOI templates (E+F) the time and amplitude axes are exchanged (in order to facilitate endplate localization in the horizontal bipolar electrode montage). The 2-D orientation of these MUAPs (outlined by double arrows) is in good agreement with the anatomical position and fibre direction of the contracted facial muscles (Blair 1986; Braus and Elze 1954; Salmons 1995).

applied in the whole recording area (Masuda and Sadoyama 1988). The low impedance values also explain the lower noise level at rest when compared with signals recorded with gold-coated metal pin electrodes (Blok et al. 2002). In this respect it has to be taken into account that the calculated median noise level (at rest) of $2.32\mu V_{rms}$ (RTI) not only includes thermal noise of the electrodes, but also amplifier noise ($0.8\mu V_{rms}$(RTI) were specified from tests on the instrument) and some physiologic noise. Based on these values, thermal electrode noise plus physiologic noise was $2.18\mu V_{rms}$(RTI). The good noise performance of the electrode grid may prove to be particularly advantageous in the detection of small and/or deeply located MU potentials. The good baseline stability, demonstrated by the recording during a short contraction, results from the chlorided pure-silver electrode surfaces; this material is known to have excellent metal-tissue properties over a broad frequency range (Cooper et al. 1980; Geddes 1972; Janz and Taniguchi 1953; Tassinary et al. 1990).

Due to the exceptionally high mechanical flexibility of the electrode carrying Polyimid* substrate, good electrical connections of the single electrodes could be achieved even in areas with very uneven contours (e.g. in subjects having a particularly deep mentolabial sulcus). A flexible electrode arrangement (at least in one dimension) was already achieved in previous high-density sEMG arrays, by mounting metal pin electrodes either on springs (KC McGill, personal communication) or on a semi-flexible print supported by a cushion of plastic foam (Blok et al. 2002). Indeed, such array versions led to an improvement regarding a more even pressure distribution on the skin surface (the latter is important for minimising the risk of poor electrical contacts in marginal parts of the recording area and for reducing the mechanical deforma-

tion of the underlying muscle). However, the flexibility obtainable with such conventional techniques is limited (at least it is much less compared with that of Polyimid* flexprints). Moreover, the crucial advantage of our new sensor is the combination of both high flexibility and minimal thickness. In investigations in which measured and modelled 2-D sEMG data are compared, it may be advantageous if measurements are taken with a rigid (i.e. inflexible) electrode array applied with pressure, because a curved spatial electrode arrangement (and also changes of the array's shape during the contraction) would make modelling very complicated. These circumstances can also be realised with our high flexible electrode grid; its electrode arrangement can be kept flat by bonding a rigid plastic foil on the reverse side, and pressure can be exerted using medical plasters or Velcro tied around a limb.

The new technique in which the electrode grid was attached to the skin turned out to be very efficient. In the majority of measurements, the electrode-to-skin attachment proved to withstand moisture (i.e. saliva in the perioral region) as well as large and dynamic tensile forces. We observed a loss of electrical connection or instable electrode-to-skin impedance values during the measurements in a few electrodes at the borders of the grids, in a few subjects showing extremely contoured soft-tissue in the chin and lower lip region and (i.e. a deep mentolabial sulcus). Contact loss is explained by these extreme conditions together with the insertion of the MEN muscle fibres in an obtuse angle directly in the mental dermis. Thus, the electrode-to-skin bonding of the grid was obviously exposed to very high tensile forces during maximal contractions of this muscle. An explanation for loss of electrical connection during measurements in the area immediately around the oral opening was the presence of saliva that may have dissolved the adhesive. The fact that contact loss mainly

occurred in the chin and lower lip region, i.e. in the lower face, explains the less pronounced impedance reduction during the recordings in this part of the face when compared with the upper face. The firm skin fixation of the flexible electrode grid arranged by means of double adhesive tape has the disadvantage that the orientation of the electrode grid cannot be changed after it is definitively attached to the skin. This is of significance, as in some muscles (e.g. in large limb muscles) it may be difficult to find the suitable sensor position and orientation (relative to the course of the muscle fibres) without monitoring signal amplitude distribution in the recording area. Possible solutions are to improve the criteria for guiding placement or to repeat the whole attachment procedure if inaccurate grid placement occurs. Another, probably more practicable possibility would be to perform a quick pre-measurement with an electrode grid pressed to the skin by hand. In this manner, the optimal orientation and position might be determined prior to definitive skin attachment. A final possibility that might be feasible is to correct the misalignment in data analysis using special alignment correction algorithms. Possible solutions still have to be explored.

By applying this technique to the facial musculature, we were not only able to demonstrate the good performance of our new electrode grid, but also to illustrate the general possibilities and advantages of the 2-D high-density sEMG technique. The topographical information of decomposed MUAPs makes it possible to determine the position of the motor endplate zones (Hilfiker and Meyer 1984; Masuda and Sadoyama 1988) and the area with highest signal amplitude ("go where the action is" principle). The results as presented here reveal some of the distinctive characters of facial MU topography; the occurrence of asymmetrically located endplate zones and neuromuscular junctions distrib-

uted over distinct areas of the muscle. These findings agree with those of histo-chemical studies (Happak et al. 1997). Knowledge of the location of neuromuscular junctions and areas of high signal amplitude is indispensable in establishing guidelines for placement of conventional electrode configurations (Falla et al. 2002; Tassinary et al. 1989). The decomposition of the sEMG interference pattern into the contributions of single MUs appears particularly useful in the complex facial muscle system consisting of many interweaving and overlying muscular slips (Blair 1986; Braus and Elze 1954; Salmons 1995). The spatial profile of extracted MUAPs allows them to be classified as belonging to certain facial muscle subcomponents. It is therefore possible to map the highly variable facial muscle structure (Kennedy and Abbs 1979; Sato 1968). From the clinical point of view, this may be particularly useful (1) for describing characteristic alterations on the MU level in neuromuscular disorders (examples of such diseases affecting the facial musculature are facioscapulohumeral dystrophy and Möbius syndrome), and (2) for observing regeneration and reinnervation of MUs after peripheral nerve injuries or muscle transplantation. Another possible application, based on the spatio-temporal information of decomposed sEMG data, is the differentiation between the contributions of individual muscles to the sEMG interference pattern in the examination of specific functions. This option may prove to be an efficient strategy in the suppression of crosstalk, which is a special problem in the facial muscle system (Blair and Smith 1986; Lapatki et al. 2003). Our results demonstrate that decomposed multichannel sEMG data even provide information regarding the 3-D orientation of muscle fibres. The progressive decrease of the signal amplitude in cranial direction in the MEN template can be explained by an increasing distance between the bio-electric source and the elec-

5

trodes (the MEN fibres course from the mental dermis in dorso-cranial direction towards their origin at the mandibular bone in the depth of the mental soft-tissues).

Although high-density sEMG is not yet used in daily clinical practice, our universally applicable and relatively inexpensive sensor might bring this non-invasive technique closer to the physician. Since sEMG electrodes cannot detect single fibre potentials, they can not replace intra-muscular electrodes for clinical diagnostic purposes. In the characterisation of single MUs an overlap exists between these two techniques. Especially here, our new multi-electrode sEMG grid offers an attractive alternative to conventional needle or fine-wire electrodes, whereby the non-invasive sEMG character is particularly appealing in some recording areas (as shown here for the face), in children, and in long-term studies (Wood et al. 2001). At present, a number of patho-physiological mechanisms causing neuromuscular disorders have escaped the keen eye of the needle electromyographer due to the topographic character of the pathology (Drost et al. 2001); studying topographic aspects of neuromuscular diseases (on the level of both the muscle and MU) clearly belongs to the domain of high-density sEMG. In this respect, it is worthwhile to further explore clinical applications and possibilities of this technique.

5

Part III

Utilising topographical information of motor unit action potentials

The fundamental research part of this thesis comprises the collection of topographical information on facial motor units in a group of healthy volunteers. We aimed at utilising this information for refining the understanding of the anatomical and functional properties of this part of the human musculature by an analysis on the level of the smallest functional units of the neuromuscular system. The knowledge obtained on motor unit territories, muscle fibre orientations and motor endplate zones should be interpreted in the context of the available macro-anatomical knowledge which has been derived from dissected human cadavers. A second goal was to utilise the extracted topographical motor unit amplitude profiles for improving measurements with conventional bipolar surface EMG electrodes in the face. Bipolar surface EMG has proven to be a valuable research and diagnostic tool for studying facial muscle function in several medical fields. In the face, the reliability and validity of this tool is limited, because objective guidelines for electrode positioning are lacking and recordings are confounded by cross-talk from multiple adjacent muscles. The complete muscle-selectivity of data on the motor unit level was expected to be a valuable source for resolving these problems.

6

Topographical characteristics of motor units of the lower facial musculature revealed by means of high-density surface EMG

Lapatki B.G., van Dijk J.P., Jonas I.E., Zwarts M.J., Stegeman D.F.

The objective of this study was to systematically characterise motor units (MUs) of the musculature of the lower face. MU endplate positions and principal muscle fibre orientations relative to facial landmarks were identified. This was done by the analysis of motor unit action potentials (MUAPs) in the surface EMG. Thirteen specially trained, healthy subjects performed selective contractions of the depressor anguli oris, depressor labii inferioris, mentalis, and orbicularis oris inferior muscles. Signals were recorded using recently developed, 0.3mm-thin and flexible high-density surface electromyography (sEMG) grids (120 channels). For each subject and each muscle and for different low contraction levels, representative MUAPs ("MU fingerprints") were extracted from the raw sEMG data according their spatio-temporal amplitude characteristics. We then topographically characterised the lower facial MUs' endplate zones and main muscle fibre orientations on the individual faces of the subjects. These topographical MU parameters were spatially warped to correct for the different sizes and shapes of the faces of individual subjects. This electrophysiological study revealed a distribution of the lower facial MU endplates in more or less restricted, distinct clusters on the muscle often with eccentric locations. The results add substantially to the basic neurophysiologic and anatomical knowledge of the complex facial muscle system. They can also be used to establish objective guidelines for placement of conventional (surface or needle) EMG electrodes as well as for clinical investigations on neuromuscular diseases affecting the facial musculature. The localised endplate positions may also indicate optimal locations for botulinum toxin injection in the face.

6

Introduction

The facial musculature is a three-dimensional assembly of multiple small muscle bundles and sheet-like muscle fibre arrays. The independently controlled subcomponents of this complex muscle system are of great importance for the functioning of the orofacial sense organs and in the mediation of emotional and affective states (mimic expression). Characteristic anatomical features of the facial muscles are: (1) non-tendenous attachments to soft tissue (in some muscles including origins), i.e., to facial skin or other muscle tissue, (2) interdigitation and overlap in relatively small areas (especially in the lower facial area), and (3) high inter- and intra-individual variability in location and morphology (Blair 1986; Braus and Elze 1954; Kennedy and Abbs 1979; Nairn 1975; Salmons 1995). Facial movements are mediated by an integrated network which includes neural systems mediating both voluntary and emotional drive from the cortex and the facial nucleus (Hopf et al. 1992; Morecraft et al. 2001).

Despite the great functional importance and the unique morphological and neural characteristics of the facial musculature, "there is no doubt that very little research of any sort has been done on the muscles innervated by the facial nerve" (May and Schaitkin 2000). This is especially true for systematic electrophysiological investigations at a single motor unit (MU) level. In the few EMG studies on facial MU characteristics, firing behaviour (Blair 1988; Kamen and De Luca 1992), recruitment patterns and reflex responses (Lansing et al. 1991; Mateika et al. 1998; McClean and Smith 1982; McClean 1991; Smith et al. 1981; Valls-Sole et al. 1992; Wohlert 1996b) were examined mostly with needle electrodes (the standard technique for electrophysiolog-

ical studies at a MU level). Until now, other basic properties of facial MUs, such as their spatial spread and orientation, and the location of the endplate zones, were not specified (except a rough determination of MU territories in the human lip musculature (Goffman and Smith 1994)). High-density sEMG (Blok et al. 2002; Farina et al. 2000; Huppertz et al. 1997; Masuda and Sadoyama 1988; Prutchi 1995; Wood et al. 2001; Yamada et al. 1987) is the obvious method of choice to fill that gap of knowledge. However, this technique could not be applied to the facial musculature due to technical limitations and lack of appropriate signal processing tools, combined with the methodological demands for EMG studies in the facial area (Cole et al. 1983; Lapatki et al. 2003). The latter are related to: (1) uneven skin contours in the face requiring highly flexible electrode arrays, (2) skin distortions during facial muscle contractions and flow of saliva, both increasing the risk of sensor attachment loss, as well as (3) general problems in attaching an electrode array to the face. These problems have been solved by the development of thin and highly flexible multi-electrode grids together with a suitable skin attachment technique for this type of sensor (Lapatki et al. 2004).

This study was undertaken to systematically determine topographical MU characteristics (i.e. their location, spatial orientation and endplate zone) of the facial musculature by means of high-density sEMG, and to compare the results to basic anatomical knowledge and data obtained in histo-chemical studies. It is expected that the results will significantly contribute to our basic knowledge on human (neuro-)physiology, and also enable informed guidelines to be derived for the placement of conventional (surface or needle) EMG electrodes. In this article, results of measurements in the lower face are presented. In a subsequent paper we will publish the results from the mid-

and upper face.

Methods

Subjects

The study group consisted of 13 subjects (6 men and 7 women, mean age 27.2 yr, range 21 – 43 yr) without known neurological or general health disorders. Nine of the subjects were trumpeters (7 music students and 2 professionals), who were expected to have good facial motor control and to be motivated to improve on that. In the run-up to the measurements, a special training program was designed and implemented to improve the ability of the participants in performing selective contractions, i.e. isolated activations of the individual facial muscles. The Ethics Commission of the University Medical Centre Nijmegen (NL) approved the protocol of the study.

Sensors for high-density sEMG measurements

The recently developed multielectrode sEMG grids (Digiraster Tetzner GmbH, Stuttgart, Germany) applied in this study were manufactured using flexprint techniques. They consist of regularly arranged, chlorided silver electrodes 2 mm in diameter with an interelectrode distance (IED) of 4 mm (centre to centre) in both directions. This IED value allowed a sufficient spatial sampling for the facial musculature. These electrode grids (Fig. 6-1A) were attached to the skin using double-sided adhesive tape (1522 Medical double coated tape, 3M, St. Paul, MN, USA) that had been prepared for this application by creating regular perforation patterns. The elaborated skin attachment procedure yields firm sensor fixation without requiring external fixations. High signal quality was achieved due to the relatively low electrode-to-skin impedances (Lapatki et al. 2004).
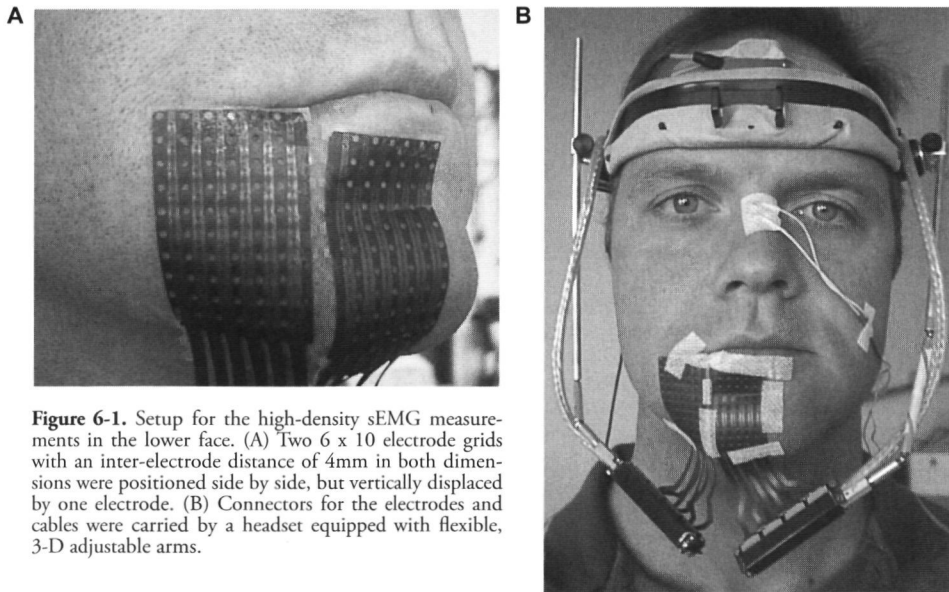
Figure 6-1. Setup for the high-density sEMG measurements in the lower face. (A) Two 6 x 10 electrode grids with an inter-electrode distance of 4mm in both dimensions were positioned side by side, but vertically displaced by one electrode. (B) Connectors for the electrodes and cables were carried by a headset equipped with flexible, 3-D adjustable arms.

6

Data acquisition

Electrical connections to the amplifiers were made with help of a headset equipped with flexible arms and connectors for the electrodes (Fig. 6-1B). Data were acquired "monopolarly", i.e. referred to a remote reference electrode (material: Ag/AgCl, diameter: 4 mm) attached on the dorsum nasi. A second reference electrode provided a common mode signal (CMS). In addition, a driven right leg (DRL) electrode was attached at the forehead (Metting van Rijn et al. 1990).

The system used for data acquisition (Mark-6, BioSemi Inc., Amsterdam, NL) has an input impedance > 100 MΩ and a CMRR > 120 dB. Signals were band-pass filtered (3.2 – 400 Hz; high-pass: first order Bessel, low-pass: fourth order Bessel) and synchronously sampled at 2000 Hz with a resolution of 0.5 µV/bit over a range of +/-16 mV (16 bits). The acquisition software allows the experiments to be controlled by on-line inspection of the raw monopolar or bipolar data of selected electrode rows or columns (Blok et

al. 2002). Since contractions of facial muscles at a constant level are difficult to perform, we implemented an sEMG amplitude feedback tool in the acquisition software that visually displayed the normalised mean RMS value of selected bipolar signals (and so the activity level of the underlying muscle) to the subject via the PC monitor. The RMS was calculated for data windows of 500 ms; normalisation was made to a maximal reference contraction of the muscle.

Setup for the measurements and electrode positioning

We examined the subjects' lower facial musculature unilaterally either on the right (7 subjects) or the left (6 subjects) side of the face. Two grids of 6 x 10 electrodes were positioned side by side, but vertically displaced by one electrode row according to criteria explained in the legends to Fig. 6-2.
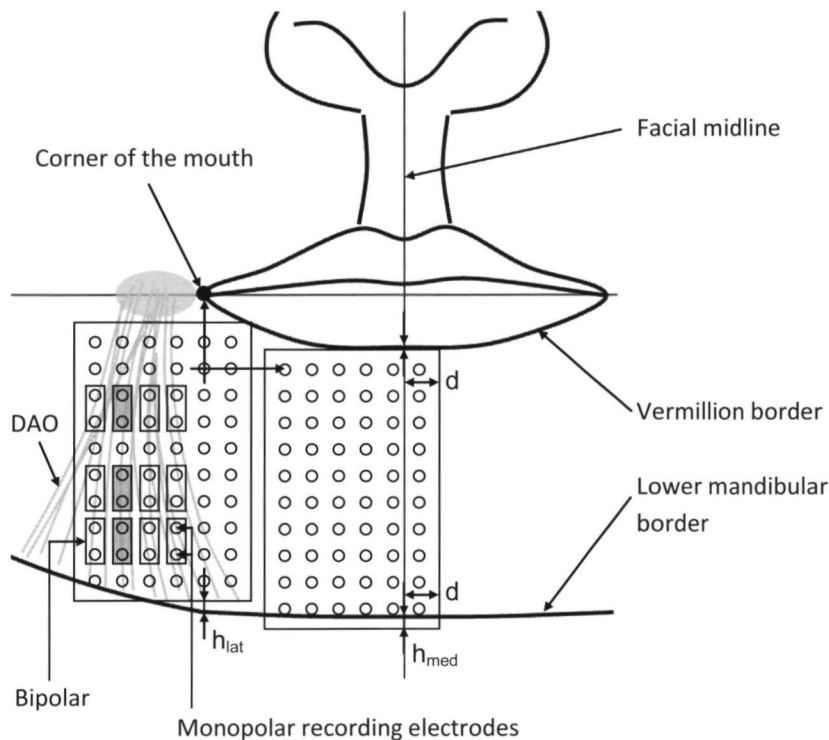
Figure 6-2. Details regarding electrode grid placement and input channel selection for decomposition of the raw data. The black circles represent the 120 (2 x 60) recording electrodes. One electrode column in between the medial and lateral electrode grid was missing so that the inter-electrode distance in the corresponding area was (exactly) double. Grid positioning was guided by the corner of the mouth, the facial midline and the inferior border of the lower lip vermilion. Medial-lateral placement criterion was the alignment of the 5th electrode column (from lateral) with the corner of the mouth. In the vertical dimension, the upper border of the medial grid was aligned with the lower lip vermilion. The third placement criterion was the parallel position between the medial grid border and the facial midline resulting in an equal distance d in the upper and lower part of the grid. According to the individual subject's facial dimensions, the lower grid borders were above or below the mandibula's lower border (resulting in positive or negative hmed and hlat values, respectively). The vertical rectangles (enclosing two recording electrodes each) illustrate that bipolar signals were calculated from two adjacent monopolar signals in vertical direction. For decomposition of the sEMG pattern, peaks were detected in three bipolar signals (in this example corresponding with the small grey rectangles). Signal input for the peak classification was extended (in this example to 12 bipolar signals, see grey and transparent rectangles) to get a better representation of the MUAPs' topography in both the vertical and horizontal facial dimension.

Recording procedure

After electrically connecting the grids, subjects were again instructed and trained in the performance of the experimental tasks now controlled by on-line inspection of selected signal amplitudes (i.e. the visual amplitude feedback derived above). When the selective motor control in the lower face was considered to be sufficient and the subjects were accu-tomed to the recording conditions, data (120 channels) were acquired while the depressor anguli oris (DAO), the depressor labii inferi-oris (DLI), the mentalis (MEN), or the orbicu-laris oris inferior (OOI) muscle was selectively activated at different levels. The facial poses corresponding to the selective contractions of these four lower facial muscles are shown in Fig. 6-3.

A: Rest

B: DAO

C: DLI

6
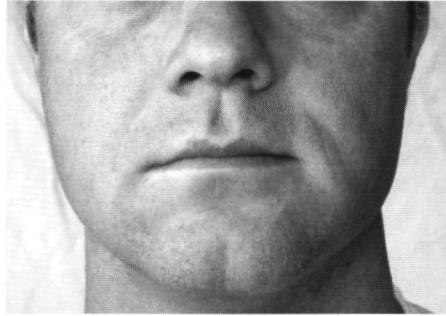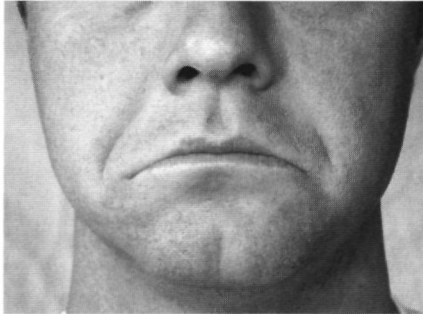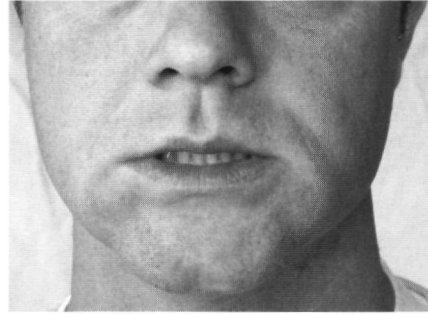
D: MEN
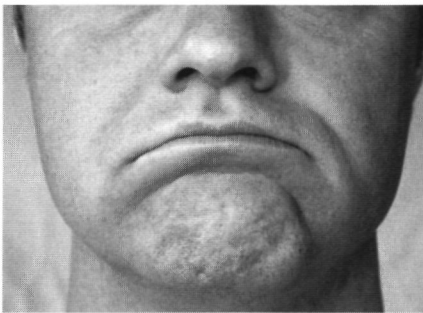
E: OOI
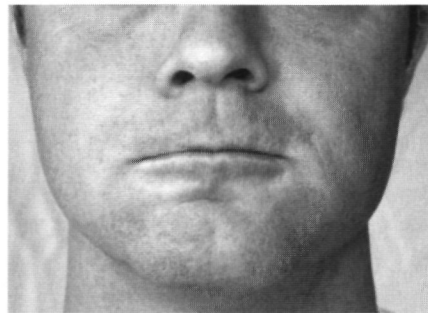
Figure 6-3. Photographs of facial expressions taken during selective, moderate contractions of the four subcomponents of the lower facial musculature. (A) Face at rest. Contractions of (B) the depressor anguli oris, (C) depressor labii inferioris, (D) mentalis, and (E) orbicularis oris muscles.

In each muscle we performed two recordings per activity level with approximately 20 s duration each. The first recordings were made at the activity level at which clear MU firings could be determined in the bipolar signals over the area of the corresponding muscle; this level corresponded most often with 2-3 % of maximal voluntary contraction (MVC). Then, the subjects were asked to perform contractions at 5 %, 10 %, 15 %, 20 %, 25 %, and 30 % of MVC so that in total 14 x 20 s of data was recorded per subject and muscle.

Data analysis

Data were analyzed off-line using algorithms programmed in Matlab, Version 6.5 (The Mathworks Inc., Natick, MA, USA). After extracting MUAPs from all recorded data (decomposition) we selected for each subject and muscle a data file containing a representative set of MUAPs; the physiological parameters of interest, the MU endplate positions and muscle fibre orientations, were then extracted from these MUAPs; finally, to allow the comparison and combination of the individual results, the extracted topographical MU parameters were normalised.

Decomposition of the sEMG pattern

MU action potentials (MUAPs) were extracted from the first 16 s of the recorded data on the basis of the specific topographical profiles and amplitude characteristics of the peaks. The decomposition procedure was based on a previously described method (Kleine et al. 2000a) and principally consisted of the following three components: (1) peak detection in three selected bipolar signals, (2) classification of the data around the detected peaks according to their differential spatio-temporal amplitude characteristics, and (3) averaging broader data windows around the classified peaks, for each peak group, and for all recording channels. Most of these steps were largely automated.

Peak detection was performed in three bipolar signals recorded in distinct locations along the fibres of the contracted muscle (indicated as an example by the three small grey rectangles in the left grid of Fig. 6-2). Thus we took into account that facial MUs can lie in distinct areas of the muscle. The algorithm guaranteed that peaks within one channel occurring less than 8 ms apart were eliminated from the determined list of peak-occurrence times, and that peaks resulting from a specific MU firing that were detected in several channels, were considered only once.

Peak classification was based on the Ward's clustering algorithm (Everitt et al. 2001) using "Euclidean distances" between the spatio-temporal amplitude characteristics of 16 ms of data around the detected peaks. One important issue in this classification is the consideration of the differential amplitude topographies of the peaks. Preliminary observation of data from the facial muscles revealed that the amplitude topographies of facial MUAPs could be significantly distinguished in both the dimensions perpendicular and parallel to the muscle fibre direction. As a consequence, we selected an extended set of input channels for the peak classification procedure that represented distinct topographical regions of the corresponding muscle in both dimensions (indicated by the three rows of four bipolar signals illustrated in Fig. 6-2). The time-shift between peaks from distinct channels, due to signal propagation, was accounted for by determining the peak latency (using a cross-correlation technique) and aligning the signals accordingly. The stopping criterion of the hierarchical clustering algorithm requires that the number of clusters be pre-defined. We chose this number to be approximately four times the number of active MUs expected. The latter number was estimated from the length of the evaluated data segment, the number of detected peaks, and the average firing rates of facial MUs (Blair 1988; Kamen and De Luca 1992). In this manner we ensured that there was a low probability that peaks with significantly distinct amplitude topographies (i.e. peaks belonging to distinct MUs) were classified into one group.

After performing spike triggered averaging of the peaks for each classified peak group and recording channel (here we used 80 ms of data around the classified peaks in order to include the whole width of the MUAP), we obtained a set of low-noise MUAP templates for each activity level and repetition, which could be

regarded as representative "fingerprints" of the MUs that contributed to the contraction. From this data set, MUAPs averaged from a small number of peaks were removed.

Selection of a representative MUAP template set

All decomposed data were inspected in order to select one set of MUAP templates (belonging to a certain recording level and repetition, respectively) per subject and muscle which best represented the distinct MUAP topographies observed in the template sets obtained from all recording levels and repetitions. To facilitate the differentiation of the MUAPs' distinct amplitude topographies, we scanned the template sets in their bipolar montage (see also Fig. 6-5). Topographical MU parameters were only determined for the selected MUAP template sets. The corresponding methods used the MUAP data in a monopolar montage.

Determination of innervation zone location and muscle fibre orientation

The location of the innervation zone and the main muscle fibre orientation of a MU correspond to the location where the MUAP starts and in which direction it propagates. From the spatial and temporal information contained in an averaged monopolar MUAP, which can be illustrated either as a template or as a time sequence of amplitude maps (see Fig. 6-4A or Fig. 6-4D), both of these parameters can be derived. Our method included the following steps: (1) two-dimensional interpolation of the monopolar MUAP data, (2) determination of the initial phase of the MUAP (MUAP initiation), (3) localisation of the standing maximal amplitude area in the initial MUAP phase (and endplate zone, respectively) on the electrode grid, (4) determination of the latencies (in both directions of signal propagation) when the propagation terminated or became diffuse (MUAP termination), and (5) locali-

sation of the maximal amplitude area on the electrode grid at the terminal MUAP latency (in both directions of propagation) and subsequent calculation of the main muscle fibre orientations.

The interpolation was performed in two stages using a bicubic method. First, we calculated the monopolar data of the missing electrode column in between the two attached electrode grids (see Fig. 6-2). Then, we interpolated the complete template data set in both dimensions 8 times between adjacent electrodes. In this manner we increased the topographical resolution of the localisation of the MUAP initiation and termination to a value of 0.5 mm (instead of the IED value of 4 mm).

The method for determining the initial phase of the MUAP was based on the fact that the main peak of the monopolar MUAP appears first in the grid area around the endplates. Another important aspect is that the monopolar amplitude values in this area are usually high compared to the amplitudes in other grid areas and, therefore, significantly contribute to the average of the absolute monopolar MUAP signals over the whole grid (called "single time series", see Fig. 6-4C). For these reasons, the MUAP initiation can be determined by means of a predefined amplitude threshold in the single time series. We used a threshold of 40 % of the maximum level: this value was on the one hand usually above the average noise and smaller peaks in the single time series, and on the other below the average value of the signals around the endplate (so that their leading edge was detected). It is important to note that not the real start of the MUAP but a slightly longer latency was determined by our algorithm. However, since there is no apparent signal propagation in the initial MUAP stage, this had only a negligible influence on the accuracy of localising the endplate zone.

6
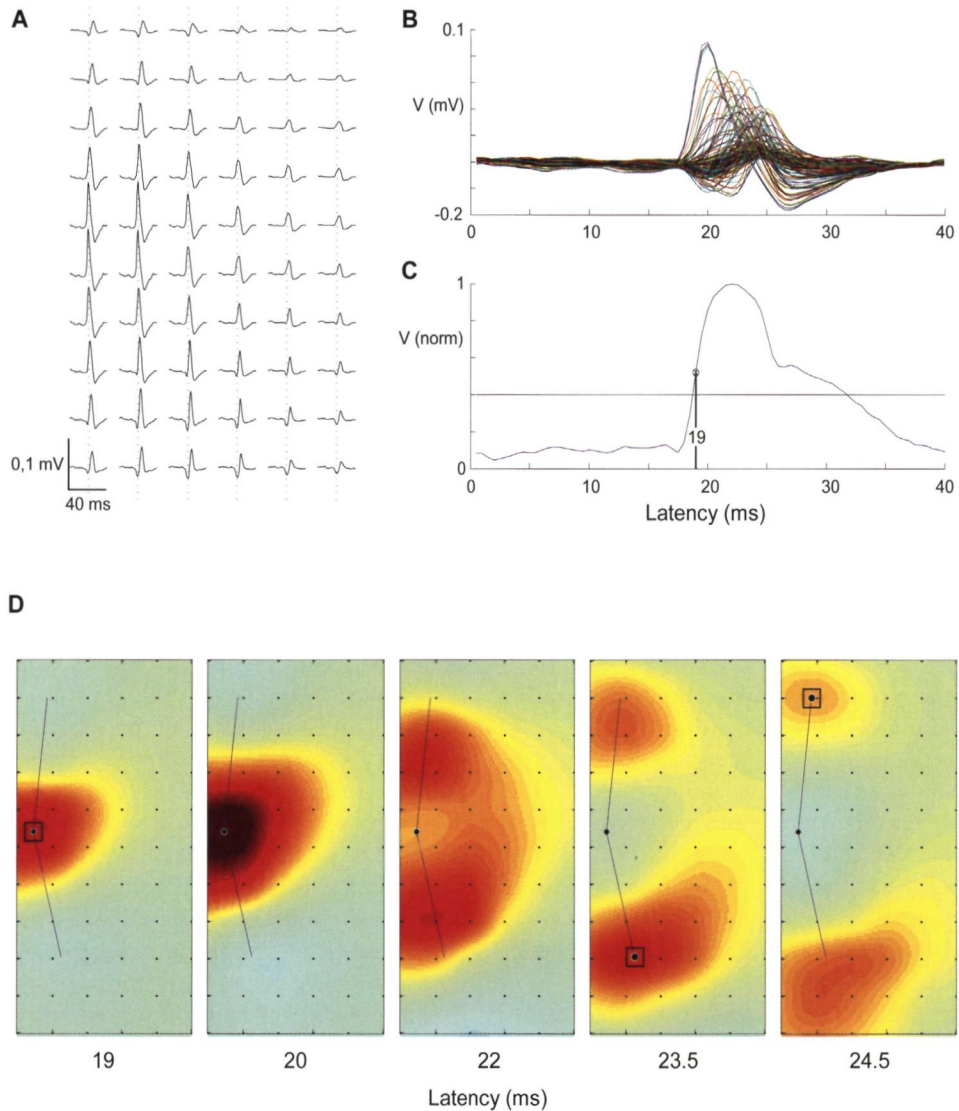
Figure 6-4. Illustration of the methods for determination of endplate position and muscle fibre orientation. (A) Example of a monopolar MUAP template decomposed from a recording during a depressor anguli oris muscle (DAO) contraction. Only the signals of the lateral 6 by 10 electrode grid (see Fig. 6-2) are shown. (B) Superimposition of these signals. (C) For determination of the endplate position, monopolar MUAP signals were averaged. The MUAP initiation was defined as the latency where the 40%-level was exceeded for the first time in the normalised average MUAP signal. (D) A sequence of interpolated monopolar amplitude maps illustrates topographically the initiation of the potential (latencies 19, 20) and its conduction in the upper and lower part of the DAO muscle (latencies 20, 22, 23.5, 24.5). Endplate position and muscle fibre orientation were determined by localising the grid areas of maximal amplitude (area size was ½ IED in both dimensions) in the interpolated monopolar amplitude maps at the latencies of MUAP initiation or termination.

The MUAP initiation was topographically characterised by searching for the (interpolated) electrode grid location of maximal amplitude in the corresponding interpolated monopolar amplitude map (Fig. 6-4D, latency 19). In order to reduce the influence of inhomogeneities in the area of maximal MUAP amplitude, the algorithm did not localise the single maximum amplitude value, but a maximal amplitude area (see black frame in Fig. 6-4D, latency 19).

The two latencies indicating the terminal stage of signal propagation away from the endplate zone in both (opposite) directions were determined by observing the complete amplitude map sequences of the corresponding MUAP. The main criteria for detecting the terminal MUAP stage included finding either a drastic reduction in amplitude, i.e. a decrease of approximately 50% within one IED (Fig. 6-4D, upper fibre direction), a beginning diffuse displacement of the propagating high amplitude zone (Fig. 6-4D, lower fibre direction), or a stationary amplitude maximum.

The position on the electrode grid corresponding to MUAP termination was localised in the same way as described for MUAP initiation, i.e. we also determined the position of the zone of maximal amplitude in the interpolated monopolar amplitude maps of the corresponding latencies (as shown by the black frames in Fig. 6-4D, latencies 23.5 and 24.5). The orientation of the muscle fibres could then be characterised as two vectors pointing from the endplate position to the (two) positions where the MUAP termination was localised. Accurate MUAP endplate location and muscle fibre orientation was verified by a final, careful observation of the complete amplitude map sequence (or "MUAP movie") with the superimposed results. If necessary, determination of these parameters was repeated with adapted threshold values and latencies, respectively.

Normalisation

The electrode grids were positioned according to the criteria specified in the legend of Fig. 6-2. The distances from the electrode grids to the facial midline, to the corner of the mouth, as well as to the median and lateral lower mandibular border were quantitatively determined after the sEMG recordings directly on the subject's face. Using the known interrelations between these specified facial landmarks and the electrodes it was possible to define the endplate positions and muscle fibre orientations (previously determined in electrode coordinates) in an individual facial coordinate system. Separately for each subject, we then applied a spatial scaling of the data to account for the different sizes and shapes of the subjects' faces; the individual facial dimensions (characterised by the centre and corner of the mouth as well as the lower mandibular border at the facial midline and at the medio-lateral level of the corner of the mouth) were warped so that they agreed with the average facial dimensions of the study group. The (constant) horizontal scaling factor for this warp was determined by the relation between the individual and average distance between the corner and the centre of the mouth. In the vertical dimension, separate scaling factors were calculated at the facial midline and at the corner of the mouth. The vertical scaling at other medio-lateral levels varied linearly between these two scaling factors. After applying this spatial normalisation, we could combine the data of all subjects in one figure and perform interindividual comparisons. Since no systematical differences between endplate positions and fibre orientations determined on the right and left face were found in any muscle, we finally performed a "mirror-image-transformation" of the parameters obtained from measurements on the left facial side to facilitate inter-individual comparison.

6

Results

Fig. 6-5 shows two monopolar (Figs. 6-5A and 5B) and two bipolar (Figs. 6-5C and 6-5D) MUAP templates decomposed from data recorded during a 5% (MVC) contraction of the DAO muscle. Only the signals derived from the lateral electrode grid (grey area in central graphic) are presented, because the signal amplitudes of the medial electrode grid were negligible for this muscle. Endplate positions and muscle fibre orientations are represented by grey dots and lines, respectively.

The correct localisation of the endplate (our method used the monopolar MUAPs) can be verified in the bipolar templates (Figs. 6-5C and 6-5D), in which the endplate position is indicated by low signal amplitude (in between signals of high amplitude) or reversal of signal polarity. The MUAP with higher mono- and bipolar amplitudes (Figs. 6-5A and 6-5C) represents the majority of the templates decomposed from this recording and has its endplates in the cranio-caudal (i.e. vertical) centre of the grid. The graphic in the middle of Fig. 6-5 shows that this location approximately corresponds with the cranio-caudal centre of the muscle. The MUAP presented on the right side (in monopolar and bipolar montage) has a smaller amplitude territory and its endplate zone has a more cranial and medial location.

Fig. 6-6 shows the endplate zones and DAO muscle fibre orientations of two representative subjects (Figs. 6-6A and 6-6B) and those parameters for all subjects included in our study (Figs. 6-6C and 6-6D). The data illustrated in Fig. 6-6A were derived from the MUAP template set from which two examples were presented in Fig. 6-5. The occurrence of a dominant endplate zone could be observed in 12 of the 13 subjects (one subject could not voluntarily contract the DAO muscle at all). In 9 of these 12 subjects, a second endplate cluster (or single additional endplates) was

found either in cranial-medial direction (in 8 subjects; examples see Figs. 6-6A and 6-6B), or in caudal-lateral direction (in 1 subject). With the exception of one subject, the MUs of this additional cluster had a smaller electrical size (i.e. the MUAPs had lower amplitude magnitudes) and smaller territories (indicated by the somewhat shorter muscle orientation lines).

Fig. 6-6C showing the data of all subjects proves that most DAO endplates are concentrated in a band-shaped area (running across the muscle in medio-lateral direction) which is located slightly inferior to half the distance between the modiolus and the mandibular's lower border. The dispersed endplates above this "band" were those of the additional cluster as mentioned above. The course of the muscle fibres was obviously different from subject to subject (Fig. 6-6D), varying from almost straight to rather curved courses (the latter is indicated by increased angulations of the superior and inferior muscle orientation lines). To demonstrate the effect of the normalisation procedure, endplate locations and fibre orientations of all subjects are also presented in this muscle in absolute facial coordinates (Figs. 6-6E and 6-6F). Comparisons of Figs. 6-6C with 6-6E and Figs. 6-6D with 6-6F illustrate the reduction of the inter-individual variability after correction for the individual sizes and shapes of the subject's faces. In the following figures only normalised data are shown.

The data from two representative subjects from the DLI muscle (Figs. 6-7A and 6-7B), demonstrate the occurrence of MU endplates only in the lower portion of the muscle, typically in a lateral and medial cluster. The fibres above the endplates are mainly orientated towards the medial portion of the respective lower lip quadrant. Fibre orientation in the caudal portion of the DLI muscle could not be determined for most decomposed MUAPs due to the short distance from the endplates to the origin.

A: Template #1 (monopolar)

B: Template #2 (monopolar)

Modiolus

DAO fibres

Template area

0.1 mV

40 ms

Monopolar electrodes

6

C: Template #1 (bipolar)
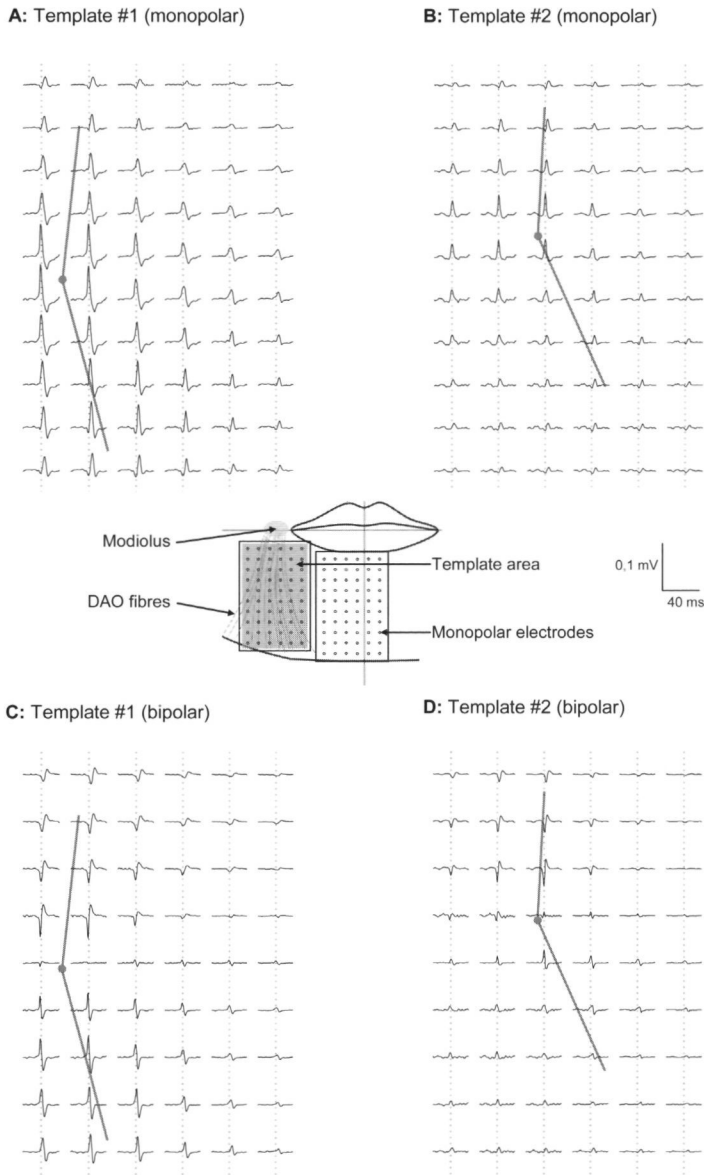
D: Template #2 (bipolar)

Figure 6-5. DAO muscle: Two monopolar and two corresponding bipolar templates showing the spatial amplitude profile of representative DAO MUAPs and superimposed results of endplate location and main muscle fibre orientation (in total, eight MUAPs were decomposed from the corresponding raw data). Only the signals derived from the lateral electrode grid are shown (grey area). The MUAPs were decomposed from signals recorded during a 5% MVC contraction of this muscle. Amplitudes were calibrated to a value of 0.1 mV (vertical inter-signal distance); data window width was 40 ms. The bipolar montage (C and D) was constructed by subtracting the (recorded) monopolar signals of consecutive electrodes in vertical direction. The position of the motor endplate zone can be detected from the bidirectional propagation pattern of the action potentials, which also results in low amplitude at and opposite signal polarity on both sides of the endplate (Masuda et al. 1983).

A: Subject #3, normalised values

B: Subject #7, normalised values

C: All subjects, normalised values

D: All subjects, normalised values

E: All subjects, absolute values (mm)

F: All subjects, absolute values (mm)
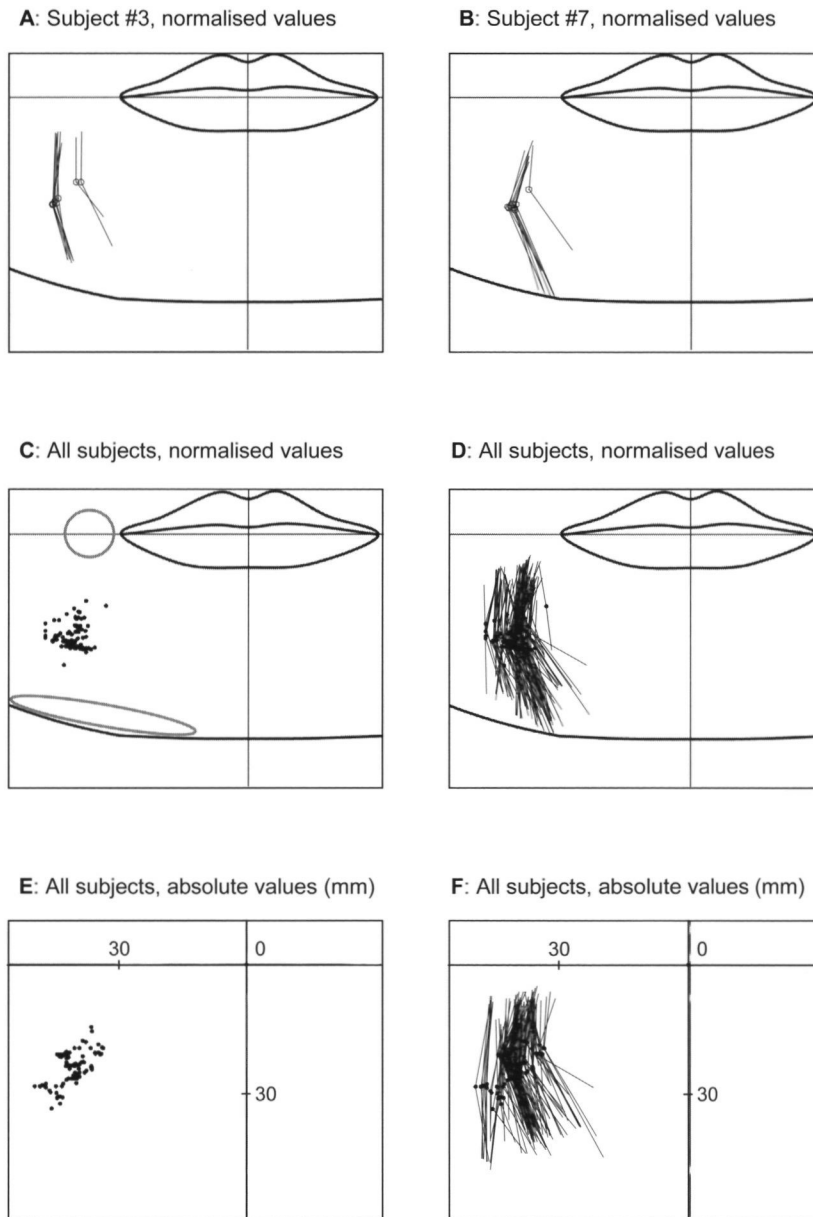
Figure 6-6. DAO endplate locations and muscle fibre orientations plotted on the schematic (average) face. (A) Results from the subject presented in Fig. 6-5. (B) Data from another individual subject. (C) Combined, normalised DAO endplate locations of all subjects with schematic representation (grey ovals) of the origin (at the lower lateral mandibular border) and the insertion (in the modiolus) of this muscle. (D) Combined, normalised DAO fibre orientations of all subjects. (E, F) Corresponding endplate locations (of all subjects) prior to their normalisation, i.e. given in millimeters (absolute coordinates).

A: Subject #2

B: Subject #9

C: All subjects

D: All subjects

6
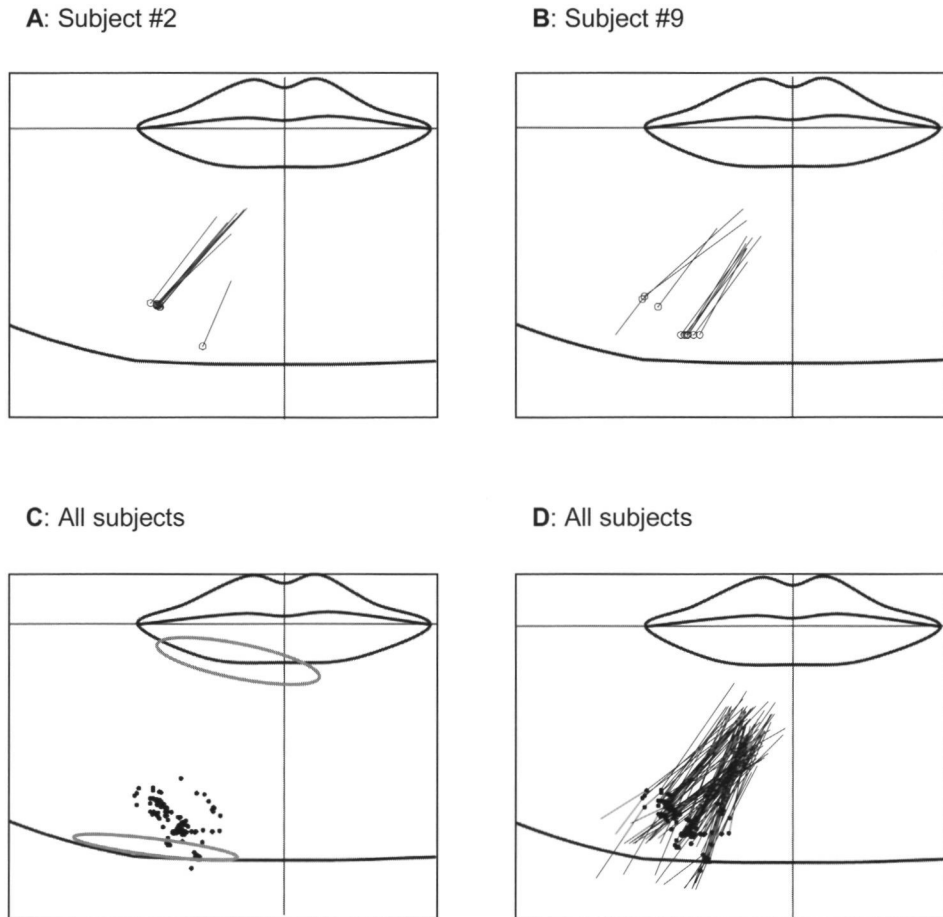
Figure 6-7. DLI endplate locations and muscle fibre orientations. (A, B) Individual data from two subjects showing clustered endplate distribution, i.e. accumulation of endplates in the muscle's lateral and medial portion. (C) Normalised DLI endplate positions of all subjects. In all subjects, DLI endplates were found to lie extremely eccentric between the origin of the muscle at the lower border of the mandibula and its insertion in the lower lip (grey ovals). (D) Normalised DLI fibre orientations of all subjects.

Fig. 6-7C proves that eccentric locations of DLI MU endplates (near the origin of this muscle) were a typical finding. The clear separation of the endplate locations in medial and lateral clusters in most of the individual data is only vaguely visible in the combined data of all subjects (obviously due to the inter-individual variability). DLI fibre orientation as specified above was a common finding in all subjects.

Moreover, in some MUAPs, signal propagation could be traced across the lower mandibular border.

Figs. 6-8A and 6-8B exemplify that MEN MU endplates could be found in both superior and inferior muscle portions, with a predominance of the superior location in most of the subjects. Typically, the superior endplates were concentrated in a relatively delimited area;

A: Subject #6

B: Subject #4

C: All subjects
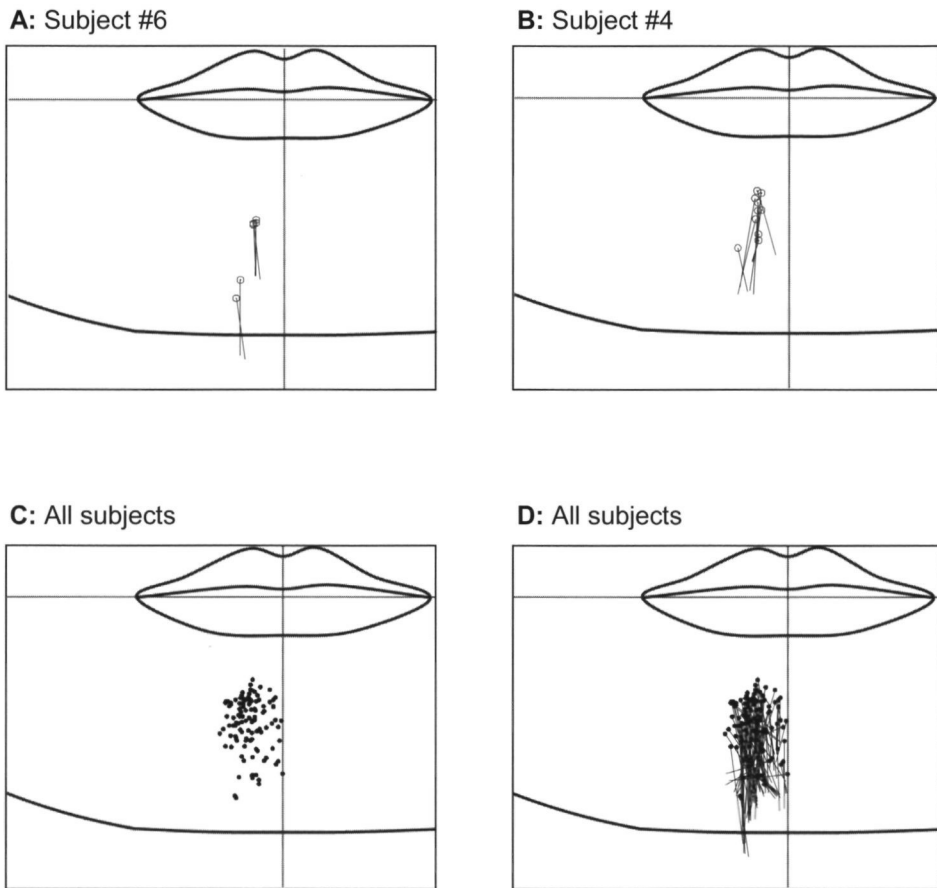
D: All subjects

Figure 6-8. Endplate locations and muscle fibre orientations of the MUs of the MEN muscle. (A, B) Representative results from two subjects. (C) Combined, normalised endplate positions of all subjects with schematic representations (grey ovals) of the muscle's origin (apical region of lower lateral incisors) and insertion (in the soft tissue mass of the chin). (D) Normalised MEN fibre orientations of all subjects, showing the relatively high inter- and intra-individual variability in this parameter.

a few inferior endplates were more widely distributed in the muscle's caudal portion (see as an example Fig. 6-8A).

Fig. 6-8C, showing the combined data of all subjects, indicates that the main concentration of MEN MU endplates lies approximately between 25 % - 50 % of the distance from the inferior border of the lower lip vermilion to the median inferior border of the mandibula. MEN muscle fibre orientation could only be

determined inferiorly to the endplates due to the very low amplitude values in the higher portions of the muscle. Inferior fibre orientation was predominantly vertical, with a relatively large variability (Figs. 6-8B and 6-8D).

Figs. 6-9A and 6-9B, which show individual results from the OOI muscle, exemplify the distribution of endplates on the whole area of the muscle and the presence of horizontal and short skew OOI fibres, as well as stationary

A: Subject #4
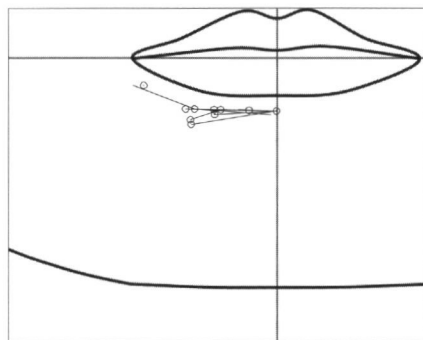
B: Subject #5
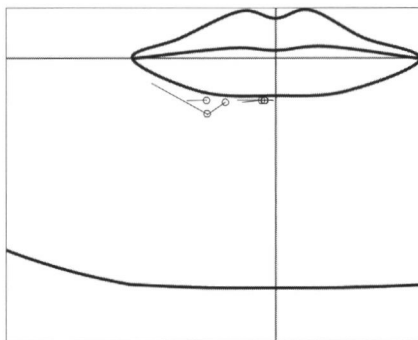
C: All subjects
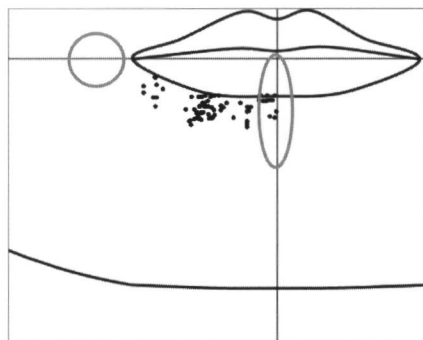
D: All subjects
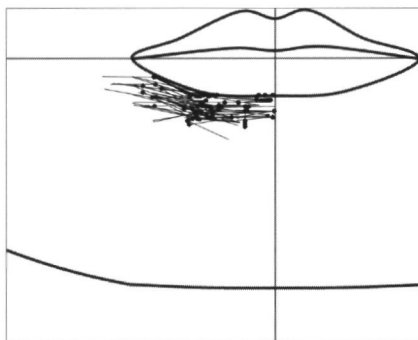
Figure 6-9. MU endplate locations and muscle fibre orientations in the OOI muscle. (A, B) Individual results from two subjects exemplifying the relatively dispersed endplate distribution in this muscle and the presence of both horizontal and skew OOI fibres. (C) Combined, normalised endplate locations of all subjects indicating a high density of endplates in the medio-lateral centre of the lower lip quadrant. (D) Combined, normalised muscle fibre orientations of all subjects showing the predominance of the horizontal OOI fibres.

(i.e. non-propagating) MUAPs.

Although in the individual data from the OOI we could not find clearly delimited endplate clusters, there was a tendency in 11 subjects for muscle innervation in the medio-lateral centre, i.e. at a location about half way between the corner of the mouth and the facial midline (Fig. 6-9C). Additional endplates were found in the medial OOI portion (in 10 subjects) and/or in an area medial and inferior to the corner of the mouth (in 4 subjects). One subject showed endplates only near the facial midline and near the modiolus, i.e. the typical occurrence of endplates in the centre of the lower lip quadrant was missing. Fig. 6-9D indicates the dominant OOI fibre orientation in parallel to the lower vermillion border, although short skew OOI fibres could also be found in most of the subjects.

Discussion

Sensor technique and data analysis

High signal quality was achieved with the multi-electrode sEMG grids especially developed for this study (Lapatki et al. 2004). Because of the high mechanical flexibility of the new sensors, good electrical connections of the single electrodes could be achieved even in subjects with very uneven contours in the recording area, e.g. due to a deep mentolabial sulcus. Moreover, the flexible electrode grids could, to a large extent, follow the skin movements resulting from the lower facial muscle contractions. As a result the sensors did not significantly hinder the performance of the experimental tasks.

Two-dimensional topographical information about the electrical activity of a muscle allows the extraction of single MU potentials from the sEMG interference pattern (Masuda et al. 1985; Rau and Disselhorst-Klug 1997; Stegeman et al. 2004). Since we applied a largely automated decomposition method and we did not consider the information about the firing moments of the MUs, the signal decomposition in our study was inherently incomplete. The risk that peaks of MUs with distinct amplitude profiles could have been grouped together and averaged respectively was largely minimised by classifying the detected peaks into a much greater number of groups than the number of expected active MUs. Thus, the only possible compromises for our results were (1) either the averaging of more or less identical MUAP peaks belonging to distinct, but electrophysiologically (and probably anatomically) similar MUs, or (2) the subdivision of the peaks belonging to a single MU into two (or more) different peak groups. In both cases, the consequences for the determined endplate zone distributions and muscle fibre orientations were only of minor significance with regard to the mapping of these topographical

MU parameters and the interpretation of the results with respect to anatomical features.

Besides histological and histochemical techniques (Aquilonius et al. 1984; Christensen 1959; Desmedt 1958; Snobl et al. 1998), high-density sEMG techniques (Hilfiker and Meyer 1984; Masuda et al. 1983; Masuda and Sadoyama 1988), and EMG techniques with several inserted invasive electrodes (Lateva et al. 2002) have already proven in previous studies to be suitable to determine the locations of the MU endplates and their distribution on the muscle. The underlying hypothesis that the MUAP amplitude waveforms are closely related to aspects of MU (and muscle fibre) morphology is well studied and an important issue in electrodiagnostic medicine (Dumitru 2000; Lateva and McGill 2001). In the present study, we focused on two main aspects of MU topography: the endplate zone location and the main muscle fibre orientation. With respect to the latter parameter, it is important to note that we determined the muscle fibre orientation in the main (central) area of each MU, and did not always trace the propagating signal to the end of the muscle fibres (e.g. in case of diffuse terminal propagation). The only possibility to localise fibre ends with an electrophysiological technique would rely on the detection of "end-effects" in the MUAP (Dumitru and King 1999; Dumitru 2000; Stegeman et al. 1997) which were in most instances not visible in our averaged facial MUAPs. End-effects may not be visible from these data due to relatively short muscle fibre lengths (i.e. the end-effects would be covered by the main peak of the MUAP), and aspects of facial muscle architecture (i.e. the diffuse interdigitation and interweaving of muscles at their origins and insertions) which reduce the "sharpness" of the end-effect. A general problem in the interpretation of sEMG data in anatomical respects is connected with the differential movement of the muscle tissue

and the electrodes during the contraction. This problem can be especially relevant in recordings with multi-electrode sEMG grids which reduce the mobility of the skin in the relatively large recording area and therefore may impede the skin in following the contracting muscle tissue. In our study, the MUAP template sets selected for further evaluation were decomposed from contractions between 5 % and 15 % of MVC. In an exemplary analysis in the DAO muscle (contraction of this muscle is accompanied by relatively large skin movements) in three subjects and three MUs per subject, we estimated an average relative movement between the electrode grid and the underlying muscle when the contraction level was increased from 5% to 15% MVC of about 1 mm. This value indicates the possible, relatively small bias of our results due to this effect. Accurate determination of topographical MU characteristics requires that the recording area completely spans the skin area above the examined muscles. With the 128 available recording channels and an IED of 4 mm, the recording area of the two attached electrode grids was approximately 20 cm² in size. Since we optimally adapted the shape of this area to the average anatomical configuration of the underlying facial musculature, it was rare that a MU territory occurred at the border or even out of the recording area. An exception in this respect were the OOI MUs; in this muscle, endplate locations above the upper border of the medial electrode grid were unavoidable, because sEMG grids cannot be placed on the lip vermilion where the density of the OOI fibres is the highest (Blair 1986). To minimise this "vertical" bias in our results as far as possible we positioned the sensors directly at the lower lip's vermilion border.

Discussion of results in an anatomical and physiological context

Topographical facial MU parameters, i.e. endplate positions and muscle fibre orientations, were imaged and quantitatively determined in relation to facial landmarks. The characteristic spatial profile allowed the decomposed MUAPs to be classified as belonging to certain facial muscle subcomponents. Thus, it can be concluded that the complex facial muscle architecture could be successfully mapped with the applied techniques. Discussion of our results is possible in the context of both macro- and micro-anatomical knowledge.

In general, we found the facial muscle positions (estimated from the mono- and bipolar amplitude profiles and endplate locations) and fibre orientations in good agreement with descriptions and drawings in anatomical textbooks (Braus and Elze 1954; Nairn 1975; Salmons 1995; Sobotta 2000), as well as quantitative macro-anatomical data (Kennedy and Abbs 1979). In anatomical literature, facial muscle architecture has often been described as having considerable inter-individual variability when compared to other musculature. An interesting finding in our study was that inter-individual variability, mainly those of the MU endplate positions, could be significantly reduced by the spatial scaling of the data on the basis of the individual and average facial dimensions (see Fig. 6-6). Based on this finding, it is possible that a great part of the variation in facial muscle anatomy discussed in the literature is due to complex inter-individual variations in facial size and shape.

Detailed histological studies on the myoneural junctions revealed that normal adult mammalian skeletal muscles are innervated by a single motoneuron (i.e. consist of fibres with a single MU endplate in the middle) and that the MU endplates are usually arranged to form a narrow band crossing the muscle's

6

central region, described as the "motor band" (Aquilonius et al. 1984; Christensen 1959). This dogma of classical anatomy and physiology has been revised in several respects. There is growing histological and electrophysiological evidence that some mammalian muscles - including the human laryngeal muscles (Perie et al. 1997; Rossi 1990) - may contain fibres with more than one endplate (Lateva et al. 2002, 2003). Further studies with sophisticated electrophysiological techniques indicate that a variety of architectural organisations of MUs, including the presence of single and multiple endplate zones in central and non-central locations (Lateva and McGill 2001), are present in normal human limb muscles. Such differences from the classical arrangement of MU endplates in one motor zone or band could also be observed in human facial muscles. Histo-chemical studies revealed that myoneural junctions are distributed on the facial muscles in round or oval-shaped clusters (Happak et al. 1997). Histological examinations provided evidence that most investigated facial muscles show a small number of clusters corresponding to the number of innervating terminal motor nerve branches. Exceptions were the orbicularis oris, orbicularis occuli, and buccinator muscles, in which MU endplates were found to be spread over the whole muscle resulting in a greater number of small motor zones. Other characteristic findings in these studies were a predominance of one MU endplate cluster (in most of the examined muscles), and eccentric positions of the MU endplates on the corresponding muscle fibre bundles. These distinctive characteristics of facial MU topography could also be observed in our electro-physiologic study.

In the DAO muscle, which is innervated by two nerve branches from the lateral margin (Happak et al. 1994; Happak et al. 1997), MU endplates were typically identified in two clusters (Fig. 6-6). The finding in a few subjects

of DAO endplates only in a single cluster might be due to either an absence of a second endplate cluster (as a sign of inter-individual variability) or, more likely, peaks of the smaller MUs belonging to an additional cluster were "covered" by the peaks of the larger MUs (Fig. 6-5) and were therefore not detected by our peak detection algorithm.

The DLI, which is innervated from several motor nerve branches of the marginal mandibular branch, showed extreme eccentric endplate locations near its lower border, with a distribution of endplates in medio-lateral dimension in two (or in some subjects three) clusters (Fig. 6-7). Position of the MU endplates near the origin of this muscle at the lower mandibular border might be connected with the phylogenetic migration of the fibres from the neck to the area near the corners of the mouth and the interconnection with the platysma, respectively (Braus and Elze 1954). The predominance of either lateral or medial endplate location in the DLI muscle varied from subject to subject. Most DLI MUAPs had amplitude territories which spanned the region of the lower lip. This confirms histological findings of serial sagittal sections of human lower lip in which groups of vertical and skew muscle fibres with an origin inferior to the lower lip (i.e. in the central DLI muscle area) were found in between the horizontal OOI fibres (Blair 1986; Blair and Smith 1986). An interesting additional finding during our experiments was that some subjects were able to contract the DLI muscle either in its lateral or medial region. This ability reflects the endplate zone distribution on this muscle and can be interpreted as compartmentalisation, i.e. within-muscle differences of anatomical and physiological parameters that partition the motoneuron pool of a single muscle into independently controlled subsets (Binder and Stuart 1980). Such possibility of heterogenic contraction was also observed in masticatory

muscles (Blanksma and van Eijden 1995; Phanachet et al. 2001), which – similar to the facial muscles - stem from the branchial arches.

In the MEN muscle, a predominant MU endplate cluster was usually found in a location slightly lateral to the facial midline, (vertically) between quarter and half the distance from the lower lip vermilion's inferior border to the lower bony margin of the mandible. One or two additional, often less clearly delimited endplate zones were often located in the muscle's inferior portion. These results cannot be compared to other data because, to our knowledge, no histological study has been carried out on the MEN muscle. The finding of relatively dispersed MEN endplate locations in the combined data of all subjects might be connected with the high inter-individual variability in soft-tissue thickness and contour in the lower lip and chin area (Kennedy and Abbs 1979), because the measured sEMG signals are a "projection" onto the surface of the electrode grids (which follows the uneven skin contours; see Fig. 6-1A). The difficulties in the determination of the superior MEN muscle fibre orientation and the low amplitudes of the MEN MUAPs above the endplates respectively are explained by the three-dimensional fibre course and the filtering properties of the soft-tissues: the MEN muscle has its origin on the anterior border of the alveolar process of the mandible and is therefore covered by the thick soft-tissue mass of the chin and the lower lip in its superior part.

The orbicularis oris muscle consists of four (upper / lower / right / left) quadrants, each of them anatomically subdivided in a marginal portion located within the lip vermilion, and a peripheral portion around the lips. The marginal and peripheral subcomponents of the investigated inferior orbicularis oris muscle (OOI) could not be separately examined in our study due to the impossibility of positioning sEMG electrode grids directly over the lip vermilion

and the incapability of most subjects (even trained trumpeters) to contract the subcomponents separately. Anatomical and histological studies have shown that the orbicularis oris is innervated from its lateral side by two terminal nerve branches and has MU endplates spread over the muscle in multiple clusters. In agreement with these data from former studies, we observed dispersed MU endplate locations in the investigated inferior part of this muscle in most of the subjects, with a main concentration of endplates, however, in the centre of the right or left lower orbicularis oris quadrants (i.e. approximately half distance between the corner of the mouth and the facial midline). We were surprised to find only MUs with relatively small territories (when compared to the whole muscle's length), because in the anatomical literature horizontal OOI fibres are described to run from the modiolus to the facial midline without interruption (Braus and Elze 1954). This issue requires further electrophysiological and histological investigations. On the other hand, the small territories and distinct muscle fibre orientations might reflect the muscle's complicated fibre architecture. As already mentioned in the context of overlapping electrical territories of OOI and DLI MUs, serial sagittal sections of human lower lip revealed the presence of fibre groups with distinct orientation (i.e. horizontal, tangential and vertical fibres) in the region "traditionally described as OOI". The relative masses of these fibre groups showed considerable variation as a function of medial-lateral and superior-inferior position (Blair 1986). Electrophysiological studies suggest that these distinct fibre groups in the OOI belong to MUs that are independently controlled and have differential mechanical functions (Abbs et al. 1984; McClean and Smith 1982). From all these electrophysiological and anatomical / histological data it can be concluded that MU architecture of the muscle tissue in the area of the lower lip is highly

6

developed and very complex. Dispersed location of horizontal OOI MUs along the lips as well as the presence of intrinsic non-horizontal OOI MUs and DLI MUs in this area, endow the lips with the ability of highly differential variation of tension and 3-D shape. Such fine and differential motor control is required e.g. in production of speech sounds, drinking, mastication and other oral functions.

An additional, frequent finding in averaged OOI MUAPs was the presence of two widely (i.e. up to 10 mm) separated, propagating zones of high amplitude. Possible explanations for this phenomenon are either branching of the motor nerve in its distal part (Happak et al. 1994; Happak et al. 1997) or synchronisation of the firings of distinct MUs. Synchronisation of facial MUs has been described in previous studies (Folkins et al. 1988; Wohlert 1996a) and seems to be one of the components of differential neural regulation of lip muscle activity on pre-motoneuron level depending on the motor task (Wohlert and Goffman 1994).

Conclusions

In this electrophysiological study, the position and distribution of MU endplates, and principal muscle fibre orientations of facial muscles have been mapped and quantitatively determined. Such fundamental data add substantially to the basic neuro-physiologic and anatomical knowledge of the complex facial muscle system. The results obtained can also be regarded as a basis for improving accuracy and reproducibility of conventional facial sEMG measurements. Facial sEMG has been proven to be a valuable, non-invasive tool in many research and clinical applications in psychophysiology (Jancke et al. 1996; Lundqvist 1995; Root and Stephens 2003; Sloan et al. 2002), speech physiology and pathophysiology (Kelly et al. 1995; Leanderson

et al. 1971; Ruark and Moore 1997; Wohlert 1996a, b; Wohlert and Hammen 2000), as well as in general dentistry and orthodontics (Lapatki et al. 2002; Tosello et al. 1998, 1999; Yamaguchi et al. 2000). Electrode placement in these studies has only been orientated towards the estimated positions and fibre directions of the examined muscles, with the intention in most of the studies to position the sensors on the centre or "belly" of the examined muscle. Our results prove that this electrode position is suboptimal at least in some muscles, e.g. in the DAO muscle due to the central location of most endplates (Fig. 6-6). That means, that relevant factors for electrode placement (Freriks et al. 1999) had to be ignored in previous studies, due to the lack of quantitative data on these variables. In our study, these gaps in fundamental anatomical and neurophysiological knowledge have been bridged to a large extent, and consequently, foundations have been laid for objective guidelines for facial EMG electrode placements. The presented results may also be relevant from a clinical point of view. The information about MU topography obtained in a group of healthy individuals is useful as normal data in the observation of regeneration and reinnervation of MUs after peripheral nerve injuries or muscle transplantation, and in the study of the topographical aspects and the characteristic alterations on the MU level of neuromuscular diseases affecting the facial musculature (e.g. facioscapulohumeral dystrophy and Möbius syndrome). Finally, maxillo-facial surgical reconstruction of facial musculature (e.g. in patients with cleft lip or tumours in the face) and therapeutic interventions with botulinum toxin (with respect to the definition of optimal locations for injections) may also benefit from this fundamental data on the facial musculature and myoneural junctions in healthy individuals.

7

Optimal placement of bipolar surface EMG electrodes in the face based on single motor unit analysis

Lapatki B.G., Oostenveld R., van Dijk J.P., Jonas I.E.,
Zwarts M.J.,Stegeman D.F.

Locations of surface electromyography (sEMG) electrodes in the face are usually chosen on a macro-anatomical basis. In this study we describe optimal placement of bipolar electrodes based on a novel method and present results for lower facial muscles. We performed high-density sEMG recordings in thirteen healthy subjects. Raw sEMG signals were decomposed into motor unit action potentials (MUAPs). We positioned virtual electrode pairs in the interpolated monopolar MUAPs at different positions along muscle fibre direction and calculated the bipolar potentials. Electrode sites were determined where maximal bipolar amplitude was achieved and were validated. Objective guidelines for sEMG electrode placement improve the signal-to-noise ratio and may contribute to reduce cross-talk, which is particularly important in the face. The method may be regarded as an important basis for improving the validity and reproducibility of sEMG in complex muscle areas.

Introduction

Particularly when complex musculature such as that of the face is examined, the validity of surface EMG measures depends significantly on methodological aspects. To improve spatial resolution and noise rejection, a bipolar (i.e. a single differential) electrode configuration is commonly used (De Luca and Knaflitz 1992). Aside from the sensor characteristics, electrode placement plays a crucial role, because sEMG recordings at different positions on the muscle gave greatly varying estimates of EMG variables (Beck et al. 2008; Campanini et al. 2007; Farina et al. 2002a; Hogrel et al. 1998; Jensen et al. 1993; Mesin et al. 2009a; Roy et al. 1986). However, establishing electrode positioning guidelines is a challenging task. It requires consideration and balancing of several aspects, such as (1) proximity of a proposed electrode site to underlying muscle with minimal intervening tissue, (2) alignment of a bipolar electrode parallel to muscle fibre direction, (3) avoiding that a bipolar electrode is positioned across the motor unit endplate region, (4) electrode attachment to a proposed site without undue problems e.g. from skin folds or curvatures, and (5) minimising crosstalk from adjacent muscles (Fridlund and Cacioppo 1986). The first three

factors are important in detecting the maximal potential gradient between the two electrodes of the bipolar montage resulting in maximal sEMG signal amplitude. The relevance of the endplate zone location in this context is connected with the propagation of the motor unit action potentials (MUAPs) in both directions away from the endplates. A location of the two electrode surfaces over the endplate region therefore leads to partial or even complete cancellation of the bipolar signal (Loeb and Gans 1986; Masuda and Sadoyama 1988; Stegeman et al. 2004).

Neither anatomical studies, nor electrophysiological investigations with conventional techniques can provide sufficient information regarding all relevant criteria for bipolar electrode placement. High-density sEMG allows to fill this gap, because this technique records muscle activity on the skin surface with a large number of small, densely spaced electrodes (Stegeman et al. 2004). This non-invasive tool provides detailed two-dimensional information about the electrical activity of the underlying musculature and allows for extraction of MUAPs from the recorded interference EMG reflecting the contributions of single motor units to the signal (Kleine et al. 2007; Masuda et al. 1985; Rau and Disselhorst-Klug 1997; Stegeman et al. 2004). Such "motor

7
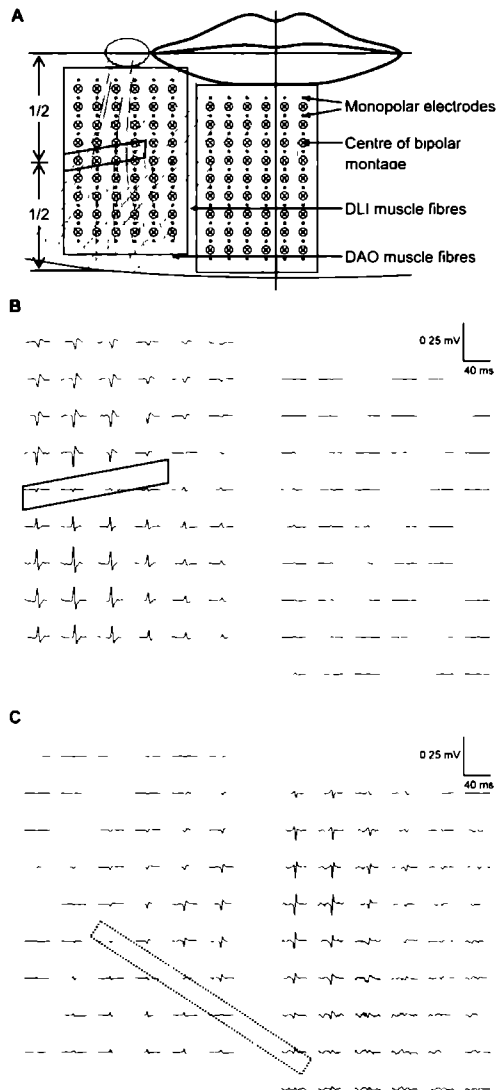
Figure 7-1. (A) Topographical relation of two attached multielectrode grids with the individual facial structures (vermillion border, facial midline, and lower mandibular border) and the underlying musculature (grey lines) of subject #3. Each grid consisted of 60 monopolar electrodes (small grey dots). A MUAP template describes the spatial amplitude distribution of a decomposed MUAP over the grid area. A bipolar MUAP template is obtained by subtracting consecutive monopolar potentials (in this example in vertical direction). The centres of these bipolar montages are indicated by black circles with crosses. (B) Example of a bipolar MUAP template belonging to a motor unit of the depressor anguli oris (DAO) muscle. In a bipolar template, the location of the endplate zone is indicated by low signal amplitude (in between signals of high amplitude) and/or reversal of signal polarity. In this subject and motor unit, the endplate zone (open parallelogram) is located halfway between the modiolus (open grey circle lateral to the corner of the mouth) and the lower mandibular border, i.e. over the DAO muscle's centre. (C) Bipolar MUAP template belonging to a motor unit of the depressor labii inferioris (DLI) muscle (same subject). In this MUAP example, the endplate zone (open dotted rectangle) is located eccentrically, i.e. more close to the lower mandibular border than to the lower lip.

unit fingerprints" (Fig. 7-1) can be used to topographically characterise motor units including determining their endplate zone location (Castroflorio et al. 2005; Hilfiker and Meyer 1984; Masuda et al. 1983; Masuda and Sadoyama 1988) and main muscle fibre directions (Gronlund et al. 2005; Lapatki et al. 2006).

In previous sEMG studies, relevant aspects for electrode placement have been ignored due to a lack of quantitative data on motor unit topography. For instance, in the face, bipolar electrodes were usually positioned parallel to the estimated muscle fibre direction and over the centre or "belly" of the muscle to be examined. Corresponding information was taken either from sparse quantitative anatomical studies (Kennedy and Abbs 1979) or from illustrations in anatomical textbooks (Salmons 1995). This usual procedure can be very problematic, as shown in Fig. 7-1B for the depressor anguli oris. In this example, the bipolar sEMG and the signal-to-noise ratio obtained at the muscle's vertical centre would be quite low, and (if a relative medial electrode location, e.g. at the medio-lateral level of the corner of the mouth, would be chosen) the risk for crosstalk from the adjacent depressor labii inferioris (Fig. 7-1C) would be relatively high. In contrast, positioning the electrode pair for the depressor anguli oris more cranially or caudally would improve the situation decisively.

For the present study we developed a method for systematically utilising topographical motor unit parameters and two-dimensional amplitude information obtained with high-density sEMG in determining the optimal placement of bipolar sEMG electrodes. Here we consider the electrode position to be optimal if the maximal bipolar sEMG is registered from the examined muscle. We show the application of this method for the lower facial musculature, as in this area several small muscle subcomponents interdigitate and

overlap in a relatively small area. Thus, objective placement guidelines for optimal electrode positioning in the lower face are challenging and of special importance.

Materials and Methods

Subjects

The study group consisted of 13 volunteers (6 men and 7 women, mean age 27.2 yr, range 21 – 43 yr) without known neurological or other general health disorders. The ethics commission of the Radboud University Nijmegen Medical Centre (The Netherlands) approved the study protocol and subjects gave informed consent prior to the experiment.

Electrode grids and equipment for high-density sEMG recordings

We used two multielectrode sEMG grids (Digiraster Tetzner GmbH, Stuttgart, Germany), each consisting of 6×10 regularly arranged, chlorided silver electrodes with a diameter of 1.7 mm (Fig. 7-2A). The centre-to-centre distance between adjacent electrodes (inter-electrode distance) was 4 mm in both directions, allowing for a sufficient spatial sampling for the facial musculature. The electrode grids were attached to the skin using specially prepared double-sided adhesive tape (basic material: 1522 medical tape, 3M, St. Paul, MN, USA) which allowed the selective application of conductive cream (GE Medical Systems Information Technologies GmbH, Freiburg, Germany) in the area of the electrodes. An elaborate procedure led to firm electrode fixation and high signal quality due to relatively low electrode-to-skin impedances (Lapatki et al. 2004).

The electrode grids were connected to the amplifiers with help of a headset equipped with flexible arms and connectors for the electrodes (Fig. 7-2B). The electric potential at each of the 120 single electrodes was acquired

7
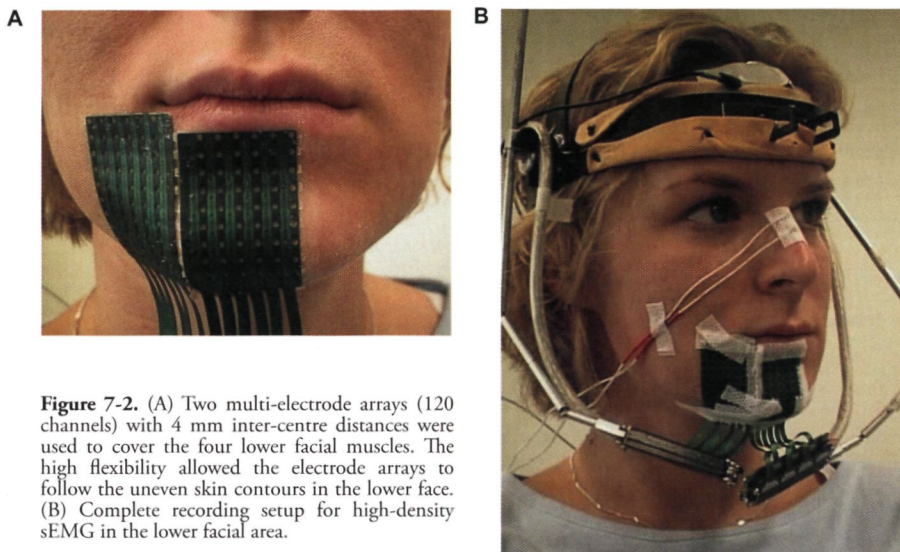
Figure 7-2. (A) Two multi-electrode arrays (120 channels) with 4 mm inter-centre distances were used to cover the four lower facial muscles. The high flexibility allowed the electrode arrays to follow the uneven skin contours in the lower face. (B) Complete recording setup for high-density sEMG in the lower facial area.

"monopolarly", i.e. referenced to a common electrode (material: silver/silver-chloride, diameter: 4 mm) attached to the dorsum of the nose. EMG was acquired using a 128 channel amplifier (Mark-6, BioSemi Inc., Amsterdam, NL). Signals were band-pass filtered (3.2 – 400 Hz) and subsequently synchronously sampled at 2000 Hz with a resolution of 0.5 µV/bit over a range of +/-16 mV (16 bits) (Blok et al. 2002).

Electrode grid positioning

The lower facial musculature was examined either on the right (7 subjects) or left (6 subjects) side of the face. The two electrode grids were positioned side by side, vertically displaced relative to each other by one electrode row (Fig. 7-3A). At the border between the medial and the lateral grid the horizontal distance between consecutive electrodes was exactly twice the inter-electrode distance within each grid.

Electrode grid positioning was guided by the corner of the mouth, the inferior border of the lower lip vermilion and the facial midline

(Fig. 7-3A). The medial-lateral placement principle was the alignment of the 5th electrode column (from lateral) with the corner of the mouth. In the vertical dimension, the upper border of the medial grid was aligned with the lower lip vermilion. A further principle for placement was to align the medial grid border parallel to the facial midline.

Recording procedure

After application of the electrodes but prior to actual recordings, the subjects were instructed and trained in selective lower facial muscle contractions supported by visual amplitude feedback. This feedback was given by displaying the Root Mean Square (RMS) value of selected bipolar signals (and so the activity level of the underlying muscle) to the subject by the PC monitor. The feedback tool was normalised to a maximal voluntary contraction of the examined muscle. When subjects were accustomed to the recording conditions, data were acquired while it was attempted to selectively contract the four muscles of the lower face, i.e. the depressor anguli oris, the depressor

labii inferioris, the mentalis, or the orbicularis oris inferior, at various contraction levels. The first recordings were made at the lowest contraction at which clear motor unit firings could be discerned in the bipolar signals over the corresponding muscle. For most measurements this level corresponded approximately to 2-3% of the maximal voluntary contraction level, estimated on the basis of the RMS value of the selected channels. Subsequently, the contraction level was increased in 5% steps up to 30%, and then in 10% steps up to the maximal voluntary contraction level (100%). Per subject, per muscle and per contraction level, we performed two recordings of ca. 20 s duration. Although facial muscles are relatively resistant to fatigue (van Boxtel et al. 1983), recovery breaks of approximately 20 – 60 s were made between subsequent contractions to prevent local fatigue effects. Additionally, subjects paused for a longer rest when they had the feeling of beginning fatigue
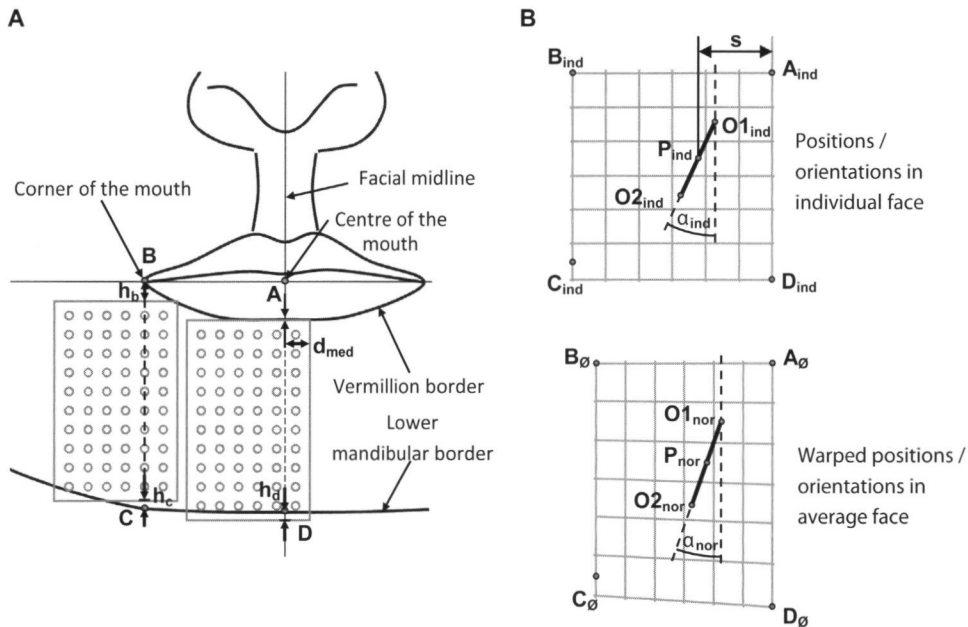
Figure 7-3. (A) Electrode grid placement. Landmark definitions: A: Centre of mouth; B: Corner of mouth; C: lower border of the mandible at the medio-lateral level of mouth corner; D: lower border of the mandible at the facial midline. The grey circles and rectangles represent the 120 (2 x 60) recording electrodes and the electrode grid borders, respectively. The topographical relation between the grids and the face was determined by measuring the vertical distances of the upper or lower grid borders from points B, C and D (h_b, h_c and h_d) as well as the horizontal distance of the medial grid's medial border from the facial midline (d_{med}). (B) Spatial scaling of individual positions and orientations. Lower facial dimensions of the individual subject (upper panel) were broader and shorter, with a more horizontal course of the lower mandibular border when compared to the average facial dimensions of the 13 subjects (lower panel). In the individual coordinate system, point P is located at a distance s from the centre of the mouth, and the line between points $O1_{ind}$ and $O2_{ind}$ has an angulation α_{ind} relative to the facial midline. The lower panel shows point P and the orientation α_{nor} of the line $O1$-$O2$ in the average coordinate system, i.e. after a spatial warp of the individual data. The (constant) horizontal scaling factor (ScF_{hor}) for this warp was determined by the relation between the individual (BA_{ind}) and average distance ($BA_{\emptyset}$) between the corner (B) and the centre of the mouth (A) using equation $ScF_{hor} = BA_{\emptyset} / BA_{ind}$. In the vertical dimension, separate scaling factors were calculated at the facial midline and at the corner of the mouth using equations $ScF_{ver1} = AD_{\emptyset} / AD_{ind}$ and $ScF_{ver2} = BC_{\emptyset} / BC_{ind}$, respectively. The vertical scaling at other medio-lateral levels (e.g. at a distance s from A) varied linearly between these two scaling factors according to the equation $ScF_{ver(P)} = (ScF_{ver2} - ScF_{ver1}) / BA_{ind} \times s + ScF_{ver1}$.

Data analysis

EMG data were analysed using a protocol programmed in Matlab, Version 7.04 (The Mathworks Inc., Natick, MA, USA). First, we applied a high-pass zero-phase 4th order Butterworth filter to eliminate low-frequency movement artifacts. Since the subjects were asked to activate the muscles at a constant level, these artifacts were found to be very small. Therefore, a cut-off frequency of 10 Hz, i.e. a lower value than 15 - 25 Hz recommended for recording spontaneous activity of facial muscles (van Boxtel 2001), was sufficient. Table 7-1 provides a schematic overview over the different steps of further data evaluation which are described below.

Table 7-1. Flow chart of the data analysis procedure

```
        ┌────────────────────────────────────────┐
        │            Raw EMG data file             │
        │ (per subject, muscle and contraction level) │
        └────────────────────────────────────────┘
                   │ (1)   Decomposition
                   ▼
        ┌────────────────────────────────────────┐
        │    Motor unit action potentials (MUAPs)  │
        │ (per subject, muscle and contraction level) │
        └────────────────────────────────────────┘
                   │ (2)   Selection
                   ▼
        ┌────────────────────────────────────────┐
        │        Representative MUAP sample         │
        │         (per subject and muscle)          │
        └────────────────────────────────────────┘
                   │ (3)   Topographical analysis
                   ▼
        ┌────────────────────────────────────────┐
        │ MU endplate position and two muscle fibre vectors │
        │                (per MUAP)                 │
        └────────────────────────────────────────┘
                   │ (4)   Virtual bipolar electrode montages
                   │       along the two muscle fibre vectors
                   ▼
        ┌────────────────────────────────────────┐
        │       Optimal bipolar electrode position  │
        │      (per MUAP and fibre direction)       │
        └────────────────────────────────────────┘
                   │ (5)   Averaging over MUAPs
                   ▼
        ┌────────────────────────────────────────┐
        │    Intra-individual mean electrode position │
        │  (per subject, muscle and fibre direction)  │
        └────────────────────────────────────────┘
                   │ (6)   Spatial normalisation
                   ▼
        ┌────────────────────────────────────────┐
        │ Normalised individual optimal electrode position (per │
        │     subject, muscle and fiber direction)  │
        └────────────────────────────────────────┘
                   │ (7)   Averaging over subjects
                   ▼
        ┌────────────────────────────────────────┐
        │        Group mean electrode position      │
        │      (per muscle and fibre direction)     │
        └────────────────────────────────────────┘
```

Decomposition and topographical motor unit analysis (steps 1, 2 and 3)

Data analysis in these three steps is described in full detail in a previous publication providing basic neurophysiologic and anatomic information on the lower facial musculature (Lapatki et al. 2006). To summarise, raw sEMG data files up to a contraction level of 30% of the maximal voluntary contraction level were decomposed resulting in one set of MUAPs per recorded file (each belonging to a certain subject, muscle, recording level and repetition, respectively) reflecting the contributions of different motor units to the corresponding interference EMG. All decomposed MUAP template sets were visually inspected in order to select one set per subject and muscle which best represented the distinct MUAP topographies observed in the MUAP sets obtained from all decomposed recording levels and repetitions belonging to this subject and muscle. Scanning the MUAP templates in their bipolar electrode montage (Figs. 7-1B and 7-1C) facilitated the differentiation of the MUAPs' distinct amplitude topographies during this selection. Only the selected MUAP template set was then topographically analyzed using the data in its monopolar montage. Prior to this analysis, the monopolar MUAPs were completed in two stages using a bicubic inter- or extrapolation method. Firstly, we calculated the monopolar data of the missing electrodes in between the two attached electrode grids (by interpolation) and at the upper or lower grid borders (by extrapolation). Secondly, we interpolated the complete template data set in both dimensions 8 times between adjacent electrodes to obtain a regular 0.5-mm resolution of the data. From each of these interpolated monopolar MUAPs we extracted the location of the motor unit endplate zone and the muscle fibre orientation at both sides of the endplate zone by inter-active evaluation of the MUAPs visualised as amplitude map

sequences ("MUAP movies"). This procedure is based on the principle that the location of the endplate zone and the main muscle fibre orientation of a motor unit correspond to the location where the MUAP starts and in which direction it propagates. Both could be determined by localising the maximal amplitude area on the electrode grid at different latencies of the MUAP. Further data evaluation described in the following steps also used the completed monopolar MUAPs.

Virtual construction of bipolar electrode montages along muscle fibre direction (step 4)

The optimal position for a bipolar electrode was in our definition the location on the muscle where a sEMG signal with maximal amplitude is registered. To achieve this, an electrode pair has to be orientated parallel to the direction of signal propagation along the muscle fibre direction. In that case the maximal spatial potential gradient is spanned (Loeb and Gans 1986). We followed this rule separately for each MUAP by placing a virtual bipolar electrode pair with a given inter-electrode distance (see below) over the endplate zone and shifting this electrode pair (in steps of 0.4 mm) along the muscle fibre orientation vectors towards the muscle's origin and insertion, respectively (Fig. 7-4A).

For each position of the electrode pair, the bipolar signal was obtained by determining the monopolar potentials of two virtual point electrodes for all MUAP latencies using a 3D spline interpolation algorithm, and then calculating the bipolar signal as the difference between the two monopolar potentials. This procedure was repeated for different inter-electrode distances ranging from 0 to 20 mm in steps of 0.8 mm. To evaluate the possible influence of the detection surface geometry on the optimal bipolar electrode position we repeated the whole procedure also for bipolar montages
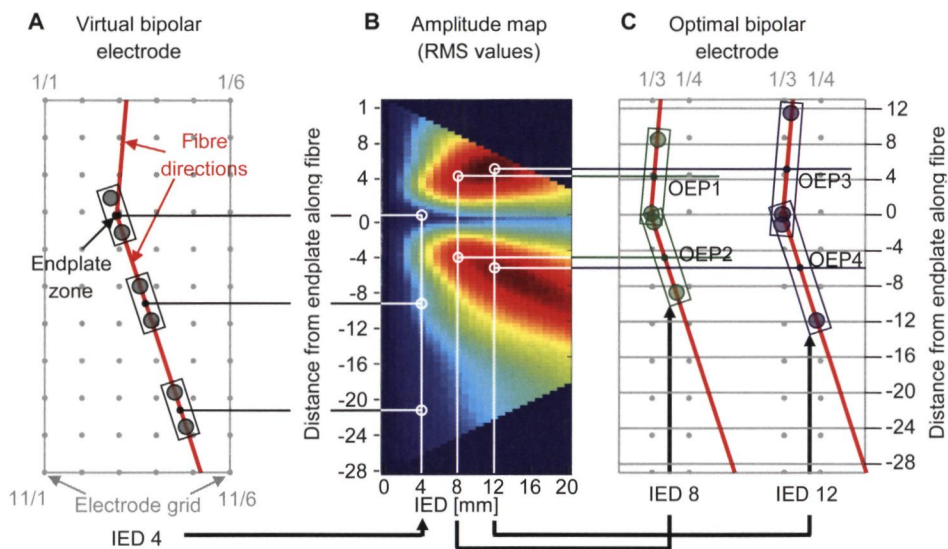
7

Figure 7-4. Methodological principle for determining the optimal bipolar sEMG electrode position (OEP) on the level of individual motor units. (A) Virtual construction of bipolar electrode montages (rectangles with two grey filled circles) at different positions on the muscle fibre orientation vectors. This example shows a motor unit of the depressor anguli oris and bipolar electrodes with an inter-electrode distance (IED) of 4 mm. The small grey dots indicate the electrodes of the lateral grid (electrode coordinates: electrode row from the top / electrode column from the lateral). Note that the lowest electrode row (row 11) was extrapolated. (B) Amplitude map describing the RMS value of the sEMG signal that would be obtained with different inter-electrode distances (horizontal axis) at different positions on the fibre orientation vectors (vertical axis). RMS value increases from blue to red. The amplitudes resulting from the electrode montages exemplified in part A are indicated by the three white circles above the inter-electrode distance of 4 mm. The minimal RMS value is obtained near the endplate zone represented by the narrow blue horizontal band. The two white circles above the inter-electrode distances of 8 mm and 12 mm indicate the RMS maxima that can be picked up above and below the endplate zone when using these inter-electrode distances. (C) Localisation of these maxima (i.e. the optimal bipolar electrode positions for inter-electrode distances of 8 mm and 12 mm) in electrode coordinates is possible.

with square detection surfaces (instead of point electrodes) with different sizes, i.e. 2×2 mm^2, 4×4 mm^2 and 6×6 mm^2. The monopolar potentials for calculating the bipolar signals were obtained by averaging the interpolated monopolar MUAP amplitude values in the area of the individual detection surfaces. This has proven to be a valid principle under most practical conditions (van Dijk et al. 2009). The amplitude of the calculated bipolar signals was characterised using the RMS value over time. Optimal bipolar electrode sites were localised where the maximal RMS value was achieved.

The results can be illustrated (for a given detection surface size) by means of two-dimensional amplitude maps for each MUAP with the inter-electrode distance along the horizontal axis and the distance from the endplate zone along the vertical axis. As it can be taken from Fig. 7-4B, RMS maxima were determined in these amplitude maps separately for the muscle fibre direction at both sides of the motor unit endplate zone (if both directions could be determined) and for different inter-electrode distances (Fig. 7-4C).

Intra-individual averaging of optimal electrode positions of different motor units (step 5)

Optimal electrode positions for individual MUAPs were intra-individually averaged (per subject, muscle, fibre direction and inter-electrode distance) to obtain electrode positions representative for the whole muscle.

Spatial normalisation of individual results to correct for facial size and shape differences (step 6)

The distances from the electrode grids to the facial midline, to the corner of the mouth, as well as to the median and lateral lower mandibular border were measured in each subject's face after the sEMG recording (Fig. 7-3A). Using the known relation between these facial landmarks, the electrode grids and the single electrodes, it was possible to define the optimal electrode positions and orientations in an individual facial coordinate system. Separately for each subject we then applied a spatial scaling of the data so that the individual facial dimensions agreed with the average facial dimensions of the study group (Fig. 7-3B). For this warp, the facial size was characterised in the horizontal dimension by the distance between the corner and centre of the mouth (distance BA), and in the vertical dimension by the distance between the centre of the mouth and the lower mandibular border at the facial midline (distance AD). In addition, differences in lower facial shape were described by determining the vertical distance between the mouth and the lower mandibular border at the medio-lateral level of the corner of the mouth (distance BC). Optimal electrode positions were then normalised, i.e. expressed in percentages of the distances BA (horizontally) and AD (vertically).

Inter-individual averaging of optimal electrode positions (step 7)

Since no systematical differences between (spatially scaled) results for the right and left side of the face were found in any muscle, we performed a "mirror-image-transformation" of the parameters obtained from measurements on the left side to the right side. Moreover, we did also not observe any statistical or systematical differences between the optimal electrode positions of male and female subjects (Student's t-test, $p > 0.05$). Thus, we could combine the results of all subjects for inter-individual comparisons and for calculation of mean values over all subjects.

Validation of the results using measured interference EMG signals

Optimal electrode positions were validated by examining whether the placement of bipolar electrodes at those positions identified in the MUAP analysis (steps 1 – 7) as optimal indeed resulted in maximal interference EMG signal amplitude. To address this issue, multiple bipolar electrode montages were constructed in the relevant grid area (i.e. around the intra-individual averages of optimal electrode positions) using the monopolar raw sEMG signals registered during attempted selective muscle contractions at different levels. Aiming at an alignment of the bipolar montages in muscle fibre direction as far as possible, we constructed montages with either a vertical (depressor anguli oris and mentalis), 45°-skew (depressor labii inferioris) or horizontal (orbicularis oris inferior) orientation relative to the arrangement of the high-density sEMG electrode grid. Moreover, we only analyzed those subjects (see results) in which the misalignment of the bipolar montages relative to the muscle's average fibre direction was in between ± 10°. In constructing the bipolar montages, one monopolar electrode was passed over resulting in bipolar electrodes with inter-elec-

7

trode distances of 8 mm (for vertical and horizontal montages) or 11.3 mm (for 45°-skew montages). These values are similar to those of commonly used bipolar sEMG electrodes. Bipolar signal amplitude was characterised by calculating RMS values from the first 10 s of the analyzed interference EMG signals. Two variables were determined per subject, muscle and contraction level: (1) the distance between the optimal electrode position (intra-individual mean value) and the location of maximal interference EMG amplitude, and (2) the percentage of the interference EMG amplitude obtained by that bipolar montage with the closest distance to the optimal electrode position using the amplitude maximum in the grid area as 100% reference. All recordings from 5% - 100% of the maximal voluntary contraction level were evaluated to analyze the dependency of the location of maximal interference EMG amplitude on the muscle's activity.

Results

Fig. 7-5 illustrates for two subjects the endplate zones, muscle fibre orientations and optimal bipolar electrode positions for the depressor labii inferioris. Values for individual motor units as well as intra-individual mean values are given. The individual data shown here are already spatially scaled to allow a direct comparison between the subjects. For both subjects two endplate clusters were found with a typical dominance of the medial-caudal cluster. For this facial muscle, the fibre orientation in the caudal portion could not be determined for most decomposed MUAPs. This is due to very eccentric endplate locations near the depressor labii inferioris muscle's origin at the lower mandibular border, resulting in short and unclear signal propagation in caudal-lateral direction. The optimal recording positions displayed in this particular illustration refer to bipolar electrodes with an inter-electrode distance of 8 mm and detection surfaces of 4 × 4 mm² which are practicable values for facial sEMG (Lapatki, Stegeman, & Jonas,

A: DLI, subject #3

Weighted mean value of (upper) optimal bipolar electrode position

Upper fibre directions of individual MUs

Optimal bipolar electrode positions of individual MUs (upper DLI)

Endplate zone

B: DLI, subject #7

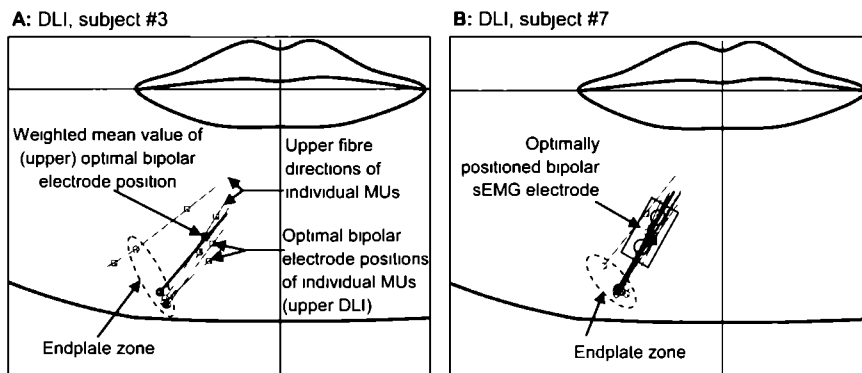Optimally positioned bipolar sEMG electrode

Endplate zone

Figure 7-5. Endplate zone locations (open circles), muscle fibre orientations (lines) and optimal bipolar electrode positions (open squares centre of bipolar montages) for different motor units (grey), mean values are indicated with corresponding black symbols All results in this illustration correspond to an inter-electrode distance of 8 mm (A) Results for subject #3 Motor unit locations were found to be distributed on two clusters though the lateral cluster consisted of one motor unit only The bold black square indicates the optimal position for sEMG recordings from the depressor labii inferioris' upper portion in this subject based on maximal amplitude In this muscle we generally calculated a mean values only for the muscle portion above the endplate zone, because only few motor units (here only one) allowed tracing of the amplitude maximum in lower fibre direction (B) Corresponding results for another subject (#7) The rectangle with two open circles depicts an optimally positioned bipolar electrode configuration

2003). However, for larger or smaller inter-electrode distances (ranging between 0 and 20 mm, see Fig. 7-4B), the optimal recording positions were very similar in all four muscles. Table 7-2 exemplifies the small differences in optimal bipolar electrode position obtained by increasing the inter-electrode distance from 4 to 8 mm and 4 to 12 mm, respectively. Also the differences in optimal electrode positions when using two monopolar point electrodes or two monopolar electrodes with detection surfaces of different sizes (2×2 mm^2, 4×4 mm^2 and 6×6 mm^2) for determining bipolar signal amplitude were found to be negligible in all muscles (Table 7-3).

Fig. 7-6 (left) illustrates the inter-individual variability in optimal bipolar recording positions and orientations for the four examined lower facial muscles as well as group mean values for these parameters. The depressor anguli oris (Fig. 7-6A) showed endplate zone locations near its anatomical centre. Propagation of this muscle's MUAPs could be determined in both directions away from the endplates resulting in two optimal bipolar electrode locations (for the upper and lower portion of this muscle each). The optimal bipolar electrode positions for recordings from the upper and lower muscle portions (average percentage ± standard deviation) were 32 ± 4.1% and 69 ± 7.4%, i.e. were located at ca. 1/3 and 2/3 of the vertical reference distance. Their horizontal positions with respect to the facial midline were both ca. 1.3 times the horizontal reference distance (135 ± 8.5% and 129 ± 10.5%, respectively). Optimal angulations of bipolar sEMG electrodes were 7 ± 6.4 ° and -19 ± 8.9 ° relative to the facial midline for recordings from the upper and lower muscle portions, respectively.

As mentioned before, the depressor labii inferioris (Fig. 7-6B) allowed determination of optimal electrode positions for its upper portion only. The optimal electrode location over all subjects corresponded to 62 ± 5.9% and 49 ± 5.0% of the vertical and horizontal reference distances, respectively. Electrodes were optimally orientated when the angle between the bipolar montage and the facial midline was 36 ± 10.8 °.

The deep location and the skewed fibre course in the mentalis muscle's upper portion made it impossible to trace the propagation of the MUAPs there. The group mean value of the optimal bipolar electrode position for recordings from the mentalis muscle's lower portion corresponded to vertical and horizontal percentages of 67 ± 8.0% and 20 ± 7.9%, respectively (Fig. 7-6C). We found an optimal electrode angulation of -5 ± 11.1 °, i.e. an orientation almost parallel to the facial midline and with relatively high inter-individual variability.

The orbicularis oris inferior (Fig. 7-6 D) consists of motor units with relatively short fibres and with high inter-individual variability of their positions within the lower lip quadrant. Due to such variable locations we calculated intra-individual mean values of optimal electrode positions for both (right and left) fibre directions together instead of determining separate values for optimal positions at both sides of the endplates. The group mean value of this position was horizontally located at 47 ± 16.6% and vertically at 20 ± 4.2%. Almost all motor units were found to be very close to the upper electrode grid border which agreed with the lower lip vermillion. The angle of -84 ± 6.1 ° indicated an almost horizontal optimal electrode orientation for bipolar recordings from this muscle.

The distances between the intra-individual average of optimal electrode position and the position of maximal interference EMG amplitude determined for validation of the optimal electrode positions are separately illustrated for the four examined facial muscles in Figs. 7-7 to 7-10. Only results for those subjects were

7

Table 7-2. Differences in optimal electrode position between bipolar montages with different inter-electrode-distances (IED).

	Difference in optimal electrode position [mm] between bipolar montages with different IED					
	[a] IED 8 vs. 4 mm			[a] IED 12 mm vs. 4 mm		
Muscle	[b]Diff. of group mean	[c]Mean of individual differences	[d]Std of individual differences	[b]Diff. of group mean	[c]Mean of individual differences	[d]Std of individual differences
DAO						
pars sup.	**0**	0.6	0.4	**0.1**	1.3	0.6
pars inf.	**0.2**	0.4	0.2	**0.1**	1.0	0.7
DLI						
pars sup.	**1.0**	1.1	0.8	**2.3**	2.4	1.4
MEN						
pars inf.	**0.3**	0.5	0.8	**0.2**	1.4	1.7
OOI	**0.3**	1.3	1.3	**0.2**	1.8	1.7

[a] All bipolar montages were constructed using two point electrodes
[b] Difference in the mean values of the study group.
[c] Mean value of the differences in individual subjects.
[d] Standard deviation of the differences in individual subjects.

Table 7-3. Differences in optimal electrode positions when the virtual bipolar electrode positioned in muscle fibre direction is configured by two monopolar point electrodes or two square electrode surfaces of different sizes (2 x 2, 4 x 4, and 6 x 6 mm²).
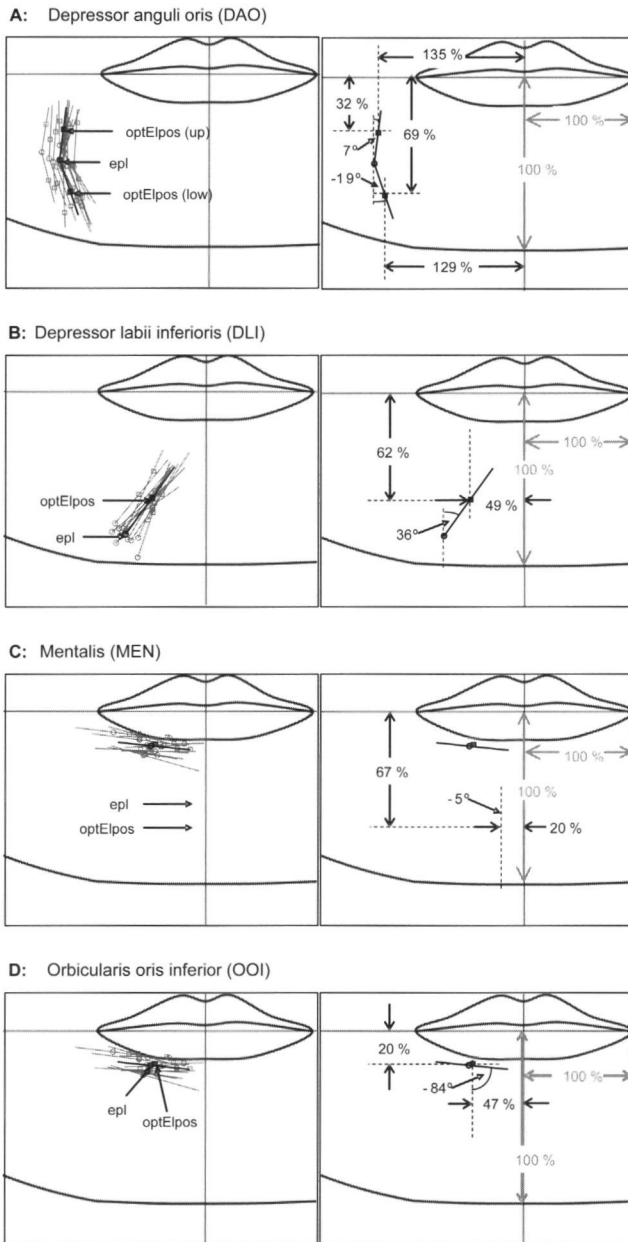
	Difference in optimal electrode position [mm] between bipolar montages with point electrodes and squared electrode surfaces of different sizes								
IED 12 mm	[a] Point vs. 2 x 2 mm²			[a] Point vs. 4 x 4 mm²			[a] Point vs. 6 x 6 mm²		
Muscle	[b]Diff. of group mean	[c]Mean of indiv. diffs.	[d]Std of indiv. diffs.	[b]Diff. of group mean	[c]Mean of indiv. diffs.	[d]Std of indiv. diffs.	[b]Diff. of group mean	[c]Mean of indiv. diffs.	[d]Std of indiv. diffs.
DAO									
pars sup.	**0.1**	0.1	0.2	**0.3**	0.3	0.5	**0.7**	0.8	0.8
pars inf.	**0.0**	0.1	0.1	**0.1**	0.3	0.3	**0.2**	0.8	0.6
DLI									
pars sup.	**0.1**	0.1	0.3	**0.2**	0.3	0.3	**0.2**	0.4	0.2
MEN									
pars inf.	**0.1**	0.1	0.1	**0.3**	0.4	0.6	**0.6**	0.7	0.8
OOI	**0.1**	0.3	0.3	**0.2**	0.8	0.7	**0.4**	1.3	0.8

[a] All bipolar montages had an inter-electrode-distance (IED) of 12 mm.
[b] Difference in the mean values of the study group.
[c] Mean value of the differences in individual subjects.
[d] Standard deviation of the differences in individual subjects.

A: Depressor anguli oris (DAO)

B: Depressor labii inferioris (DLI)

C: Mentalis (MEN)

D: Orbicularis oris inferior (OOI)

Figure 7-6. (A-D) Endplate zone locations (epl; open circles), muscle fibre orientations (lines) and optimal bipolar electrode positions (optElpos; squares indicate the centre of bipolar montages, see Fig. 7-5B) for the four lower facial muscles. The left panels illustrate individual values (grey,) and mean values of the study group (bold black). All results illustrated here refer to bipolar electrodes with an inter-electrode distance of 8 mm and detection surfaces of 4 × 4 mm². In the right panels, mean optimal electrode positions are given in percentages of the horizontal and vertical reference distances, i.e. the distance between the centre and corner of the mouth, and the distance between the centre of the mouth and the bony lower mandibular border at the facial midline, respectively.

determined fulfilling the inclusion criteria of misalignment of the horizontal or skew bipolar electrode montages relative to muscle fibre direction < ± 10°. The locations of maximal interference EMG amplitude had a spatial resolution of only 4 mm corresponding to the high-density grid's inter-electrode-distance. Thus, deviations smaller than half the diagonal of a square built by four grid electrodes (i.e., 2.83 mm) were still considered as agreement between the two positions mentioned above.

In the upper portion of the depressor anguli oris (Fig. 7-7), the highest bipolar amplitudes were actually registered by those electrode montages with the closest distance to the recommended electrode position (Fig. 7-7A). Exceptionally, peaks in the curves indicating higher distances could be observed mostly at very low activity levels. Fig. 7-7B indicates that in eight of the nine evaluated subjects, the bipolar amplitudes registered at the recommended positions were very close to or even corresponded to the maximal amplitude in the grid area. Only one subject showed a systematical amplitude reduction > 10% at this position, though the corresponding distance to the location of maximal interference EMG signal amplitude was only ca. 4 mm (Fig. 7-7A).

Comparably small deviations of the locations of the interference EMG amplitude maxima from the recommended electrode positions and high signal amplitudes at these positions respectively were also found for the depressor labii inferioris (Fig. 7-8). Moreover, also in this muscle relatively low variability of the calculated distances and amplitude percentages was observed in the majority of evaluated subjects when interference EMG data from different activity levels were compared.

In the mentalis (Fig. 7-9) and orbicularis oris inferior (Fig. 7-10), however, greater deviations and smaller amplitude percentages were found. It has to be noted that in the mentalis muscle, the displacements of the interference EMG maxima and, even more markedly, the resulting amplitude decreases seemed to be positively correlated with the activity level. Nevertheless, up to contraction levels of 40% of the maximal voluntary contraction level, RMS values calculated for the bipolar signals registered at the recommended positions were still > 90% of the corresponding maxima in the grid area in nine of the ten evaluated subjects (Fig. 7-9B).

The diagrams for the orbicularis oris inferior (Figs. 7-10A and 7-10B) indicate relatively high inter-individual variability in both the deviations of the interference EMG maxima and the amplitude reductions when compared to the findings for the other three muscles. In spite of this, in five of the nine evaluated subjects, placement of bipolar electrodes according to our recommendations allowed for registering amplitudes percentages >90% of the corresponding maxima in the whole activity level range. A conspicuous finding in the orbicularis oris inferior was that in one subject a constant displacement of the amplitude maxima from the recommended electrode position of only 6.2 mm resulted in a tremendous amplitude decrease of more than 50%.

Discussion

The present study describes a novel method for establishing electrode positioning guidelines for bipolar sEMG recordings based on motor unit analysis, i.e. evaluation of the decomposed sEMG. This method was applied to establish electrode positioning guidelines for the complex musculature of the lower face. Results were validated by comparing the optimal electrode positions determined by motor unit analysis to those positions where the interference EMG recorded during (attempted) selective contractions of corresponding muscles had its maximal amplitude.

A

B
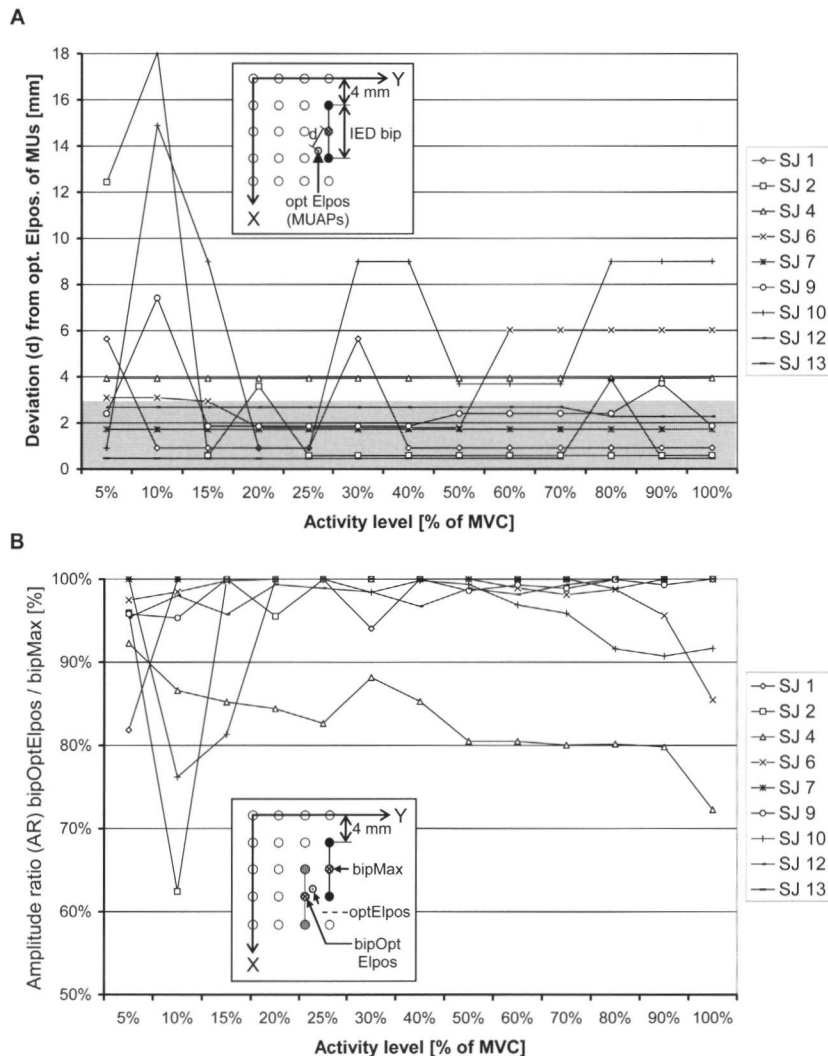
Figure 7-7. Validation of the bipolar electrode positions for sEMG recordings from the upper portion of the depressor anguli oris. (A) The distance *d* (inset) describes the deviation (intra-individual mean value) of the centre of that bipolar electrode montage with maximal interference EMG signal amplitude (RMS value) from the optimal electrode position (opt Elpos) obtained by evaluation of motor unit action potentials (MUAPs). In this muscle, bipolar electrode montages with an inter-electrode distance (IED bip) of 8 mm were constructed in vertical direction using corresponding measured monopolar signals. The deviation d was determined for interference EMG signals recorded during attempted selective contractions of the depressor anguli oris at different levels. Only contractions of those nine subjects were evaluated in which the main fibre orientation differed less than ± 10º from the vertical direction of the bipolar montage. Deviations up to 2.83 mm (grey area) were considered as agreement between the two positions described above due to the spatial resolution of the interference EMG data of 4 mm. (B) The illustrated amplitude ratios describe the relation between the interference EMG amplitude (RMS value) obtained by that bipolar electrode montage (bipOptElpos) with the closest distance to the averaged optimal electrode position of the motor unit action potentials (optElpos), and the maximal interference EMG amplitude of the grid area (bipMax). Amplitude ratios were determined for contractions at different levels.
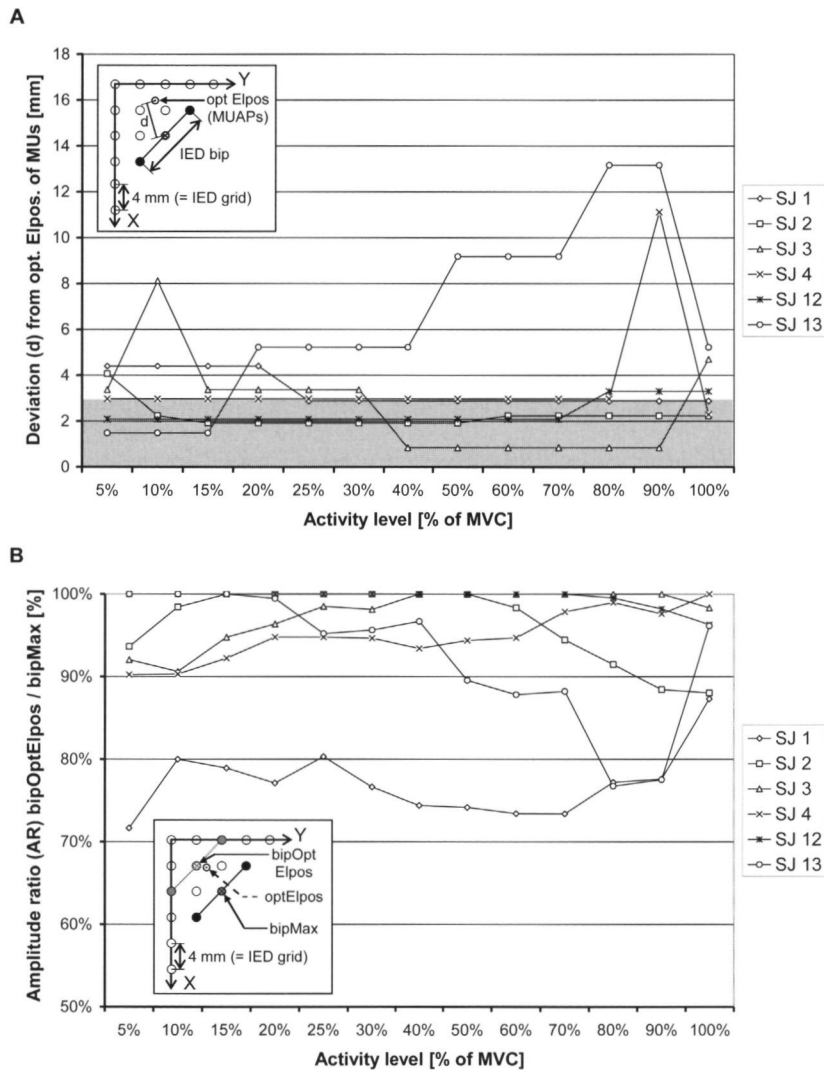
A

B

Figure 7-8. Validation of the bipolar electrode positions determined for the depressor labii inferioris. In this muscle, skew (45° in latero-caudal / medio-cranial direction) bipolar montages with an inter-electrode-distance of 11.3 mm were constructed (see inset). Only six subjects fulfilled the inclusion criterion of main muscle fibre orientation within 45 ± 10°. (A) Deviations d were determined as described in the legend to Fig. 7-7A. (B) Amplitude ratios (AR) bipOptElpos / bipMax were calculated as described in the legend to Fig. 7-7B.

Motor units of the depressor anguli oris are typically located in two regions, with a clear dominance (in number and electrical size) of the more lateral location (Lapatki et al. 2006). Thus, the electrode positions proposed in our study for recordings in the upper and lower muscle portions mainly represent these lateral motor units. Usually, functional studies

A

B
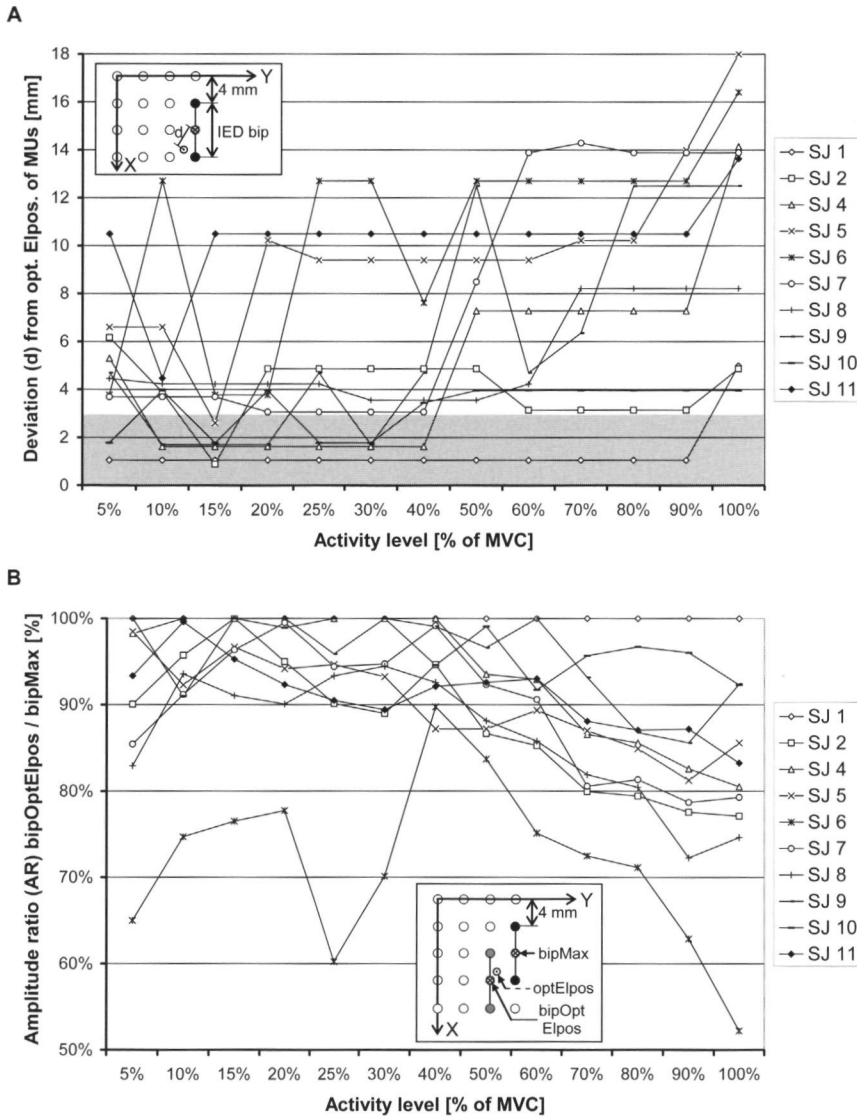
Figure 7-9. Validation of the bipolar electrode positions determined for the mentalis muscle. Bipolar montages with an inter-electrode-distance of 8 mm were constructed in vertical direction (see inset). Ten subjects had main muscle fibre orientations within ± 10°. (A) Deviations d were determined as described in the legend to Fig. 7-7A. (B) Amplitude ratios (AR) bipOptElpos / bipMax as described in the legend to Fig. 7-7B.

require only attachment of one bipolar electrode per muscle. Due to greater distances to adjacent facial muscles potentially resulting in less cross-talk from these adjacent sources, we recommend attachment of a bipolar electrode in the upper portion of the depressor anguli oris. However, this recommendation has to be supported yet by quantitative studies on cross-talk in the lower face. In the validation of individual optimal electrode positions for
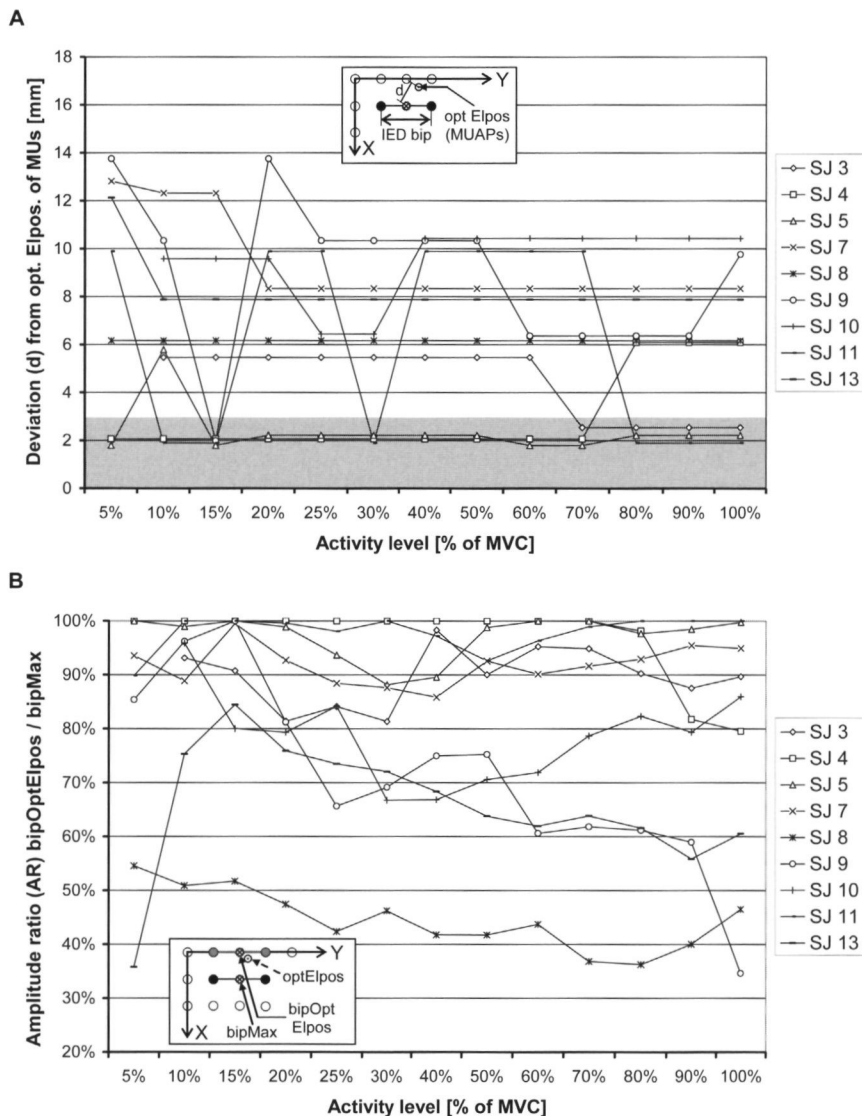
7

A

B

Figure 7-10. Validation of the bipolar electrode positions determined for the orbicularis oris inferior. In this muscle, bipolar montages (inter-electrode-distance: 8 mm) were constructed in horizontal direction (see inset). Nine subjects fulfilled the inclusion criterion, i.e. misalignment of the horizontal montages relative to the main muscle fibre direction < ± 10°. (A) Deviations *d* were determined as described in the legend to Fig. 7-7A. (B) The amplitude ratios (AR) bipOptElpos / bipMax as described in the legend to Fig. 7-7B.

sEMG recordings in the upper portion of the depressor anguli oris, we observed good agreement with the locations of maximal interference EMG and high signal amplitude at the proposed positions respectively in the majority of evaluated subjects and in a wide range of activity levels.

Extreme eccentric endplate locations in

the depressor labii inferioris near its origin at the lower mandibular border allows only for recording from this muscle superior to the endplate zone. Topographical data from the lower face revealed that motor units of the depressor labii inferioris are distributed in the medio-lateral dimension in two or three groups with a varying predominance of either more lateral or medial locations (Lapatki et al. 2006). Obviously, such variable motor unit distribution resulted in an average optimal electrode position approximately in the muscle's anatomical centre. This finding is contrasting with that of the depressor anguli oris, where in the anatomical centre the bipolar signal amplitude was found to be very low (e.g., see Fig. 7-1), and exemplifies the relevance of topographical amplitude information for the determination of electrode placement guidelines. The validation of individual results for the depressor labii inferioris has mainly shown that the determined optimal electrode positions indeed allow for recording bipolar sEMG signals with maximal or at least nearly maximal amplitude. With regard to the possibility of electrode attachment, the proposed location might interfere with the mentolabial fold. If this is actually the case, we recommend shifting the bipolar electrode laterally-cranially (i.e. perpendicular to muscle fibre direction) until its medial border adjoins the mentolabial fold. In spite of such transversal displacement of the electrode pair, high signal amplitude can still be expected due to the broad, sheet-like shape of the depressor labii inferioris which is also reflected by the topographical amplitude profiles of this muscle's MUAPs (as exemplified in Fig. 7-1C).

Anatomical studies have shown that the mentalis muscle consists of fibres with an oblique inclination relative to the skin surface (Braus and Elze 1954; Nairn 1975; Salmons 1995). Increasing muscle fibre depth results in an attenuation of the bipolar sEMG

(Roeleveld et al. 1997c). This attenuation prevented tracing of MUAPs of the mentalis muscle in cranial direction and generally leads to an accessibility of the mentalis for sEMG only in its caudal portion. There, the optimal recording position was vertically located near the centre of the mental soft-tissue, slightly lateral to the facial midline. The validation of the results for ten individual subjects revealed some disagreement between the (averaged) positions of maximal bipolar amplitude along fibre direction in the decomposed MUAPs and the positions of maximal bipolar amplitude in the interference EMG. The relatively high fluctuations of the curves describing the distances between these two positions suggest that co-contraction of adjacent muscles may be one causative factor for displacement of the amplitude maximum in the interference EMG. In addition, during the topographical MUAP analysis we could observe that MUAPs belonging to the mentalis muscle are often characterised by a relatively wide zone of high amplitude with two or more local maxima in the area of the soft-tissue chin. This might also explain why (at least in low and moderate contraction levels), amplitude reductions at the individual optimal electrode positions were limited to 10% (Fig. 7-9B) in spite of partly large metric deviations of the amplitude maxima (Fig. 7-9A).

The typical distribution of motor units of the orbicularis oris inferior in small territories over the whole lower lip (Lapatki et al. 2006) suggested calculating a common mean value for the optimal electrode positions for both (right and left) fibre directions. In addition, this characteristic feature for orbicularis oris inferior motor units makes it generally impossible to avoid straddling of (at least some) motor unit endplates in placing a bipolar electrode. Previous electrophysiological and anatomical studies revealed the existence of different fibre groups of the orbicularis oris inferior with

either horizontal or skewed course (Abbs et al. 1984; Blair 1986; Braus and Elze 1954; McClean and Smith 1982) providing evidence for a highly developed and very complex muscle fibre architecture within the lower lip region. Our sEMG study indicates that – at least in the lower lip area below the vermillion border (i.e., the area covered by the electrode grids) – the horizontal orbicularis oris inferior muscle fibres are predominant. One factor that might have biased this finding is the relatively large inter-electrode spacing of our multi-electrode grids (4 mm) when compared with the very short projected length of the skewed orbicularis oris inferior muscle fibres. More research is necessary to clarify this aspect. The amplitude maxima of most MUAPs of this muscle were vertically located close to, or at the medial multi-electrode grid's upper border (which agreed with the lower lip vermillion). Their average horizontal location was found to be ca. halfway between the centre and the corner of the mouth. Here electrophysiological findings agree well with results from a previous anatomical-histological study providing differential data on the surface area of muscle tissue at different vertical and horizontal levels in histological cross-sections of the human lower lip (Blair and Smith 1986). Based on combined electrophysiological and histological data we suggest positioning a bipolar electrode on the orbicularis oris inferior as close as possible to the lower lip vermillion in the centre between the facial midline to the corner of the mouth, and with an orientation parallel to the course of the vermillion border. We can only speculate as to why in many evaluated subjects the interference EMG signal amplitude at (or close to) this position was submaximal. Both, phase cancellation effects which probably occur in regions where MUAPs belonging to different territories propagate in opposite directions, and/or the possibility that short, skew orbicularis oris inferior fibres are under-represented

in the MUAP samples (as mentioned before), might play a role here.

In previous studies, only interference EMG signals recorded during voluntary contractions were evaluated for the determination of optimal electrode placement in the face (Tassinary et al. 1989; Williamson et al. 1980) or other recording areas (Campanini et al. 2007; Mesin et al. 2009a). Particularly in the face where selective contractions of individual muscle subcomponents are difficult, this approach contains a high risk for cross-talk from co-activated adjacent muscle to bias the results (Lapatki et al. 2003). Actually, this seems to be confirmed in the present study by the unsystematic displacements of the interference EMG amplitude maxima when attempted selective contractions of the mentalis muscle were performed at different levels (Fig. 7-9A), confirming the statement that, without verifying the selectivity of voluntary muscle activation for determining variables for individual muscles, questions remain about the validity of the conclusions (van Vugt and van Dijk 2001).

In the present study we analyzed decomposed MUAPs for establishing electrode positioning guidelines. Indeed, this approach leads to 100% muscle selectivity, because MUAPs represent the activity of a single muscle only and can be unambiguously assigned to their corresponding muscle on the basis of the characteristic amplitude topography. An alternative method for achieving complete muscle selectivity may include electrical stimulation, as e.g. applied in quantitative studies of cross-talk (De Luca and Merletti 1988; Farina et al. 2002b; Koh and Grabiner 1993; van Vugt and van Dijk 2001). However, both selective stimulation of facial nerve branches innervating single muscle subcomponents only, and direct stimulation of these relatively small muscle bundles or sheets at their motor points without co-stimulating adjacent muscles, are hardly achievable in practice (Delbeke 1982).

Utilising muscle-selective MUAPs containing spatio-temporal amplitude information has a further advantage. Their propagation can be followed two-dimensionally on the electrode grid and in time. This allows for defining both the optimal location and orientation of a bipolar sEMG electrode. In contrast, the evaluation of interference EMG signals using linear or two-dimensional electrode arrays is based on the a priori defined orientation of the consecutive electrodes which is difficult to assess and often compromised in complex musculature such as that of the face in particular.

When muscle parameters are extracted by means of single motor unit analysis, it is crucially important that the selected MUAP sample is representative for all MUAPs of the corresponding muscle. In structural respects, a MUAP sample can be considered to be representative if all different MUAP topographies are reflected, and single motor units or a class of motor units are not biasing the results. The latter can be a particular challenge when the selected MUAP sample comprises MUAPs from different recordings during distinct contraction levels, because the recruitment order implies that motor units with lower recruitment threshold are also active at higher recording levels resulting in double-consideration of (groups of) motor units in the MUAP sample. The strategy we have chosen as a compromise for minimising such a selection bias and, simultaneously, achieving greatest possible representation of the whole muscle's motor unit pool was to consider only MUAPs extracted from a single recording file, and to select that recording file showing the greatest topographical variability in MUAP amplitudes. A consequence of this decision was that MUAP sample sizes were relatively small, with averages between 7 and 8 for the four examined muscles and individual sample sizes ranging between 3 and 12. In this context

it has to be emphasised that visual comparison of the MUAP template sets belonging to different high contraction levels indicated that the selected MUAP samples represented the topographical variability of the MUAPs to a great extent.

Usually, the raw sEMG files selected for further evaluation were recorded during contraction between 5% and 15% of the maximal voluntary contraction level. In theory, two aspects may challenge optimal electrode positions extracted from data recorded during such low muscle activity also being valid for recordings during higher contraction levels. First, motor units with different recruitment thresholds may have different spatial distributions of their action potentials leading to a different location of the average amplitude maximum for different contraction levels; as mentioned before, this possibility was not confirmed in visual inspection of the decomposed MUAP template sets belonging to different contraction intensities. Secondly, isotonic contraction of facial muscles is always accompanied by some movement of the muscle tissue relative to the electrode-skin complex. This could result in larger displacements of the amplitude maximum on the electrode grid when the contraction intensity is increased. Since the optimal electrode positions determined in the present study were topographically related to the interference EMG maxima obtained during contractions at different levels, the combined effect of these two factors could be quantitatively assessed. A remarkable finding in most of the evaluated subjects was the high local stability of the interference EMG amplitude maxima close to the proposed electrode positions in a wide range of activity levels, i.e. from low to moderate (in the mentalis) or even up to submaximal levels (in the depressor anguli oris and depressor labii inferioris). It is important to note that this might be different in other muscles consisting

7

of both superficially and deeply located motor units, where the MUAPs recorded on the skin surface may not represent the whole muscle's motor unit sample, or where the relative movement between the electrode-skin complex and the muscle tissue due to the contraction may be more pronounced as a result of more unfavorable anatomical conditions (Farina et al. 2001).

In agreement with most of the previously described approaches for establishing electrode positioning guidelines for studying muscle functions, we considered an electrode location to be optimal when the sEMG registered from the examined muscle subcomponent has maximal amplitude. Principally, this approach should lead to the best signal-to-noise ratio, as demonstrated by the MUAP templates of Fig. 7-1 showing large amplitude differences between electrode montages at different locations. Amplitude maximisation may simultaneously contribute to minimise the relative portion of the sEMG signal generated by co-activation of adjacent muscles. It has to be emphasised, however, that it is difficult to assess the contribution of amplitude maximisation to reduction in such "cross-talk" quantitatively, due to complex interrelations of causative factors of this phenomenon (Farina et al. 2002b; Mesin et al. 2009b). An alternative, potentially more promising strategy against cross-talk suggests to shift the electrodes to the side of the muscle away from the edge with other subdivisions or adjacent muscles, so that the geometrical distance of the recording site to adjacent (unwanted) sources is maximised (Freriks et al. 1999). Though this approach may be efficient in some recording areas, it is certainly confronted with fundamental limitations when anatomically complex musculature such as that of the face is examined. First, facial muscles may have adjacent muscles on both sides and, therefore, reduction in cross-talk from the adjacent muscle on one side

would result in an increased cross-talk from the muscle on the other side. Second, small muscle subcomponents are often composed of fibres arranged in narrow bands or bundles. Shifting the electrodes perpendicular to the muscle fibre direction would then markedly decrease the signal registered from the muscle of interest leading to a compromised signal-to-noise ratio. Thus, it seems that with optimising the recording technique alone, the problem of cross-talk in facial sEMG cannot be solved.

In a previous anatomical study, electrode placements for examining the facial musculature with fine-wire electrodes were proposed by giving absolute distances (Kennedy and Abbs 1979). The high degree of inter-individual variation in facial size and shape was not accounted for in that study. In contrast, in the present study we performed a spatial scaling of the individual electrode positions and orientations and specified these parameters in relative measures, i.e. in percentages of distances between facial anatomical landmarks. As demonstrated in a recent study on facial motor unit topography, spatial scaling of topographical parameters significantly decreases inter-individual variability (Lapatki et al. 2006). As a consequence, average positions calculated from spatially scaled data are more accurate.

For transferring the electrode positions suggested in this study for the four lower facial muscles to novel subjects, measurements of the horizontal and vertical reference distances have to be taken along the curved skin surface. Subsequently, these lengths and the corresponding percentages (Fig. 7-6) have to be used for calculating the vertical and horizontal electrode positions for the corresponding subject in millimeters. This applies to all positions except for the vertical coordinate (and angle) of the bipolar electrode over the orbicularis oris inferior, where we recommend referring to the level and to the course of the lower lip vermillion. Our high-density sEMG study in

the lower face revealed that optimal positions for bipolar electrodes with different inter-electrode distances seem to be quite similar (see also Table 7-2). Thus, the decision regarding an appropriate inter-electrode distance for bipolar sEMG recordings in the face can be based on other factors, such as signal amplitude, spatial filter properties, as well as practical methodological issues. From the latter point of view, we suggest using a bipolar electrode simply consisting of two thin, 4-mm diameter silver/silver-chloride disks. Such small electrode dimensions are still handy in research or clinical applications since a special skin attachment technique allows firm and secure electrode fixation without requiring an acrylic housing (usually the housing causes increased outer dimensions). An important advantage of such small electrodes is that an inter-electrode distance of 8 mm can be realised which should increase spatial selectivity (Loeb and Gans 1986). Moreover, in a previous study we could successfully demonstrate that such bipolar electrodes allow for the simultaneous observation of multiple facial muscles with a minimal functional obstruction (Lapatki et al. 2003).

To conclude, we developed methods for determining optimal positions of bipolar electrodes using topographical parameters and two-dimensional amplitude profiles of MUAPs extracted from high-density sEMG recordings. This approach can be generally applied to all musculature accessible to sEMG. Electrode positioning guidelines were established for the challenging muscle area of the lower face consisting of subcomponents with very close topographical relationships. The results were validated using interference EMG signals recorded during attempted selective contractions of the four lower facial muscles at different levels. Facial sEMG has proven to be a valuable research and diagnostic tool for applications in psychophysiology, speech physiology and dentistry. In previous sEMG studies in these fields, several important criteria for electrode positioning had to be ignored due to the lack of information on relevant topographical electrophysiological aspects. These limitations have been taken care of in the present study. Finally, an important general principle has been established for improving both the validity and reproducibility of sEMG investigations.

7

8

ESTIMATION AND REMOVAL OF EMG CROSS-TALK IN THE LOWER FACE

Lapatki B.G., van Dijk J.P., Jonas I.E., Zwarts M.J., Stegeman D.F., Oostenveld R.
Submitted

Surface electromyograms (sEMG) from facial muscles are confounded by activity of adjacent muscles. In this study we estimated this unwanted "EMG cross-talk" and introduce a novel method for estimating the true individual muscle activity. High-density sEMG was recorded in the lower face in 13 subjects. Muscle-selective motor unit action potentials (MUAPs) were extracted and used to quantify cross-talk as the ratio between the MUAP amplitudes at an adjacent electrode and at the electrode above the contracted muscle. These cross-talk ratios (CTRs) were used in a matrix inversion algorithm to separate cross-talk from co-activation in interferencing EMG patterns. We found mean CTRs ranging from 0.03 to 0.52, reflecting the contribution of neighbouring muscle activity on the recorded sEMG. The CTRs are of great importance for a correct interpretation of the facial sEMG and may substantially improve the estimate of individual muscle activity.

Introduction

The facial musculature is of great importance in a variety of functions, such as speech, vision, food intake, and the mediation of emotional and affective states. Most physiologic facial muscle functions are relatively complex and involve many muscles simultaneously (Nairn 1975; Salmons 1995). This shows in the variety of facial expressions as well as in the highly developed activation patterns in which the perioral muscles participate during speech or other oral functions. A consequence of the simultaneous participation of multiple muscles in facial activities is the need for multi-muscle observations in functional studies.

Surface electromyography (sEMG) is a widely used, non-invasive tool for studying muscle activity. The large pick-up volume of surface electrodes is usually considered to be an advantage over intramuscular recording technique, because it enables the behaviour of many simultaneously active motor units to be studied and, therefore, provides an overview over the activity of a muscle as a whole. However, a limited "spatial selectivity" also means that signals from muscles lying in the vicinity of the muscle of interest may be co-registered due to volume conduction through the tissue between the muscle and the electrode (De Luca and Merletti 1988). Such unwanted co-registration of activity of adjacent muscles is referred to as "EMG cross-talk" and is a particular problem in recordings from musculature with complex architecture, as for example the facial muscle system consisting of multiple small, blending and interweaving muscle subcomponents (Braus and Elze 1954; Nairn 1975; Salmons 1995).

EMG cross-talk has been examined in a number of studies, including mathematical simulations and experimental designs which provide an important basis for understanding this phenomenon. For example, the amount of cross-talk has proven to be significantly influenced by the physical properties of the volume conductor, such as the thickness of subcutaneous layers (Kuiken et al. 2003; Mesin et al. 2009b; Roeleveld et al. 1997a; Solomonow et al. 1994), skin conductivity (Lowery et al. 2003; Mesin et al. 2009b; Roeleveld et al. 1997a) and the presence of superficial bone (Lowery et al. 2002; Mesin 2008). Recent studies have also shown that especially the non-propagating components of the EMG related to the generation and extinction of the action potential at the endplate and muscle fibre endings (so-called "far-field potentials" (Stegeman et al. 1997)) contribute significantly to cross-talk (Dimitrova et al. 2002;

8

Farina et al 2002b)

Cross-talk obviously confounds estimates of muscle activity and is therefore considered to be one of the most significant limiting factors in the interpretation of sEMG (Lowery et al 2003, Rau et al 2004) A common measure to suppress cross-talk consists of spatial high-pass filtering using a bipolar (i e , single differential) or higher order electrode montage (Disselhorst-Klug et al 1997, van Vugt and van Dijk 2001) Such a spatial filter makes use of the spatial low-pass filtering characteristics of the volume conductor which is separating the muscle tissue from the electrodes (Gath and Stalberg 1977) Since cross-talk signals have to cover a longer distance through the volume conductor to reach the electrode site than signals from the underlying muscle, the former are expected to contain more spatial low-frequency components These low-frequency components are suppressed by "common-mode rejection" leading to a relative attenuation of cross-talk (van Vugt and van Dijk 2001) Experimental studies demonstrated that the longitudinal double-differential electrode montages and the branched electrode type are the most effective spatial filters for cross-talk reduction (De Luca and Merletti 1988, Disselhorst-Klug et al 1999, Farina et al 2002b, Koh and Grabiner 1993, van Vugt and van Dijk 2001) Decreasing the inter-electrode distance(s) (IED) of bipolar or higher order electrode montages has also been found to reduce cross-talk (Disselhorst-Klug et al 1999, Farina et al 2002b, Fuglevand et al 1992) and is therefore often recommended for minimising this phenomenon However, the variable composition of cross-talk signals of propagating and non-propagating signal components (Dimitrova et al 2002, Farina et al 2002b, Mesin et al 2009b) makes it difficult to generalise or predict the effectiveness of spatial filtering In some recording areas it may be effective to shift the electrodes

to the side of the muscle away from the edge with other subdivisions or adjacent muscles, thereby increasing the geometrical distance of the recording site to the adjacent unwanted sources (Freriks et al 1999) However, this approach is obviously confronted with limitations when a muscle is surrounded by other muscles on several sides

So far, elimination of cross-talk by optimising recording techniques or data processing are limited Thus, it seems obligatory to identify and quantitatively estimate the bias resulting from cross-talk Computer model simulations indicated that neither cross-correlation analysis of two EMG signals from different electrodes (Lowery et al 2003), nor temporal high pass filtering (Dimitrova et al 2002), are suitable means for this purpose, although often suggested (Lowery et al 2003, Mogk and Keir 2003, Morrenhof and Abbink 1985, Winter et al 1994) This is certainly due to the composition of the sEMG signals of propagating and non-propagating components (Farina et al 2002b, Farina et al 2004, Lowery et al 2003) Further limitations in the application of cross-correlation in this context occur if cross-talk signals from more than one muscle contribute to a recording (Disselhorst-Klug et al 1999), which applies to facial sEMG In these conditions a comparison of pairs of signals is not sufficient

Perhaps the most straightforward procedure to detect and quantify cross-talk is to evaluate voluntary or electrically stimulated "selective" contractions of a specific muscle and to relate this activity to the recordings over the contracted and over neighbouring muscles In this manner, reference values for cross-talk have been provided for leg muscles (De Luca and Merletti 1988, Farina et al 2002b, van Vugt and van Dijk 2001) and perioral muscles (Lapatki et al 2003) However, it has to be emphasised that both voluntary contractions and electrical stimulation do not guarantee

the absence of co-activation or co-stimulation of neighbouring muscles. Without verifying the absence of this collateral muscle activity, by e.g. on-line control using additional intra-muscular (i.e., spatially more selective) fine-wire electrodes, the validity of the corresponding conclusions remains questionable (van Vugt and van Dijk 2001). Fundamental limitations in "isolated" voluntary contractions and selective electrical stimulation of individual muscle components for achieving muscle selectivity concern the facial muscle system in particular, because both are barely achievable in practice (Delbeke 1982; Lapatki et al. 2003).

In a recent high-density sEMG study we proposed guidelines for optimal bipolar electrode placement in the lower facial area (Lapatki et al. 2010). We considered electrode locations and orientations to be optimal when the registered sEMG signals had maximal amplitudes. The purpose of the present study was to quantify the amount of cross-talk for the recommended electrode placement parameters using a novel approach based on the analysis of muscle-selective motor unit action potentials. A second goal was to exemplify the utilisation of these quantitative cross-talk estimations for distinguishing between cross-talk and co-activation in interference sEMG signals recorded during attempted isolated facial muscle contractions.

Materials and Methods

Subjects

Thirteen volunteers (6 men and 7 women, mean age 27.2 yr, range 21 – 43 yr) without known neurological or other general health disorders participated in the study. The ethics commission of the Radboud University Nijmegen Medical Centre, the Netherlands, approved the study protocol and subjects gave informed consent prior to the experiment.

High-density sEMG recordings

We acquired sEMG data using two flexible multi-electrode sEMG grids manufactured by Digiraster Tetzner GmbH (Stuttgart, Germany), each consisting of 6 × 10 regularly arranged, chlorided silver electrodes with a diameter of 1.7 mm. The distance between adjacent electrodes was 4 mm (centre-to-centre) in both directions, allowing for a sufficient spatial sampling for the facial musculature. By positioning the two electrode grids side by side and vertically displaced to each other by one electrode row, the four muscles of the lower face, i.e. the depressor anguli oris, depressor labii inferioris, mentalis and orbicularis oris inferior muscles, were largely covered. At the border between the medial and the lateral grid the horizontal distance between consecutive electrodes was exactly twice the inter-electrode distance within each grid. The electrode grids were attached to the skin using specially prepared double-sided adhesive tape. An elaborate procedure led to firm electrode fixation and high signal quality due to relatively low electrode-to-skin impedances (Lapatki et al. 2004).

The electric potential at each of the 120 single electrodes was acquired "monopolarly" with the reference electrode attached to the dorsum of the nose. A 128-channel Mark-6 amplifier (BioSemi Inc., Amsterdam, The Netherlands) band-pass filtered (3.2 – 400 Hz) and subsequently synchronously sampled the sEMG signals at 2000 Hz at a resolution of 0.5 µV/bit over a range of +/-16 mV (16 bits).

Experimental procedure

The lower facial musculature was examined either on the right (7 subjects) or left (6 subjects) side of the face. After application of the electrodes, but prior to actual recordings, the subjects were instructed in selective lower facial muscle contractions supported by visual amplitude feedback. The feedback consisted

8

of displaying the Root Mean Square (RMS) over the last 500 ms of selected bipolar channels to indicate the activity level of the muscle to be contracted. When subjects were familiar with the experimental tasks, sEMG data were acquired while it was attempted to selectively contract one of the four examined lower facial muscles.

The high-density sEMG recordings were made at different activity levels, starting at 2-3% of the maximal voluntary contraction level (this level was estimated on the basis of the RMS value of the selected channels during an initial maximal voluntary contraction). Subsequently, the contraction level was increased in 5% steps up to 30%, and then in 10% steps up to the maximal voluntary contraction level (100%). Per subject, per muscle and per contraction level, we performed two recordings of about 20 s duration. Although facial muscles are relatively resistant to fatigue (van Boxtel et al. 1983), recovery breaks of approximately 20 – 60 s were made between subsequent contractions to prevent local fatigue effects. Additionally, subjects were allowed a longer rest when they felt upcoming fatigue

Data analysis
EMG data were analyzed using a protocol programmed in Matlab, Version 7.04 (The Mathworks Inc., Natick, MA, USA). First, we applied a 10 Hz high-pass filter to eliminate low-frequency movement artifacts. Table 8-1 provides a schematic overview over the further steps for more specific data evaluation.

Up to the determination of the optimal electrode position (step 3), the procedures are described in full detail in two previous publications providing information on the lower facial muscle architecture (Lapatki et al. 2006) and guidelines for optimal placement of bipolar sEMG electrodes in this area (Lapatki et al. 2010). These steps are only summarised here.

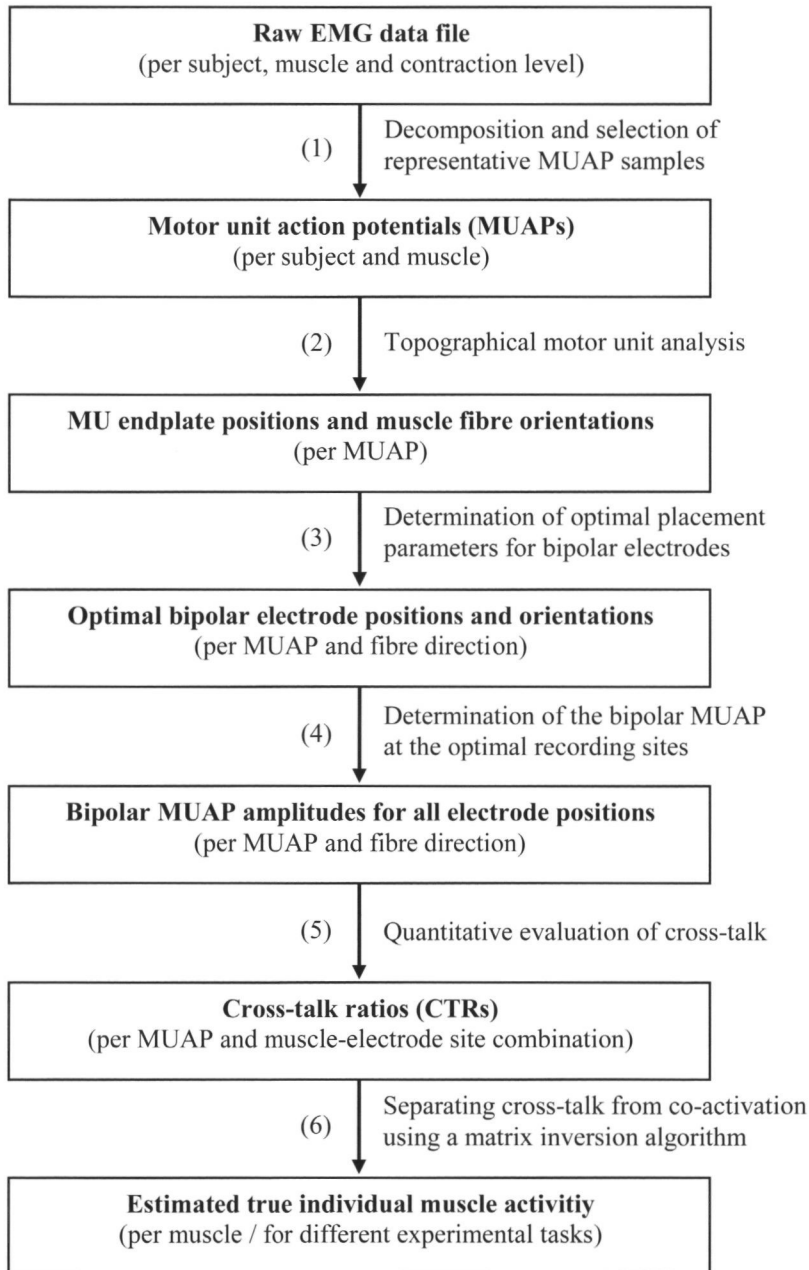## Decomposition and selection of representative MUAP samples (step 1)
The raw sEMG data files for the contraction levels up to 30% of the maximal voluntary contraction level were decomposed on the basis of the specific topographical profiles and amplitude characteristics of firings of individual motor units (Kleine et al. 2007). Per recorded file (i.e., for a certain subject, muscle, recording level and repetition) we obtained a set of motor unit action potentials (MUAPs). All MUAP sets were then visually inspected to select one of them per subject and muscle which best represented the distinct MUAP topographies observed in the different recording levels and repetitions. Visualising the MUAPs as bipolar templates (Kleine et al. 2007) facilitated the differentiation of their distinct amplitude topographies during this selection. On average, the selected MUAP sets consisted of 8 distinct MUAPs. Only MUAPs belonging to these MUAP sets were subsequently topographically analyzed.

Topographical motor unit analysis (step 2)
To determine the motor unit endplate and muscle fibre orientation, we used the MUAPs in their monopolar montage. As an initial step, the monopolar MUAPs were spatially interpolated in two stages using a bicubic inter- or extrapolation method. First, we obtained the potential at the position of the missing electrodes in between the two attached electrode grids and at the upper or lower grid borders. Second, we interpolated the complete template data set in both dimensions eight times between adjacent grid electrodes to achieve a regular 0.5-mm spatial resolution.

From each of these interpolated monopolar MUAPs we extracted the location of the motor unit endplate zone and the muscle fibre orientation at both sides of the endplate zone by interactive evaluation of the MUAPs visualised as amplitude map sequences (which can

Table 8-1. Flow chart of the data analysis procedure

```
┌─────────────────────────────────────────────────────┐
│              Raw EMG data file                        │
│    (per subject, muscle and contraction level)        │
└─────────────────────────────────────────────────────┘
                    │  (1)   Decomposition and selection of
                    │        representative MUAP samples
                    ▼
┌─────────────────────────────────────────────────────┐
│        Motor unit action potentials (MUAPs)           │
│            (per subject and muscle)                   │
└─────────────────────────────────────────────────────┘
                    │  (2)   Topographical motor unit analysis
                    ▼
┌─────────────────────────────────────────────────────┐
│  MU endplate positions and muscle fibre orientations  │
│                  (per MUAP)                           │
└─────────────────────────────────────────────────────┘
                    │  (3)   Determination of optimal placement
                    │        parameters for bipolar electrodes
                    ▼
┌─────────────────────────────────────────────────────┐
│    Optimal bipolar electrode positions and orientations│
│            (per MUAP and fibre direction)             │
└─────────────────────────────────────────────────────┘
                    │  (4)   Determination of the bipolar MUAP
                    │        at the optimal recording sites
                    ▼
┌─────────────────────────────────────────────────────┐
│   Bipolar MUAP amplitudes for all electrode positions  │
│            (per MUAP and fibre direction)             │
└─────────────────────────────────────────────────────┘
                    │  (5)   Quantitative evaluation of cross-talk
                    ▼
┌─────────────────────────────────────────────────────┐
│              Cross-talk ratios (CTRs)                 │
│  (per MUAP and muscle-electrode site combination)     │
└─────────────────────────────────────────────────────┘
                    │  (6)   Separating cross-talk from co-activation
                    │        using a matrix inversion algorithm
                    ▼
┌─────────────────────────────────────────────────────┐
│       Estimated true individual muscle activitiy       │
│      (per muscle / for different experimental tasks)   │
└─────────────────────────────────────────────────────┘
```

8

be regarded as "MUAP movies"). This procedure is based on the principle that the location of the endplate zone and the main muscle fibre orientation of a motor unit correspond to the location where the MUAP starts and in which direction it propagates. Both could be determined by localising the amplitude maximum on the electrode grid at different latencies of the MUAP.

Determination of optimal bipolar electrode positions and orientations (step 3)

According to our previous definition (Lapatki et al. 2010) we considered the orientation and the location of a bipolar electrode to be optimal when the maximal sEMG amplitude is registered. In theory, a maximal bipolar signal is obtained by orientating the electrode

pair parallel to the muscle fibre direction at a certain location between the endplate zone and the muscle's origin or insertion (Freriks et al. 1999; Loeb and Gans 1986). Since both the complete topographical amplitude information (contained in the monopolar MUAPs) and muscle fibre directions were available, we could determine the optimal bipolar electrode positions for the individual MUAPs from our data. We tried to determine these positions for both fibre directions away from the endplate (for reasons discussed below, this was only possible for the depressor anguli oris muscle). Moreover, we determined optimal electrode positions for different inter-electrode distances and for bipolar electrodes with different electrode surface sizes.

Results for individual MUAPs were aver-
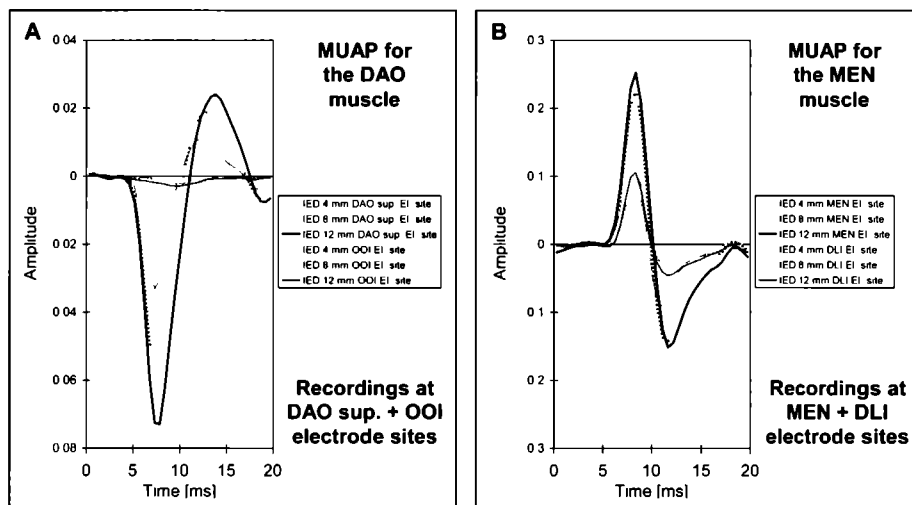
Figure 8-1. Bipolar MUAP shapes determined for optimal electrode sites for different muscles and for bipolar electrodes with different inter-electrode distances (IEDs) (A) Shape of a MUAP belonging to the depressor anguli oris (DAO) muscle when registered by the bipolar electrode positioned directly over this muscle (bold signals) and by the electrode positioned over the orbicularis oris inferior (OOI) muscle (thin "cross-talk signals") The signals for bipolar electrodes with IFDs of 4, 8 and 12 mm are plotted in light grey dashed, grey dotted, and black solid lines, respectively As expected, a nearly linear increase in signal amplitude can be observed with increasing IED (Roeleveld et al 1997c) Due to the relatively large distance of this adjacent recording site to the source of the potential and the unfavourable orientation of the bipolar montage with respect to the muscle fibre direction, the OOI cross-talk is small (B) Bipolar mentalis (MEN) MUAP recorded over the MEN (bold signals) and depressor labii inferioris (DLI) muscles (thin signals) The cross-talk signals (DLI recording site) have relatively high amplitudes (ca 25% of those obtained above the MEN muscle) and also increase approximately linearly with increasing IED Signal amplitude over the MEN muscle increased markedly when the IED was enlarged from 4 mm to 8 mm, but increased much less when the IED was further increased to 12 mm

aged within each subject (per muscle, fibre direction and inter-electrode distance) to determine electrode positions and orientations representative for the whole muscle. For each individual subject we then spatially warped the facial dimensions including the electrode locations and orientations in such a way as to obtain agreement with the average facial dimensions of the whole study group (see (Lapatki et al. 2010) for more details regarding this normalisation procedure). Results from measurements on the left side of the face were transformed to the right side. We then combined the results of all subjects for inter-individual comparisons and for the calculation of mean values of optimal electrode positions and orientations over all subjects.

Determination of the bipolar MUAP at all optimal recording sites in the lower face (step 4)

From step 3, optimal bipolar electrode locations and orientations are available for each of the four lower facial muscles (and in the
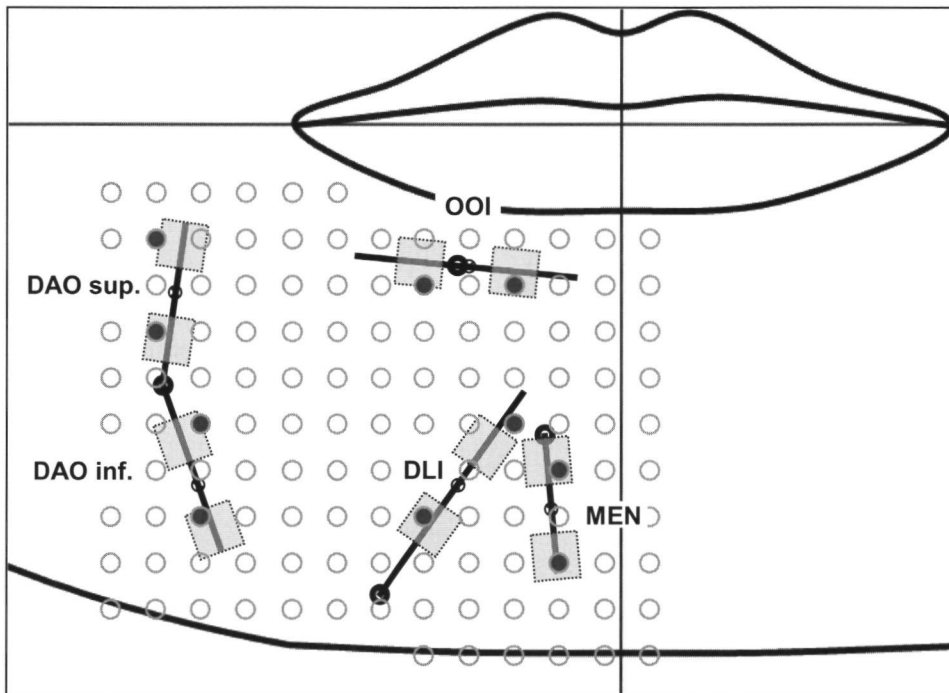
Figure 8-2. CTRs were primary determined for the optimal electrode placements established in our previous study (Lapatki et al. 2010) having skew orientations and positions somewhere in between the grid electrodes (dotted rectangles filled with light grey color). For calculating the true muscle activity by multiplication of the inverted CTR matrix with the vector of RMS values for measured composite EMG signals, we calculated a second set of CTRs for bipolar montages constructed using the grid electrodes themselves (filled circles). In this manner, an important precondition for the application of the matrix inversion algorithm, i.e. the agreement of the locations for which CTRs are calculated and from which EMG signals are available, was fulfilled. In each individual subject we chose those grid montages which were most similar to the optimally positioned bipolar electrodes. These montages had always a vertical direction for the depressor anguli oris and mentalis muscles, a horizontal direction for the orbicularis oris inferior, and an inter-electrode distance of 8 mm in these muscles. Due to more skew fibre orientation, bipolar montages on the depressor labii inferioris muscle were constructed with a 45° orientation, leading to an inter-electrode distance of 11.3 mm. Muscle abbreviations: superior and inferior portions of the depressor anguli oris (DAO sup., DAO inf.); depressor labii inferioris (DLI); mentalis (MEN); and orbicularis oris inferior (OOI).

depressor anguli oris muscle for the upper and lower muscle portion). These positioning parameters allow registering the MUAPs from the corresponding muscle with maximal amplitude. To quantify the EMG cross-talk, we evaluated from each MUAP the corresponding potential at the optimal bipolar electrode position(s) above the contracted muscle itself as well as at the positions optimal for bipolar sEMG recordings from the three adjacent muscles (examples for such "cross-talk potentials" can be taken from Fig. 8-1).

The procedure for obtaining the bipolar MUAP at the different positions included the determination of the monopolar potentials of two virtual square electrodes (Fig. 8-2) with equal distances (along fibre direction) from the corresponding optimal position. These potentials were determined for all latencies of the corresponding MUAP by interpolating the monopolar MUAP amplitude values in the area of the two square electrode surfaces with a resolution of 0.5 mm using a 3D spline interpolation algorithm, and by subsequent averaging the interpolated potentials over each electrode surface (averaging of the potential in the electrode area has proven to be a valid principle under most practical conditions (van Dijk et al. 2009)). Then we calculate the RMS amplitude value of the bipolar MUAP determined from these two averaged monopolar potentials. We repeated the whole procedure for square electrodes with a size of 2×2 mm^2, 4×4 mm^2 and 6×6 mm^2, and with a distance ranging from 0.8 to 20 mm (in steps of 0.8 mm) to evaluate possible influences of the detection surface geometry and the inter-electrode distance of the bipolar montages on the MUAP amplitudes and the amount of cross-talk, respectively. Moreover, bipolar signal amplitudes were determined for both the intra-individual averages of optimal electrode position and orientation as well as for the group averages for these parameters.

Quantitative characterisation of cross-talk (step 5)

To quantify the cross-talk occurring between the contracted muscle and an adjacent recording site, we defined the cross-talk ratio (CTR) according to

$$CTR_{MUAP\,(i)\,to\,electrode\,(j)} = \frac{RMS_{electrode\,(j)}}{RMS_{electrode\,(i)}}$$

(Eq. 1)

The CTR describes for a certain MUAP the ratio between the RMS amplitude value obtained by an adjacent bipolar electrode (j) and that obtained by the bipolar electrode optimally positioned over the contracted muscle (i).

Since we assumed that the evaluated MUAP samples were representative for the whole muscle, we averaged the CTR values for individual MUAPs intra-individually (per subject, muscle, fibre direction and inter-electrode distance) to obtain cross-talk estimates representative for the whole muscle. Since no systematical differences between CTRs for the right and left side of the face, as well as between male and female subjects were found (Student's t-test, $p > 0.05$), we combined the results of all subjects for characterisation of inter-individual variability in cross-talk and for the calculation of mean values over all subjects.

Separating cross-talk from co-activation using a matrix inversion algorithm (step 6)

The averaged CTRs for all possible combinations of the lower facial muscles with the different electrode sites can be combined in a matrix M (Eq. 2). We defined this matrix to reflect the different muscles to which the CTRs belong in different columns, and to reflect the different electrode sites in different rows. Moreover, only CTRs referring to one optimal electrode position per muscle are considered resulting in a 4×4 matrix.

$$M = \begin{pmatrix} 1 & CTR_{DLI\,to\,DAO} & CTR_{MEN\,to\,DAO} & CTR_{OOI\,to\,DAO} \\ CTR_{DAO\,to\,DLI} & 1 & CTR_{MEN\,to\,DLI} & CTR_{OOI\,to\,DLI} \\ CTR_{DAO\,to\,MEN} & CTR_{DLI\,to\,MEN} & 1 & CTR_{OOI\,to\,MEN} \\ CTR_{DAO\,to\,OOI} & CTR_{DLI\,to\,OOI} & CTR_{MEN\,to\,OOI} & 1 \end{pmatrix}$$

(Eq. 2)

As mentioned before, in the depressor anguli oris muscle we could determine an optimal electrode position for the fibre directions (i.e., the muscle portions) above and below the motor endplates (this is in contrast to the remaining three muscles, where only one fibre direction could be evaluated). This required the selection of CTRs referring to either one of the two positions and in the forthcoming, the results obtained by using the upper depressor anguli oris electrode position will be reported. (See legend to Fig. 8-2 for muscle abbreviations used in Eqs. 1-8).

Each (vertical) column of the CTR matrix describes the fractions of the activity of a certain muscle that is registered at the four different electrode sites, with the amplitude registered over the contracted muscle itself as reference value (i.e., 1). Conversely, each (horizontal) row of the matrix describes the composition of the potential v recorded by a certain electrode. Assuming that the MUAP sets from which the CTRs were extracted were representative for the interference EMG signals obtained from the corresponding muscles, this potential is the weighted sum of the true activity s of the four muscles with the CTR values given in the corresponding row as weighting factors. For instance, Eq. 3 specifies the potential recorded by the depressor anguli oris electrode.

Given bipolar interference sEMG signals over the four muscles that are simultaneously recorded, we obtain four linear equations with four unknowns, namely the true activities s of the individual muscles. These equations can be combined in a matrix equation, with the measured interference EMG signals as vector v and the CTR matrix M from the MUAP analysis as known variables, and the vector s describing true muscle activities as unknown variables:

$$\vec{v} = \mathbf{M} \times \vec{s};\ \vec{v} = \begin{pmatrix} v_{DAO} \\ v_{DLI} \\ v_{MEN} \\ v_{OOI} \end{pmatrix};\ \vec{s} = \begin{pmatrix} s_{DAO} \\ s_{DLI} \\ s_{MEN} \\ s_{OOI} \end{pmatrix}$$

(Eq. 4)

The true muscle activity can now be estimated by multiplying the inverted CTR matrix (M^{-1}) with the measured interference EMG signals:

$$\vec{s} = \mathbf{M}^{-1} \times \vec{v}$$

(Eq. 5)

It should be noted that calculation of the true muscle activity should be possible for any combination of four bipolar electrodes (and corresponding CTRs, respectively) positioned somewhere in the lower face, and not only for the four optimally positioned electrodes. This is true on condition that the CTRs and EMG interference signals used in the matrix inversion algorithm refer to identical electrode positions and orientations. However, the optimal electrode positions (which were determined in the interpolated data) did not precisely coincide with the grid electrodes, but were located somewhere in between. As a solution, we determined a second set of CTRs for (vertical, horizontal or 45°-skew) bipolar grid electrode montages closest to the optimal electrode positioning parameters (Fig. 8-2).

8

$$v_{Electrode\,DAO} = s_{DAO} + CTR_{DLI\,to\,DAO} \times s_{DLI} + CTR_{MEN\,to\,DAO} \times s_{MEN} + CTR_{OOI\,to\,DAO} \times s_{OOI}$$

(Eq. 3)

The estimation of the "true" activity of the four muscles by separating the cross-talk from co-activation is demonstrated by means of two examples: in the first, we eliminated cross-talk from recordings during selective contractions of all four examined lower facial muscles at different activity levels in one individual subject; in the second, we compared the ability of the subjects to selectively contract one muscle (the depressor labii inferioris). The possibility to use a single matrix M between subjects is also tested and discussed.

Results

CTRs from optimal electrode placements

Mean CTRs of the study group for the muscle-electrode site combinations are presented in Fig. 8-3A (as mentioned before, for the depressor anguli oris muscle, it was possible to determine CTRs for both fibre directions away from the endplates resulting in a 5 × 5 table). The presented cross-talk estimates correspond to bipolar electrodes with an inter-electrode distance of 8 mm and detection surface sizes of 4 × 4 mm², which are practicable dimensions for bipolar sEMG recordings in the face (Lapatki et al. 2003). The electrode positions and orientations used correspond to the optimal placement established in our previous study (Lapatki et al. 2010). Fig. 8-3B gives an overview over these optimal electrode placements and the table in Fig. 8-3C includes their (relative) horizontal and vertical facial coordinates as well as their angulations relative to the facial midline.

Depressor anguli oris MUAPs showed maximally 20% of their amplitudes at the electrode sites over the other three muscles indicated by the CTRs being ≤ 0.20 in the first two columns of Fig. 8-3A. The smallest CTR (0.06) was found for the orbicularis oris inferior's electrode which has the greatest distance to the depressor anguli oris muscle (Fig. 8-3B).

Very high CTRs were determined for the MUAPs of the depressor labii inferioris at the mentalis electrode site (0.52) and, conversely, for the MUAPs of the mentalis at the depressor labii inferioris electrode site (0.40). In comparison, mean CTRs of depressor labii inferioris and mentalis MUAPs reached maximally 0.13 at the electrodes above the other two muscles. Moderate CTRs were found for the orbicularis oris inferior MUAPs with mean values ranging from 0.11 to 0.21 (Fig. 8-3A).

To show the inter-individual variability, an overview of CTRs is given in Fig. 8-4 as box-plot diagrams. The black lines within the grey boxes are the median values which may slightly differ from the mean values given in the table in Fig. 8-3A. The Figs. 8-4A and 8-4B allow a comparison of the cross-talk for the two alternative electrode sites for sEMG recordings from the depressor anguli oris muscle. In the majority of subjects we registered higher amplitudes on the superior muscle portion.

Dependency of the CTRs from recording parameters

Small and non-systematic changes in the CTRs were observed when comparing electrodes with detection surface sizes of 2 × 2 mm², 4 × 4 mm² and 6 × 6 mm². The inter-quartile range of the CTR differences between the three different detection surface sizes was mostly within ± 0.01 for all muscle-electrode site combinations and all inter-electrode distances.

Bipolar electrodes with small inter-electrode distances have been recommended for facial sEMG to minimise the cross-talk. Our results indicate, however, that the increase in cross-talk with increasing inter-electrode distance is relatively small (Fig. 8-5). Some muscle-electrode site combinations even showed slightly decreasing CTRs with an increase in the inter-electrode distance.
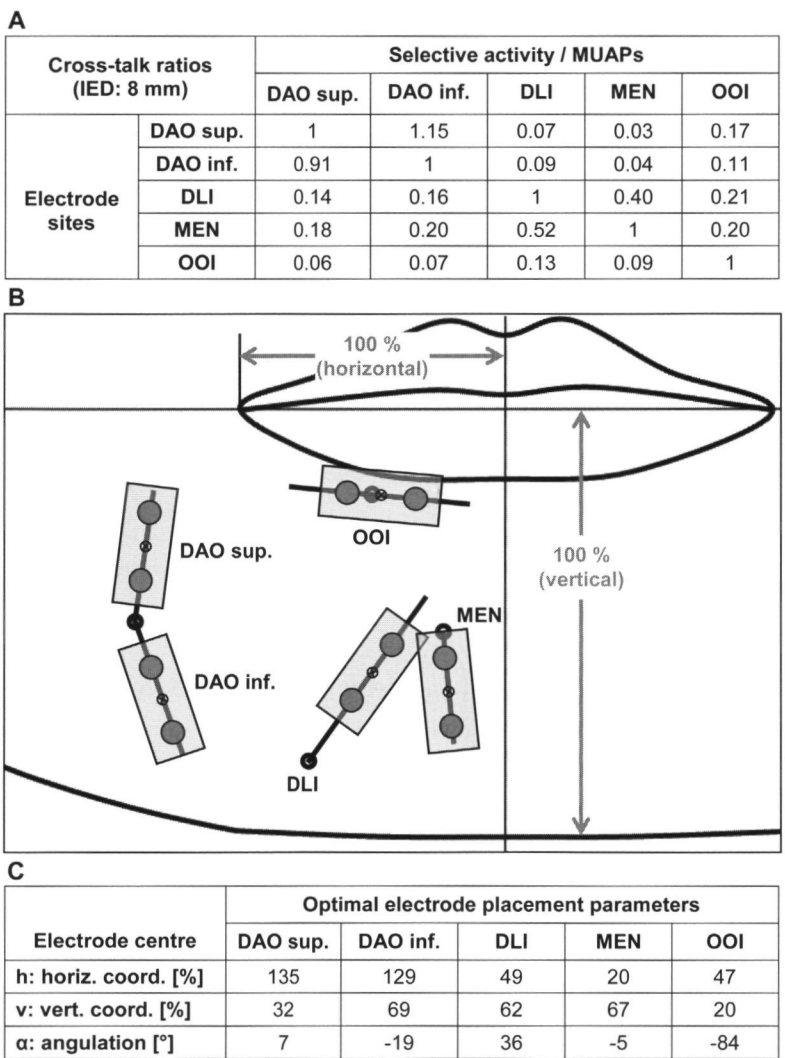
A

Cross-talk ratios (IED: 8 mm)		Selective activity / MUAPs				
		DAO sup.	DAO inf.	DLI	MEN	OOI
Electrode sites	DAO sup.	1	1.15	0.07	0.03	0.17
	DAO inf.	0.91	1	0.09	0.04	0.11
	DLI	0.14	0.16	1	0.40	0.21
	MEN	0.18	0.20	0.52	1	0.20
	OOI	0.06	0.07	0.13	0.09	1

B

C

Electrode centre	Optimal electrode placement parameters				
	DAO sup.	DAO inf.	DLI	MEN	OOI
h: horiz. coord. [%]	135	129	49	20	47
v: vert. coord. [%]	32	69	62	67	20
α: angulation [°]	7	-19	36	-5	-84

8

Figure 8-3. (A) Mean cross-talk ratios (CTRs) for all muscle-electrode site combinations in the lower face. These combinations include MUAPs and electrode sites of the depressor anguli oris (DAO), the depressor labii inferioris (DLI), mentalis (MEN), and orbicularis oris inferior (OOI) muscles. The DAO muscle is accessible for surface EMG in both its superior (DAO sup.) and inferior (DAO inf.) portions. The given CTRs refer to the group mean optimal electrode positions (as specified in B, C) established in our previous study (Lapatki et al. 2010), and to bipolar electrodes with an inter-electrode distance (IED) of 8 mm and detection surface sizes of 4 × 4 mm². The numbers within the columns multiplied by 100% describe the mean amplitude percentages of the corresponding muscle's MUAPs registered at the four adjacent electrode sites. (B) Schematic representation of the lower face and optimally placed bipolar electrodes (symbolised by the pairs of grey squares). The lines connecting the two electrodes of a bipolar montage coincide with the mean muscle fibre orientations of the corresponding muscles and muscle portions, respectively. Endplate locations are symbolised as bold open circles. The DLI and MEN electrode sites are relatively close to each other, while the electrode above the DAO and OOI muscles had relatively large distances to all three neighbouring muscles. (C) Numerical values (vertical and horizontal coordinates and angulations with reference to facial landmarks and the facial midline, respectively) for the optimal bipolar electrode placements as illustrated in (B).
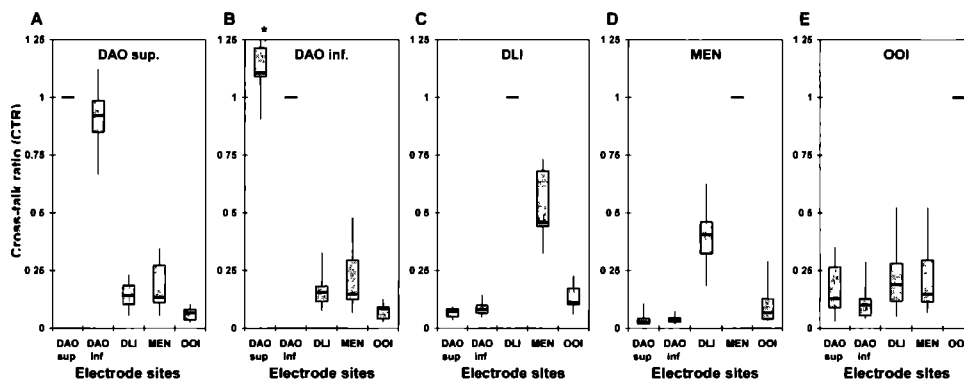
Figure 8-4. Inter-individual variability of EMG cross-talk in the lower face as indicated by CTRs. The grey boxes illustrate the distribution of the intra-individual mean CTRs of all subjects for all combinations of MUAPs and electrode sites. The lower and upper box limits are the 25th and 75th percentiles, and the horizontal lines indicate the median values. At the top of each boxplot diagram it is indicated to which muscle the MUAPs belong. CTRs are normalised to the optimal electrode site above this muscle. Different electrode sites are given below each boxplot diagram. (A), (B) Two diagrams are given for the MUAPs belonging to the depressor anguli oris muscle (DAO), because CTRs were normalised to both the electrode site above its superior (DAO sup.) and inferior (DAO inf.) portion. (C) CTRs for the depressor labii inferioris (DLI). (D) CTRs for the mentalis (MEN). (E) CTRs for the orbicularis oris inferior (OOI). *: The maximum CTR for the DAO sup. electrode side in (B) is 1.56.
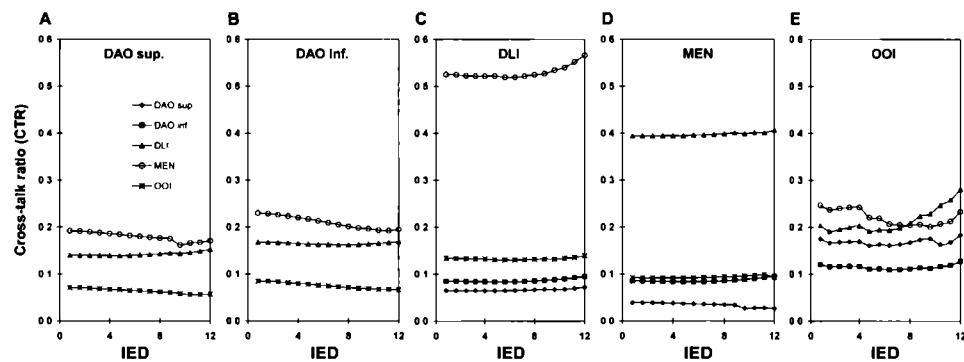
Figure 8-5. Dependency of the CTRs on the inter-electrode distance of the bipolar montage. CTR mean values for the whole study group are given. The different symbols illustrate the CTRs for the five different electrode sites. X-axis: different inter-electrode distances between 0.8 mm and 12 mm. Only CTRs for adjacent electrode sites are given. At the top of each diagram it is indicated which muscle's MUAPs are given in the corresponding panel. CTRs are normalised to the optimal electrode site above this muscle. (A), (B) Cross-talk for the depressor anguli oris (DAO) MUAPs normalised to the electrode site above the superior (DAO sup.) and inferior (DAO inf.) muscle portion. (C) CTRs for the depressor labii inferioris (DLI). (D) CTRs for the mentalis (MEN). (E) CTRs for the orbicularis oris inferior (OOI).

Comparison between CTRs for individual subjects and for the study group

To evaluate to which extent the EMG cross-talk can be reduced when the electrode positions are individually optimised, we also calculated CTRs for the individual subjects' optimal elec-

trode positions. Fig. 8-6 illustrates the corresponding differences. Indeed, for most of the muscle-electrode site combinations, lower CTRs were found when the electrode positions were individually optimised (this finding coincides with a positive difference). However,
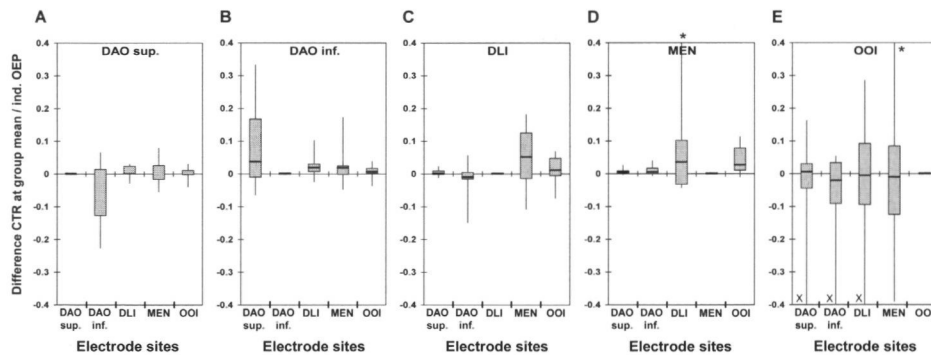
Figure 8-6. Difference between the CTRs determined for the group mean optimal electrode position (OEP) and those determined for the within-subject optimal electrode position illustrated in boxplot diagrams. Positive numbers indicate higher CTRs at the group mean optimal electrode position. Each panel shows the difference in CTR for one activated muscle and for the five electrode positions at which the muscle activity can be detected. (A), (B) CTR differences for MUAPs belonging to the depressor anguli oris muscle (DAO) when this muscle is examined in its superior (DAO sup.) or inferior (DAO inf.) portion. (C) Differences in CTRs for the depressor labii inferioris (DLI). (D) CTR differences for the mentalis (MEN). (E) CTR differences for the orbicularis oris inferior (OOI).
*: The minimum CTR differences for the DLI electrode site in (D) and the MEN electrode site in (D) are between 0.42 and 0.44, respectively.
x: The minimum CTR differences in (E) are between -0.42 and -0.67 for the DAO sup., DAO inf. and DLI electrode sides.

the median of the difference between CTRs at individual optimal and at global optimal electrode positions were relatively small (≤ 0.05). Moreover, for most MUAP-electrode site combinations, also the inter-quartile ranges (grey boxes) indicating the inter-individual variability of these differences were quite small. High individual differences between CTRs at individual optimal and global optimal electrode positions were particularly found for the orbicularis oris inferior MUAPs (Fig. 8-6E), as indicated by several maxima exceeding the diagram's range of ± 0.4.

CTRs used in the matrix inversion algorithm to remove interference EMG cross talk

Using the quantitative estimate of the EMG cross-talk, it is possible to correct for the confounding effect of adjacent muscles on the estimate of individual muscle activity. Eq. 4 describes the linear mixture between the four individual muscle activities and the measured EMG signals. Using the mean estimated

CTRs (as described in Fig. 8-3A), the relation between measured EMG signal and individual muscle activity becomes

$$
\begin{pmatrix} v_{DAO\,\mathrm{sup}} \\ v_{DLI} \\ v_{MEN} \\ v_{OOI} \end{pmatrix} = \begin{pmatrix} 1 & 0.07 & 0.03 & 0.17 \\ 0.14 & 1 & 0.40 & 0.21 \\ 0.18 & 0.52 & 1 & 0.20 \\ 0.06 & 0.13 & 0.09 & 1 \end{pmatrix} \times \begin{pmatrix} s_{DAO} \\ s_{DLI} \\ s_{MEN} \\ s_{OOI} \end{pmatrix}
$$

(Eq. 6)

It has to be noted that from the two possible electrode positions for recording from the depressor anguli oris muscle, the superior one was chosen in Eq. 6; correspondingly, the interference EMG registered by the superior electrode and the CTRs referring to this electrode were included in this equation (and also in the following ones).

Based on the matrix inversion of M as explained in Eq. 5, the individual muscle activity can be estimated from the measured sEMG using

8

$$\begin{pmatrix} s_{D4O} \\ s_{DII} \\ s_{MF\lambda} \\ s_{OOI} \end{pmatrix} = \begin{pmatrix} 1.02 & -0.05 & 0 & -0.16 \\ -0.09 & 1.29 & -0.50 & -0.15 \\ -0.13 & -0.64 & 1.27 & -0.10 \\ -0.04 & -0.11 & -0.05 & 1.04 \end{pmatrix} \times \begin{pmatrix} v_{D4Osup} \\ v_{DII} \\ v_{MF\lambda} \\ v_{OOI} \end{pmatrix}$$

(Eq. 7)

For instance, the true activity of the orbicularis oris inferior muscle can be estimated as

$$s_{OOI} = -0.04 \times v_{D4Osup} - 0.11 \times v_{DII} - 0.05 \times v_{MF\lambda} + 1.04 \times v_{OOI}$$

(Eq. 8)

In an individual well-trained subject we exemplify the use of individual CTRs in the matrix inversion approach to separate cross-talk from co-activation. Fig. 8-7A shows RMS values of EMG signals measured during attempted selective contractions of the four lower facial muscles at different activity levels. Estimates of true individual muscle activities during these tasks are given in Fig. 8-7B. The comparison of the measured and estimated muscle activity for the depressor anguli oris and depressor labii inferioris contractions (upper two panels each) reveals that the "co-activity" registered by the adjacent electrodes was nearly pure cross-talk. This means that this subject performed an almost perfect selective contraction. For higher contraction levels in the depressor anguli oris, some co-activation of the depressor labii inferioris is observed. Note the progressively increasing "negative" mentalis activity in the depressor anguli oris and depressor labii inferioris contractions, which is a physically impossible effect of the matrix inversion algorithm (Fig. 8-7B).

During the attempted selective mentalis muscle contractions, the subject showed some varying co-activity of the depressor labii inferioris and very little co-activity of the orbicularis oris inferior. In contrast, selective contraction of the orbicularis oris inferior was more difficult for this subject, as demonstrated

by the partially higher degree of co-activity when compared to the voluntary orbicularis oris inferior activity in low contraction levels (up to 25% MVC), and highly variable co-activity of all three adjacent muscles during (sub)maximal contractions.

Results of all subjects for attempted selective depressor labii inferioris contractions at a level of 15% of the maximal voluntary contraction level are shown in Fig. 8-8. The activity measured above the adjacent muscles (Fig. 8-8A) disappeared to a great extent in nearly all subjects after multiplying these activities with the inverted individual CTR matrices (Fig. 8-8B), with exception of subject #11. Fig. 8-8C illustrates estimations of the activities of the four muscles when the group's mean CTR matrix instead of the individual CTR matrices was used. Although in the majority of the subjects the results for both alternatives are similar, larger differences could be observed in some subjects (notably #1 and #13) for the mentalis in particular. For these subjects, the group's mean CTR matrix does obviously not accurately reflect the individual cross-talk. The bias in the estimated true muscle activity when using group mean CTRs instead of individual CTRs is indicated by the inter-individual variability of the CTRs in Fig. 8-4. High inter-individual variability in the differences between CTRs at individual optimal and global optimal electrode positions indicate those MUAP-electrode site combinations which contribute the most to an inaccuracy in the estimations of true individual muscle activity.

Discussion

EMG cross-talk is a largely distance-dependent phenomenon and, therefore, a key problem in EMG examinations of the facial musculature due to its anatomical structure. The present study provides estimates of the cross-
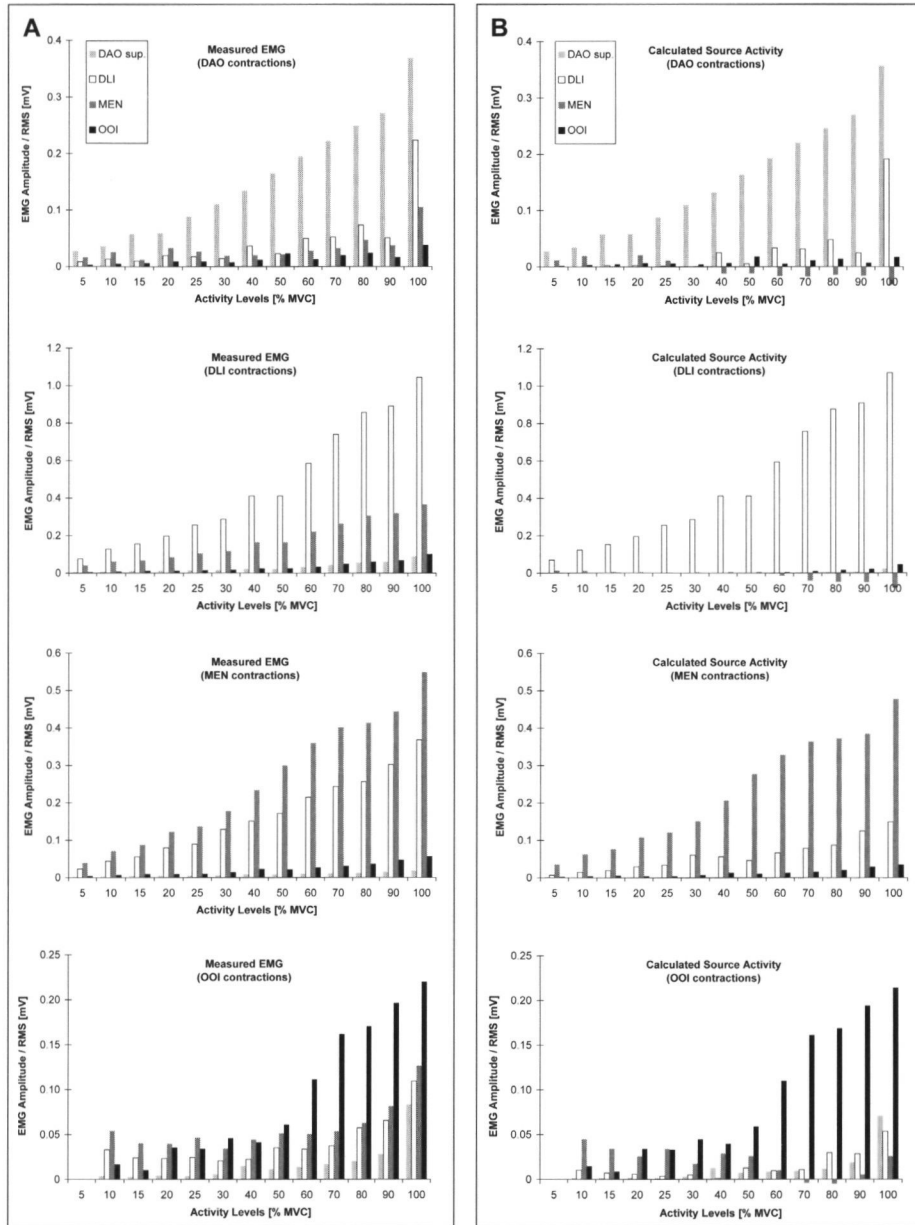
Figure 8-7. Attempted selective contractions of the four lower facial muscles at different activity levels performed by one individual subject. (A) RMS values of the measured EMG signals. (B) Calculated source activity for these contractions using the individual 4×4 CTR matrix for this subject in the matrix inversion algorithm (Eq. 6). From the two electrode sites for recordings from the depressor anguli oris muscle, the superior one was chosen.
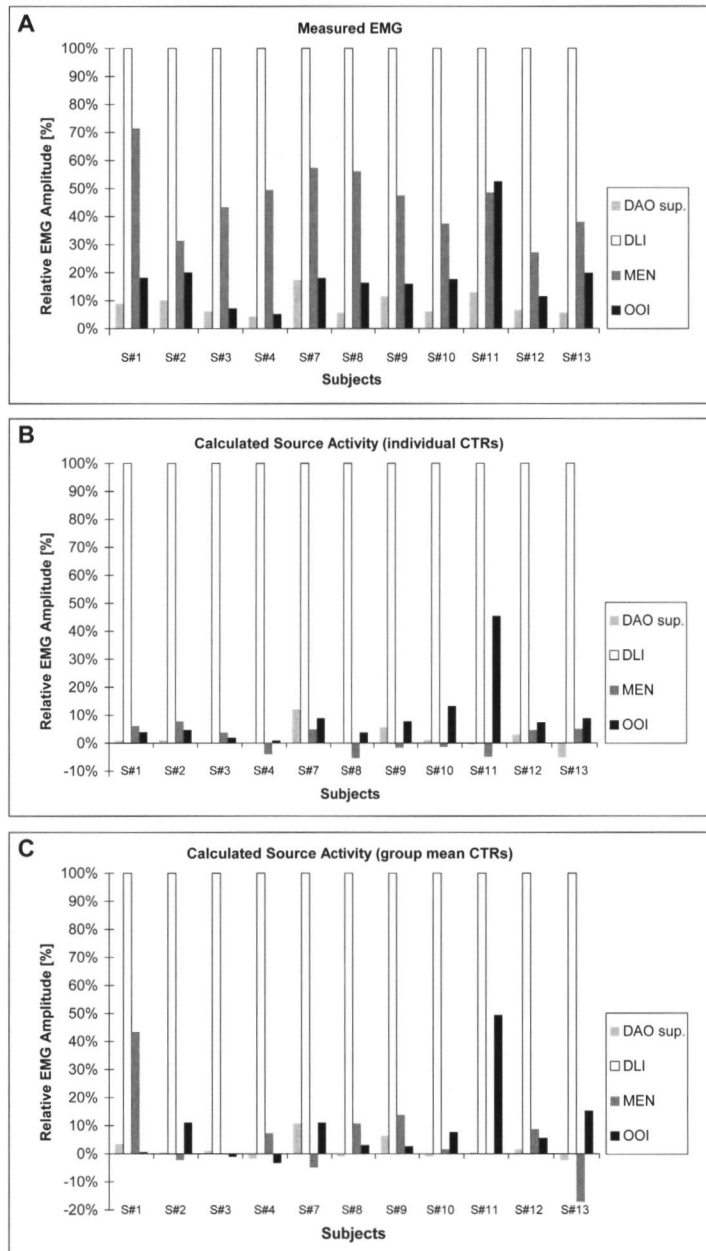
Figure 8-8. Attempted selective depressor labii inferioris contractions of all subjects at a level of 15% of the maximal voluntary contraction level. (A) RMS values of the measured EMG signals normalised to the RMS value of the signal registered over the contracted muscle. (B) Calculated source activity for these contractions using the individual subject's 4 × 4 CTR matrices. (C) Calculated source activity for these contractions using the group mean 4 × 4 CTR matrix in all subjects.

talk for recordings of muscle activity in the lower face. The estimates are based on the analysis of decomposed MUAPs which are muscle-selective and contain complete spatial amplitude information and, therefore, make accurate quantitative cross-talk estimates possible. When muscle parameters are determined by single motor unit analysis, the representativity of the analyzed MUAP sample is of crucial importance. In contrast, approaches for the assessment of cross-talk based on interference EMG recorded during attempted selective contractions of individual facial muscles, as performed in a previous study (Lapatki et al. 2003), contain a high risk to be biased from co-activated adjacent muscles. Also electrical stimulation, an alternative for achieving muscle selectivity which has been applied in previous quantitative studies of cross-talk (De Luca and Merletti 1988; Farina et al. 2002b; Koh and Grabiner 1993; van Vugt and van Dijk 2001), is not practicable in the face. It is not possible to separately stimulate facial nerve branches innervating single muscle subcomponents or to directly stimulate the small facial muscle bundles or sheets at their motor points without co-stimulating adjacent muscles (Delbeke 1982).

In the present study we established for those muscle-adjacent electrode site combinations in the lower face with the closest distance, i.e. the depressor labii inferioris muscle and the mentalis electrode and vice versa, mean CTRs of 0.52 and 0.40, respectively. These values can be interpreted as the fractions of the activity of these muscles that are registered with an electrode above the neighbouring muscle. These values also reflect the possible bias when conclusions are drawn on their activity without taking cross-talk quantitatively into account. In this regard, our results support the opinion of other authors advising caution in attributing facial EMG signals to specific muscles or functions (Blair and Smith 1986; Fridlund

and Cacioppo 1986). The CTRs found for the other muscle-electrode site combinations (except those between the two sites of the depressor anguli oris which are discussed below) were between 0.03 and 0.21 and their differences within this range are largely plausible when the topographical interrelationships of the corresponding muscles and electrode sites are considered. This does not apply to the orbicularis oris inferior muscle showing relatively high mean CTRs and large inter-individual variability in relation to the small motor unit territories and short fibre lengths as well as to the relatively large distances between the muscle's fibres and the adjacent recording sites (see Fig. 8-3A, last column, also Fig. 8-3B). Large intra- and inter-individual variability of the optimal electrode positions for orbicularis oris inferior MUAPs (Lapatki et al. 2010) might be one explanation. Due to the small amplitude territories, calculation of the bipolar MUAP at the averaged electrode positions may result in a significant amplitude decrease if the MUAP has its amplitude maximum at a relatively large distance from the average optimal electrode position. By definition, this amplitude decrease leads to an increase in the CTR. Visual observation of orbicularis oris inferior MUAPs for determining topographical motor unit parameters (data analysis step 2) revealed another aspect probably contributing to increased variability and an overestimation of CTRs for the orbicularis oris inferior muscle. In MUAPs belonging to this muscle, remaining activity in grid areas beyond the muscle's anatomical territory could be observed in spite of averaging a great number of firing events and corresponding data windows, respectively. The topographical characteristic of this remote activity showed very often similarities with that of motor units of adjacent muscles. Such "physiological noise" in the decomposed MUAPs might be the result of synchronisation of motor unit firings and

8

cannot be eliminated within our approach. Indeed, synchronisation of facial motor units has been described in previous studies (Folkins et al. 1988; Wohlert 1996a) and seems to be one of the components of differential neural regulation of lip muscle activity on a premo-toneuron level depending on the motor task (Wohlert and Goffman 1994).

In the present study, cross-talk was quantified and presented for both the optimal electrode locations above the superior and inferior portion of the depressor anguli oris muscle. In principle, only one electrode for examining this muscle is required. The comparison of the CTRs determined for both locations indicates that in almost all subjects higher signal amplitude were obtained by the superior electrode site with a mean difference of approximately 15%. Recording of maximal amplitude from a certain muscle has the advantage of reducing the relative contribution of activity of adjacent muscles to the signal. However, the two recording sites have also to be compared regarding the relative distances to the adjacent muscles. Our results indicated less cross-talk from the depressor labii inferioris and mentalis muscles to the superior depressor anguli oris electrode site (due to amplitude maximisation and larger distances), and the converse finding for the orbicularis oris inferior muscle (due to a greater distance between this muscle and the inferior depressor anguli oris electrode site). Thus, it seems that both locations are similarly suitable. For the latter reason, we provided the equations required for calculating the true individual muscle activity including the measured sEMG signal and CTRs of the electrode above the inferior portion of the depressor anguli oris muscle in an appendix to this article. Cross-talk in the facial area was quantitatively assessed in a previous study by evaluating the amplitudes of composite EMG signals recorded during attempted isolated facial muscle contractions (Lapatki et al. 2003). In that study, consid-

erably higher mean CTRs and higher inter-individual variability were observed apparently because co-activation was still included in the analysis.

Our result suggest that spatial filtering using bipolar electrodes with a small inter-electrode distance, though recommended in the literature (Basmajian and De Luca 1985; Loeb and Gans 1986), is rather ineffective for increasing the measurement selectivity and reducing the cross-talk in facial surface EMG. We found only a slight, non-systematic tendency in most muscle-electrode site combinations for increasing CTRs with enlarging the inter-electrode distance (Fig. 8-5). The minor influence of the inter-electrode distance on cross-talk in the face is due to similar (relative) signal amplitude increases with increasing inter-electrode distance at both the electrode sites above the contracted muscle and above the adjacent muscles. The mentalis MUAP of Fig. 8-1B exemplifies how the relation between these two parameters can be influenced by the topographical interrelationships between the bipolar electrode and the endplate zone. The absent increase of the bipolar MUAP amplitude above the mentalis with increasing the inter-electrode distance from 8 mm to 12 mm was obviously due to the fact that in the larger inter-electrode distance, the superior detection surface of the bipolar montage was located superiorly to the endplate leading to partial signal extinction (Stegeman et al. 2004). More generally, it has to be noted that the minor influence of the inter-electrode distance of a bipolar montage on the amount of cross-talk is in good agreement with recent studies including model simulations and experimental data (Farina et al. 2002b; Mesin et al. 2009b). Future studies in the face might be of interest in order to explore the limits of cross-talk reduction with higher order spatial filters.

We consider quantitative cross-talk estimates to be very promising for estimating

the true individual muscle activity without the confounding effect of activity of neighbouring muscles. In the example for the individual subject, almost all measured EMG "co-activity" (Fig. 8-7A) was actually identified as cross-talk. The ability of the subject in selective facial motor control would have been considerably under-estimated when relying on the measured EMG alone. The same effect is demonstrated for the whole study group for the depressor labii inferioris contraction at a low level (Fig. 8-8). In both examples, little "negative" source estimates were observed, indicating an over-correction by the matrix inversion algorithm. This bias in the estimation of the true individual muscle activity has to be attributed to inaccurate CTRs for corresponding individual subjects. One possible reason for inaccurate CTRs is differential movement of the muscle tissue and the electrodes during muscle contractions leading to different topographical interrelations and thus, alterations in the CTRs. This problem becomes more important for larger differences between the contraction level used for extraction of the MUAP sample (and hence, the CTR estimate), and the contraction level for estimating the muscle activity, as clearly demonstrated by the submaximal to maximal contractions of the depressor anguli oris and depressor labii inferioris in the individual subject (see Fig. 8-7); the lack of mentalis co-activity in these contractions reveals itself as "negative" activity. Indeed, while the contraction intensity was increased in these examples, the amount of "negative" mentalis activity progressively increased as well. Imprecision in the assessment of the true activity may also be connected to limitations in the representativity of the decomposed MUAP sample, which means that some of the different MUAP topographies representing the corresponding muscle as a whole are not sufficiently reflected in the analyzed MUAP sample. In the present

study we minimised this problem by decomposing all recorded files and scanning corresponding MUAP samples up to 30% of the maximal voluntary contraction level and selecting those samples containing greatest variability in MUAP topography. In this context it should be noted that general limitations exist in sEMG mapping of the orbicularis oris MUAPs. Since sEMG grids cannot be placed on the lip vermillion where the density of orbicularis oris fibres is the highest (Blair and Smith 1986), it could happen that certain motor units, having their small territories superior to the attached grids, were under- or even not represented. This especially concerns motor units consisting of marginal or intrinsic non-horizontal fibre populations (Blair 1986; Braus and Elze 1954). The estimate of the individual muscle activity can be expected to be more biased if not all confounding adjacent muscles are included in the EMG measurements.

One question addressed in the present study with potential relevance for future facial sEMG studies was to which extent inaccuracies in the estimation of the true muscle activity are introduced when group mean CTRs instead of individual CTRs are applied. Although in some subjects and certain muscles large differences occurred (see Figs. 8-8B and 8-8C), these differences were relatively small compared to the bias of muscle activity estimations when measured EMG signals (which contain the full confounding cross-talk) are considered only. Utilising mean CTRs for assessment of muscle facial function may therefore be regarded as superior to utilising measured EMG signals only, because interindividual differences in CTRs are considerably smaller than the magnitude of the ratios themselves. Consequently, a preferred future strategy for sEMG studies in the face might be to attach bipolar electrodes according to the proposed placement guidelines and to use the

8

mean (inverted) CTR matrix (as given in Eq. 7 or, alternatively, in Eq. A2 of the Appendix) for improving the accuracy of the muscle activity estimation.

Not many alternative approaches for quantifying cross-talk in the face are available. Simultaneous surface and intra-muscular EMG recordings cannot exclude co-activity or co-stimulation of an adjacent muscle, because due to their high spatial selectivity, intra-muscular EMG signals reflect the activity of only a few motor units in the vicinity of the needle or wire electrode. The lack of suitable methods for establishing a "gold standard" makes it difficult to assess the validity of the CTRs and corresponding coefficients of the inverted CTR matrix for calculating the true individual muscle activity provided in the present study. However, it should be noted in this context that the methodological concept of the present study for determining cross-talk estimates is based on the evaluation of amplitude profiles of monopolar MUAPs and, therefore, principally coincides with that applied in our previous study for determining optimal electrode placements. The latter method has been validated using interference sEMG signals (Lapatki et al. 2010). In both studies we used identical MUAP samples. Moreover, the application of the same individual CTR matrix to contractions of different muscles led to plausible estimates of true individual muscle activity (Fig. 8-7), which supports the validity of our methodological approach for determining quantitative cross-talk estimates.

To conclude, in the present study we quantified EMG cross-talk in the lower face based on the analysis of muscle-selective MUAPs. Our methodological approach is not limited to the face and can be applied to other musculature as well. Practically, the presented results can readily be used for facial sEMG in future by attaching electrodes at the proposed positions for which mean CTRs are available and use the given inverted CTR matrix to improve the estimate of individual muscle activity.

Appendix

If the mean CTR matrix is configured using the CTRs referring to the inferior (instead of the superior) depressor anguli oris electrode position, the relation between measured EMG signal and individual muscle activity becomes

$$\begin{pmatrix} v_{DAOinf} \\ v_{DLI} \\ v_{MEN} \\ v_{OOI} \end{pmatrix} = \begin{pmatrix} 1 & 0.09 & 0.04 & 0.11 \\ 0.16 & 1 & 0.40 & 0.21 \\ 0.20 & 0.52 & 1 & 0.20 \\ 0.07 & 0.13 & 0.09 & 1 \end{pmatrix} \times \begin{pmatrix} s_{DAO} \\ s_{DLI} \\ s_{MEN} \\ s_{OOI} \end{pmatrix}$$

(Eq. A1)

Correspondingly, the individual muscle activity can be estimated from the measured EMG using

$$\begin{pmatrix} s_{DAO} \\ s_{DLI} \\ s_{MEN} \\ s_{OOI} \end{pmatrix} = \begin{pmatrix} 1\,02 & -0.07 & 0 & -0.10 \\ -0.10 & 1\,29 & -0\,50 & -0.16 \\ -0\,14 & -0\,64 & 1\,27 & -0\,11 \\ -0\,05 & -0\,10 & -0\,05 & 1\,04 \end{pmatrix} \times \begin{pmatrix} v_{DAOinf} \\ v_{DLI} \\ v_{MEN} \\ v_{OOI} \end{pmatrix}$$

(Eq. A2)

For instance, the true activity of the orbicularis oris inferior muscle can then be estimated using

$$s_{OOI} = -0\,05 \times v_{DAOinf} - 0\,10 \times v_{DLI} - 0\,05 \times v_{MEN} + 1\,04 \times v_{OOI}$$

(Eq. A3)

8

Part IV

Clinical applications

In this part we explore and prepare clinical applications of high-density surface EMG in the face. This comprises the use of high-density surface EMG for myofeedback training of selective facial muscle contractions. Such training might be also clinically helpful for restoring facial muscle function. In addition, we investigate in an extensor digitorum brevis muscle model whether precise localisation of the motor endplate zones for injection of botulinum neurotoxin increases the therapeutic efficacy of this drug. This question is particularly relevant for application of botulinum neurotoxin to facial muscles, due to their eccentric and variable endplate zone locations. It is hypothesised that endplate targeted injection with high-density surface EMG guidance might allow the reduction of injected toxin dose and both side-effects and costs of the therapy

9

Training of facial muscle contractions using high-density surface EMG myo-feedback

Introduction

Visual examination has certain limitations in the assessment of the contributions the individual facial muscles make to a specific facial movement. High-density surface EMG provides topographical information and therefore might be a suitable monitoring tool.

This issue was addressed in a group of professional trumpeters who were trained to improve their ability in facial motor control.

Methods

The training scheme consisted of:
1. three training sessions, in which isolated facial muscle contractions were demonstrated and individually instructed by an experienced trainer,
2. a booklet with descriptions and illustrations for independent training of the participants, and
3. myo-feedback training at the beginning of the measurements with the high-density sEMG system.

In three training sessions the trainer (the author of this thesis) demonstrated isolated facial muscle contractions, which were then practiced by the participants with the aid of visual feedback (i.e. by using a mirror). The trainer controlled and corrected performance of the tasks. In between the training sessions, which were separated by about two weeks, the participants were asked to practice independently with the aid of a booklet and under visual feedback control using a mirror. The booklet included instructions about how facial muscle subcomponents can be contracted in isolation, and which changes in facial appearance accompany these contractions (see Chapter 2).

The myo-feedback training was performed in connection with high-density sEMG measurements. High-density sEMG allows the topographical profiles of electrophysiological responses of contracted muscles to be studied (Fig. 9-1). The topographical information is especially useful in the present context of muscle recruitment and interaction in the face. For monitoring sEMG signals, we implemented an sEMG amplitude feedback tool into the acquisition software that visually displays (on-line) the EMG amplitude distribution in the recording area of the grid with a 500 ms update to the subject via the PC monitor. To help the subjects in keeping the selective contractions at a constant level during the recordings, activity from a subset of

A

B

9
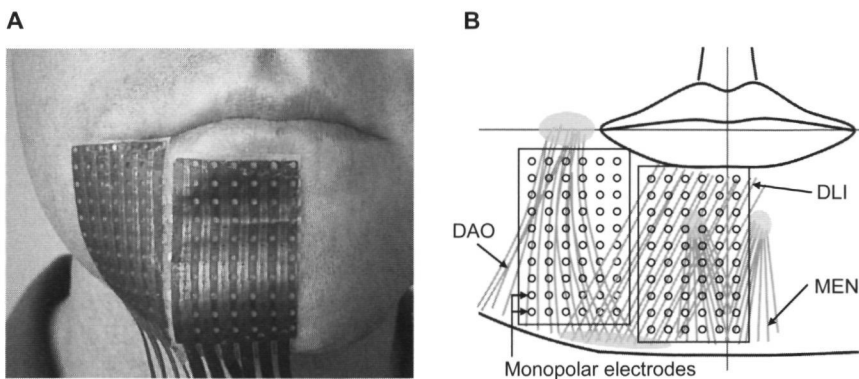
Figure 9-1. (A) Two 6 by 10 multi-electrode grids attached to the lower face for monitoring high-density sEMG signals (myo-feedback). (B) Position of the electrode grids relative to the underlying mm. depressor anguli oris (DAO), depressor labii inferioris (DLI), and mentalis (MEN). Origins of these muscles are indicated by grey areas.

grid electrodes of the underlying muscle was also visually displayed on the PC monitor in a dynamic diagram.

Results and discussion

The developed training scheme was a great support in training selective facial muscle contractions at constant activity levels. The myo-feedback provided in form of dynamic EMG amplitude maps enabled both the experimenter and subject to easily detect and localise unwanted co-contraction of adjacent muscles (Fig. 9-2). By this means, deficits in selectively contracting facial muscles could be identified and largely eliminated.

On the basis of these positive experiences we hypothesise that myo-feedback training with high-density surface EMG might be a useful clinical tool for supporting physio-therapeutic approaches in restoring facial muscle function. This aspect needs further exploration in patients with facial weakness.
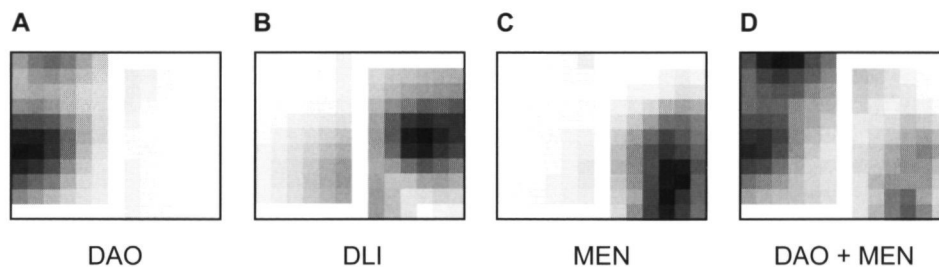
Figure 9-2. Example of amplitude maps showing the activity of underlying facial muscle subcomponents during contraction of lower facial muscles. The amplitude is expressed in grey levels (darker is higher). For electrode grid positions relative to the face, see Fig. 9-1. Maps during (A) selective contraction of the m. depressor anguli oris (DAO), (B) selective contraction of the m. depressor labii inferioris (DLI), (C) selective contraction of the m. mentalis (MEN), and (D) attempted selective DAO contraction with co-contraction of the MEN (DAO + MEN).

10

INCREASED EFFECT OF BOTULINUM NEUROTOXIN WHEN TARGETED TOWARD THE MUSCLE'S MOTOR ENDPLATE ZONE

Lapatki B.G., van Dijk J.P., van de Warrenburg B.P.C., Zwarts M.J.
Submitted

Toxin spread to adjacent muscles and antibody formation are major problems in the clinical application of Botulinum neurotoxin (BoNT). Clinical studies have proven these adverse effects to be dose-dependent. Animal studies indicated that endplate-targeted injection potentiates the effect of BoNT-A. In this study we compared the effect of endplate-targeted injections of a low BoNT-A dose with that of injections at defined distances from the motor endplate zone. In eight healthy volunteers, the main endplate zones of the right and left extensor digitorum brevis (EDB) muscles were localised using high-density surface EMG. On the study side, 10 IU BoNT-A (Dysport®, Ipsen) were injected at distances of 2-12mm from the endplate zone. On the control side, the same BoNT-A dose was administered into the endplate zone. The effect of BoNT-A was assessed by recording the compound muscle action potential (CMAP) prior to the injection and 2, 12, and 24 weeks later. On the control side, the mean CMAP reduction 2 weeks after BoNT-A injection was 79.3%. The intra-individual difference in CMAP reduction between both EDB muscles revealed a significant interrelation with the injection distance from the endplate zone on the study side (linear regression analysis, $R^2=0.51$, p=0.03). Increasing the injection distance from the endplate zone by 1cm reduced the effect of BoNT-A by 46%. Guided injection of a reduced BoNT dose into the muscle's endplate zone(s) is a promising strategy for optimising the therapeutic effectiveness of BoNT and, possibly, for minimising side-effects such as unwanted weakening adjacent muscles and immunoresistance.

Introduction

Botulinum neurotoxin (BoNT) blocks the release of acetylcholine at the neuromuscular junction or in the autonomic nervous system (Breidenbach and Brunger 2005). The clinical use of this effect comprises various conditions caused by muscle or exocrine gland hyperactivity including dystonia and a variety of other neurologic, ophthalmologic, urologic, gastrointestinal, and dermatologic conditions (Collins and Jankovic 2006; Naumann et al. 2008; Simpson et al. 2008a; Simpson et al. 2008b; Truong and Jost 2006).

BoNT, in therapeutical doses, is a relatively safe drug (Bakheit 2006). The main adverse effects can be subdivided into three categories (Simpson et al. 2008b): first, diffusion of the toxin from the intended site of action possibly leading to unwanted inhibition of acetylcholine release at neighbouring motor and autonomic nerve endings; second,

sustained blockage of transmission which can produce anatomic denervation including muscle atrophy; third, immunoresistance to BoNT (Dressler and Hallett 2006; Greene et al. 1994).

In the treatment of disorders characterised by excess motor activity, spread of the toxin to the muscles adjacent to that targeted for treatment is one of the commonest unwanted effects of BoNT-A reported in the literature (Bakheit 2006). Clinical studies have proven this adverse effect to be dose-dependent (Borodic et al. 1990; Eleopra et al. 1996). The relevance of the administered toxin dose for toxin spread was also supported by a rabbit longissimus dorsi model showing by means of histochemical techniques that morphologic effects of BoNT-A correlate with the administered toxin dose, and that low doses of BoNT-A cause a graduated effect in a defined field within the muscle (Borodic et al. 1994).

10

The most logical strategy for reducing adverse effects of BoNT is to administer the lowest effective toxin dose (Bakheit 2006). Indeed, clinical studies in patients with cervical dystonia revealed that adverse effects (e.g. dysphagia) could be reduced by injecting a reduced total BoNT-A dose (Borodic et al. 1990; Brans et al. 1995), though earlier studies (Jankovic and Schwartz 1990; Ludlow et al. 1988) could not provide sufficient evidence for such a relationship.

In current clinical practice, dose reduction may be difficult due to the requirement for a sufficient and reliable treatment effect. Theoretically, because BoNT acts at the neuromuscular junctions, the area(s) within the muscle with the highest concentration of neuromuscular junctions should be most sensitive to the toxin. So, targeted injection of BoNT might be the key for reducing the dose while maintaining clinical efficacy (Childers 2004). This assumption seems to be supported by data from animal studies. In a rat tibialis anterior muscle model it was found that even small BoNT-A doses that would normally be considered subclinical induced significant muscular weakness if injected near the motor endplate zone (Shaari and Sanders 1993). Also in a canine model it was demonstrated that endplate-targeting potentiates the effect of BoNT-A (Childers et al. 1998).

The present study was undertaken to evaluate the effect of endplate-targeted injection of a low dose of BoNT-A in a human extensor digitorum brevis muscle (EDB) model. More specifically, we aimed at characterising muscular weakness after injecting BoNT-A precisely into the motor endplate zone and at different distances from it. The EDB muscle was chosen for its isolated location and easy accessibility, the lack of clinically relevant manifestations resulting from EDB weakness as well as the availability of dose-response interrelationships after BoNT-A

injections into this muscle (Sloop et al. 1996). We hypothesised that BoNT-A injections are most potent when specifically targeted toward the motor endplate zone, and that a reduction in the effect of BoNT-A is observed if the distance between the injection site and the endplate zone is increased.

Materials and Methods

Subjects
The study group consisted of eight volunteers (3 non-pregnant females and 5 males, mean age 31.8 yr, range 21 – 56 yr) without known neurological or general health disorders. The subjects provided written informed consent and the study protocol was approved by the Ethics Commission of the Radboud University Nijmegen Medical Centre.

Motor endplate zone localisation
High-density surface EMG was used to localise the main motor endplate zone of the EDB muscle (Fig. 10-1A). This technique records muscle activity on the skin surface with a large number of small, densely spaced electrodes (Stegeman et al. 2004). To cover the whole EDB muscle we applied a flexible multielectrode grid manufactured by Digiraster Tetzner GmbH (Stuttgart, Germany) consisting of 8×15 chlorided silver electrodes (Lapatki et al. 2004). The amplifier system (ActiveOne, BioSemi, Amsterdam, The Netherlands) had a sample rate of 2048 Hz. The electric potentials of the 120 single electrodes were acquired with reference to a common electrode attached to the ankle and were displayed in a bipolar montage. In the bipolar interference signals from consecutive electrodes in muscle fibre direction (Fig. 10-1B), the position of the motor endplate zone could be detected on-line from the bidirectional propagation pattern of the motor unit action potentials resulting in low amplitude at and opposite signal polarity
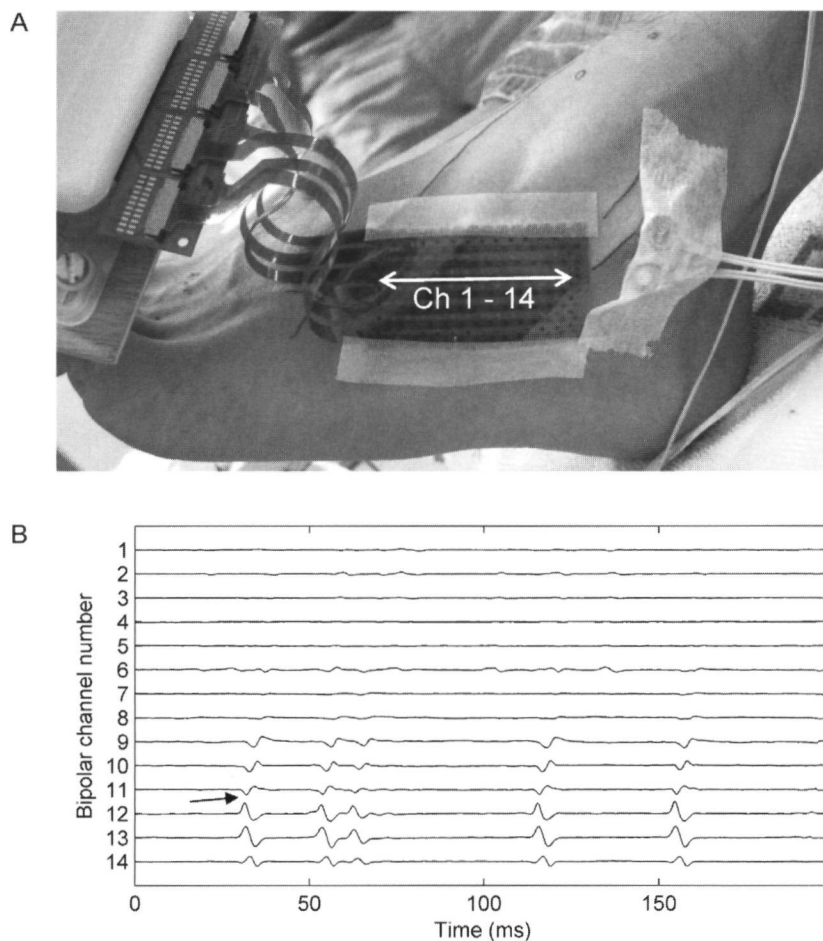
Figure 10-1. Motor endplate zone detection using high-density surface EMG. (A) Endplate zone localisation using a high-density surface EMG electrode grid (120 channels) with inter-electrode distances of 4 mm in both dimensions. The white double arrow indicates one electrode row in fibre direction (14 bipolar channels). (B) Bipolar surface EMG signals (200 ms) of consecutive electrodes of the electrode row indicated by the white double arrow in (A). Channels are numbered from distal to proximal locations. Inter-signal distance is 0.5 mV. The black arrow points to the endplate zone of one motor unit. Endplate zones of all motor units firing in this data window were located between the 11th and 12th bipolar channel. The corresponding position could be transferred back onto the subject's foot.

on both sides of the endplates (Masuda et al. 1983).

Study protocol

In the beginning of the first recording session, we determined the locations of both EDB muscles' main motor endplate zones during voluntary contractions of this muscle at low levels. Compound muscle action potentials (CMAPs) were then obtained by supramaximal electrical stimulation of the peroneal nerve using a constant current stimulator (pulse width: 100µs). Its electrodes were attached to the ankle approximately 70 mm away from the EDB muscle. Three repetitions of the CMAP measurements were performed on each side.

10

Foot temperature was maintained between 33 and 35° C. The baseline CMAPs were recorded prior to BoNT-A administration using the high-density electrode grids.

The positions of the grids and other relevant coordinates indicating the main motor endplate zone and the assigned injection site were documented by markings with indelible ink through small perforations in between the electrodes. These markings were necessary for guiding the subsequent BoNT-A injection and the electrode placement for follow-up CMAP recordings.

After removing the high-density electrode grids, 10 IU BoNT-A (Dysport®, Ipsen Pharmaceuticals Ltd.) were injected in the right and left EDB muscles at the predefined locations (Fig. 10-2A): on the study side at a randomly assigned distances between 2 and 12 mm proximal from the previously determined main endplate zone, and on the control side directly into the main endplate zone.

BoNT-A injections were performed by an experienced clinical neurophysiologist (MJZ) under EMG-guidance with TECATM MyoJect needle electrodes (Viasys Heathcare) to ensure the correct injection depth. The injected toxin dose was chosen on the basis of the dose-response curve of human EDB muscle function to BoNT-A (Sloop et al. 1996). In that study an equivalent dose of 3 IU BoNT-A (Botox®, Allergan Corp.) resulted in a ca. 50% CMAP reduction. The physician who administered BoNT-A was not aware of whether the injection was on the study or control side. At the end of the first session, the marked electrode grid coordinates were registered relative to the vein topography on the dorsum of the foot (Fig. 10-2B) and superposed on a transparent plastic foil.
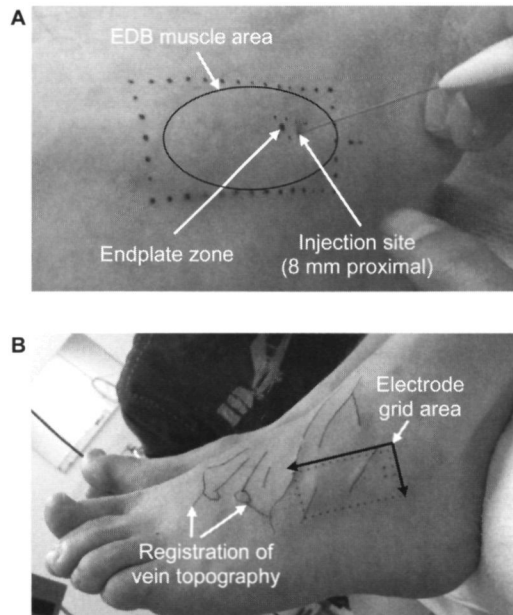
Figure 10-2. BoNT-A injection on the study side at a defined distance to the motor endplate zone. (A) Precise BoNT-A injection on the study side at a defined distance (here 8 mm) proximal to the EDB muscle's main endplate zone. (B) Relevant electrode grid coordinates and the vein topography on the dorsum of the foot were marked. Subsequently, these markings were copied to a transparent plastic foil which guided the placement of the single large electrode used for the follow-up CMAP recordings.

Follow-up CMAP registrations were performed at 2, 12, and 24 weeks after BoNT-A injection. To reduce examination time, these recordings were performed by means of a single large electrode instead of the high-density electrode grid used for the measurements at baseline (T0). Electrode size was 10×10 mm^2 precisely matching an area of 3×3 electrodes of the high-density electrode grid. The principle of averaging the potential over a defined high-density electrode grid area has been proven experimentally and by a simulation model to be valid under practical conditions (van Dijk et al. 2009). The follow-up CMAP measurements using the single large electrode were taken at two different sites: (1) at the location where the maximal CMAP amplitude area was found at T0 (see below), and (2) at the location of the main motor endplate zone. Registration of electrode grid position at T0 allowed for placing the single large electrode in that area from which the CMAP values were obtained at T0.

The examiner was not aware of the CMAP amplitude values of T0 when obtaining the follow-up CMAPs.

Data analysis and statistics

EMG data were analyzed using a protocol programmed in Matlab, Version 7.04 (The Mathworks Inc., Natick, MA, USA). All recorded signals were bandpass filtered (10 – 400Hz). As mentioned before, the baseline CMAPs were registered with the multi-electrode grids. By utilising the complete topographical amplitude information of these grids, we could determine the position of the single large electrode for the follow-up measurements. To obtain a regular 1-mm resolution for localising the maximal CMAP area on the grid, high-density surface EMG data were interpolated in both dimensions four times between adjacent electrodes applying a bicubic interpolation method. One CMAP

was then determined for each possible 10×10 mm^2 subarea of the electrode grid by averaging the interpolated potentials in the corresponding subarea (van Dijk et al. 2009). The average CMAPs were quantitatively evaluated by determining their negative peak area. The maximum of this parameter in the electrode grid area as well as the corresponding value for the location of the main endplate zone were further analyzed. The follow-up CMAPs obtained with a single large electrode were also quantitatively evaluated by determining the negative peak area.

For each subject and time-point, the mean CMAP amplitude value of the three repetitions was calculated. As a measure of the effect of the BoNT-A injection we normalised these values relative to the mean CMAP value obtained at baseline (T0).

Results were statistically evaluated using SPSS statistical software version 16.02 (Chicago, USA). Differences in the relative changes of the CMAP values on the control side (endplate-targeted injection) were analyzed by means of the paired T-test including 95% confidence intervals (CI). The distance of BoNT-A injection from the main motor endplate zone (study side) and the difference in the relative CMAP reduction between the study and control side were subjected to linear regression.

Results

CMAP reduction on the control side (endplate-targeted BoNT-A injection)

At the position above the motor endplate zone, the mean CMAP reduction 2 weeks after BoNT-A injection (T1) directly in the motor endplate zone (control side) was 79.3% (range: 63.4% – 95.0%). During the follow-up period the mean CMAP reduction decreased only to 76.4% (61.0% – 95.5%) at 12 weeks (T2), and to 70.1% (46.3% – 87.9%) at 24 weeks
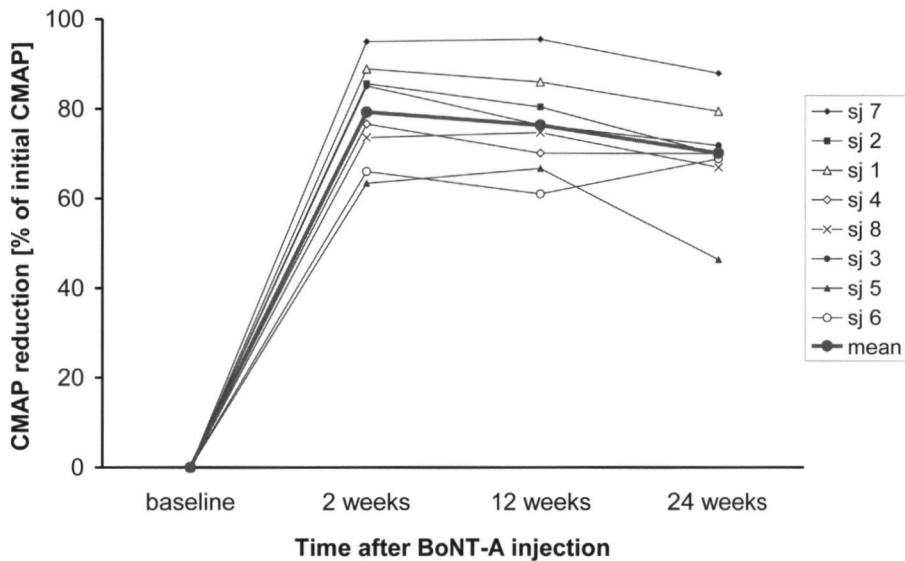
10

Figure 10-3. CMAP reduction in the follow-up period relative to the baseline CMAP. The CMAP reductions at T1, T2, and T3 are given as percentage of the baseline CMAP value. The data refer to the electrode area above the motor endplate zone.
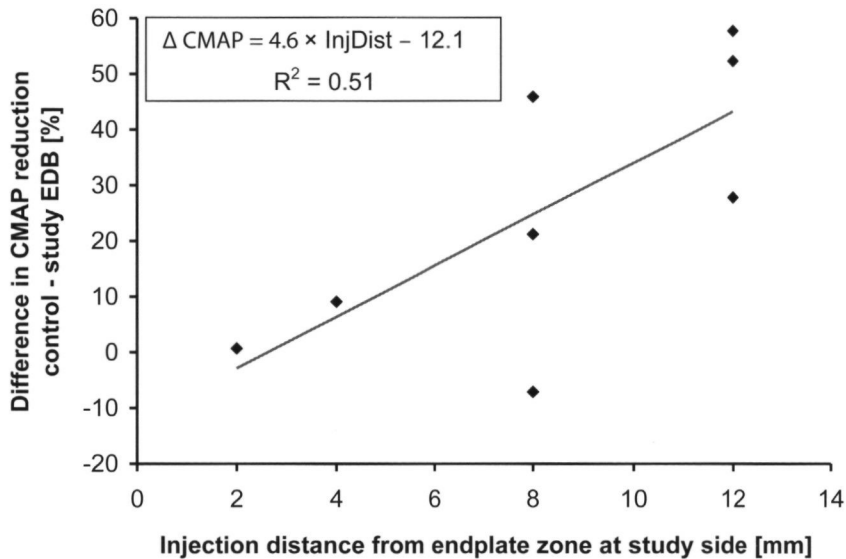

Figure 10-4. Difference in CMAP reduction (study vs. control side). Dependency of the difference in the relative CMAP reduction between the study and control side (Δ CMAP) two weeks after BoNT-A administration from the distance of the injection to the endplate zone on the control side (InjDist). The equation of the corresponding linear regression model is given in upper left corner of the diagram.

(T3) (Fig. 10-3). The difference between the follow-up CMAP reductions at T1 and at T3 was statistically significant (paired T-test, p = 0.005, CI = 3.8 – 14.5%). At the position where the CMAP was maximal, a similarly high CMAP reduction at the first follow-up examination of 75.1% (41.7% – 95.0%) and similar recovery of the EDB muscle function was found. Detailed individual results are provided as supplemental data (Table 10-1).

Table 10-1. CMAP reductions in percent of the baseline CMAP in the follow-up period

		Control side (endplate-targeted injection)					
		Δ CMAP (endpl. pos.)			Δ CMAP (max. CMAP pos.)		
Subject	InjDist	T_1	T_2	T_3	T_1	T_2	T_3
7	0	95.0	95.5	87.9	95.0	94.0	85.8
2	0	85.6	80.4	69.8	74.2	67.6	52.0
1	0	88.9	86.0	79.4	88.7	88.0	84.2
4	0	76.6	70.1	70.0	77.3	68.4	69.2
8	0	73.6	74.7	66.9	68.2	65.8	58.9
3	0	85.1	76.4	71.8	85.4	75.2	74.2
5	0	63.4	66.7	46.3	41.7	28.4	2.1
6	0	66.0	61.0	68.8	70.0	61.7	68.1
Mean		79.3	76.4	70.1	75.1	68.6	61.8
SD		11.2	11.0	11.9	16.4	19.8	26.7
Confid. interval	Upper	87.1	84.0	78.3	86.4	82.3	80.3
	lower	71.5	68.7	61.9	63.7	54.9	43.3

		Study side					
		Δ CMAP (endpl. pos.)			Δ CMAP (max. CMAP pos.)		
Subject	InjDist	T_1	T_2	T_3	T_1	T_2	T_3
7	2	94.3	81.0	79.6	75.1	48.8	52.5
2	4	76.5	62.3	58.5	53.3	42.2	42.7
1	8	43.0	11.2	19.3	38.0	16.6	26.7
4	8	83.7	81.7	77.7	84.2	75.8	75.7
8	8	52.4	44.7	26.3	60.8	48.8	29.5
3	12	57.3	49.1	38.7	64.3	56.0	47.8
5	12	11.1	28.4	-10.8	-3.5	-10.1	-36.3
6	12	8.3	20.3	16.8	-25.3	-35.0	-6.4

10

Δ CMAP: CMAP reduction in percent of the initial CMAP two weeks (T_1), 12 weeks (T_2), and 24 weeks (T_3) after injection of BoNT-A (10 IU Dysport®, Ipsen). Control side: injection directly into the main motor endplate zone. Study side: high-density surface EMG guided injection at distances (InjDist) between 2 - 12 mm to the main endplate zone. CMAP values were determined in a 10×10 mm² area both over the main endplate zone (endpl. pos.) and over the location of the maximal initial CMAP value (max. CMAP pos.). Subjects are ordered according to the injection site distance from the main endplate zone on the study side.

Comparison of CMAP reduction on study and control side

The linear regression model with the difference in CMAP reduction between the control and study side (two weeks after BoNT-A injection) as dependent variable provided evidence for a significant interrelation between this variable and the distance of the injection from the main motor endplate zone on the study side (p = 0.03). The calculated model (see inset of Fig. 10-4) explained 51% of the variability in this interrelation. The regression coefficient indicates a 4.6% (CI = 0.1 – 9.1%) lower drug effect when the injection distance from the motor endplate zone is increased by 1 mm (Fig. 10-4).

Discussion

Common adverse effects of BoNT-A reported in clinical studies, such as weakening of muscles not intended to be treated, are mainly dose-dependent and related to local spread of the toxin (Bakheit 2006). The total amount of BoNT-A applied at each injection series is also a major risk factor for antibody-induced therapy failure (Dressler and Benecke 2007). A plausible strategy to reduce these adverse effects is to administer only the minimal toxin dose necessary for achieving the desired therapeutic effect. Histochemical studies in animal muscle models indicated that this requires precise toxin application in the region of the motor endplates (Borodic et al. 1994; Shaari and Sanders 1993). In the present study we could demonstrate the feasibility of this strategy in a human EDB muscle model using high-density surface EMG for localising the main endplate zone. We found that muscular weakness after BoNT-A injection (characterised by the reduction of the CMAP) is significantly dependent on the distance of the injection from the main endplate zone, and that even a very small BoNT-A dose can be highly effec-

tive when precisely targeted toward the region where the neuromuscular blockade occurs. More specifically, the comparison between the CMAP values obtained from the EDB muscle on the study and control sides revealed an almost 50% lower drug effect in those subjects where BoNT-A was administered at a distance of 12 mm from the main endplate zone. The statistical significance of this interrelation was confirmed in the linear regression model describing a 4.6% lower CMAP reduction per mm increase of the injection distance from the main motor endplate zone. These findings are supported by a recent study reporting a low-dose targeted toward the motor endplate of the biceps brachii (based on anatomical endplate location data) was more effective than a non-targeted low-dose (Gracies et al. 2009).

Current BoNT administration techniques do not use electrophysiological localisation of the endplate zone for guiding toxin injection, although EMG is sometimes used to ensure that the injection needle is actually inserted in the targeted muscle. Instead, clinicians rely primarily on anatomical landmarks and/or on empirical observation as to where injections produced the best clinical response (Borodic et al. 1991; Childers 2004). Due to relatively high individual variability in endplate zone location (Lapatki et al. 2006) we assume that misplacement of toxin injection more than 1 cm away from the endplate zone can easily occur in a clinical situation. This might be one factor responsible for the considerable variability regarding the clinical efficacy of BoNT (Simpson et al. 2008b).

Our study revealed a relatively high mean CMAP reduction of nearly 80% after endplate-targeted BoNT-A injections (on the control side) despite the injection of a strongly reduced toxin dose of only 10 IU Dysport®. Such remarkable weakening of the EDB muscle has to be interpreted in the context of the dose-response relationships

established for this muscle in a previous study (Sloop et al. 1996). In that study, an equivalent dose of 3 IU Botox® (Sampaio et al. 2004) resulted in only 50% CMAP reduction, and even with considerably high BoNT-A doses, CMAP reductions did not exceed 90%. Also this comparison supports the hypothesis that if BoNT-A is precisely administered in the region of the motor endplates, a significant reduction of the clinically applied toxin doses, and possibly also of adverse effects, might be feasible while achieving sufficient weakening of the treated muscle.

Different strategies for targeting BoNT injections are described in the literature (Childers 2003, 2004). These include the identification of the motor point, i.e. the skin area above the muscle where the threshold is lowest for its electrical excitability (Borodic et al. 1991; Childers 2003), and determining the region of most motor unit activity (i.e. the maximal CMAP location) by means of supramaximal stimulation of the motor nerve (Sloop et al. 1996). It has to be noted that these strategies are only of minor relevance for clinical therapy with BoNT, probably also due to severe limitations in electrical stimulation in many muscles. Moreover, injecting BoNT into the motor point would certainly be suboptimal, since this location does not necessarily coincide with the motor endplate zone, i.e. the actual anatomical target of the toxin (Borodic et al. 1991; Farina et al. 2002b; Warfel 1985). The latter seems also to be true for the maximal CMAP location. For instance, in the present study we observed a mean distance of 5.8 mm (range: 2.0 – 15.3 mm) between this location and the endplate zone. Our regression model provides a rough estimate for a possible reduction of the therapeutic effect when injecting the toxin at such a distance from the actual injection target. In contrast to the injection site localisation methods proposed in the literature, high-density surface EMG

has successfully demonstrated its potential for topographically characterising the position and distribution of motor endplates (i.e., those structures into which BoNT injections are most effective) in both the present study and applications in other fields (Castroflorio et al. 2005; Falla et al. 2002; Lapatki et al. 2006; Masuda and Sadoyama 1988).

In principle, the conceptual design of targeting the motor endplate zone for BoNT administration is tailored to those muscles having motor endplates clustered in single or several well-defined areas with centric or eccentric locations. Broad endplate zones ("motor bands"), as can be expected in larger muscles, may require several injections. Multiple point injections are probably still the preferable option for treating muscles having diffuse or multifocal distribution of neuromuscular junctions over the whole muscle, as seems to be the case for the orbicularis oris and orbicularis occuli muscles (Borodic et al. 1991; Happak et al. 1997; Lapatki et al. 2006). A further requirement for the approach introduced in the present study is the muscles' accessibility to surface EMG recordings. This means that high-density surface EMG guided BoNT injection may not be feasible when deep musculature has to be injected, as e.g. for the treatment of hip flexor spasticity. Precise endplate zone detection by means of high-density surface EMG requires special equipment and is certainly somewhat time-consuming (approximately 10 - 15 minutes are needed for this procedure). However, we argue that the injection site would have to be localised only once, as it should be possible to mark this location permanently, e.g. by minimal dermal color administration (like a small "tattoo").

In spite of these restrictions, it has to be emphasised that the conditions for the application of high-density surface EMG seem to be met by a large number of skeletal muscles

10

considered for BoNT injection, for example by the sternocleidomastoid muscle (often involved in cervical dystonia) as shown by previous electrophysiological studies (Falla et al. 2002) and own preliminary experiments. Moreover, multi-channel amplifiers and surface EMG electrode grids are already commercially available. The promising results of the present study certainly justify testing the approach introduced here in a clinical trial.

Conclusions

The results of this study provide evidence that injection of BoNT-A precisely in the endplate zone optimises the effect of this drug. Endplate targeted injection of a minimal effective dose might be a promising strategy for minimising the amount of injected toxin and, consequently, unwanted weakness of adjacent muscles and other adverse effects. Further studies are needed to demonstrate the clinical benefit of this strategy.

10

Part V

Discussion and summary

11

General discussion and outlook

Introduction

A review of the anatomical and neurophysiological literature shows that in comparison to other musculature facial muscles have been somewhat neglected (D'Andrea and Barbaix 2006; May and Schaitkin 2000). This may be due to the fact that only a relatively small group of specialised physicians, therapists and scientists has a particular interest in the orofacial musculature. Another reason may be that investigations in the facial area seem to be particularly challenging – regardless of whether they include dissection or neurophysiological methods. Some anatomists consider dissection of the facial musculature as the most difficult subject of practical anatomy. As a consequence, nearly all dissection studies include a very limited number of human cadavers, and only few thorough, complete and detailed descriptions can be found in anatomy handbooks. A burden of electrophysiological methods for studying facial motor unit properties has been the necessity to confront patients and subjects with invasive methods in the face. High-density surface EMG, which is used in other musculature for non-invasive detailed examination of muscles, was difficult to apply due to limitations of technical and signal processing tools.

The lack of basic anatomical and neurophysiologic knowledge on the facial musculature has impeded various aspects of diagnosis and treatment of facial muscle dysfunctions and disorders. For instance, (conventional) surface EMG studies for examining orofacial muscle (dys-)functions were lacking objective guidelines for electrode positioning , substantially limiting their reproducibility and validity (Fridlund and Cacioppo 1986; Van Boxtel and Jessurun 1993). Furthermore, therapeutic concepts for reconstructive maxillo-facial surgery in cleft lip, trauma and tumor patients as well as injection of botulinum neuro-

toxin for treatment of dyskinesis have been confronted with similar limitations. The goal of the research described in this thesis was to map facial motor units topographically using high-density surface EMG. In addition to contributing to the basic anatomic and neurophysiologic knowledge on the facial musculature, collected data were utilised to improve the methodology of (conventional) bipolar surface EMG measurements in the face and increase the validity by quantitative estimation and removal of cross-talk, i.e. the confounding activity of adjacent muscles. Moreover, clinical applications of high-density surface EMG have been exemplified.

Sensor technique

The first obstacle that had to be overcome was to develop an appropriate sensor technique which allowed high-density surface EMG to be applied to the facial area. This step was crucial because available multi-electrode arrays usually consisted of metal pins or bars (as single electrodes) mounted in apertures of a substrate sheet and integrated in container. Such containers have a height of several centimeters (Fig. 11-1A) and are therefore relatively bulky. The problems in applying these electrode containers to the face as well as the discomfort for the subject during the measurement due to the required pressure of the serrated metal pins on the skin are obvious (Fig. 11-1B).

These limitations have been largely eliminated by the development of a 50 μm-thin and highly flexible electrode grid consisting of flat, electrochemically deposited electrodes. A key aspect in the practical application of this novel electrode grid type was the development of a specific skin attachment technique that used specially prepared double-sided adhesive tape. This method allowed the selective application of conductive cream only directly below the detection surfaces, leading to relatively low
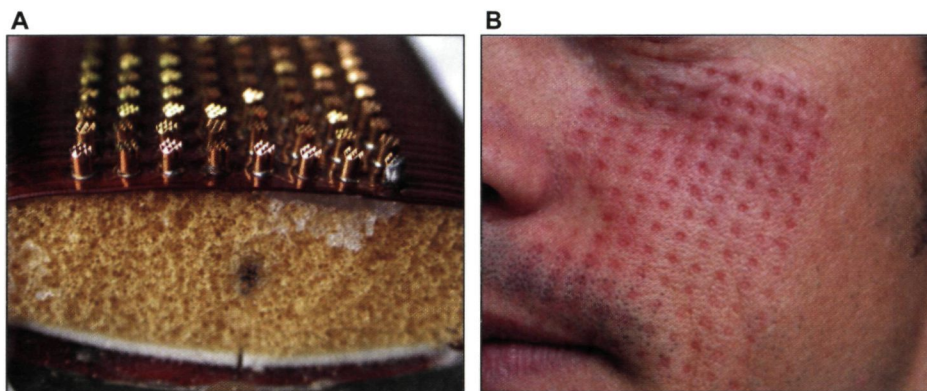
11

Figure 11-1. (A) Multi-electrode array with serrated metal pin electrodes. (B) Facial skin after a 10-min measurement session using this array type.

electrode-to-skin impedances (in spite of flat electrode surfaces) and firm sensor fixation without requiring external fixations. Moreover, since our sensor is manufactured using a thin electrode carrier substrate and an industrial process (the so-called "flexprint technique"), it was relatively inexpensive and allowed grids of different sizes to be cut out of a basic grid version with a common pair of scissors. This allowed adaptation of the size of the recording area to the underlying musculature.

The advantages of the newly developed sensors are not only relevant for facial application, but also in other areas comprising relatively small muscles and pronounced skin curvatures such as the foot and hand. For instance, our flexible sensor has been successfully used for MUNE in the thenar muscles to monitor the disease progression in patients with amyotrophic lateral sclerosis (ALS) (van Dijk et al. 2010, in press) and to study the association between motor axon loss with hand dysfunction in Charcot-Marie-Tooth disease 1a (Videler et al. 2008).

With regard to more broad clinical application of the novel technique, certain limitations still exist. Firstly, the procedure of sensor attachment and electrical connection takes ca.

10-15 minutes which would be rather time-consuming for routine use in clinical diagnostics. Secondly, after the sensor is attached to the skin, it cannot be easily rotated or shifted during the recording session to optimise its orientation or position on the investigated muscle. The latter would require de- and reattachment which is much easier and faster in conventionally (i.e., non-adhesively) fastened metal pin electrode arrays. Part of our current work is focused on finding solutions for these issues. One approach is aimed at combining the advantages of both electrode types by replacing each electrochemically deposited, flat grid electrode by a circular micro-needle array with a diameter of 1.5 mm. In our prototypes (Fig. 11-2A-D), these arrays are equipped with 21 platinum-coated micro-needles each 150 µm in height.

To achieve sufficiently low electrode-to-skin impedances, the micro-needles were designed to penetrate the electrically poorly conductive skin layer. As a result, the distribution of only a minimal amount of electrode cream in the whole sensor area prior to attachment of the electrode grid together with the adhesive tape in a one-step procedure would be sufficient to obtain good signal quality. The
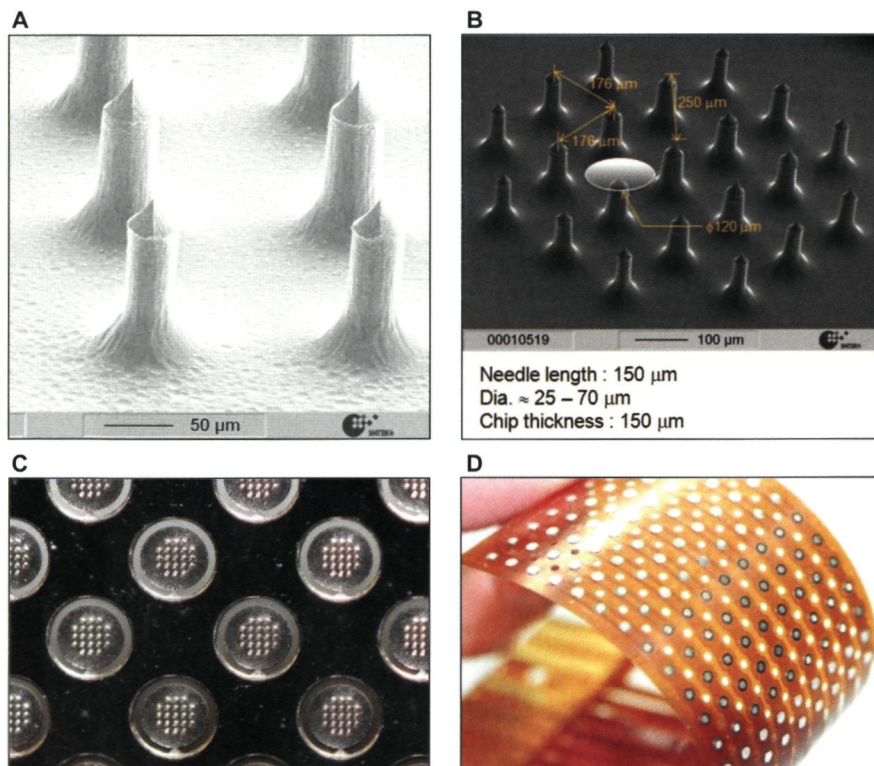
Figure 11-2. (A) Micro-needles with a height of ca. 150 μm. They are dimensioned to penetrate only the outer layers of the epidermis, but not the dermis comprising the capillaries and nerve endings. (B) Several of these needles form an array with a diameter of ca. 1mm. (C) The micro-needle arrays are manufactured by dry-etching of a silicon waver and subsequently coated with platinum. (D) Bending test after attachment of 13 × 9 micro-needle arrays to a flexible polyimid substrate using electrically conductive adhesive.

results of pilot measurements with such needle arrays are promising. We are working on a second approach for dealing with grid misalignment by "rotating" the data by of off-line data processing instead of grid re-attachment. We are exploring the correction of misalignment by means of both reverse modelling (Schad et al. 2008) and movement analysing techniques (Bruhn et al. 2005; Horn and Schunck 1981).

Anatomic and physiological results

We demonstrated various possibilities for utilising the two-dimensional amplitude infor-mation contained in the decomposed facial motor unit action potentials. Most facial muscles lie directly under the skin surface. Thus, the locations on the electrode grid where the action potentials arise and the direction in which they propagate must actually be very close to the motor unit's endplate position and main muscle fibre direction. In this manner, we mapped the neuromuscular junctions and fibre architecture of the lower facial musculature on the level of the smallest functional units in thirteen healthy individuals. Previous approaches for illustrating facial muscle anatomy have been based on graphic or

11

photographic material from dissected human cadavers. Also the clustered distribution of facial motor endplate could only be imaged in cadaveric material using histochemical techniques. In contrast, our electrophysiologic method is non-invasive and can be applied in-vivo. Moreover, the possibility of examining a larger group of subjects allowed the collection of more representative data and the consideration of inter-individual variability in facial size and shape. The non-linear spatial normalisation procedure applied prior to averaging of individual results led to a clear reduction of the inter-individual variability.

In addition to the measurements taken in the lower face, we performed high-density surface EMG recordings also in other facial areas (Fig. 11-3). The evaluation of the data from the midfacial musculature including the orbicularis oris superior, upper incisivus, levator anguli oris, zygomaticus major, levator labii superioris complex and the inferior part of the orbicularis occuli is nearly completed.

Limits in the spatial resolution of our recording technique are met in the orbicularis oris muscle. This complex muscle is actually comprised in each of its quadrants of at least three populations of relatively short fibres with distinct orientations (Blair 1986; Salmons 1995). We are currently preparing complementary studies in this muscle using refined multi-electrode arrays with shorter inter-electrode
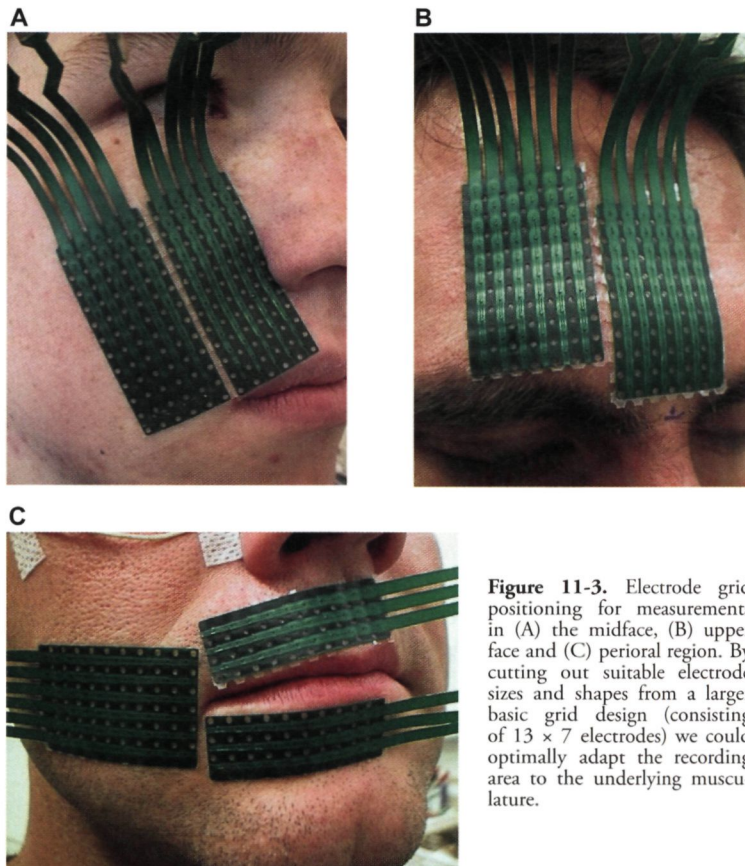
Figure 11-3. Electrode grid positioning for measurements in (A) the midface, (B) upper face and (C) perioral region. By cutting out suitable electrode sizes and shapes from a larger basic grid design (consisting of 13 × 7 electrodes) we could optimally adapt the recording area to the underlying musculature.

distances. An interesting observation during our experiments was that some subjects were able to selectively activate distinct regions of individual facial muscles, particularly the case in the depressor labii inferioris, and that this ability seemed to reflect the muscle-specific endplate zone distribution. We interpret these findings as compartmentalisation, i.e. partitioning of the muscle's motoneuron pool into independently controlled subsets (Binder and Stuart 1980). Future studies are necessary to explore whether this is an attribute shown only in some specific muscles or if it extends to all facial muscles. Moreover, it is necessary to assess the importance of compartmentalisation for the complexity and diversity of specific facial motor tasks.

Besides topographical motor unit properties, high-density surface EMG can also be applied to study facial motor unit firing and recruitment behaviour (Kleine et al. 2000a) as well as for the previously mentioned improvement of motor unit number estimation (van Dijk et al. 2008). In pilot studies (Fig. 11-4) we have experienced that a full decomposition of interference EMG recordings from facial muscles as needed to determine the full firing characteristics of motor units is relatively difficult, compared to limb musculature. One difficulty is that during "constant" contractions motor units are frequently switched on and off indicating that motor unit recruitment is not stable. Using the complementary information provided by multi-electrode surface

A
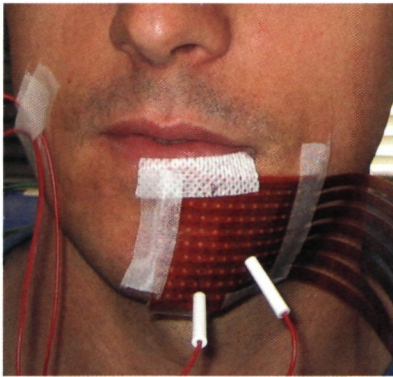
Figure 11-4. Pilot experiments for studying recruitment behaviour of facial muscles. (A) Surface and needle EMG signals were simultaneously recorded using a flexible high-density surface EMG grid and concentric needle electrodes inserted through perforations in the grid. (B) The subject performed a ramp contraaction up to 50% of the maximal voluntary contraction level. The force exerted by the mentalis to pull the chin in cranial direction was monitored using a special transducer. Seven motor units of the mentalis muscle were decomposed. The observed firing rates (up to 40 Hz) are much higher than in other skeletal muscles where seldom firing rates above 20 Hz are seen. (Needle EMG signals were decomposed by K. McGill and Z. Lateva).

B

11
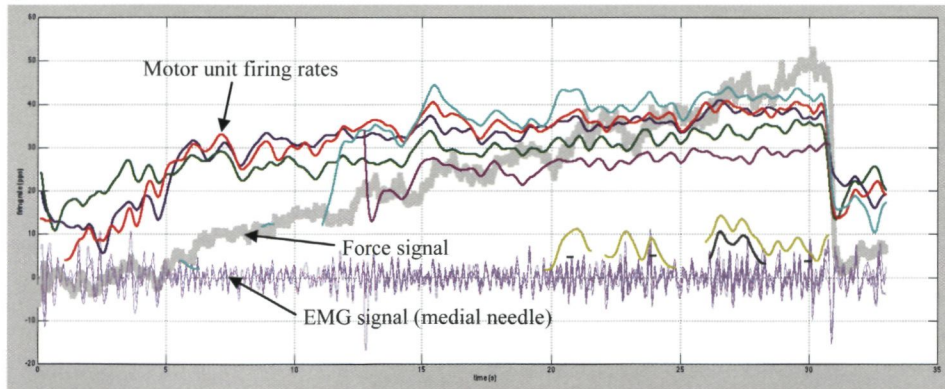
EMG grids and intra-muscular needle or wire electrodes (the latter can be inserted through the wholes in the flexible electrode array) seems to be the best approach for both reliable decomposition and correct assignment of decomposed MUAPs to certain muscle subcomponents of the facial musculature Further research on these topics is on-going

Optimised bipolar electrode postioning

Another important issue we were able to address with the newly developed methodology was the optimisation of the recording positions for conventional bipolar surface EMG The latter method has proved to be a valuable, non-invasive tool in many research and clinical applications in psychophysiology, speech physiology and pathophysiology, general dentistry and orthodontics

A significant limitation of bipolar surface EMG in the face has been the lack of standardised electrode positions (Fridlund and Cacioppo 1986, Van Boxtel and Jessurun 1993) In previous studies, bipolar electrodes were usually positioned parallel to the estimated muscle fibre direction and over the centre or "belly" of the muscle to be examined The anatomical information underlying this procedure had to be taken from illustrations of facial muscle architecture in anatomical textbooks, more objective data were available only from few muscles (Tassinary et al 1989, Williamson et al 1980) Thus, previous surface EMG studies in the face could not meet current methodological standards recommended for surface EMG (Freriks et al 1999) Our high-density surface EMG study has successfully filled this gap in knowledge By constructing virtual bipolar electrode montages in the fibre direction in the monopolar MUAPs, we localised the position for each muscle where the maximal signal amplitude is

achieved Our results revealed that – depending on the specific muscle to be examined – either centric or eccentric electrode positions on the muscle are preferred This finding exemplified the fundamental problem of relying on anatomical knowledge alone for standardising electrophysiological measurements

The problem of cross-talk

In surface EMG recordings from the facial musculature consisting of multiple muscles in a relatively small area, co-registration of activity of adjacent muscles is unavoidable Cross-talk can considerably bias the estimates of muscle activity and is therefore considered to be one of the most significant limiting factors in the interpretation of sEMG (Lowery et al 2003, Rau et al 2004) So far, both elimination and quantitative estimation of cross-talk by optimising recording techniques or data processing were limited, especially for recordings from the facial musculature due to restricted muscle-selectivity in both voluntary contractions and electrical stimulation (Delbeke 1982, Lapatki et al 2003) In the present work we propose a novel method for quantifying the amount of cross-talk based on single motor unit analysis In contrast to attempted "selective" voluntary muscle contractions as used in previous studies in the face (Lapatki et al 2003, O'Dwyer et al 1981), MUAPs are 100% muscle-selective and thus allow unbiased and accurate quantitative cross-talk estimates As indicator for the amount of cross-talk we used the ratio between the MUAP amplitudes at an adjacent electrode and at the electrode above the contracted muscle The mean cross-talk ratios established in our study (ranging from 0 03 to 0 52) are of fundamental importance for the correct interpretation of surface EMG data from the face, as they reflect the possible measurement bias of the recorded interference EMG caused by activity of neighbouring muscles Beyond that,

we were even able to remove the confounding cross-talk, since by examination of the whole musculature of the lower face we obtained cross-talk ratios for all muscle-electrode site combinations in this area. This opened the possibility of applying a matrix inversion algorithm for extracting the "true" individual muscle activity from interferencing EMG patterns. Applying this method to recordings during attempted isolated facial muscle contractions, we observed that in the measured surface EMG, the ability of the subjects to selectively contract the lower facial muscles was considerably under-estimated.

In principle, estimation of true individual muscle activity by applying our matrix inversion approach and cross-talk ratios should be possible for interference EMG measurements alone, provided that one bipolar surface EMG electrodes is positioned on each lower facial muscle according to our guidelines. Theoretically, this estimate requires cross-talk ratios from the same individual. An interesting issue which has been addressed was how accurate true individual muscle activity can be estimated when mean, instead of individual, cross-talk ratios are applied. Generally, we found this error to be relatively small, especially when compared to that error inherent in the measured surface EMG. Thus we consider our approach to be useful for improving the estimate of true individual muscle activity in future studies. Application of our method is not restricted to surface EMG measurements in the facial area, recordings from other musculature confounded by cross-talk can benefit as well.

We included two examples of clinical application of the developed sensor technique. On-line illustration of topographical amplitude information from a complex muscle system provides objective myo-feedback on the activity of the system's subcomponents. During training wind instrumentalists in selective facial muscle contractions, we observed that such myo-feedback aided the improvement of differentiated facial motor control. We hypothesise that high-density surface EMG myo-feedback may also be clinically useful, e.g. as a complementary tool for restoring facial muscle weakness. Considering this, one has to relate the benefit of this tool to the relatively time-consuming sensor application procedure and the expensive multi-channel recording equipment. Objective balancing of the benefits and the costs is only possible on the basis of broad clinical experience and/or comparative clinical trials.

Another interesting clinical application could be the improvement of the treatment with the neurotoxin of *Clostridium botulinum*. We demonstrated in a human extensor digitorum brevis muscle model that the effect of toxin injection depends significantly on the distance of the injection from the motor endplate zone (i.e., the location where the neuromuscular blockade occurs). We observed that injection misplacement of only 1 cm away from the endplate zone reduced the therapeutic effect by ca. 50%. This suggests that, if precisely targeted toward the endplate zone, a smaller toxin dose is sufficient for achieving the desired therapeutic effect. Besides reducing therapy costs, this strategy might help in minimising adverse effects such as unwanted weakening of adjacent muscles not intended to be treated or antibody formation. Presumably, endplate targeted botulinum neurotoxin injection might be particularly beneficial in muscles with variable and atypical motor endplate zone locations such as those of the face. It has to be mentioned that besides histochemical techniques (Aquilonius et al. 1984; Christensen 1959; Snobl et al. 1998) and EMG techniques with several inserted invasive electrodes (Lateva et al. 2002), high-density surface EMG has already proven in previous studies to be suitable for determining the locations of

11

the motor endplates and their distribution on the muscle. However, in the context of clinical use of this tool for targeted administration of botulinum neurotoxin both the applicability of our flexible electrode grids in challenging muscle areas such as that of the face, and the possibility of injecting the toxin through the holes in the electrode grids are unique characteristics. The possible clinical advantages of our approach will be investigated in a planned clinical trial including patients with cervical dystonia.

The described examples used simple monitoring of amplitude maps or visual observation of interference EMG signals. Recently, fast algorithms for automatic decomposition of high-density surface EMG have been developed (Holobar et al. 2009; Zazula and Holobar 2005). It is conceivable that these improved software tools for automated single motor unit analysis together with progress in sensor technology will facilitate practical application of multi-electrode arrays (as promoted by us) and provide important key factors for advancing clinical application of multi-electrode techniques and improving the diagnosis of neuromuscular diseases. Since surface EMG electrodes cannot detect single fibre potentials, they cannot replace intra-muscular electrodes for clinical diagnostic purposes. However, in the characterisation of single motor units an overlap exists between these two techniques. Especially here, our new multi-electrode sEMG grid offers an attractive alternative to conventional needle or fine-wire electrodes, whereby the non-invasive sEMG character is particularly appealing in the face, in general EMG studies in children, and in long-term

studies. A number of pathophysiological mechanisms causing neuromuscular disorders show a specific topographic character (Drost et al. 2001). Studying topographic aspects of neuromuscular diseases – on the level of both the muscle and motor unit – clearly belongs to the domain of high-density surface EMG. In this respect it is worthwhile to further explore clinical applications and possibilities of this technique. For instance, early affection of the facial muscles is a hallmark feature of facioscapulo-humeral dystrophy causing a considerable loss of mimic expression. Detailed morphological or electrophysiological studies in this disease on topographical alterations of facial motor units are still lacking. Pilot studies show that motor units affected by the dystrophic process are smaller and show a reduced spatial spread (Fig. 11-5). Furthermore, we could localise the peculiar distribution of muscle-dystrophy reflected by regions of affected muscle tissue. These findings are promising and suggest further exploration of the clinical potential of high-density surface EMG techniques for early diagnosis in this and other neuromuscular disorders affecting facial muscles. The collateral advances in sensor techniques and signal processing tools as described before might be helpful in this context. In addition to the possible application of our optimised sensor technique for clinical diagnosis, fundamental research on the alterations of facial motor units in neuromuscular diseases might contribute to the understanding of the pathophysiological mechanisms and might give clues for new therapeutic approaches and for further genetic, biochemical and neurophysiologic research.
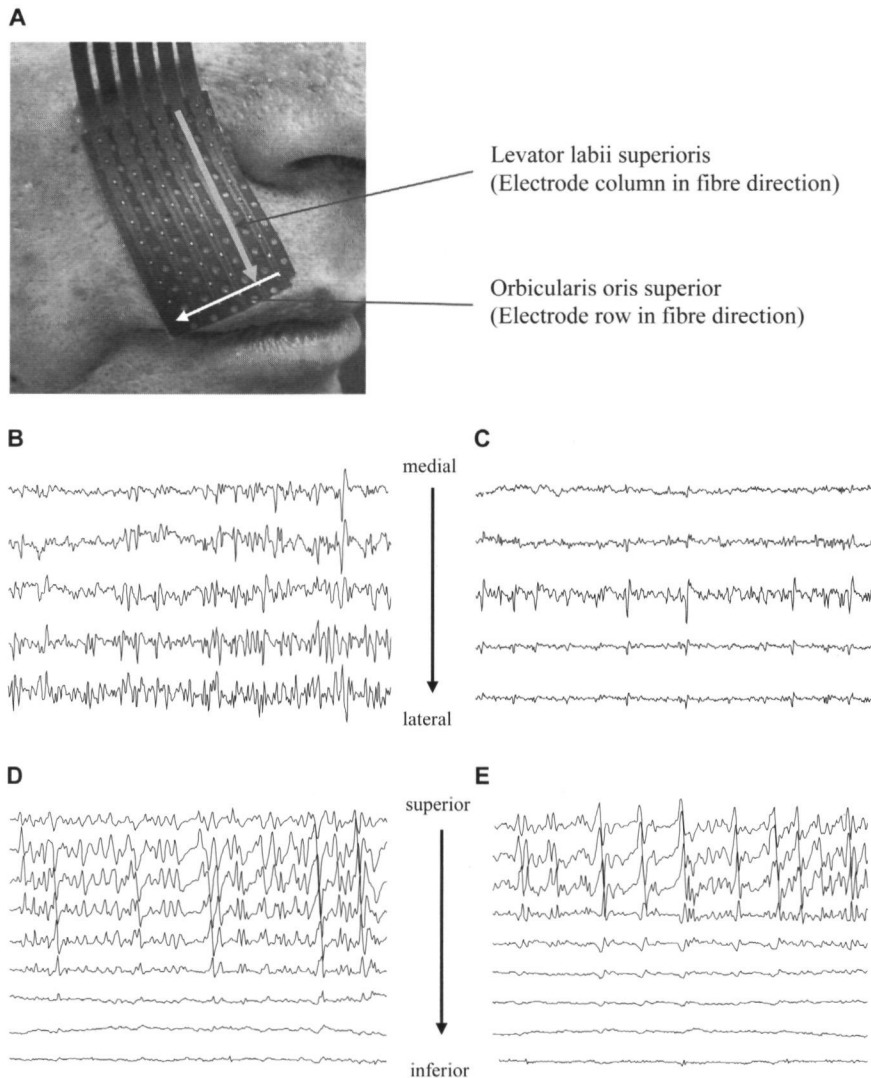
Figure 11-5. (A) Pilot measurements in a patient with facioscapulohumeral dystrophy. An array of 6×10 electrodes was attached on each facial side. (B) Bipolar signals (400 ms) from the right orbicularis oris superior muscle derived from consecutive electrodes in fibre direction (this electrode row is marked by the white arrow in panel (A). Signals show a normal interference pattern. (C) Similar signals from the left orbicularis oris superior. They have much lower amplitudes (except the middle signal) and show a relative poor interference pattern. (D) Bipolar signals (200 ms) derived from an electrode column (grey arrow in panel (A) located over the right levator labii superioris muscle. (E) Similar signals from the more affected, left levator labii superioris. On the left side (E), attenuation of signal amplitudes was observed more cranially when compared to the contralateral side. This may indicate shortening of muscle fibres on their inferior endings. These findings indicate that primarily the left upper lip is affected by the muscle dystrophic process which agrees with the clinical symptoms in this patient.

11

12

SUMMARY

The diagnosis and treatment of facial muscle dysfunctions and disorders have been hampered by major deficiencies in the anatomic and neurophysiologic knowledge on the complex facial musculature. A particular concern was the lack of knowledge on topographical motor unit properties. High-density surface electromyography is the most appropriate method presently available to fill this gap. However, while in many muscle areas this technique has been successfully used, applications in the face could not be considered. The main disadvantages preventing the use of high-density surface EMG for the facial musculature were the limitation of the construction principles and the application techniques of conventional electrode array systems, combined with the special methodological demands for surface EMG in the facial area.

The research described in this thesis included the development of a reusable, highly flexible multi-electrode surface EMG grid and of a specific skin attachment technique using specially prepared double-sided adhesive tape that allowed selective electrode cream application only in the electrode areas. The silver-chloride electrode surfaces and their low electrode-to-skin impedances guaranteed high baseline stability and a low signal noise level. Due to its high mechanical flexibility, the electrode grid follows the skin curvature even in areas with very uneven contours. The electrode grid attachment procedure also demonstrated resistance to saliva and tensile forces due to mimic contractions.

The improved sensor technique was subsequently used to record high-density surface EMG in thirteen healthy subjects during selective contractions of the four lower facial muscles, i.e. the depressor anguli oris, depressor labii inferioris, mentalis, and orbicularis oris inferior, at different activity levels. Recorded interference EMG signals were decomposed into MUAPs which reflect the signal contributions of single motor units. The combined spatial and temporal amplitude characteristics of the extracted MUAPs enabled their assignment to individual lower facial muscles and their compartments. Moreover, this information allowed us to extract motor endplate positions and principal muscle fibre orientations of the lower facial motor units and to map these parameters on the subjects' individual faces. Prior to averaging the individual results were spatially warped to correct for the different sizes and shapes of the faces of individual subjects. This non-invasive electrophysiological study revealed a distribution of the lower facial motor endplates in distinct clusters on the muscle often with eccentric locations which principally confirms findings of previous histochemical studies in human cadavers. These results contribute topographical information on the facial musculature on the level of its smallest functional units to the basic anatomic and neurophysiologic knowledge.

Facial surface EMG has been proven to be a valuable, non-invasive tool in many research and clinical applications in psychophysiology, speech physiology and pathophysiology as well as in general dentistry and orthodontics. Electrode locations in previous studies were mainly chosen on a macro-anatomical basis due to the lack of relevant quantitative information on topographical motor unit properties. We developed a method for establishing objective electrode placement guidelines using the extracted topographical motor unit parameters and the MUAPs' two-dimensional amplitude profiles. Electrode positions were considered to be optimal when the surface EMG registered from the corresponding muscle has maximal amplitude which principally should lead to the best signal-to-noise ratio. The determined optimal electrode positions were validated using interference EMG signals recorded during attempted selective

12

lower facial muscle contractions at different levels. More generally, we have established in this study an important methodological principle for improving both the validity and reproducibility of surface EMG investigations.

In complex musculature such as that of the face, surface EMG recordings are significantly confounded by activity of adjacent muscles. We quantitatively estimated this unwanted "EMG cross-talk" in the lower face by determining (for all muscle-electrode site combinations) the MUAP amplitude ratio between an adjacent electrode and the electrode positioned above the muscle to which the MUAP belonged. We found mean cross-talk ratios for bipolar surface EMG recordings in the lower face ranging from 0.03 to 0.52. These values reflect the contribution of neighbouring muscles to the measured EMG activity and are therefore of great importance regarding a correct interpretation of the measurement. Moreover, we have demonstrated that these cross-talk ratios can be used in a matrix inversion algorithm to eliminate the confounding cross-talk from conventional bipolar surface EMG signals. This was empirically tested on data from four electrode positions in the lower face recorded during attempted isolated muscle contractions. The ability of the subjects to selectively contract the lower facial muscles is considerably under-estimated when evaluating measured EMG instead of estimating the "true" individual muscle activity. Practically, given the condition that one bipolar electrode is attached for each muscle according to the proposed guidelines, the inverted cross-talk matrix can readily be used for improving the estimate of individual muscle activity in future surface EMG studies in the lower face. In contrast to methods used in previous studies for quantitative cross-talk estimates, our approach is based on the analysis of muscle-selective MUAPs leading to complete muscle-selectivity. Although this is particularly important in the face where selective voluntary muscle contractions or electrical stimulation is limited, our methodological approach can also be applied to bipolar surface EMG recordings from other more or less complex muscle areas.

The results presented here may also be relevant from a clinical point of view. Our novel, highly flexible, relatively inexpensive and universally applicable sensor might bring high-density surface EMG closer to the physician. Especially in the characterisation of single motor units, high-density surface EMG offers an attractive alternative to conventional needle or fine-wire EMG, whereby its non-invasive character is particularly appealing. The facial motor unit topography obtained in a group of healthy individuals is useful as normal data in the observation of regeneration and reinnervation of MUs after peripheral nerve injuries or muscle transplantation, and in the study of the topographical aspects and the characteristic alterations on the motor unit level of neuromuscular diseases affecting the facial musculature (as indicated in pilot measurements in patients with facioscapulohumeral dystrophy or Möbius syndrome). Finally, we demonstrated in the human EDB muscle that therapeutic interventions with botulinum neurotoxin may benefit from the possibility of localising motor endplate zone(s) in-vivo. We assume that – if precisely targeted to the location where the neuromuscular blockade occurs – a sufficient therapeutic effect can be achieved by administering a lower toxin dose. We expect this approach to be particularly useful in treating muscles with atypical motor endplate locations and distributions, such as the facial muscles. Our strategy might help to reduce both therapy costs and side-effects such as unwanted paralysis of adjacent muscles and antibody formation.

12

Diagnose en behandeling van aandoeningen van de aangezichtspieren worden gehinderd door gebrek aan kennis over de anatomie en de neurofysiologie van de complexe gezichtsmusculatuur. Een probleem daarbij is het gebrek aan kennis over de topografische eigenschappen van gezichtspieren en meer specifiek hun bouwstenen, de motorische eenheden. High-density oppervlakte elektromyografie (EMG) is tot op heden de meest geschikte methode om dit probleem te benaderen. Hoewel de techniek al in veel andere gebieden succesvol werd toegepast, was toepassing in het gezicht vrijwel onmogelijk. Het belangrijkste obstakel dat toepassing van high-density oppervlakte EMG in de weg stond waren de problemen rond de constructie en de manier van aanbrengen van de elektrodegrids, gecombineerd met de speciale methodologische eisen die oppervlakte EMG in het aangezicht stelt.

In dit proefschrift is de ontwikkeling van een herbruikbaar, licht en flexibel elektrodegrid voor oppervlakte EMG beschreven samen met een speciale techniek voor het aanbrengen ervan. Dat laatste gebeurt door middel van speciaal voor dit doel aangepast dubbelzijdige plakband wat het mogelijk maakt een geleidende elektrodepasta zo aan te brengen dat onderlinge elektroden geen elektrisch contact maken. De zilverchloride elektrodeoppervlakken zorgen voor een goede elektrode-huid impedantie met een stabiele half-cell potentiaal en een laag ruis niveau. Door de hoge flexibiliteit van deze grid kunnen de contouren van de huid goed gevolgd worden, zelfs in gebieden met grote krommingen. De bevestiging van de elektrode is ook bestand tegen vocht en de krachten die ontstaan bij gelaatsbewegingen.

Deze verbeterde elektrodetechniek werd vervolgens gebruikt bij de registratie van high-density oppervlakte EMG bij dertien gezonde vrijwilligers tijdens het selectief aanspannen op verschillende activiteitsniveaus van vier facialis spieren in het onderste deel van het gezicht, namelijk de m. depressor anguli oris, de m. depressor labii inferioris, de m. mentalis en de m. orbicularis oris inferior. De opgenomen EMG signalen zijn vervolgens ontrafelt in motor unit actie potentialen (MUAPs) die de bijdrage van de individuele functionele bouwstenen van de spier, de motor units representeren. Het spatio-temporele profiel van MUAPs maakte het mogelijk om de individuele MUAPs specifiek toe te wijzen aan een enkele spier. Met deze informatie was het mogelijk om de positie van de motor eindplaten, daar waar de motor units worden geactiveerd, alsmede de richting van de spiervezels vast te stellen om die vervolgens te projecteren op de gezichten van de individuele proefpersonen. Voordat een gemiddelde van deze uitkomsten bepaald werd, zijn de individuele resultaten spatieel gecorrigeerd naar de verschillen in grootte en vormen van de gezichten van de proefpersonen. Deze non-invasieve elektrofysiologische studie laat een distributie zien van motor eindplaten in afzonderlijke clusters in de spier, vaak excentrisch gelokaliseerd, hetgeen eerder histologisch onderzoek bij humane cadavers bevestigt. De resultaten voegen topografische informatie op het niveau van de functionele eenheden van de gelaatspieren toe aan het totaal van anatomische en neurofysiologische kennis van het menselijke spierstelsel.

Oppervlakte EMG van het gelaat is een waardevolle non-invasieve techniek gebleken in psychofysiologisch, spraakfysiologisch en pathofysiologisch onderzoek, maar ook in de tandheelkunde en orthodontie. Door gebrek aan kwantitatieve informatie over de topografische eigenschappen van motor units werd positionering van elektroden voornamelijk gebaseerd op macro-anatomische kennis. In dit proefschrift staat daarom een methode beschreven voor het vaststellen van objectieve elektrodeposities gebaseerd op de topogra-

12

fische eigenschappen van motor units en de spatio-temporele amplitude profielen van de MUAPs. De positie van de elektroden werd optimaal verondersteld indien de amplitude van het oppervlakte EMG signaal voor de betreffende spier maximaal was, wat in principe leidt tot de beste signaal-ruis verhouding. De zo bepaalde optimale elektroden posities zijn gevalideerd aan de hand van het EMG interferentie patroon tijdens zo selectief mogelijke contracties van de individuele spieren op verschillende contractieniveaus. Meer in zijn algemeenheid hebben we met dit onderzoek een methode ontwikkeld waarmee zowel de validiteit als de reproduceerbaarheid van oppervlakte EMG verbeterd kan worden.

Bij complexe spieren, zoals die in het aangezicht, wordt het oppervlakte EMG sterk beïnvloed door de activiteit van naastliggende spieren. Deze ongewenste overspraak of "cross-talk" hebben we gekwantificeerd in het onderste deel van het gezicht door (voor alle spier-elektrode combinaties) de zogenoemde "cross-talk-ratio" tussen een naastliggende elektrode en de elektrode boven de spier waartoe de MUAP hoorde. De gemiddelde cross-talk-ratios voor bipolaire oppervlakte EMG opnames lagen tussen de 0.03 en 0.51. Deze waarden representeren de (ongewenste) bijdrage van naastliggende spieren aan het oppervlakte EMG en zijn daarom van groot belang voor de juiste interpretatie van de data. We hebben laten zien dat het mogelijk is om deze cross-talk-ratios te gebruiken in een matrix inversiealgoritme om daarmee de beïnvloeding van cross-talk op een conventioneel gemeten bipolair EMG signaal te corrigeren. Dit hebben we empirisch getoetst op data van vier elektrodeposities in het aangezicht gemeten tijdens selectieve spiercontracties. De mate waarin proefpersonen in staat zijn de onderste gezichtspieren selectief aan te spannen wordt fors onderschat indien uitgegaan wordt van het gemeten EMG signaal in relatie tot de

"echte" individuele spieractiviteit. De geïnverteerde cross-talk matrix kan direct worden gebruikt om een betere schatting te krijgen van de individuele spieractiviteit voor toekomstig onderzoek met oppervlakte EMG in het gezicht indien een bipolaire elektrode voor elke spier wordt aangebracht op grond van voorgestelde objectieve posities. In tegenstelling tot andere studies naar cross-talk, maken we bij onze methode gebruik van de spier-selectieve MUAPs wat resulteert in een volledige selectiviteit van spieractiviteit. Hoewel dit met name van belang is bij de aangezichtspieren waarbij selectieve aanspanning en elektrische stimulatie van de spieren lastig is, kan onze methode ook toegepast worden voor oppervlakte EMG in andere gebieden.

De resultaten van het hier gepresenteerde onderzoek zijn ook vanuit klinisch oogpunt potentieel relevant. Onze nieuwe, flexibele, relatief goedkope en universeel toepasbare elektrodegrid kan het high-density oppervlakte EMG ook dichter bij de clinicus brengen. Voor de karakterisering van motor units vormt het high-density oppervlakte EMG een aantrekkelijk alternatief in vergelijking tot het naald of "fine wire" EMG, waarbij met name het non-invasieve karakter aantrekkelijk is. De topografie van motor units van de aangezichtspieren uit de groep van gezonde proefpersonen is ook waardevol als referentieset bij de bestudering van regeneratie en reïnnervatie van motor units na perifeer zenuw letsel of een spiertransplantatie. Tevens zijn de data van belang bij de bestudering van topografische aspecten en karakteristieke veranderingen op het niveau van motor units bij neuromusculaire aandoeningen waarbij de gezichtspieren zijn aangedaan (zoals we gezien hebben in een pilot-studie bij facioscapulohumerale dystrofie (FSHD) en Möbius syndroom). Tot slot hebben we in de extensor digitorum brevis spier van de voet laten zien dat het therapeutisch effect van botulinum toxine mogelijk

positief beïnvloed kan worden door een goede lokalisering van de motor eindplaat zone(s). Daarbij gaan we ervan uit dat door precieze toediening van de toxine op de plaats waar de neuromusculaire overgang wordt geblokkeerd, met een lagere dosis een voldoende therapeutisch effect kan worden bereikt. We verwachten dat dit met name interessant is bij de behandeling van spieren bij atypische posities van de motor eindplaat zoals het geval is bij de gezichtspieren. Daarbij kan onze strategie therapiekosten en ongewenste bijeffecten, zoals verlamming van naastliggende spieren en de formatie van antilichamen, helpen reduceren.

12

Part VI

Appendix

REFERENCES

Abbs JH, Gracco VL and Blair C. Functional muscle partitioning during voluntary movement: facial muscle activity for speech. *Exp Neurol* 85: 469-479, 1984.

Andreassen S and Rosenfalck A. Relationship of intracellular and extracellular action potentials of skeletal muscle fibers. *CRC Crit Rev Bioeng* 6: 267-306, 1981.

Aquilonius SM, Askmark H, Gillberg PG, Nandedkar S, Olsson Y and Stalberg E. Topographical localization of motor endplates in cryosections of whole human muscles. *Muscle Nerve* 7: 287-293, 1984.

Armstrong JB, Rose PK, Vanner S, Bakker GJ and Richmond FJ. Compartmentalization of motor units in the cat neck muscle, biventer cervicis. *J Neurophysiol* 60: 30-45, 1988.

Arsos GA and Dimitriu PP. A fractal characterization of the type II fiber distribution in the extensor digitorum longus and soleus muscles of the adult rat. *Muscle Nerve* 18: 961-968, 1995.

Bakheit AM. The possible adverse effects of intramuscular botulinum toxin injections and their management. *Curr Drug Saf* 1: 271-279, 2006.

Basmajian JV and De Luca CJ. *Muscles alive. Their functions revealed by electromyography*. Baltimore, London, Los Angeles, Sydney: Williams & Wilkins, 1985.

Beck TW, Housh TJ, Cramer JT and Weir JP. The effects of electrode placement and innervation zone location on the electromyographic amplitude and mean power frequency versus isometric torque relationships for the vastus lateralis muscle. *J Electromyogr Kinesiol* 18: 317-328, 2008.

Binder MD and Stuart DG. Motor unit - muscle receptor interactions: Design features of the neuro-muscular control system. In: *Progress in clinical neurophysiology. Spinal and supraspinal mechanisms of voluntary motor contol and locomotion*, edited by Desmedt JD. Basel: Karger, 1980, p. 72-98.

Blair C. Interdigitating muscle fibers throughout orbicularis oris inferior: preliminary observations. *J Speech Hear Res* 29: 266-269, 1986.

Blair C and Smith A. EMG recording in human lip muscles: can single muscles be isolated? *J Speech Hear Res* 29: 256-266, 1986.

Blair C. Firing and contractile properties of human lower lip motor units during sustained isometric contractions. *Exp Neurol* 99: 269-280, 1988.

Blanksma NG and van Eijden TM. Electromyographic heterogeneity in the human temporalis and masseter muscles during static biting, open/close excursions, and chewing. *J Dent Res* 74: 1318-1327, 1995.

Blok JH, van Dijk JP, Drost G, Zwarts MJ and Stegeman DF. A high-density multichannel surface electromyography system for the characterization of single motor units. *Review of Scientific Instruments* 73: 1887-1897, 2002.

Bodine-Fowler S, Garfinkel A, Roy RR and Edgerton VR. Spatial distribution of muscle fibers within the territory of a motor unit. *Muscle Nerve* 13: 1133-1145, 1990.

Borodic GE, Joseph M, Fay L, Cozzolino D and Ferrante RJ. Botulinum A toxin for the treatment of spasmodic torticollis: dysphagia and regional toxin spread. *Head Neck* 12: 392-399, 1990.

Borodic GE, Cozzolino D, Ferrante R, Wiegner AW and Young RR. Innervation zone of orbicularis oculi muscle and implications for botulinum A toxin therapy. *Ophthal Plast Reconstr Surg* 7: 54-60, 1991.

R

Borodic GE, Ferrante R, Pearce LB and Smith K. Histologic assessment of dose-related diffusion and muscle fiber response after therapeutic botulinum A toxin injections. *Mov Disord* 9: 31-39, 1994.

Brans JW, de Boer IP, Aramideh M, Ongerboer de Visser BW and Speelman JD. Botulinum toxin in cervical dystonia: low dosage with electromyographic guidance. *J Neurol* 242: 529-534, 1995.

Braus H and Elze C. *Anatomie des Menschen. Ein Lehrbuch für Studierende und Arzte. Bd 1 Bewegungsapparat.* Berlin: Springer-Verlag, 1954.

Breidenbach MA and Brunger AT. New insights into clostridial neurotoxin-SNARE interactions. *Trends Mol Med* 11: 377-381, 2005.

Bruhn A, Weickert J, Feddern C, Kohlberger T and Schnorr C. Variational optical flow computation in real time. *IEEE Trans Image Process* 14: 608-615, 2005.

Buchthal F. The functional organization of the motor unit: a summary of results. *Am J Phys Med* 38: 125-128, 1959.

Burba M. *Brass Master-Class. Methode für Blechbläser Der logische Weg zu grenzenloser Sicherheit, Ausdauer und Hohe.* Mainz: Edition Schott, 1994.

Burke D and Gandevia SC. Skeletal muscle: structure and function. In: *Clinical Neurophysiology of disorders of muscle and neuromuscular junction, including fatigue,* edited by Stalberg E. Amsterdam: Elsevier, 2003, p. 7-26.

Campanini I, Merlo A, Degola P, Merletti R, Vezzosi G and Farina D. Effect of electrode location on EMG signal envelope in leg muscles during gait. *J Electromyogr Kinesiol* 17. 515-526, 2007.

Castroflorio T, Farina D, Bottin A, Debernardi C, Bracco P, Merletti R, Anastasi G and Bramanti P. Non-invasive assessment of motor unit anatomy in jaw-elevator muscles. *J Oral Rehabil* 32: 708-713, 2005.

Childers MK, Kornegay JN, Aoki R, Otaviani L, Bogan DJ and Petroski G. Evaluating motor endplate-targeted injections of botulinum toxin type A in a canine model. *Muscle Nerve* 21: 653-655, 1998.

Childers MK. The importance of electromyographic guidance and electrical stimulation for injection of botulinum toxin. *Phys Med Rehabil Clin N Am* 14: 781-792, 2003.

Childers MK. Targeting the neuromuscular junction in skeletal muscles. *Am J Phys Med Rehabil* 83 Suppl 10: 38-44, 2004.

Christensen E. Topography of terminal motor innervation in striated muscles from stillborn infants. *Am J Phys Med* 38: 65-78, 1959.

Cole KJ, Konopacki RA and Abbs JH. A miniature electrode for surface electromyography during speech. *J Acoust Soc Am* 74: 1362-1366, 1983.

Collins A and Jankovic J. Botulinum toxin injection for congenital muscular torticollis presenting in children and adults. *Neurology* 67: 1083-1085, 2006.

Cooper R, Osselton JW and Shaw JC. *EEG technology.* London: Butterworths, 1980.

Crossman AR. Neuroanatomy. In: *Gray's anatomy,* edited by Standring S. Oxford: Churchill Livingstone Elsevier, 2008, p. 275-297.

D'Andrea E and Barbaix E. Anatomic research on the perioral muscles, functional matrix of the maxillary and mandibular bones. *Surg Radiol Anat* 28: 261-266, 2006.

Daube JR. Motor unit number estimates--from A to Z. *J Neurol Sci* 242: 23-35, 2006.

Davis RA, Anson BJ, Budinger JM and Kurth LR. Surgical anatomy of the facial nerve and parotid gland based upon a study of 350 cervicofacial halves. *Surg Gynecol Obstet* 102: 385-412, 1956.

De Luca CJ and Merletti R. Surface myoelectric signal cross-talk among muscles of the leg.

Electroencephalogr Clin Neurophysiol 69: 568-575, 1988.

De Luca CJ and Knaflitz M. *Surface Electromyography: what's new?* Torino: Edizioni C.L.U.T., 1992.

Delbeke J. Reliability of the motor unit count in the facial muscles. *Electromyogr Clin Neurophysiol* 22: 277-290, 1982.

Desmedt JE. Methods of studying neuromuscular function in humans: isometric myogram, excitation electromyogram, and topography of terminal innervation. *Acta Neurol Psychiatr Belg* 58: 977-1017, 1958.

Dimitrova NA, Dimitrov GV and Nikitin OA. Neither high-pass filtering nor mathematical differentiation of the EMG signals can considerably reduce cross-talk. *J Electromyogr Kinesiol* 12: 235-246, 2002.

Disselhorst-Klug C, Silny J and Rau G. Improvement of spatial resolution in surface-EMG: a theoretical and experimental comparison of different spatial filters. *IEEE Trans Biomed Eng* 44: 567-574, 1997.

Disselhorst-Klug C, Blanc Y and Rau G. Examination of the reduction of crosstalk between the leg muscles by spatial filtering techniques. In: *Future applications of surface electromyography*, edited by Hermens HJ FB. Enschede: Roessingh Research and Development, 1999, p. 38-40.

Dressler D and Hallett M. Immunological aspects of Botox, Dysport and Myobloc/NeuroBloc. *Eur J Neurol* 13 Suppl 1: 11-15, 2006.

Dressler D and Benecke R. Pharmacology of therapeutic botulinum toxin preparations. *Disabil Rehabil* 29: 1761-1768, 2007.

Drost G, Blok JH, Stegeman DF, van Dijk JP, van Engelen BG and Zwarts MJ. Propagation disturbance of motor unit action potentials during transient paresis in generalized myotonia: a high-density surface EMG study. *Brain* 124: 352-360, 2001.

Dumitru D and King JC. Motor unit action potential duration and muscle length. *Muscle Nerve* 22: 1188-1195, 1999.

Dumitru D. Physiologic basis of potentials recorded in electromyography. *Muscle Nerve* 23: 1667-1685, 2000.

Ekbom KA, Jernelius B and Kugelberg E. Perioral reflexes. *Neurology* 2: 103-111, 1952.

Ekman P and Friesen WV. *Manual for the facial action coding system*. Palo Alto: Consulting Psychologists Press, 1977.

Ekman P, Friesen WV and Hager JC. Psychology, appearance and behavior of the human face: http://face-and-emotion.com/dataface/facs/new_version.jsp, 2002 (2010 February 8).

Eleopra R, Tugnoli V, Caniatti L and De Grandis D. Botulinum toxin treatment in the facial muscles of humans: evidence of an action in untreated near muscles by peripheral local diffusion. *Neurology* 46: 1158-1160, 1996.

English AW and Letbetter WD. A histochemical analysis of identified compartments of cat lateral gastrocnemius muscle. *Anat Rec* 204: 123-130, 1982.

Enoka RM. Morphological features and activation patterns of motor units. *J Clin Neurophysiol* 12: 538-559, 1995.

Everitt BS, Landau S and Leese M. *Cluster analysis*. London: Arnold, 2001.

Falla D, Dall'Alba P, Rainoldi A, Merletti R and Jull G. Location of innervation zones of sternocleidomastoid and scalene muscles--a basis for clinical and research electromyography applications. *Clin Neurophysiol* 113: 57-63, 2002.

Farina D, Fortunato E and Merletti R. Noninvasive estimation of motor unit conduction velocity distribution using linear electrode arrays. *IEEE Trans Biomed Eng* 47: 380-388, 2000.

R

Farina D, Merletti R, Nazzaro M and Caruso I. Effect of joint angle on EMG variables in leg and thigh muscles. *IEEE Eng Med Biol Mag* 20: 62-71, 2001.

Farina D, Madeleine P, Graven-Nielsen T, Merletti R and Arendt-Nielsen L. Standardising surface electromyogram recordings for assessment of activity and fatigue in the human upper trapezius muscle. *Eur J Appl Physiol* 86: 469-478, 2002a.

Farina D, Merletti R, Indino B, Nazzaro M and Pozzo M. Surface EMG crosstalk between knee extensor muscles: experimental and model results. *Muscle Nerve* 26: 681-695, 2002b.

Farina D, Merletti R and Enoka RM. The extraction of neural strategies from the surface EMG. *J Appl Physiol* 96: 1486-1495, 2004.

Feinstein B, Lindegard B, Nyman E and Wohlfart G. Morphologic studies of motor units in normal human muscles. *Acta Anat (Basel)* 23: 127-142, 1955.

Fleshman JW, Munson JB, Sypert GW and Friedman WA. Rheobase, input resistance, and motor-unit type in medial gastrocnemius motoneurons in the cat. *J Neurophysiol* 46: 1326-1338, 1981.

Folkins JW, Linville RN, Garrett JD and Brown CK. Interactions in the labial musculature during speech. *J Speech Hear Res* 31: 253-264, 1988.

Freilinger G, Happak W, Burggasser G and Gruber H. Histochemical mapping and fiber size analysis of mimic muscles. *Plast Reconstr Surg* 86: 422-428, 1990.

Freriks B, Hermens HJ, Disselhorst-Klug C and Rau G. The recommendations for sensors and sensor placement procedures for surface electromyography. In: *European recommendations for surface electromyography. Results of the SENIAM project*, edited by Hermens HJ. Enschede (NL)· Roessingh Research and Development, 1999, p. 15-25.

Fridlund AJ and Cacioppo JT. Guidelines for human electromyographic research. *Psychophysiology* 23: 567-589, 1986.

Frucht SJ, Fahn S, Greene PE, O'Brien C, Gelb M, Truong DD, Welsh J, Factor S and Ford B. The natural history of embouchure dystonia. *Mov Disord* 16: 899-906, 2001.

Frucht SJ. Embouchure dystonia--Portrait of a task-specific cranial dystonia. *Mov Disord* 24: 1752-1762, 2009.

Fuglevand AJ, Winter DA, Patla AE and Stashuk D. Detection of motor unit action potentials with surface electrodes: influence of electrode size and spacing. *Biol Cybern* 67: 143-153, 1992.

Gandiglio G and Fra L. Electrophysiological study of the facial reflexes in normal subjects. *Electroencephalogr Clin Neurophysiol* 23: 191-192, 1967a.

Gandiglio G and Fra L. Further observations on facial reflexes. *J Neurol Sci* 5: 273-285, 1967b.

Gath I and Stalberg E. On the volume conduction in human skeletal muscle: in situ measurements. *Electroencephalogr Clin Neurophysiol* 43: 106-110, 1977.

Geddes LA. *Electrodes and the measurement of bioelectric events*. New York: Wiley, 1972.

Glendinning DS and Enoka RM. Motor unit behavior in Parkinson's disease. *Phys Ther* 74: 61-70, 1994.

Goffman L and Smith A. Motor unit territories in the human perioral musculature. *J Speech Hear Res* 37: 975-984, 1994.

Goodmurphy CW and Ovalle WK. Morphological study of two human facial muscles· orbicularis oculi and corrugator supercili. *Clin Anat* 12: 1-11, 1999.

Gracies JM, Lugassy M, Weisz DJ, Vecchio M, Flanagan S and Simpson DM. Botulinum toxin dilution and endplate targeting in spasticity: a

double-blind controlled study. *Arch Phys Med Rehabil* 90: 9-16 e12, 2009.

Greene P, Fahn S and Diamond B. Development of resistance to botulinum toxin type A in patients with torticollis. *Mov Disord* 9: 213-217, 1994.

Grimby L and Hannerz J. Firing rate and recruitment order of toe extensor motor units in different modes of voluntary conraction. *J Physiol* 264: 865-879, 1977.

Gronlund C, Ostlund N, Roeleveld K and Karlsson JS. Simultaneous estimation of muscle fibre conduction velocity and muscle fibre orientation using 2D multichannel surface electromyogram. *Med Biol Eng Comput* 43: 63-70, 2005.

Haig AJ, Gelblum JB, Rechtien JJ and Gitter AJ. Technology assessment: the use of surface EMG in the diagnosis and treatment of nerve and muscle disorders. *Muscle Nerve* 19: 392-395, 1996.

Happak W, Burggasser G and Gruber H. Histochemical characteristics of human mimic muscles. *J Neurol Sci* 83: 25-35, 1988.

Happak W, Burggasser G, Liu J, Gruber H and Freilinger G. Anatomy and histology of the mimic muscles and the supplying facial nerve. *Eur Arch Otorhinolaryngol* 7 Suppl 1: 85-86, 1994.

Happak W, Liu J, Burggasser G, Flowers A, Gruber H and Freilinger G. Human facial muscles: dimensions, motor endplate distribution, and presence of muscle fibers with multiple motor endplates. *Anat Rec* 249: 276-284, 1997.

Henneman E. Functional organization of motoneuron pools: the size principle. In: *Integration in the nervous system*, edited by Asanuma H and Wilson VJ. Tokyo: Igaku-Shoin, 1977, p. 13-25.

Henneman E and Mendell LM. Functional organization of motoneuron pool and its inputs. In: *Handbook of physiology*, edited by Brooks VB. Bethesda, Maryland: American Physiological Society, 1981, p. 423-507.

Hilfiker P and Meyer M. Normal and myopathic propagation of surface motor unit action potentials. *Electroencephalogr Clin Neurophysiol* 57: 21-31, 1984.

Hogrel JY, Duchene J and Marini JF. Variability of some SEMG parameter estimates with electrode location. *J Electromyogr Kinesiol* 8: 305-315, 1998.

Holobar A, Farina D, Gazzoni M, Merletti R and Zazula D. Estimating motor unit discharge patterns from high-density surface electromyogram. *Clin Neurophysiol* 120: 551-562, 2009.

Holstege G, Kuypers HG and Dekker JJ. The organization of the bulbar fibre connections to the trigeminal, facial and hypoglossal motor nuclei. II. An autoradiographic tracing study in cat. *Brain* 100: 264-286, 1977.

Holstege G. Descending motor pathways and the spinal motor system: limbic and non-limbic components. *Prog Brain Res* 87: 307-421, 1991.

Holstege G. Emotional innervation of facial musculature. *Mov Disord* 17 Suppl 2: S12-16, 2002.

Hopf HC, Muller-Forell W and Hopf NJ. Localization of emotional and volitional facial paresis. *Neurology* 42: 1918-1923, 1992.

Horn BKP and Schunck BG. Determining Optical Flow. *Artificial Intelligence in Medicine* 17: 185–203, 1981.

Huppertz HJ, Disselhorst-Klug C, Silny J, Rau G and Heimann G. Diagnostic yield of noninvasive high spatial resolution electromyography in neuromuscular diseases. *Muscle Nerve* 20: 1360-1370, 1997.

Hwang K, Kim DJ and Hwang SH. Musculature of the pars marginalis of the upper orbicularis oris muscle. *J Craniofac Surg* 18: 151-154, 2007a.

Hwang K, Kim DJ and Hwang SH. Immunohistochemical study of differences between the muscle fiber types in the pars peripheralis and marginalis. *J Craniofac Surg* 18: 591-593, 2007b.

R

Isley CL and Basmajian JV. Electromyography of the human cheeks and lips. *Anat Rec* 176: 143-147, 1973.

Ito J, Moriyama H and Shimada K. Morphological evaluation of the human facial muscles. *Okajimas Folia Anat Jpn* 83: 7-14, 2006.

Jancke L, Vogt J, Musial F, Lutz K and Kalveram KT. Facial EMG responses to auditory stimuli. *Int J Psychophysiol* 22: 85-96, 1996.

Jankovic J and Schwartz K. Botulinum toxin injections for cervical dystonia. *Neurology* 40: 277-280, 1990.

Janz GJ and Taniguchi H. The silver-silver halide electrodes: Preparation, stability, reproducibility and standard potentials in aqueous and non-aqueous media. *Chemical Review* 53: 397-437, 1953.

Jenny AB and Saper CB. Organization of the facial nucleus and corticofacial projection in the monkey: a reconsideration of the upper motor neuron facial palsy. *Neurology* 37: 930-939, 1987.

Jensen C, Vasseljen O and Westgaard RH. The influence of electrode position on bipolar surface electromyogram recordings of the upper trapezius muscle. *European Journal of Applied Physiology and Occupational Physiology* 67: 266-273, 1993.

Johnson MA, Polgar J, Weightman D and Appleton D. Data on the distribution of fibre types in thirty-six human muscles. An autopsy study. *J Neurol Sci* 18: 111-129, 1973.

Kakuda N, Nagaoka M and Tanaka R. Discrimination of different motor units by spike-triggered averaging of surface electromyograms. *Neurosci Lett* 122: 237-240, 1991.

Kamen G and De Luca CJ. Firing rate interactions among human orbicularis oris motor units. *Int J Neurosci* 64: 167-175, 1992.

Keizer K and Kuypers HG. Distribution of corticospinal neurons with collaterals to the lower brain stem reticular formation in monkey (Macaca fascicularis). *Exp Brain Res* 74: 311-318, 1989.

Kelly EM, Smith A and Goffman L. Orofacial muscle activity of children who stutter: a preliminary study. *J Speech Hear Res* 38: 1025-1036, 1995.

Kennedy JG and Abbs JH. Anatomic studies of the perioral motor system: foundations for studies in speech physiology. In: *Speech and language*, edited by Lass N. New York: Academic Press, 1979.

Kernell D. Organized variability in the neuromuscular system: a survey of task-related adaptations. *Arch Ital Biol* 130: 19-66, 1992.

Kleine BU, Blok JH, Oostenveld R, Praamstra P and Stegeman DF. Magnetic stimulation-induced modulations of motor unit firings extracted from multi-channel surface EMG. *Muscle Nerve* 23. 1005-1015, 2000a.

Kleine BU, Schumann NP, Stegeman DF and Scholle HC. Surface EMG mapping of the human trapezius muscle: the topography of monopolar and bipolar surface EMG amplitude and spectrum parameters at varied forces and in fatigue. *Clin Neurophysiol* 111: 686-693, 2000b

Kleine BU, van Dijk JP, Lapatki BG, Zwarts MJ and Stegeman DF. Using two-dimensional spatial information in decomposition of surface EMG signals. *J Electromyogr Kinesiol* 17: 535-548, 2007.

Koh TJ and Grabiner MD. Evaluation of methods to minimize cross talk in surface electromyography. *J Biomech* 26 Suppl 1: 151-157, 1993.

Kugelberg E. Facial reflexes. *Brain* 75: 385-396, 1952.

Kugelberg E. The motor unit: anatomy and histochemical functional correlations *Riv Patol Nerv Ment* 97: 251-258, 1976.

Kuiken TA, Lowery MM and Stoykov NS. The effect of subcutaneous fat on myoelectric signal amplitude and cross-talk. *Prosthet Orthot Int* 27: 48-54, 2003.

Kumagai K and Yamada M. The clinical use of multichannel surface electromyography. *Acta Paediatr Jpn* 33: 228-237, 1991.

Kuypers HG. Corticobular connexions to the pons and lower brain-stem in man: an anatomical study. *Brain* 81: 364-388, 1958.

Lansing RW, Solomon NP, Kossev AR and Andersen AB. Recording single motor unit activity of human nasal muscles with surface electrodes: applications for respiration and speech. *Electroencephalogr Clin Neurophysiol* 81: 167-175, 1991.

Lapatki BG, Mager AS, Schulte-Moenting J and Jonas IE. The importance of the level of the lip line and resting lip pressure in Class II, Division 2 malocclusion. *J Dent Res* 81: 323-328, 2002.

Lapatki BG, Stegeman DF and Jonas IE. A surface EMG electrode for the simultaneous observation of multiple facial muscles. *J Neurosci Methods* 123: 117-128, 2003.

Lapatki BG, Van Dijk JP, Jonas IE, Zwarts MJ and Stegeman DF. A thin, flexible multielectrode grid for high-density surface EMG. *J Appl Physiol* 96: 327-336, 2004.

Lapatki BG, Oostenveld R, Van Dijk JP, Jonas IE, Zwarts MJ and Stegeman DF. Topographical characteristics of motor units of the lower facial musculature revealed by means of high-density surface EMG. *J Neurophysiol* 95: 342-354, 2006.

Lapatki BG, Oostenveld R, Van Dijk JP, Jonas IE, Zwarts MJ and Stegeman DF. Optimal placement of bipolar surface EMG electrodes in the face based on single motor unit analysis. *Psychophysiol* 47: 299-314, 2010.

Lateva ZC and McGill KC. Estimating motor-unit architectural properties by analyzing motor-unit action potential morphology. *Clin Neurophysiol* 112: 127-135, 2001.

Lateva ZC, McGill KC and Johanson ME. Electrophysiological evidence of adult human skeletal muscle fibres with multiple endplates and polyneuronal innervation. *J Physiol* 544: 549-565, 2002.

Lateva ZC, McGill KC and Johanson ME. Increased jitter and blocking in normal muscles due to doubly innervated muscle fibers. *Muscle Nerve* 28: 423-431, 2003.

Lawson VH, Bromberg MB and Stashuk D. Comparison of conventional and decomposition-enhanced spike triggered averaging techniques. *Clin Neurophysiol* 115: 564-568, 2004.

Leanderson R, Persson A and Ohman S. Electromyographic studies of facial muscle activity in speech. *Acta Otolaryngol* 72: 361-369, 1971.

Loeb G and Gans C. Electromyography for experimentalists. Chicago: The University of Chicago Press, 1986.

Lowery MM, Stoykov NS, Taflove A and Kuiken TA. A multiple-layer finite-element model of the surface EMG signal. *IEEE Transactions on Biomedical Engineering* 49: 446-454, 2002.

Lowery MM, Stoykov NS and Kuiken TA. A simulation study to examine the use of cross-correlation as an estimate of surface EMG cross talk. *J Appl Physiol* 94: 1324-1334, 2003.

Ludlow CL, Naunton RF, Sedory SE, Schulz GM and Hallett M. Effects of botulinum toxin injections on speech in adductor spasmodic dysphonia. *Neurology* 38: 1220-1225, 1988.

Lundqvist LO. Facial EMG reactions to facial expressions: a case of facial emotional contagion? *Scand J Psychol* 36: 130-141, 1995.

Macefield VG, Gandevia SC, Bigland-Ritchie B, Gorman RB and Burke D. The firing rates of human motoneurones voluntarily activated in the absence of muscle afferent feedback. *J Physiol* 471: 429-443, 1993.

Masuda T, Miyano H and Sadoyama T. The propagation of motor unit action potential and the location of neuromuscular junction investigated

R

by surface electrode arrays. *Electroencephalogr Clin Neurophysiol* 55: 594-600, 1983.

Masuda T, Miyano H and Sadoyama T. A surface electrode array for detecting action potential trains of single motor units. *Electroencephalogr Clin Neurophysiol* 60: 435-443, 1985.

Masuda T and Sadoyama T. The propagation of single motor unit action potentials detected by a surface electrode array. *Electroencephalogr Clin Neurophysiol* 63: 590-598, 1986.

Masuda T and Sadoyama T. Skeletal muscles from which the propagation of motor unit action potentials is detectable with a surface electrode array. *Electroencephalogr Clin Neurophysiol* 67: 421-427, 1987.

Masuda T and Sadoyama T. Topographical map of innervation zones within single motor units measured with a grid surface electrode. *IEEE Trans Biomed Eng* 35: 623-628, 1988.

Mateika JH, Essif EG, Dellorusso C and Fregosi RF. Contractile properties of human nasal dilator motor units. *J Neurophysiol* 79: 371-378, 1998.

May M and Barnes L. Pathologic considerations in facial nerve disorders: clinicopathologic correlations. In: *The facial nerve*, edited by Schaitkin BM. New York: Thieme, 2000.

May T and Schaitkin BM. *The facial nerve*. New York - Stuttgart: Thieme, 2000.

McClean MD and Smith A. The reflex responses of single motor units in human lower lip muscles to mechanical stimulation. *Brain Res* 251: 65-75, 1982.

McClean MD. Lip muscle EMG responses to oral pressure stimulation. *J Speech Hear Res* 34: 248-251, 1991.

McComas AJ and Thomas HC. Fast and slow twitch muscles in man. *J Neurol Sci* 7: 301-307, 1968.

McComas AJ, Fawcett PR, Campbell MJ and Sica RE. Electrophysiological estimation of the number of motor units within a human muscle. *J Neurol Neurosurg Psychiatry* 34: 121-131, 1971.

McComas AJ. Oro-facial muscles: internal structure, function and ageing. *Gerodontology* 15: 3-14, 1998.

Merletti R, Lo Conte L, Avignone E and Guglielminotti P. Modeling of surface myoelectric signals--Part I: Model implementation. *IEEE Trans Biomed Eng* 46: 810-820, 1999.

Mesin L. Simulation of surface EMG signals for a multi-layer volume conductor with a superficial bone or blood vessel. *IEEE Transactions on Biomedical Engineering* 55: 1647-1657, 2008.

Mesin L, Merletti R and Rainoldi A. Surface EMG: the issue of electrode location. *J Electromyogr Kinesiol* 19: 719-726, 2009a.

Mesin L, Smith S, Hugo S, Viljoen S and Hanekom T. Effect of spatial filtering on crosstalk reduction in surface EMG recordings. *Medical Engineering and Physics* 31: 374-383, 2009b.

Metting van Rijn AC, Peper A and Grimbergen CA. High-quality recording of bioelectric events. Part 1. Interference reduction, theory and practice. *Med Biol Eng Comput* 28: 389-397, 1990.

Metting van Rijn AC, Peper A and Grimbergen CA. High-quality recording of bioelectric events. Part 2. Low-noise, low-power multichannel amplifier design. *Med Biol Eng Comput* 29: 433-440, 1991.

Mogk JP and Keir PJ. Crosstalk in surface electromyography of the proximal forearm during gripping tasks. *J Electromyogr Kinesiol* 13: 63-71, 2003.

Monti RJ, Roy RR and Edgerton VR. Role of motor unit structure in defining function. *Muscle Nerve* 24: 848-866, 2001.

Morecraft RJ and Van Hoesen GW. Convergence of limbic input to the cingulate motor cortex in the rhesus monkey. *Brain Res Bull* 45: 209-232, 1998.

Morecraft RJ, Louie JL, Herrick JL and Stilwell-Morecraft KS. Cortical innervation of the facial nucleus in the non-human primate: a new interpretation of the effects of stroke and related subtotal brain trauma on the muscles of facial expression. *Brain* 124: 176-208, 2001.

Morecraft RJ, Stilwell-Morecraft KS and Rossing WR. The motor cortex and facial expression: new insights from neuroscience. *Neurologist* 10: 235-249, 2004.

Morecraft RJ, McNeal DW, Stilwell-Morecraft KS, Gedney M, Ge J, Schroeder CM and van Hoesen GW. Amygdala interconnections with the cingulate motor cortex in the rhesus monkey. *J Comp Neurol* 500: 134-165, 2007.

Morrenhof JW and Abbink HJ. Cross-correlation and cross-talk in surface electromyography. *Electromyogr Clin Neurophysiol* 25: 73-79, 1985.

Moss ML. The functional matrix hypothesis revisited. 1. The role of mechanotransduction. *Am J Orthod Dentofacial Orthop* 112: 8-11, 1997.

Nairn RI. The circumoral musculature: structure and function. *British Dental Journal* 138: 49-56, 1975.

Naumann M, So Y, Argoff CE, Childers MK, Dykstra DD, Gronseth GS, Jabbari B, Kaufmann HC, Schurch B, Silberstein SD and Simpson DM. Assessment: Botulinum neurotoxin in the treatment of autonomic disorders and pain (an evidence-based review): report of the Therapeutics and Technology Assessment Subcommittee of the American Academy of Neurology. *Neurology* 70: 1707-1714, 2008.

Nemeth PM, Solanki L, Gordon DA, Hamm TM, Reinking RM and Stuart DG. Uniformity of metabolic enzymes within individual motor units. *J Neurosci* 6: 892-898, 1986.

O'Dwyer NJ, Quinn PT, Guitar BE, Andrews G and Neilson PD. Procedures for verification of electrode placement in EMG studies of orofacial and mandibular muscles. *J Speech Hear Res* 24: 273-288, 1981.

Ohyama M, Obata E, Furuta KS, Sakamoto K, Ohbori Y and Iwabuchi Y. Face EMG topographic analysis of mimetic movements in patients with Bell's Palsy. *Acta Otolaryngol, Suppl.*: 47-56, 1988.

Ounjian M, Roy RR, Eldred E, Garfinkel A, Payne JR, Armstrong A, Toga AW and Edgerton VR. Physiological and developmental implications of motor unit anatomy. *J Neurobiol* 22: 547-559, 1991.

Perie S, St Guily JL, Callard P and Sebille A. Innervation of adult human laryngeal muscle fibers. *J Neurol Sci* 149: 81-86, 1997.

Petajan JH. Motor unit frequency control in man. In: *Motor unit types, recruitment and plasticity in health and disease*, edited by Desmedt JE. Basel: Karger, 1981, p. 184-200.

Phanachet I, Whittle T, Wanigaratne K and Murray GM. Functional properties of single motor units in inferior head of human lateral pterygoid muscle: task relations and thresholds. *J Neurophysiol* 86: 2204-2218, 2001.

Phanachet I, Whittle T, Wanigaratne K and Murray GM. Minimal tonic firing rates of human lateral pterygoid single motor units. *Clin Neurophysiol* 115: 71-75, 2004.

Prutchi D. A high-resolution large array (HRLA) surface EMG system. *Med Eng Phys* 17: 442-454, 1995.

Pullman SL, Goodin DS, Marquinez AI, Tabbal S and Rubin M. Clinical utility of surface EMG: report of the therapeutics and technology assessment subcommittee of the American Academy of Neurology. *Neurology* 55: 171-177, 2000.

Rau G and Disselhorst-Klug C. Principles of high-spatial-resolution surface EMG (HSR-EMG):

R

single motor unit detection and application in the diagnosis of neuromuscular disorders. *J Electromyogr Kinesiol* 7: 233-239, 1997.

Rau G, Schulte E and Disselhorst-Klug C. From cell to movement: to what answers does EMG really contribute? *Journal of Electromyography and Kinesiology* 14: 611-617, 2004.

Reucher H, Rau G and Silny J. Spatial filtering of noninvasive multielectrode EMG: Part I--Introduction to measuring technique and applications. *IEEE Trans Biomed Eng* 34: 98-105, 1987.

Roeleveld K, Blok JH, Stegeman DF and van Oosterom A. Volume conduction models for surface EMG; confrontation with measurements. *J Electromyogr Kinesiol* 7: 221-232, 1997a.

Roeleveld K, Stegeman DF, Falck B and Stalberg EV. Motor unit size estimation: confrontation of surface EMG with macro EMG. *Electroencephalogr Clin Neurophysiol* 105: 181-188, 1997b.

Roeleveld K, Stegeman DF, Vingerhoets HM and Van Oosterom A. Motor unit potential contribution to surface electromyography. *Acta Physiol Scand* 160: 175-183, 1997c.

Roeleveld K, Stegeman DF, Vingerhoets HM and Van Oosterom A. The motor unit potential distribution over the skin surface and its use in estimating the motor unit location. *Acta Physiol Scand* 161: 465-472, 1997d.

Roeleveld K, Sandberg A, Stalberg EV and Stegeman DF. Motor unit size estimation of enlarged motor units with surface electromyography. *Muscle Nerve* 21: 878-886, 1998.

Rohen JW, Yokochi C and Lütjen-Drecoll E. *Anatomie des Menschen - Fotografischer Atlas*. Stuttgart: Schattauer, 2006.

Root AA and Stephens JA. Organization of the central control of muscles of facial expression in man. *J Physiol* 549: 289-298, 2003.

Rossi G. From the pattern of human vocal muscle fibre innervation to functional remarks. *Acta Otolaryngol* 473 Suppl: 1-10, 1990.

Roy SH, De Luca CJ and Schneider J. Effects of electrode location on myoelectric conduction velocity and median frequency estimates. *J Appl Physiol* 61: 1510-1517, 1986.

Ruark JL and Moore CA. Coordination of lip muscle activity by 2-year-old children during speech and nonspeech tasks. *J Speech Lang Hear Res* 40: 1373-1385, 1997.

Rushworth G. Observations on blink reflexes. *J Neurol Neurosurg Psychiatry* 25: 93-108, 1962.

Salmons S. Muscle. In: *Gray`s Anatomy. The anatomical basis of medicine and surgery* (38 ed.), edited by Williams PL. New York: Churchill Livingstone, 1995.

Sampaio C, Costa J and Ferreira JJ. Clinical comparability of marketed formulations of botulinum toxin. *Mov Disord* 19 Suppl 8: 129-136, 2004.

Sato S. Statistical studies on the anomalous muscles of the Kyushu Japanese. 3. The muscles of the back, breast and abdomen. *Kurume Med J* 15: 209-220, 1968.

Satoda T, Takahashi O, Tashiro T, Matsushima R, Uemura-Sumi M and Mizuno N. Representation of the main branches of the facial nerve within the facial nucleus of the Japanese monkey (Macaca fuscata). *Neurosci Lett* 78: 283-287, 1987.

Schad A, Oostenveld R, van Dijk JP, Zwarts MJ, Stegeman DF, Timmer J and Lapatki BG. Model based estimation of motor unit properties. *XVIIth Congress of the International Society of Electrophysiology and Kinesiology*, Niagara Falls, Ontario, Canada, 2008.

Schindler HJ, Turp JC, Blaser R and Lenz J. Differential activity patterns in the masseter muscle under simulated clenching and grinding forces. *J Oral Rehabil* 32: 552-563, 2005.

Scholle HC, Schumann NP, Biedermann F, Stegeman DF, Grassme R, Roeleveld K, Schilling N and Fischer MS. Spatiotemporal surface EMG characteristics from rat triceps brachii muscle during treadmill locomotion indicate selective recruitment of functionally distinct muscle regions. *Exp Brain Res* 138: 26-36, 2001.

Schumann NP, Scholle HC, Anders C and Mey E. A topographical analysis of spectral electromyographic data of the human masseter muscle under different functional conditions in healthy subjects. *Arch Oral Biol* 39: 369-377, 1994.

Shaari CM and Sanders I. Quantifying how location and dose of botulinum toxin injections affect muscle paralysis. *Muscle Nerve* 16: 964-969, 1993.

Shefner JM. Motor unit number estimation in human neurological diseases and animal models. *Clin Neurophysiol* 112: 955-964, 2001.

Simpson DM, Blitzer A, Brashear A, Comella C, Dubinsky R, Hallett M, Jankovic J, Karp B, Ludlow CL, Miyasaki JM, Naumann M and So Y. Assessment: Botulinum neurotoxin for the treatment of movement disorders (an evidence-based review): report of the Therapeutics and Technology Assessment Subcommittee of the American Academy of Neurology. *Neurology* 70: 1699-1706, 2008a.

Simpson DM, Gracies JM, Graham HK, Miyasaki JM, Naumann M, Russman B, Simpson LL and So Y. Assessment: Botulinum neurotoxin for the treatment of spasticity (an evidence-based review): report of the Therapeutics and Technology Assessment Subcommittee of the American Academy of Neurology. *Neurology* 70: 1691-1698, 2008b.

Sloan DM, Bradley MM, Dimoulas E and Lang PJ. Looking at facial expressions: dysphoria and facial EMG. *Biol Psychol* 60: 79-90, 2002.

Sloop RR, Escutin RO, Matus JA, Cole BA and Peterson GW. Dose-response curve of human extensor digitorum brevis muscle function to intramuscularly injected botulinum toxin type A. *Neurology* 46: 1382-1386, 1996.

Smith A, Zimmermann GN and Abbas PJ. Recruitment patterns of motor units in speech production. *J Speech Hear Res* 24: 567-576, 1981.

Snobl D, Binaghi LE and Zenker W. Microarchitecture and innervation of the human latissimus dorsi muscle. *J Reconstr Microsurg* 14: 171-177, 1998.

Sobotta J. *Atlas der Anatomie des Menschen*. München: Urban & Schwarzenberg, 2000.

Solomonow M, Baratta R, Bernardi M, Zhou B, Lu Y, Zhu M and Acierno S. Surface and wire EMG crosstalk in neighbouring muscles. *Journal of Electromyography and Kinesiology* 4: 131:142, 1994.

Stal P, Eriksson PO, Eriksson A and Thornell LE. Enzyme-histochemical differences in fibre-type between the human major and minor zygomatic and the first dorsal interosseus muscles. *Arch Oral Biol* 32: 833-841, 1987.

Stal P, Eriksson PO, Eriksson A and Thornell LE. Enzyme-histochemical and morphological characteristics of muscle fibre types in the human buccinator and orbicularis oris. *Arch Oral Biol* 35: 449-458, 1990.

Stal P, Eriksson PO, Schiaffino S, Butler-Browne GS and Thornell LE. Differences in myosin composition between human oro-facial, masticatory and limb muscles: enzyme-, immunohisto- and biochemical studies. *J Muscle Res Cell Motil* 15: 517-534, 1994.

Staudenmann D, Kingma I, Daffertshofer A, Stegeman DF and van Dieen JH. Heterogeneity of muscle activation in relation to force direction: a multi-channel surface electromyography study on the triceps surae muscle. *J Electromyogr Kinesiol* 19: 882-895, 2009.

Stegeman DF, Roeleveld K and Blok JH. EMG topography as an instrument in clinical neurophysiology: a unipolar recording approach. In: *Proceedings*

R

First General Workshop European concerted action (SENIAM, BIOMED II), edited by Hermens HJ, Merletti R and Freriks B. Enschede: Roessingh, 1996, p. 73-76.

Stegeman DF, Dumitru D, King JC and Roeleveld K. Near- and far-fields: source characteristics and the conducting medium in neurophysiology. *J Clin Neurophysiol* 14: 429-442, 1997.

Stegeman DF, Houtman CJ, Lapatki BG and Zwarts MJ. Multichannel surface EMG. In: *Handbook of Clinical Neurophysiology*, edited by Stalberg E. Amsterdam: Elsevier, 2004, p. 245-268.

Stuart DG and Enoka RM. Motoneurons, motor units, and the Size Principle. In: *The clinical neurosciences*, edited by Rosenberg RN and Willis WD. New York: Churchill Livingstone, 1983, p. 471-517.

Tassinary LG, Cacioppo JT and Geen TR. A psychometric study of surface electrode placements for facial electromyographic recording: I. The brow and cheek muscle regions. *Psychophysiology* 26: 1-16, 1989.

Tassinary LG, Geen TR, Cacioppo JT and Edelberg R. Issues in biometrics: offset potentials and the electrical stability of Ag/AgCl electrodes. *Psychophysiology* 27: 236-242, 1990.

Theeuwen M, Gielen CC, Miller LE and Doorenbosch C. The relation between the direction dependence of electromyographic amplitude and motor unit recruitment thresholds during isometric contractions. *Exp Brain Res* 98: 488-500, 1994.

Tosello DO, Vitti M and Berzin F. EMG activity of the orbicularis oris and mentalis muscles in children with malocclusion, incompetent lips and atypical swallowing--part I. *J Oral Rehabil* 25: 838-846, 1998.

Tosello DO, Vitti M and Berzin F. EMG activity of the orbicularis oris and mentalis muscles in children with malocclusion, incompetent lips and atyp-
ical swallowing--part II. *J Oral Rehabil* 26: 644-649, 1999.

Trotter JA. Functional morphology of force transmission in skeletal muscle. A brief review. *Acta Anat (Basel)* 146: 205-222, 1993.

Trotter JA, Richmond FJ and Purslow PP. Functional morphology and motor control of series-fibered muscles. *Exerc Sport Sci Rev* 23: 167-213, 1995.

Truong DD and Jost WH. Botulinum toxin: clinical use. *Parkinsonism Relat Disord* 12: 331-355, 2006.

Urban PP, Wicht S, Marx J, Mitrovic S, Fitzek C and Hopf HC. Isolated voluntary facial paresis due to pontine ischemia. *Neurology* 50: 1859-1862, 1998.

Valls-Sole J, Tolosa ES and Pujol M. Myokymic discharges and enhanced facial nerve reflex responses after recovery from idiopathic facial palsy. *Muscle Nerve* 15: 37-42, 1992.

van Boxtel A, Goudswaard P, van der Molen GM and van den Bosch WE. Changes in electromyogram power spectra of facial and jaw-elevator muscles during fatigue. *J Appl Physiol* 54: 51-58, 1983.

van Boxtel A and Jessurun M. Amplitude and bilateral coherency of facial and jaw-elevator EMG activity as an index of effort during a two-choice serial reaction task. *Psychophysiology* 30: 589-604, 1993.

van Boxtel A. Optimal signal bandwidth for the recording of surface EMG activity of facial, jaw, oral, and neck muscles. *Psychophysiology* 38: 22-34, 2001.

van Dijk JP, Blok JH, Lapatki BG, van Schaik IN, Zwarts MJ and Stegeman DF. Motor unit number estimation using high-density surface electromyography. *Clin Neurophysiol* 119: 33-42, 2008.

van Dijk JP, Lowery MM, Lapatki BG and Stegeman DF. Evidence of Potential Averaging over the Finite Surface of a Bioelectric Surface Electrode. *Ann Biomed Eng* 37: 1141-1151, 2009.

van Dijk JP, Schelhaas HJ, van Schaik IN, Janssen HMHA, Stegeman DF and Zwarts MJ. Monitoring disease progression using high-density motor unit number estimation in ALS. *Muscle and Nerve*, 2010 (in press).

van Vugt JP and van Dijk JG. A convenient method to reduce crosstalk in surface EMG. *Clin Neurophysiol* 112: 583-592, 2001.

Videler AJ, van Dijk JP, Beelen A, de Visser M, Nollet F and van Schaik IN. Motor axon loss is associated with hand dysfunction in Charcot-Marie-Tooth disease 1a. *Neurology* 71: 1254-1260, 2008.

Warfel J. *The extremeties - muscles and motor points*. Philadelphia: Lea & Febiger, 1985.

Welt C and Abbs JH. Musculotopic organization of the facial motor nucleus in Macaca fascicularis: a morphometric and retrograde tracing study with cholera toxin B-HRP. *J Comp Neurol* 291: 621-636, 1990.

Widmer CG, English AW and Morris-Wiman J. Developmental and functional considerations of masseter muscle partitioning. *Arch Oral Biol* 52: 305-308, 2007.

Wigley C. Cells, tissues and systems. In: *Gray's anatomy*, edited by Standring S. Oxford: Churchill Livingstone Elsevier, 2008, p. 112.

Williamson DA, Epstein LH and Lombardo TW. Methodology: EMG measurement as a function of electrode placement and level of EMG. *Psychophysiology* 17: 279-282, 1980.

Winter DA, Fuglevand AJ and Archer SE. Crosstalk in surface electromyography: theoretical and practical estimates. *Journal of Electromyography and Kinesiology* 4: 15-26, 1994.

Wohlert AB and Goffman L. Human perioral muscle activation patterns. *Journal of Speech and Hearing Research* 37: 1032-1040, 1994.

Wohlert AB. Perioral muscle activity in young and older adults during speech and nonspeech tasks. *Journal of Speech and Hearing Research* 39: 761-770, 1996a.

Wohlert AB. Reflex responses of lip muscles in young and older women. *Journal of Speech and Hearing Research* 39: 578-589, 1996b.

Wohlert AB and Hammen VL. Lip muscle activity related to speech rate and loudness. *J Speech Lang Hear Res* 43: 1229-1239, 2000.

Wood SM, Jarratt JA, Barker AT and Brown BH. Surface electromyography using electrode arrays: a study of motor neuron disease. *Muscle Nerve* 24: 223-230, 2001.

Yamada M, Kumagai K and Uchiyama A. The distribution and propagation pattern of motor unit action potentials studied by multi-channel surface EMG. *Electroencephalogr Clin Neurophysiol* 67: 395-401, 1987.

Yamaguchi K, Morimoto Y, Nanda RS, Ghosh J and Tanne K. Morphological differences in individuals with lip competence and incompetence based on electromyographic diagnosis. *J Oral Rehabil* 27: 893-901, 2000.

Yayla V and Oge AE. Motor unit number estimation in facial paralysis. *Muscle Nerve* 38: 1420-1428, 2008.

Zazula D and Holobar A. An approach to surface EMG decomposition based on higher-order cumulants. *Comput Methods Programs Biomed* 80 Suppl 1: 51-60, 2005.

Zwarts MJ, van Weerden TW, Links TP, Haenen HT and Oosterhuis HJ. The muscle fiber conduction velocity and power spectra in familial hypokalemic periodic paralysis. *Muscle Nerve* 11: 166-173, 1988.

R

Zwarts MJ and van Dijk JP Methods to determine muscle fiber conduction velocity In *State of the art on modelling methods for surface electromyography, European concerted action (BIOMED II, SENIAM)*, edited by Hermens HJ SD, Blok JH, Freriks B Enschede Roessingh, 1998, p 85-89

Zwarts MJ, Drost G and Stegeman DF Recent progress in the diagnostic use of surface EMG for neurological diseases *J Electromyogr Kinesiol* 10 287-291, 2000

Zwarts MJ and Stegeman DF Multichannel surface EMG basic aspects and clinical utility *Muscle Nerve* 28 1-17, 2003

ABBREVIATIONS

General Terms

EMG	electromyography, electromyographic
sEMG	surface electromyography
3D	three-dimensional
IED	inter-electrode-distance
Ag/AgCl	silver / silverchloride
SI	selectivity-index
CTR	cross-talk ratio
RMS	root-Mean-Square (value)
CMRR	common mode rejection ratio
CMS	common mode signal
DRL	driven right leg (electrode)
RTI	referred to input
MU	motor unit
MUAP	motor unit action potential
MUNE	motor unit number estimation
CMAP	compound muscle action potential
MVC	maximal voluntary contraction
BoNT	botulinum neurotoxin
BoNT-A	botulinum neurotoxin type A
FSHD	facioscapulohumeral dystrophy
ALS	amyotrophic lateral sclerosis

Muscles

CSC	corrugator supercili
LPS	levator palpebrae superioris
OOC	orbicularis oculi
OOC orb	orbicularis oculi pars orbitalis
OOC pal	orbicularis oculi pars palpebralis
OOC lac	orbicularis oculi pars lacrimalis
LLS	levator labii superioris
LLS an	levator labii superioris alaeque nasi
ZYG min	zygomaticus minor
LAO	levator anguli oris
ZYG maj	zygomaticus major
BUC	buccinator
DAO	depressor anguli oris
INC	incisivus (labii superioris et inferioris)
OOR	orbicularis oris (superior et inferior)
OOS	orbicularis oris superior
OOI	orbicularis oris inferior
OOR per	orbicularis oris pars peripheralis

Ab

OOR mar	orbicularis oris pars marginalis
OOR tan	orbicularis oris pars tangentialis
DLI	depressor labii inferioris
DLI med	depressor labii inferioris pars medialis
DLI lat	depressor labii inferioris pars lateralis
MEN	mentalis
DAO	depressor anguli oris
DAO sup	depressor anguli oris pars superior
DAO inf	depressor anguli oris pars inferior
EDB	extensor digitorum brevis

Acknowledgements

Ac

sailing boat and on the cross-country ski run.

Hans van Dijk, I will never forget your remark when we tensely followed the first signals recorded with the flexible electrode grid: "Yes, it looks like EMG". Not only your technical support and scientific contributions to my work were very important. I am delighted and grateful for how our friendship throve and prospered, and very glad that I can continue to work together with a person which has become one of my best friends. Your and Hanneke's unbelievable "gastvriendschap" caused a feeling of coming home, when I crossed the railway bridge over the Waal. Hanneke, thanks for your heartiness, the advices you gave me while I was lying on your "red coach", the necessary interruptions of the boring and never-ending scientific discussions between Hans and me, the excellent food and room service, etc.. Yara, you are the sweetest alarm clock I ever had. I will never forget your morning whisper "Bernd wakker worden, het is opstaan tijd, Papa is al klaar".

Scientific studies in humans are only possible if there are subjects who participate. Tonnie Kievits, your support in recruiting most of them from your trumpet class at the Music Conservatorium Arnhem and your professional colleagues, as well as your own readiness for being one of them, was really great! Besides that, your free tickets for concert events allowed me to benefit from facial muscle activities also in cultural respects, and reminded me that there is more than Matlab and science. I like to thank all the participants in the measurements for their patience in the training sessions and in the two to four recording sessions taking three to four hours each. A special thanks to my "cover-boy" Bob. Mark Massa, Hans Tuinenga, Jan Menssen, Gerhard Mühl, Thomas Bilger, Thomas Günter and Sascha Schmidt I like to thank for their technical contributions to my work, and Gabriele Wachter and Hans van Dijk for their great help in the layout of this thesis.

Bert Kleine, I am conscious of having benefited a lot from your pre-work (the decomposition algorithms), and from your excellent performance as the first German research fellow in the department. In this manner, you also opened the door for the next candidate (me). Paul Blijham, thanks for our discussions about "god and the world". We supported each other when being in similar situations … now we both finished our PhDs and are settled down – are we getting old? Mark-Rudi Massa, now with so many Dutch players in the Bundesliga we would have many topics for our football-talks. Gea Drost, thanks for your offer to live in your house and use the car during your vacations. As relaxing as it usually was when we were drinking a glass of wine, I have to admit to have had some stress that time in your house, since both your cat (probably poisoned) and Volvo (for sure: lack of oil) almost died. Nevertheless, your offer was great! Mireille van Beekvelt, you helped me with personal training and common lessons in the "Nijmegse Loopschool" to defeat the seven highest hills of the Netherlands. Also the way in which you, Erwin and Mila integrated me in your social activities and shared your friends was really nice. Also the other PhD students (e.g. Maartje, Gijs, Mireille, Rebecca, Sigrid, Edwin, Monique, …) and department members (May, Wilma, Henny, Yvonne, Sebastiaan, Nens, Jaco, …) I like to thank for the warm social atmosphere, especially during the "dagjes uit", "borrels" and refreshing midday walks.

Ac

LIST OF PUBLICATIONS

Papers in international peer-review journals as first author

1. Lapatki B.G., Oostenveld R., van Dijk J.P., Jonas I.E., Zwarts M.J., Stegeman D.F.: Optimal placement of bipolar surface EMG electrodes in the face based on single motor unit analysis. Psychophysiol 47, 299-314, 2010. Impact factor: 3,349

2. Lapatki, B.G., Paul, O.: Intelligente Brackets für 3D-Kraft-/Drehmomentmessungen in der kieferorthopädischen Grundlagenforschung und Therapie – derzeitiger Entwicklungsstand und Zukunftsperspektiven. J Orofac Orthop 68, 377-396, 2007.

3. Lapatki, B.G., Klatt A., Schulte-Mönting J., Jonas I.E.: Dentofacial parameters explaining variability in retroclination of the maxillary central incisors. J Orofac Orthop 68, 109-123, 2007.

4. Lapatki B.G., Bartholomeyczik J., Ruther P., Jonas I.E., Paul O.: Smart bracket for multi-dimensional force and moment measurement. J Dent Res 86, 73-78, 2007. Impact factor: 3,192

5. Lapatki B.G., Baustert D., Schulte-Mönting J, Frucht S., Jonas I.E.: Lip-to-incisor relationship and postorthodontic long-term stability of cover-bite treatment. Angle Orthod 76, 942-949, 2006. Impact factor: 0,778

6. Lapatki B.G., Oostenveld R., van Dijk J.P., Jonas I.E., Zwarts M.J., Stegeman D.F.: Topographical characteristics of motor units of the lower facial musculature revealed by means of high-density surface EMG. J Neurophysiol 95, 342-354, 2006. (Additionally, cover page of J Neurophysiol 94, 2006). Impact factor: 3,853

7. Lapatki B.G., Klatt A., Schulte-Mönting J., Stein S., Jonas I.E.: A retrospective cephalometric study for the quantitative assessment of relapse factors in cover-bite treatment. J Orofac Orthop 65, 475-488, 2004.

8. Lapatki B.G., Van Dijk J.P., Jonas I.E., Zwarts M.J., Stegeman D.F.: A thin, flexible multielectrode grid for high-density surface EMG. J Appl Physiol 96, 327-336, 2004. Impact factor: 3,037

9. Lapatki B.G., Stegeman D.F, Jonas I.E.: A surface EMG electrode for the simultaneous observation of multiple facial muscles. J Neurosci Meth 123, 117-128, 2003. Impact factor: 1,784

P

10. Lapatki B.G., Mager A.S., Schulte-Mönting J., Jonas I.E.: The importance of the level of the lip line and resting lip pressure in Class II, Division 2 malocclusion. J Dent Res 81, 323-328, 2002. Impact factor: 3,192

Papers in international peer-review journals as co-author

11. Van Dijk J.P., Lowery M.M., Lapatki B.G., Stegeman D.F.: Evidence of potential averaging over the finite surface of a bioelectric surface electrode. Ann Biomed Eng 37, 1141-1151, 2009. Impact factor: 2,35

12. Van Dijk J.P., Blok J.H., Lapatki B.G., van Schaik I.N., Zwarts M.J., Stegeman D.: Motor unit number estimation using high-density surface electromyography. Clin Neurophysiol 119, 33-42, 2008. Impact factor: 2,72

13. Kleine B.U., van Dijk J.P., Lapatki B.G., Zwarts M.J., Stegeman D.: Using two-dimensional spatial information in decomposition of surface EMG signals. J Electromyogr Kinesiol 17, 535-548, 2007. Impact factor: 2,181

Reviews

14. Lapatki B.G.: Dentale und neuromuskuläre Probleme bei Bläsern – Grundlagen und Therapie. Med Welt 57, 588-595, 2006. Zeitschrift im "Journal Citation Reports" nicht gelistet

15. Zwarts M.J., Lapatki B.G., Kleine B.U., Stegeman D.F.: Surface EMG: how far can you go? Suppl Clin Neurophysiol 57, 111-119, 2004. Impact factor: 2,640

Conference papers

16. Ruther P., Lapatki B.G., Trautmann A., Paul O. Micro needle based electrode arrays for surface electromyography. Proceedings Mikrosystemtechnik Kongress 2007 (Dresden), 2007.

17. Gieschke P., Lapatki B.G., Bartholomeyczik J., Paul O.: First 1:1 scale smart orthodontic bracket. Proceedings Smart Systems Integration 2007 (Paris, France, 27 – 28 Mar. 2007), pp. 207-214, 2007.

18. Lapatki B.G., Jonas I.E.: The great importance of resting lip-pressure and lip-line level for the position and post-orthodontic stability of the maxillary central incisors. In: Davidovitch Z., Mah J., Suthanarak S. (Eds.). Biological Mechanisms of Tooth Eruption, Resorption, and Movement. Vol. 8, pp. 313-321, O.S. Printing House Co. Ltd., Bangkok, 2006.

19. Bartholomeyczik J., Haefner J., Lapatki B.G., Ruther P., Schelb T., Paul O.: Integrated six-degree-of-freedom sensing for orthodontic smart brackets. Technical Digest IEEE MEMS Conference (Istanbul, Turkey, 22 - 26 Jan. 2006), pp. 690-693, 2006.

20. Bartholomeyczik J., Haefner J., Joos J., Schubert F., Lapatki B.G., Ruther P., Paul O.: Novel concept for the multidimensional measurement of forces and torques in orthodontic smart brackets. Technical Digest IEEE Sensors Conference (Irvine, USA, 31 Okt. - 3 Nov. 2005), pp. 1010-1013, 2006.

21. Bartholomeyczik J., Haefner J., Joos J., Lapatki B.G., Schubert F., Ruther P., Paul O.: Packaged multidimensional stress sensing – towards the smart orthodontic bracket. Proceedings Mikrosystemtechnik Kongress 2005 (Freiburg, 10 - 12 Oct. 2005), pp. 423-426, 2005.

22. Schmitt S, Lapatki B.G.: Gemessene Mimik – Silbersensoren auf der Haut entschlüsseln elektrische Signale der Gesichtsmuskeln. Zeitwissen 2/05 (Wissenschaftliches Magazin der Wochenzeitung „Die Zeit"). Sektion Gesundheit / Medizintechnik. Hamburg: Zeitverlag Gerd Bucerius; p. 65, 2005.

23. Lapatki B.G., Stegeman D.F., Zwarts M.J.: Selective contractions of individual facial muscle subcomponents monitored and trained with high-density surface EMG. In: Beurskens C.H.G, van Gelder R.S., Heymans P.G., Manni J.J., Nicolai J.A. (Eds.). The Facial Palsies. Complementary Approaches, pp. 89-108. Lemma, Utrecht, 2005.

24. Stegeman D.F., Houtman C.J., Lapatki B.G., Zwarts M.J.: Multichannel surface EMG. In: Stalberg E., (Ed.). Handbook of Clinical Neurophysiology, pp. 245-268, Elsevier, Amsterdam, 2004.

25. Lapatki B.G.: Quantitative Untersuchung zur Beurteilung funktioneller Parameter beim Trompetenspiel. In: Edition Wissenschaft, Reihe Humanmedizin, Vol. 187, pp. 1-130, Tektum Verlag, Marburg, 1998.

P

Curriculum Vitae

Bernd Lapatki was born in Rottweil, Germany, on May 16, 1966. In December 1994, he received his degree in dentistry from the University of Freiburg, Germany. After working for two years as a general dentist, he defended his doctoral thesis in medicine (Dr. med. dent. degree) with the title "Quantitative Analysis for the Assessment of Functional Parameters during Trumpet Playing" in 1998. In December 2000, he finished a postgraduate study at the Department of Orthodontics, Freiburg University Medical Centre, and obtained the certificate as "specialist in orthodontics". From September 2001 to October 2002 he attended as a research fellow at the Department of Clinical Neurophysiology, Radboud University Nijmegen Medical Centre (The Netherlands), with financial support from the Deutsche Gesellschaft für Kieferorthopädie (German Orthodontic Society) and the Stichting FSHD (Wassenaar, The Netherlands). After finishing his habilitation thesis (leading to a German academic degree, equivalent to the PhD degree) in dentistry with the title "Pathogenesis and treatment stability of cover-bite and Angle-Class II Division 2 malocclusion" in November 2007, he obtained a professorship for orthodontics from the Faculty of Medicine of the University of Ulm in September 2009, where he is currently working as Head of the Department of Orthodontics at the Centre of Dentistry.

In 1999, Bernd Lapatki was awarded by the Faculties of Medicine and Applied Sciences of the Albert Ludwig University Freiburg for the best dissertation in the field of medicine/medicine technnique/applied informatics/microsystems engineering. In 2004, he received the "Alex Motsch Award" of the Academy of Functional Diagnostics and Therapy (AFTD) of the German Society of Dentistry and Oral Medicine for the paper "Systematic characterisation of motor units of the facial musculature by means of high-density surface electromyography", and in 2007 the "Arnold Biber Award" (the highest scientific award of Orthodontics in Germany) of the German Orthodontic Society for the paper "Smart brackets for 3D-force-moment measurements in orthodontic research and therapy – developmental status and prospects".

Besides his research on the facial and masticatory musculature, Bernd Lapatki is also working on the development of a smart fixed appliance with integrated micro sensors for measuring the forces and moments exerted on the individual teeth during orthodontic therapy. Moreover, he is interested in the physiology and pathophysiology of wind instrument playing and is specialised in the treatment of dental problems in wind instrumentalists.

Bernd lives together with his wife Cristina in Ulm, Germany.

CV

Donders Institute
for Brain, Cognition and Behaviour